

Soluble Silicates

Soluble Silicates

James S. Falcone, Jr., EDITOR
The PQ Corporation

Based on a symposium jointly
sponsored by the Divisions of
Industrial and Engineering Chemistry
and Inorganic Chemistry at the
182nd National Meeting of the
American Chemical Society,
New York, New York,
August 26–27, 1981.

A C S S Y M P O S I U M S E R I E S **194**

AMERICAN CHEMICAL SOCIETY
WASHINGTON, D. C. 1982



Library of Congress Cataloging in Publication Data

Soluble silicates.

(ACS symposium series, ISSN 0097-6156; 194)

"Based on a symposium jointly sponsored by the Divisions of Industrial and Engineering Chemistry and Inorganic Chemistry at the 182nd National Meeting of the American Chemical Society, New York, New York, August 26-27, 1981."

Includes bibliographies and index.

1. Silicates—Congresses.

I. Falcone, James S., 1946- . II. American Chemical Society. Division of Industrial and Engineering Chemistry. III. American Chemistry Society. Division of Inorganic Chemistry. IV. Series.

TP245.S5S64 1982 661'.068324 82-11514
ISBN 0-8412-0730-5 ACSMC8 194 1-374 1982

Copyright © 1982

American Chemical Society

All Rights Reserved. The appearance of the code at the bottom of the first page of each article in this volume indicates the copyright owner's consent that reprographic copies of the article may be made for personal or internal use or for the personal or internal use of specific clients. This consent is given on the condition, however, that the copier pay the stated per copy fee through the Copyright Clearance Center, Inc. for copying beyond that permitted by Sections 107 or 108 of the U.S. Copyright Law. This consent does not extend to copying or transmission by any means—graphic or electronic—for any other purpose, such as for general distribution, for advertising or promotional purposes, for creating new collective work, for resale, or for information storage and retrieval systems. The copying fee for each chapter is indicated in the code at the bottom of the first page of the chapter.

The citation of trade names and/or names of manufacturers in this publication is not to be construed as an endorsement or as approval by ACS of the commercial products or services referenced herein; nor should the mere reference herein to any drawing, specification, chemical process, or other data be regarded as a license or as a conveyance of any right or permission, to the holder, reader, or any other person or corporation, to manufacture, reproduce, use, or sell any patented invention or copyrighted work that may in any way be related thereto.

PRINTED IN THE UNITED STATES OF AMERICA

**American Chemical
Society Library**
1155 16th St. N. W.
Washington, D. C. 20036

ACS Symposium Series

M. Joan Comstock, *Series Editor*

Advisory Board

David L. Allara

Robert Baker

Donald D. Dollberg

Robert E. Feeney

Brian M. Harney

W. Jeffrey Howe

James D. Idol, Jr.

Herbert D. Kaesz

Marvin Margoshes

Robert Ory

Leon Petrakis

Theodore Provder

Charles N. Satterfield

Dennis Schuetzle

Davis L. Temple, Jr.

Gunter Zweig

FOREWORD

The ACS SYMPOSIUM SERIES was founded in 1974 to provide a medium for publishing symposia quickly in book form. The format of the SERIES parallels that of the continuing ADVANCES IN CHEMISTRY SERIES except that in order to save time the papers are not typeset but are reproduced as they are submitted by the authors in camera-ready form. As a further means of saving time, the papers are not edited or reviewed except by the symposium chairman, who becomes editor of the book. Papers published in the ACS SYMPOSIUM SERIES are original contributions not published elsewhere in whole or major part and include reports of research as well as reviews since symposia may embrace both types of presentation.

PREFACE

SODIUM SILICATES WERE INTRODUCED commercially in the United States over 100 years ago as a replacement for rosin in soaps. Today the use of soluble silicates in industry is widespread and effective. And for the past 30 years, users of soluble silicates have considered James Vail's two volume ACS Monograph No. 116, "Soluble Silicates: Their Properties and Uses," the definitive work on the subject. Since then significant advances have been made in understanding the chemistry of both the sodium silicates and their various derivative materials.

Recently, however, the development of ^{29}Si FT-NMR spectroscopy combined with X-ray structural information on solids and the refinement of chromatographic methods for silicate solutions and solids have begun to provide a clearer picture of the distribution of species in solution. The results of these efforts are only now beginning to shed further light on the complex chemistry of these materials. It is expected that the emerging knowledge of the structure and the influence of that structure on solution properties and reactivity will further enhance the value that these materials have in industrial processes. As we learn more about these "structured solutions," we can expect better understanding of silicate glass chemistry, the equilibria of species in soil and water, cement chemistry, the synthesis of synthetic silicates, and the role of silicates in industrial and biological systems.

The 21 papers presented in this timely volume represent the recent work or summaries of studies of a significant cross section of researchers who have been studying soluble silicates and other relevant technologies. The topics may be viewed as four allied themes. The first group of papers deals with the history of these materials, modern instrumental methods for analysis and reviews their current environment, health, safety and regulatory status. Next, several papers cover aspects of the structural, colloid, and solution chemistry of soluble silicates, the solubility of amorphous silica, and a review of the chemistry of silanol groups. This last subject is included because evidence shows that the reaction chemistry of species in solutions of silicates with high $\text{SiO}_2/\text{Na}_2\text{O}$ ratios may be analogous to the surface chemistry of a high surface area porous silica gel.

The next group of papers discusses recent applications of the soluble silicates with particular emphasis on oil recovery. This is an application which arose by analogy to the use of soluble silicates in detergency; it is particularly interesting because here, as in detergency, many of the chemical properties of soluble silicates, acting in concert, play a role in the enhancement of oil production, i.e., basicity, the reactivity of silicate anions with metal ions and oxide surfaces, their hydrophilic nature and ability to form gels at higher concentration.

The last section is made up of several papers on the preparation and properties of novel silicate materials of current interest.

In closing, I would like to acknowledge The PQ Corporation for allowing me the time and support to bring together the many people interested in understanding and applying these useful materials and to acknowledge the contributions of the authors who share my enthusiasm for silicate chemistry. It is my feeling that this is simply the beginning of a new and exciting chapter in the growth of the understanding and use of these "inorganic polymers" for the future.

JAMES S. FALCONE, JR.

**The PQ Corporation
Research and Development Center
Lafayette Hill, PA 19444**

March 1, 1982.

A Short History of the Manufacture of Soluble Silicates in the United States

JOHN H. WILLS

Kennet Square, PA 19348

The manufacture of soluble silicates of soda and potash in the USA began in the 1850's and received a vigorous push when it was found to be a satisfactory replacement for rosin in the manufacture of strong soaps during the war between the states. Continuous manufacture of the glass was introduced by the Elkinton family, soap and candle makers in Philadelphia, PA. The alkaline crystallized products now used widely in detergents were developed in the early 1930's, based on the patents and phase studies of Chester L. Baker. In that decade, Dr. William Stericker took the lead in the development of coated roofing granules and the manufacture of black and white television tubes using potassium silicate to bind the pigment to the glass face. The manufacture of catalyst and other gels and replacement of phosphates in detergents by soluble silicates and other additives in the 1950's overshadowed the loss of the corrugated box industry to starch adhesives.

What I want to cover is something of the industrial beginnings of the soluble silicates, how their use has grown, perhaps a feeling of the burgeoning optimistic aspect of the world in which it took root and of the people who influenced and led its growth. Much reference is made to the Philadelphia Quartz Co. (PQ Co.) - now the PQ Corporation because this company has been a major factor throughout the whole period and because it has been able to make much more early data available.(1)

Most of you know that the soluble silicates are primarily the sodium silicates which are available over a range of concentrations and ratios of $\text{SiO}_2:\text{Na}_2\text{O}$, including water solutions, glasses, and crystals according to the needs which industry has found for them.

The story of the industry began with a German professor, Johann Nepomuk von Fuchs of the German University of Landshut.

He became interested in this chemical about 1818 and in the next twelve years worked out the basic technology for production and suggested most of the possible uses as indicated by his study of its properties. Under royal edict, it was used for a time to protect the stages and curtains of theatres from catastrophic disasters by fires current at the time. Kuhlman in France for a period took up the leadership in European development, but von Fuchs in 1855, just before he died in 1856, wrote a full report on his work and suggestions for use of soluble silicates and this was widely read.(2)

One major European application was the replacement of animal dung in a textile process called "dunging", and Gossage developed a very good soap using soluble silicate. His company, Crosfields, prospered and eventually became the leading soap and detergent producer under the style of Unilever. Also about this time, there was a series of patents in the USA for the preparation and use of waterglass, particularly in soap. These give us some insight into the men who began the industry in the USA.(3) The practice of shipping soluble glass as ballast seems to have been a major problem for would be manufacturers in New York and Boston. Philadelphia was the center of American chemical industry at the time and seems to have been better situated. Relations between the North and South were strained, and the expectation of war threatened the supply of colophony or rosin on which the many small soapers relied for the preparation of stronger laundry products.(4) Most of these soapers also made candles, and kerosene lamps were rapidly reducing the demand for them.

The Beginnings of the American Industry

Industrial development of sodium silicate in America begins with Dr. Lewis Feuchtwanger. He had studied about 1830 with Professor Dobereiner at Jena. The professor had been fascinated by Fuchs' reports and was working with soluble silicates. Feuchtwanger brought his enthusiasm home with him and writes that in 1832, with the permission of Admiral Perry, he carried out some successful tests at the Brooklyn Navy Yard. The cannons were protected from rust for several years by a coating of mixed sodium silicate and asphaltum. He also extended the life of the wooden docks several times by impregnating the wood piles and substructures with dilute sodium silicate. The saturated wood prevented attack by teredo worms. He probably bought this silicate from Germany and dissolved it here but he does claim that he was manufacturing it in 1869.(5)

I have found no other evidence that he had a plant, but a Mr. Sawyer of Pittsburgh, Pa. reported in 1864 that he had been buying from Feuchtwanger(1), and in 1867 a treatise on soap making states that Mr. Dieterichs, chemist for the "Atlantic

Quartz Co. of West Philadelphia" had also been buying from him.(6) I have found no other reference to this company in any directories. Feuchtwanger's first publication seems to have been written out longhand, although it is possible that the manuscript I saw had been copied from his book, a practice not uncommon at the time.

J.M. Ordway deserves mention in our record for besides the patents for making alkali silicates by reducing sodium sulfate and preparing an easily soluble powder by coacervating the liquid noted earlier, he published an article on the history and use of soluble silicate in Silliman's Journal in 1861 and a series of articles in the American Journal of Science in 1861, 1862, 1865 and finally in 1907; an active scientific life of 45 years. In his article of 1861 (7), he gives a complete description of the state of the art from melting to dissolving. He was already aware that the raw materials should be of the highest purity and that soda ash was easier to use. Since sodium sulfate was cheaper, the reaction was fully studied. Glass furnaces from which it was possible to draw a little fused silicate at a time and then add more charge were used. Consistent results were difficult to obtain and he recommended melting the charge completely and drawing the melt at once. He mentions furnaces with beds of 24 and 40 square feet. Four charges of $\text{Na}_2\text{O}:2.5 \text{SiO}_2$ could be completed in 24 hours. The charge was drawn into iron pots, cooled, and ground to a desired size with cast iron, toothed, crushing rollers. If drawn into water, it would break into small fragments which were difficult to dry. However they were readily dissolved by heating the water. The disilicate was easier to dissolve and was recommended for the calico printers. With soda ash as alkali source he could draw six charges a day.

In Philadelphia, a young Quaker named Thomas Elkinton was coming of age. His father had gone into the manufacture of soap and candles in 1831 after 15 years of missionary work with the Seneca and Iroquois Indians at Tunessassa, N.Y. Having served his time and needing to support his family, he followed a cousin into this new venture which required not only manual dexterity but bartering skills and familiarity with ship captains. The relationship of the Elkinton family of soap makers in Philadelphia with a group styled variously as the New York Silicate Co. or the New York Quartz Co. or the New York Liquid Silicate Co. as well as with J. M. Ordway and Hodges, Silsbee, and Richardson of Boston encompasses the real foundation of the manufacture of soluble silicates in this country.

Thomas Elkinton was a young man of 22 when in about 1857 he became interested in applying silicates to the soap made by his father.(1) After he had read van Fuch's last survey and had copied Gossage's English patent into his journal, Thomas Elkinton bought iron pans for a furnace and in 1858 spent \$2.50

for plans for a reverbratory furnace. Bricks were ordered in 1861, and the first four barrels of silicate were sold in early 1861. His US patent #39135 for a continuous furnace issued in 1863. The design included all the basic requirements for a silicate furnace. This new furnace was built in 1863 for \$1,100. While the first attempt was a failure because of inadequate or inaccurate mixing of the sand and soda ash, his next attempt (after a month given to digging out and repair) ran for a month and produced 122,000 pounds of glass.

His patent and perhaps his other activities alerted the group in New York. G. T. Vanderburg, Secretary of the New York Quartz Co., obtained US patent #31648 in 1863 and assigned it to the Liquid Quartz Co. of New York. This improvement covered a soap in which the added silicate had a ratio of $\text{SiO}_2:\text{Na}_2\text{O}$ above 1. Vanderburg had also obtained US patent #28540 in 1860 for a process for reducing a siliceous substance to a fluid state using superheated steam. At about the same time, Thomas bought 10 pounds of ground silicate of soda from the New York Quartz Co. and he also met with Vanderburg to discuss the Gossage patent, perhaps at the time the ground glass was ordered.⁽¹⁾ He had bought liquid silicate from them in April, 1861.

So, early in 1864, the president of New York Silicate or Quartz Co. John Graecen, Jr. and the Treasurer, Samuel Booth, approached Thomas and his brother Joseph at their soap factory, 783 S. 2nd St., their father having passed the company to them in 1862. The New Yorkers mentioned that they owned the Vanderburg soap patent and suggested that it was being infringed. At the same time, they hinted that they were a large and financially sound company which could afford to manufacture silicate at a price which would run the Elkinton brothers out of the business. They suggested a royalty of 1/4¢ a pound for an article which sold for 4¢ a pound, only 25% less than today's bulk price of 5.6¢. The upshot was that a partnership was arranged, and the Philadelphia Quartz Co. came into being as of February 25, 1864. The Elkinton brothers were to be the active partners and were to "carry on the business in accord with their religious principles." The New Yorkers arranged to lease a property at 9th & Mifflin Streets from their earlier partner, a Philadelphia soap and candle maker with whom the brothers declined to be associated. This property was sold to Graecen and Booth in 1867, and then on December 22, 1868 the Elkinton brothers bought out their partners for about \$23,000.

In 1863-1864, Hodges, Silsbee, and Richardson of India Wharf, Boston advertised as agents for the New York Quartz Co. and the Philadelphia Quartz Co. Hodges was curious and experimented with the production of soluble silicates using both ash and salt cake which requires C as a reducing agent and also an oxidizing agent to get rid of the discoloration by the carbon. He described his work in letters to Thomas Elkinton.

In 1872, after the bankruptcy of the New York Quartz Co., the Ordway patents were assigned first to Samuel Booth as receiver and to Ordway and thence were assigned to Hodges and Co. Also in 1872, the Vanderburgh patents were assigned to Booth by Ordway. Finally, in the same year, all of these patents were assigned equally to Coolidge and Hodges of Boston and the Elkinton brothers of Philadelphia. At about this time Hodges advertised that his firm was the sole manufacturer in New England at the Bayside Alkali Works in South Boston.

This is really the story of the beginning of alkali silicate manufactured in North America. The volume grew slowly. In 1893 Thomas wrote to Curtin, Hughes and Kellogg of Boston that the commercial papers were unlikely to quote prices for alkali silicates. He kept only small stocks for "outside users---are so trivial that a chance order for a few gallons or barrels at a time will cover the order."(1)

The Centennial Exposition held in Philadelphia in 1876 seemed to dramatize the growth and excitement of the times. Many companies had exhibits; including Feuchtwanger and the Elkinton brothers. The Philadelphia Quartz Co. received the highest award of merit for "a most beautiful exhibit of silicate of soda" according to one commentator. They had an arresting experiment in which black, oily cotton rags used to wipe clean the many steam engines at the exhibition were washed with silicate and turned out a lovely soft white cotton.

The early development of furnaces and dissolvers came at just the right time, for the war between the states in 1861-1864 did cut off the rosin supply and created a demand for their product. The Elkintons had the advantage that they also produced soap next door to the silicate plant. The sale of silicate was welcome, but early sales records show only a few barrels. However, in 1889 the Philadelphia Quartz Co. built a new plant at Anderson, Indiana right over a gas well. It is the oldest silicate plant still producing and was next door to the large soap plant of Peet Brothers. This established a custom still recognized in the industry of selling silicate by pipeline. The Fortville Chemical Co. was built near Anderson in 1896 and was bought by Grasselli Chemical Co. in 1902, as part of their expansion in the alkali business. Mechling Brothers built a plant in Camden, NJ in 1902 and the Philadelphia Quartz Co. expanded into a larger plant on the Delaware River at Chester in 1905. The Merrimac Chemical Co. at Lowell, Mass. produced silicate in 1890. This plant was acquired by Monsanto in 1929. The Mechling plants, by then owned by Allied Chemical Co, are now closed.

One reason there is very little information on producers and sellers of silicates is that few people came seeking them. I assume that a drummer for soluble silicates came into town, checked the local directory (before phone books and yellow pages) and visited all the local soap makers. In Philadelphia

in 1860 there were 45 and 22 in New York. A special factor in this sales program was Charles Goudy, an Englishman with a broad background in chemical manufacturing before crossing the Atlantic. He settled in Marshalltown, Iowa for reasons having to do with his wife's health and set up a very successful soap business. About 1876, he and Thomas Elkinton, one or both, conceived the idea of a small machine carried in a suitcase which could demonstrate the use of soluble silicate in soap in the would-be customer's office. Goudy became a leading figure in PQ Co. and continued to travel until he was 80. He was their first development chemist and one of the first in our chemical industry. In later years he was joined by his son George who had experience in soap manufacture previously and became a leader in PQ Co. as well as an industrial statesman.

The Growth of the Industry

There is a long list of companies and works built, bought, sold, merged, enlarged, or dismantled. The record is not always clear or exact and seems unnecessary to review. Figure 1 attempts to show the growth of production from 1850 to 1980 in terms of the liquid silicate which is most common. This curve is a composite from several sources, not all of which agree, and I have not tried to show the yearly ups and downs which appear when the annual census figures are plotted. The curve follows in a general way the growth of population as well as the gross national product, but it is usually hedged against depressions by the growth of the industries it serves as well as its cost which makes it a candidate for replacing more expensive items.

The first fifty years are a record compiled by W.T. Elkinton of the production by the Philadelphia Quartz Co., primarily for the Elkinton Soap Co., but for many other customers. It does not include imported material or the production by known competitors such as Fortville in 1896 or around Boston. I would suggest that the line represents from 50 to 75% of the silicate used up to 1900. This growth was primarily for use in soap.

James G. Vail joined PQ Co. in 1905 before finishing college. He then finished his formal chemical education at the Institute of Technology, Darmstadt, Germany, became president of the U.S. Society of Chemical Engineers in 1945-46 before retiring finally in 1952 and wrote the major books on soluble silicates issued in 1928 and in 1952,(3) the year he died.

Soluble silicates as an adhesive had long been used in small amounts when in the 1890's there began an intensive and continuing effort to produce paper boxes to compete with the wooden packaging then in general use. Paperboard with a corrugated ply between two sheets and complex machines were developed. The later development of adhesive and cement uses

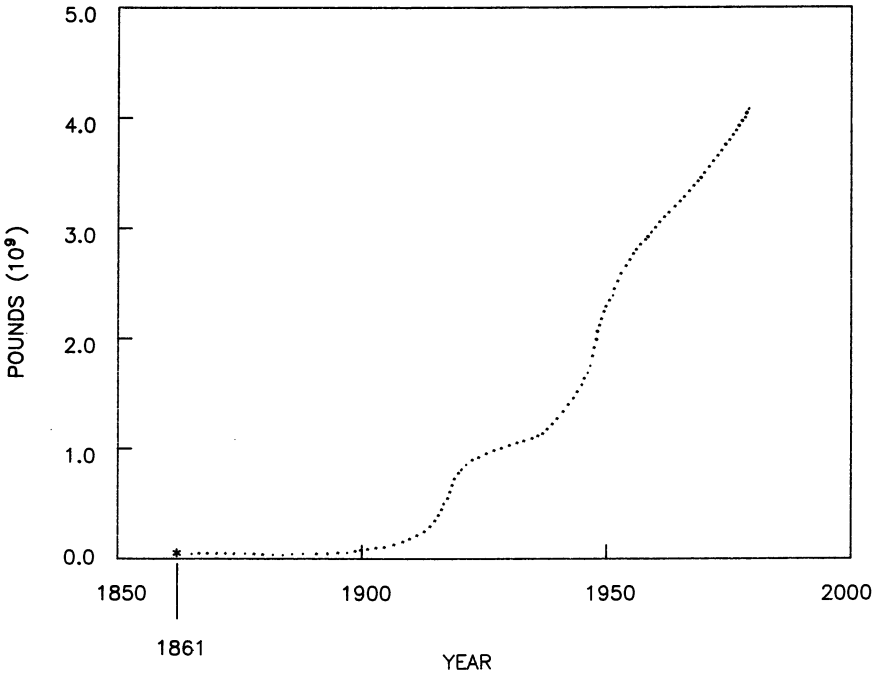


Figure 1. U.S. production of soluble silicate in 10⁹ pounds of liquid, equal to 3.22 SiO₂·Na₂O, 1.39 Sp. Gr.

of soluble silicates has been reviewed in a series of volumes on adhesives and cements.(8)

Hydrous Silicates

During much of the same period there was a less important but more generally known application that is for the preservation of eggs. Many people had their own chickens or were canny enough to buy eggs when they were cheap in the spring and summer. They kept ceramic crocks in the cellar filled with dilute waterglass. The excess eggs were placed in the crocks and the silicate reacted with the shell preventing either loss or increase in the water content of the egg, entrance of infective agents, or loss of the air cell and even when kept nine months of so they were still poachable. George Goudy conceived the need for a powdered silicate which could be readily dissolved at home. Using L.B. Edgerton's patents issued in 1916 (9), for atomizing liquid silicates, a desiccated silicate was produced and sold as "Goudy's Egg Preserver" in 56oz. packages which would make 7 gallons of diluted waterglass, all for one dollar. Demand appeared to rise after the war, and in 1930 arrangements were made to install a spray tower imported from Germany. With the increasing use of refrigeration and large scale continuous production of eggs, the market for egg preserver evaporated, but other developments such as muds for drilling through heaving shale areas kept the new larger desiccation tower in operation.

The Development of the Alkaline Silicates for Detergents

I suppose there are still soapers who consider soluble silicates an adulterant, a derogatory word. Following World War I, many researchers carried out vigorous programs of investigation and writing to demonstrate the several ways in which soluble silicates act as detergents themselves and aid as builders in cleaning in combination with soaps and other detergents. J.D. Carter's papers published about 1930 have been considered classics in the field as they set out criteria for soiling and measuring detergency.(10)

Even before the first world war, the cleaning industry had begun to desire more alkaline detergents. The Puritan Soap Co. suggested combinations of silicate and soda ash, but all such combinations seemed liable to cake in their containers. Chester L. Baker, after an early indoctrination in the crystallization of commercial borax and other salts of Searles Lake, CA, in 1927, became Chief Chemist of the Philadelphia Quartz Co. of California, an affiliate formed in 1917 and owned 50% by the Stauffers. Baker and later his assistant, Ralph Jue, worked long hours developing the phase relationships for the crystallization of hydrated metasilicates of sodium over

the range of 0 to 90°C. They established the existence of and carefully described the physical characteristics of the 5, 6, 8, and 9 hydrates and the conditions for their appearance and disappearance.(11) They also found and described the sesquisilicate $\text{Na}_3\text{HSiO}_4 \cdot 5\text{H}_2\text{O}$ ($3\text{Na}_2\text{O} : 2\text{SiO}_2 : 11\text{H}_2\text{O}$). They showed that a solution carefully prepared at the composition of $\text{Na}_2\text{SiO}_3 \cdot 5\text{H}_2\text{O}$ ($\text{Na}_2\text{O} : \text{SiO}_2 : 5\text{H}_2\text{O}$, pentahydrate) could be seeded and allowed to crystallize in a soap mold and then ground and sized. Since there was no excess liquid silicate, the product was stable enough to ship from San Francisco through the humid Panama Canal to Philadelphia without caking. This was taken as the crucial test for a commercial product, and his work became the basis for the great development of the alkaline silicate powders. The first sales were made in California in 1928. Later he brought out the sesquisilicate and later still worked out the process for a granulated sodium metasilicate.

In 1980, the capacity of sodium metasilicate as pentahydrate was about 580 million pounds. PQ Corporation is said to have the largest capacity with Stauffer and Diamond-Shamrock following in that order.

By cross license with PQ Co., Pennwalt developed a hydrated form of orthosilicate ratio about 1938. It was an integral product made by mixing NaOH with the necessary amount of another silicate or silica. If the crystallizer was kept turning, the mixture went through a higher temperature fluid state and gradually transformed into particles which were stable enough for commercial use. I know of no phase diagrams showing the existence of stable Na_4SiO_4 ($2\text{Na}_2\text{O} \cdot \text{SiO}_2$) or its hydrates, and the process is no longer used. All so-called orthosilicate is now compounded and is included in the metasilicate figures. As shown in Table I, the production of these alkaline products not available before 1928 is now very large.

Table I
USA Production in Millions of Pounds of Sodium
Metasilicate (Calculated as Pentahydrate)
and of Sodium Orthosilicate

<u>Year</u>	<u>$\text{Na}_2\text{SiO}_3 \cdot 5\text{H}_2\text{O}$</u>	<u>Na_4SiO_4</u>
1928	0.3 est.	0
1929	1.8 est.	1 est.
1930	4 est.	60
1940	40 est.	76
1950	198	60
1955	314	76
1960	386	76
1965	502	84
1970	450	72
1976	378	63
1979	433	52
1980	336	60 est.

The Development of Other End Uses

The chemist who bore the brunt of the introduction of these new detergents to the laundry and metal trades was William Stericker. He always maintained that no leading detergent or laundry soap ever held a leading position for a long period without including a good proportion of sodium silicate. From the time, 1922, when he earned his graduate degree at Mellon Institute studying the properties of sodium silicate, he developed an uncanny sense of how to use it in commercial processes.(12) It was mainly his insight which helped the developers of roofing granules, welding rod coatings, oscillograph coatings, methods for preventing corrosion in susceptible water systems, and coagulation with activated silica sols for the clarification of water and sewage. Just before the second World War the new detergents and non-soap compounds were appearing, and Stericker was a leader in working with soap and detergent associations to establish the efficacy of silicates in such systems where phosphates were generally accepted. First, he demonstrated the necessity for the anti-corrosion properties of the silicates. This development was especially welcomed by our industry because the starch adhesives developed with alkali and borax in the 30's largely replaced the silicate adhesives for box making in the 50's, and this loss caused much consternation among us.

The gelation of solutions of soluble silicates with acids and acidic salts is very old, but industrial development began with the Wheaton patents in England about 1922,(13) These were for base exchange gels for softening water and were used through the 30's when they were gradually replaced with organic agents of higher capacity. Newer versions are now being used in detergents. Desiccant gels also began to appear in the 30's and Davison Chemical Co. was the chief developer. The use of catalyst gels in the petroleum industry boomed with World War II. The silicas in finely divided form and as sols came along during and after the war. Much of the silicate production for use in these areas is captive. The lithium silicates(14, 15) which became available in the 50's are more expensive but are useful in binding corrosion resistant coatings to iron, in cements, and in molds.

The Contributions of James Vail

James Vail was a great publicist. Besides writing many articles and reports on all phases of silicate technology, he put out a small monthly sheet - P's and Q's - for over twenty years, and this was known in the chemical industry far beyond the silicate field. In 1928, he published ACS Monograph #46 "Soluble Silicates in Industry" and thirty years later he acceded to many requests and wrote ACS Monograph #116 "Soluble

Silicates" in two volumes.(3) While much has happened since 1952, the book has not yet been replaced as the primary reference for soluble silicate technology and should be reviewed for references and basic information on processes and products I have so briefly mentioned. James Vail was a man of great insight, a poet, author, and above all a humanitarian. He carried out sensitive, significant, supportive programs in many parts of the world for the American Friends Service Committee of which he was Foreign Secretary for a long period, about 1938 to 1948. He was in India on such a mission when he died. In his final paragraphs of Chapter 1 of his last book, he notes the rising world population and the need to conserve resources not readily replaced. He notes there that phosphates are irreplaceable and badly needed for fertilizer in agriculture. Food resources continue to be scarce, and he points out that a rational society would preserve phosphates both by conserving their use in detergents and refusing to spend energy and fertilizer for the production of starches and proteins for industrial use which could just as well be replaced by soluble silicates prepared from salt and sand, raw materials abundant into the foreseeable future. "...soluble silicates now serve so wide a range of industry that they are to be regarded as a fundamental part of any long range planning for the conservation of natural resources.(3)

Final Comments

Perhaps this is a good place to stop. Table II shows an estimate of the capacity for production of most of the plants in the USA.

Table II
Capacity of the Soluble Silicate Industry in the USA
in 1981 in Billions of Pounds of Sodium Silicate
Liquid Equivalent to 3.22 SiO₂:Na₂O Ratio by
Weight at 42° Baumé

<u>Producer</u>	<u>Plants</u>	<u>Capacity, pound (10⁹)</u>
Diamond Shamrock	7	1.3
duPont de Nemours	5	0.7
PQ Corp.	12	2.2
Chemical Products	1	0.1
Grace Chemical	1	0.4 captive
PG Corp.	2	1.1 "
Ethyl Corp.	1	0.4 "
Engelhard	1	0.04 "
J.M. Huber	2	0.5 "
Associated Minerals	1	0.02
Total		<u>6.8</u>

Table III gives an idea of the amounts required by major applications (75% of capacity as of 1980).²⁹

Table III
Soluble Silicate Use in 1980 in Billions of Pounds
of Liquid Product Equivalent to 3.22 SiO₂:Na₂O Weight
Ratio at 1.39 Specific Gravity

<u>Application</u>	<u>Volume, pounds (10⁹)</u>
Catalysts and Gels	1.3
Soap and Detergents	1.2
Roofing Granules, Ceramics, Textiles, Rods, Foundry, etc.	0.7
Pigments	0.6
Boxboard, Adhesives	0.3
Ore, Paper, Water Treatment	0.3
Total	4.4 (or 75% of capacity)

New applications keep cropping up and old ones appear in new guise. Soluble silicates are usually relatively inexpensive, but their sensitive properties have to be understood and handled competently. Many a potential application has failed because necessary precautions were not taken either in the use or in the storing and handling. The manufacturers have representatives ready and able to help.

I have mentioned only a few of the individuals of the many who have helped expand the application of this product which has so much to recommend it. The basic raw materials, water, salt, and pure sand are available in essentially unlimited quantities at low cost. While they require considerable energy in preparation, they seldom cause environmental problems and readily return to the soil. They are inorganic materials which, it seems to me, are only at the beginning of their development by man. Anyone who contemplates the place of silica in natural organic and inorganic systems has to realize that we have a long way to go before we realize the full potential of this product which excited the imagination of Fuchs and others 150 years ago.

As we go into the last twenty years of this century, I am filled with optimism, not only because of the applications which now appear promising and the increasingly efficient operations which the computer age suggests, but because I firmly believe we have not yet discovered all of nature's secrets about the ability of silica to bind or react with itself and other substances. The development of detergents, adhesives, gels, solar heating or power systems, fire prevention, and the increasing understanding of chemical and physical bonds all suggest to me that we can expect the production curve to continue to rise.

Literature Cited

1. Historical File - T. Elkinton's Journals and W.T. Elkinton's Compilation (1931), etc., The PQ Corporation, Valley Forge, PA.
2. Von Fuchs, J.N., "Bereitung, Eigenschaften und Nutzenanwendung des Wasserglasses mit Einschluss der Stereochromie"; Literarisch-artistische Anstalt: Munchen, 1857.
3. Vail, J.G. "Soluble Silicates" 1 and 2, ACS Monograph Series #116; Reinhold Publishing Corp.: New York, 1951 (Chap. 1, especially p. 4-7, gives a brief historical review).
4. Annual Record of Scientific Discovery, Wells, D.A., ed.; Gould and Lincoln: Boston, 1864.
5. Feuchtwanger, L. "Practical Treatise on Soluble of Waterglass" 3rd ed.: New York, 1875.
6. Ott, A. "The Art of Manufacturing Soap and Candles"; Lindsay and Blakiston: Philadelphia, 1867.
7. Ordway, J.M., American Journal of Science and Arts, 2nd Series, 1861 32 153-165, .
8. Wills, J.H. : "Adhesion and Adhesives", De Bruyne, N.A.; and Houwink, R., Ed.; Elsevier Publishing Co., Amsterdam, 1951.
9. Edgerton, L.B., U.S. Patent 1194827 and 1198203 (1916).
10. Carter, J.D., Ind. and Eng. Chem. 18, 248 1926; 23, 1289 1931.
11. Baker, C.L. and Jue, L.R. J. Physical Chem. 1938 42, 165; J. Physical and Colloid Chem. 1950 54, 208.
12. Stericker, W. in J. Alexander "Colloid Chemistry" Chemical Catalog Co., Inc.: New York, 1928 p 289.
13. Hilditch, F.P. and Wheaton, H.J., U.S. Patent 1717777 (1929); 1879239 (1929); 1848127 (1932).
14. Iler, R.K. U.S. Patent 2668149 (1945).
15. Cuneo, F.L. U.S. Patent 3392039 (1968).

RECEIVED March 2, 1982.

Modern Instrumental Methods for Analysis of Soluble Silicates

JONATHAN L. BASS

The PQ Corporation, Research and Development Center, Lafayette Hill, PA 19444

Modern analytical instrumentation has been used in the last 25 years for determining commercially important characteristics of soluble silicates, and the nature of silicate species in silicate glasses and solutions. The classical wet methods for assay of silicate solutions are alkali titration and gravimetric determination of silica, which can also be determined, with lesser precision, by the alkali fluosilicate method. The alternative instrumental assay methods, X-ray fluorescence, atomic spectroscopy and thermotitrimetry, will be compared with the classical methods for precision and ease of measurement. Instrumental methods have greatly extended the ability of the analyst to detect trace cations and anions in soluble silicates. The scope and limitations, illustrated by some applications, of atomic and X-ray fluorescence spectroscopy, ion selective electrodes, and other less common methods for impurity analysis will be discussed. The techniques of infrared, Raman, X-ray photoelectron, and sputter induced photon spectroscopy, used for identification of silicate species will be briefly reviewed.

Sodium silicate was the 45th largest volume chemical produced in the United States in 1980, according to the 1981 Chemical and Engineering News Survey (1). Obviously, the analysis of this material as well as the other major soluble alkali silicate, potassium silicate, is very important commercially. This paper will briefly review the modern analytical instrumental methods that are used to determine the quality of commercial soluble silicates and instrumental

techniques that are used in structural characterization of silicates as glasses and in solution.

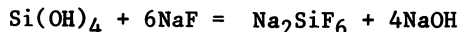
Assay of Soluble Silicates

Classical Wet Chemical Assay Methods

Before describing the instrumental methods, it is important to discuss the classical wet chemical techniques that form the foundation of analysis of soluble silicates. The most essential chemical property of silicate is the content of alkali and silica in either the glass or solution.

The standard method for determining the alkali assay involves titrating a diluted silicate solution with hydrochloric acid to either a methyl orange or methyl orange-xylene cyanole end point (2). The mixed indicator gives a more distinct end point.

Silica content may be determined by either the precise, tedious gravimetric silica procedure (2) or the more rapid but less precise fluosilicate method (3). The gravimetric method involves precipitation of the silica with acid, collecting the precipitate, ashing, volatilizing the silica with hydrofluoric acid and determining the weight loss after volatilization. The fluosilicate method involves reacting silica in a previously neutralized solution with sodium fluoride to form sodium fluosilicate and sodium hydroxide by the following reaction:



and titrating the hydroxide with hydrochloric acid to the methyl orange end point.

Silicate to soda ratios can also be determined rapidly for quality control purposes by an alkali titration and a measurement of either specific gravity or refractive index and viscosity which are correlated to $\text{SiO}_2/\text{Na}_2\text{O}$ ratios using control charts. The control charts are based on samples previously analyzed by the precise gravimetric method. The specific gravity method is more commonly used in commercial practice.

Assay by Instrumental Methods

The character of chemical analysis has changed drastically since World War II with the advent of sophisticated optical systems and electronic detection devices, which have been combined into instrumentation now commonplace in many industrial laboratories. The major advantages of instrumental

analysis are speed, sensitivity, versatility and relative ease of automation.

There are two venerable methods of instrumental silicate analysis that predate World War II, flame photometry for the alkali metals (4) and spectroscopic detection of the silicomolybdate acid complex in the visible spectrum (5). The spectroscopic method has been adapted for automated determination of silicate in detergents (6). The silicomolybdate method is also utilized to monitor the level of monomeric silica in silicate solutions (7). More recently developed instruments are capable of determining both alkali and silica (8-11). Atomic spectrometric instruments determine the total amount of an alkali ion, including that due to neutral species. Therefore the alkali assay by these methods may be greater than a titration method. Atomic absorption (AA) and plasma emission spectroscopy (PES) involve decomposition of the ions in solution to the atomic state. In the case of AA, atoms and ions of the element being analyzed are volatilized into the path of a light beam emitted from a lamp, and absorb this light, whose wavelengths are characteristic of valence electronic transitions in the atomic state. PES involves the excitation of valence electronic transitions of atoms and ions volatilized in a plasma arc. X-ray fluorescence (XRF) involves excitation of core electrons by incident X-rays, followed by X-ray emission at wavelengths that are characteristic of the elements present in either solution or solid. Finally, the thermal titrator is capable of detecting both alkali and silica by sensing a temperature increase in an adiabatic system. In the case of alkali, the increase is caused by the heat of reaction due to neutralization with acid, and for silica, by the heat produced during the fluosilicate reaction.

Comparison of Wet Chemical and Instrumental Methods

When choosing whether to use a wet chemical or instrumental methods for assay of alkali silicate, the analyst must weigh the compromise between the usually higher precision of wet chemistry and the speed and versatility of an instrument. In addition, the purchase of an instrument involves a substantial capital expense with higher operating annual expenses due to the requirements for periodic maintenance and more expensive supplies. However, if a large volume of analyses are run, the cost per sample may be lower using an instrument.

Table I summarizes the relative precision of the various assay methods. These tabulated values are conservative estimates; experienced analysts may achieve better precision between duplicate analyses. The table indicates a 3 to 5 fold advantage in precision for wet chemistry in most cases.

TABLE I
RELATIVE PRECISION OF WET CHEMICAL AND
INSTRUMENTAL ASSAY METHODS

<u>Wet Chemical</u>	<u>Instrumental</u>
Gravimetric silica <u>+0.05%</u>	Atomic absorption and emission Silica <u>+2%</u>
Fluosilicate reaction <u>+0.3%</u>	Alkali <u>+1%</u>
Alkali Titration <u>+0.1%</u>	X-ray Fluorescence Silica <u>+0.5%</u> Alkali <u>+1%</u>
Thermometric titration	Silica <u>+0.3%</u> Alkali <u>+1%</u>
Silicomolybdate	Silica <u>+0.5%</u>

However, in the commercial world the ultimate in precision is often not needed to satisfy the situational analytical requirements. Because the gravimetric procedure involves many time consuming steps, the fluosilicate reaction is generally preferable as the usual silica wet chemical assay method. It is not as precise as a normal alkali titration because of the difficulty of observing the end point.

Instrumental methods play an important role in silicate assay when the content of a specific alkali ion is required or when a large volume of samples justifies the cost of labor saved by using an instrument. For example, the titration method cannot distinguish between sodium and potassium in a mixed alkali silicate. A drawback of atomic, molecular and emission spectroscopy as assay methods is the extensive dilution required to lower analyte concentrations to the linear operating range of the instrument (8, 9). This contributes a dilution error which reduces the precision of the analysis. An advantage of X-ray fluorescence is that samples can be analyzed without dilution. It is necessary to use alkali resistant hardware. Unfortunately, X-ray fluorescence is the most expensive instrumental assay method.

Several papers have appeared within the last several years describing the application of thermometric titrations for silicate analysis (11). The instrumentation is less expensive than spectrometers but has not yet received widespread use in the U.S. silicate industry. However, somewhat analogous procedures are commonplace for analysis of caustic and alumina in the Bayer process streams of the aluminum industry (12). The method requires comparison against standards whose assay has been determined by other methods.

The silicomolybdate acid complex method is used for in-process monitors for silica content up to 50 ppm in process water. In combination with an automatic sampling and dilution system, such a monitor could assay for silica in a process stream with a precision of 0.5 to 1%, relative.

Instrumental Techniques for Silicate Impurity Analysis

The use of modern analytical instruments has greatly expanded the analyst's ability to determine impurities in silicates. Wet chemical methods usually are far too tedious, suffer from substantial interference or are not sensitive enough for impurity analysis. Even some instrumental techniques are subject to interferences, requiring separation to be used in the analytical procedure. The analyst must also decide on the sensitivity required since lowering detection limits usually increases the cost of analysis and the sophistication of the analytical procedure.

Impurities of major significance in alkali silicates are iron, alumina, calcium and magnesium, chloride, sulfate, carbonate and titania. They may originate as impurities in raw materials, be added from the manufacturing equipment, or be absorbed from the atmosphere. The degradation of product quality may be manifested as undesirable color, turbidity in solution, corrosiveness, loss of alkalinity or altered reactivity of products made from the silicate (e.g., iron or sulfate may poison a silica-based catalyst manufactured from a silicate solution).

Several instrumental techniques are available for detection of both cationic and anionic impurities in alkali silicates, with detection limits ranging down to the parts per billion or in some cases, parts per trillion level. The investigator must be aware that these sensitivities are achieved using the analyzed sample. If substantial dilution is required to bring the original material into the instrumental operating range, then the detection limit in this as-received sample is far higher. For example, if one can determine the presence of element A at the 1 ppb level in solution but a silicate requires 1000-fold dilution before it can be analyzed, then the detection limit in the original silicate is 1 ppm. Similarly, if a separation procedure is required, the detection limit in the original material is higher than in the aliquot being analyzed. Table II summarizes the capability of several instrumental methods for detection of impurities. This table provides broad guidance; in the case of a particular species, the analyst must consult the literature or perform experiments to find the actual detection limit for that species.

TABLE II
INSTRUMENTAL TECHNIQUES FOR SILICATE IMPURITY ANALYSIS

<u>Detection of Cations</u>	<u>Sample Preparation</u>	<u>Detection Limits</u>
<u>Technique</u>		
Flame AA	Separation, dilution	ppb-ppm in solution
Furnace AA	Separation, dilution	ppt-ppb in solution
Argon Plasma	Dilution	ppb-ppm in solution
X-Ray Fluorescence	Direct	ppm as received
Ion Selective Electrodes	Separation dilution	ppb-ppm in solution
Neutron Activation	Direct, separation	ppb-ppm as received ppb after separation
<u>Detection of Anions</u>		
<u>Technique</u>	<u>Sample Preparation</u>	<u>Detection Limits</u>
Ion Chromatography	Separation, dilution	ppm in solution
Ion Selective Electrodes	Separation, dilution	ppb to ppm in solution
Argon Plasma	Dilution	B, P ppm in solution
X-Ray Fluorescence	Direct	ppm as received
Raman Spectroscopy	Direct	0.5% carbonate in glass
Neutron Activation	Direct, separation	ppb-ppm as received ppb after separation

Detection of Cationic Impurities

Probably the most commonly used instruments for cation impurity analysis of silicates are flame atomic absorption spectrophotometers and ion selective electrodes. In most cases, separation of silica is required to reduce interferences. The sample may also have to be diluted to bring the analyte concentration within the linear operating range. For cations, the atomic absorption spectrophotometer is more versatile than ion specific electrodes. If the analyst is concerned with the presence of heavy metals, then accessories such as a hydride system for the elements that form high vapor pressure compounds, e.g., Sb, and a mercury vapor cold trap are useful. If a large number of elements are to be determined, a substantial investment in hollow cathode and electrode discharge lamps must be made. Several gas mixtures will also be required.

The flame atomic absorption spectrophotometer has detection limits ranging from the ppb to ppm level, depending on the element analyzed. Improved sensitivity can be achieved with the use of the graphite furnace which has lower background and atomizes more efficiently than the flame. In most cases a three order of magnitude improvement in sensitivity is achieved. However, this improvement in sensitivity requires more careful sampling, handling and ultra high purity reagents to be used in sample preparation. The calibration procedure is also more tedious.

In the last 6 to 7 years, argon plasma emission (PES) instrumentation has been commercialized with detection limits usually intermediate between flame and furnace AA. The two most common types of plasma instruments are the inductively coupled plasma (ICP) and direct current plasma (DCP). Although the ICP is somewhat more sensitive in terms of reported detection limits than DCP, the former cannot tolerate as high a dissolved solids content as the latter. Therefore, on the original silicate materials, the detection limits are similar. Another advantage of PES compared to AA is that commercial PES spectrometers can be configured for simultaneous multi-elemental analysis, while the current commercial multi-elemental AAs are sequential. The base price of PES equipment is higher than AA but if the sample load is high, the increased productivity of multi-elemental PES may result in a lower cost per analysis.

Table III lists spectral lines that are useful for the spectroscopic analysis of major components and impurities in soluble silicates.

TABLE III

TYPICAL SPECTRAL LINES FOR ATOMIC SPECTROSCOPIC ANALYSIS
OF MAJOR AND TRACE ELEMENTS IN SILICATES

<u>ELEMENT</u>	<u>AA</u>	<u>PES</u>
Iron	248 nm	238 nm
Silicon	252	252
Magnesium	285	280
Titanium	365	335
Sodium	295	590
Calcium	211	397
Aluminum	309	396
Potassium	383	770

Two less commonly used techniques, X-ray fluorescence (XRF) and neutron activation analysis (NAA) have the advantage that as-received samples can be analyzed, glasses as well as solutions. Both are more expensive than the previously mentioned techniques. The NAA technique that produces the greatest sensitivity requires irradiation in a research nuclear reactor and hence is really practical only when detection of low levels of unusual cations is required. Sodium silicate is somewhat more difficult to analyze than many other materials because of the formation of the relatively long lived radionuclide Na^{24} whose emissions interfere with the detection of other elements. Nevertheless we were able to determine, in a sample of sodium silicate, that many heavy elements of toxicological concern were undetectable down to the ppm to ppb level in the undiluted silicate (13). An XRF spectrometer can be configured to perform sequential multi-elemental analyses. It is less sensitive to the elements of lower atomic number. Also, since the X-rays penetrate only to a depth of about 10 μm , the sample must be homogeneous. Solid samples must be presented to the X-ray beam with a flat surface. However, the relative ease of sample preparation and the ability to run glasses and solutions with only minor dilution make X-ray fluorescence a useful technique where analysis for a wide range of impurities is required.

Detection of Anionic Impurities

Detection of anionic impurities in alkali silicates has not been as fully developed as for cations. The anion of greatest concern is carbonate which is absorbed from the atmosphere. Potentially, carbonate could originate from the soda ash or potash raw material used in silicate manufacture but under normal furnace operation the ash should be thoroughly decomposed. The standard classical method for carbonate analysis involves acidification and boiling of the solution to release CO_2 which is adsorbed on Ascarite. The procedure is time consuming and subject to errors resulting from difficulties in maintaining uniform flow. Two instrumental methods that show promise are ion chromatography (14) and laser Raman spectroscopy (15). Using a size exclusion column, carbonate has been determined down to the ppm level. This technique has not yet been applied to soluble silicates, which may require separation of the silica. Laser Raman spectroscopy has been applied to carbonate determination down to the 0.5% level in potassium silicate glass, using bands at 1770, 1428 and 575 cm^{-1} .

Using the proper choice of separation column, ion chromatography appears to be applicable for the sequential multicomponent analysis of other anions such as sulfate, chloride, fluoride and nitrate. The detection limits will be substantially lower than the classical gravimetric and potentiometric methods currently used. Ion selective electrodes are available for chloride and fluoride. A silicate sample requires separation in order to remove interferences.

As in the case of cations, NAA and XRF permit direct analysis for impurity elements that may be present in an anionic form. XRF is capable of detecting P, S, Cl, Br and I. NAA can determine Cl, Br and I at the ppm level in the as-received state, depending on the material and at lower levels using radiochemical separation.

Finally, argon plasma emission spectroscopy can determine the presence of two other elements, which can be present as anions, B and P. The technique is far more sensitive for the former element which can be detected at the ppb level in solution, while P can be detected at the ppm level. Both elements can also be analyzed by atomic absorption spectroscopy, but with less sensitivity.

Applications of Advanced Instrumentation to Silicate Structural Analysis

The last 25 years, and especially the last 10, have seen the application of advanced, expensive instrumental techniques

to the structural characterization of silicates both in the glass and solution states. Other contributors to this symposium have discussed extensively the use of nuclear magnetic resonance (NMR) spectroscopy and trimethyl silylation combined with gas-liquid chromatography (GLC), gel permeation chromatography (GPC) and mass spectroscopy (MS) to analyze the nature of siloxy bridging in silicate solutions. This paper will briefly describe the results of some other techniques that are less frequently used.

Vibrational spectroscopy, both laser Raman (16) and infrared (16, 17), can be applied as a useful supplement to the data developed by NMR and TMS for characterizing silicate species in solution. The number of bands observed in vibrational spectroscopy depends on the symmetry of the silicate species present. Protons attached to the Si-O bonds lower the symmetry compared to the SiO_4^{4-} ion. In this way, Marinangeli, et al (15), assigned seven laser Raman bands in a sodium metasilicate solution adjusted to pH 14 to the presence of $\text{Si}_2(\text{OH})_2^{2-}$. The spectra are shown as Figure 1. As the pH was lowered, shifts of bands to higher frequencies ($930\text{--}1000\text{ cm}^{-1}$) were observed. In unadjusted sodium metasilicate solution (pH 13.3), infrared bands attributed to the transformation of $\text{SiO}_2(\text{OH}_2)^{-2}$ into $\text{SiO}(\text{OH})^{-3}$ and the dimer $\text{Si}_2\text{O}_3(\text{OH})_4^{2-}$ appear. These bands were assigned by analogy to bands observed in the infrared spectra of crystalline silicates. When the solution is further acidified, bands at higher frequencies ($1000\text{--}1120\text{ cm}^{-1}$) assigned to polymeric species were observed. These shifts were also observed in the infrared by Beard (17) who studied silicates of different silica to alkali ratios. He also observed changes in intensities, over a period of several days, for silicate solutions produced by dissolving silica in alkali. These changes were attributed to depolymerization of the high molecular weight silicate species originally formed.

The nature of the silicon-oxygen bond in alkali silicate glasses as the sodium content increases has been investigated by electron spectroscopy for chemical analysis (ESCA) and high resolution X-ray fluorescence spectroscopy (18-21). ESCA has shown that the binding energy of oxygen 1s electrons of non-bridging oxygen is about 2eV less than that of bridging oxygens. This result is illustrated by the deconvoluted O_{1s} ESCA spectrum in Figure 2 (18). At low sodium concentration, sodium is associated with non-bridging oxygens (i.e., the network terminating oxygens). However, at higher sodium concentrations, the number of oxygen atoms with this lower binding energy as indicated by the peak intensity is less than the number of sodium ions indicating that some of these ions are dispersed in the network (18). In addition, the chemical

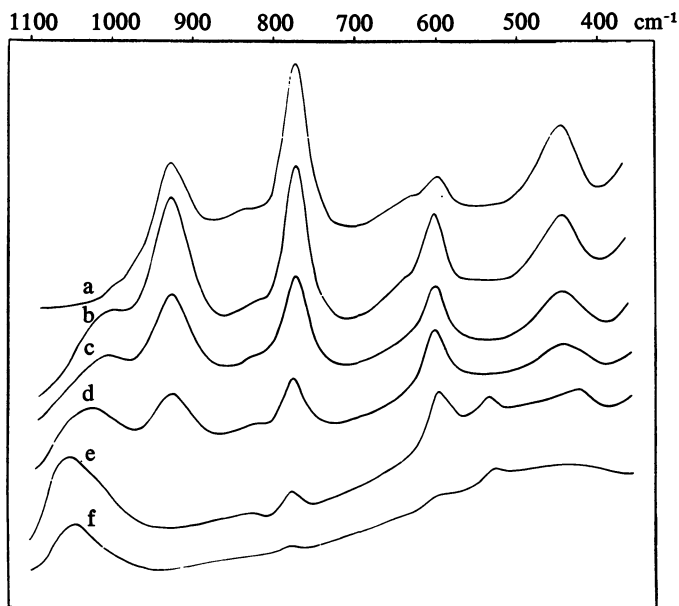


Figure 1. Raman spectra of aqueous solutions of 2.5 M Na_2SiO_3 , 4 M NaOH, pH 14 (a); 2.5 M Na_2SiO_3 , 0.5 M NaOH, pH 13.4 (b); 2.5 M Na_2SiO_3 , pH 13.3 (c); 2.5 M Na_2SiO_3 , 1.25 M HCl, pH 13 (d); 2.5 M Na_2SiO_3 , 2.5 M HCl, pH 12.5 (e); 2.5 M Na_2SiO_3 , 3.75 M HCl, pH 11.5 (f). (Reproduced, with permission, from Ref. 16. Copyright 1978, Multiscience Publications Ltd.)

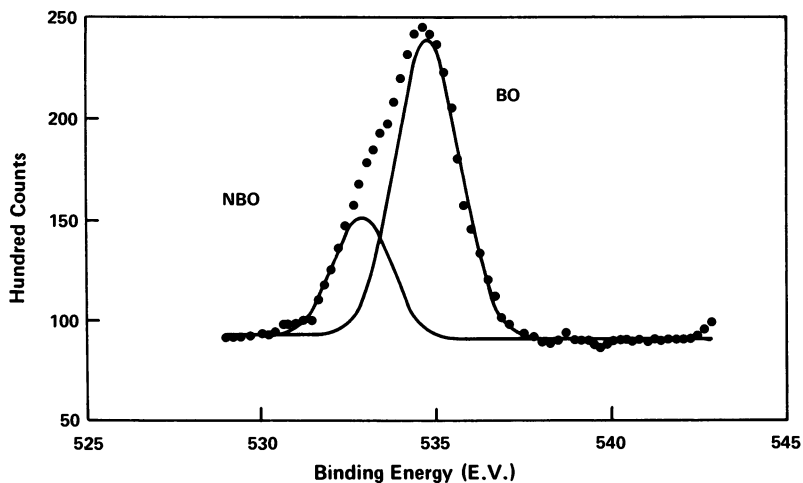


Figure 2. Binding energy (eV). ESCA $\text{O}(1s)$ spectrum of a sodium silicate glass, 30% Na_2O + 70% SiO_2 . (Reproduced, with permission, from Ref. 18. Copyright 1979, North-Holland Publishing Co.)

shift is less pronounced at higher sodium concentration, indicating a trend toward energy equivalence of the non-bridging and bridging oxygens (19). These ESCA data are complemented by high resolution X-ray fluorescence spectroscopic results which show a decrease in the average strength of silicon-oxygen bonds (20) and a relative decrease of positive charge on silicon atoms (21) with increasing sodium concentration. These trends were monitored by observing chemical shifts in silicon K X-ray lines.

The effect of hydration on hydrogen and sodium distribution in alkali silicate glasses has been studied by sputter induced photon spectroscopy (SIPS) and by infrared reflection and transmission spectroscopy (22, 23). SIPS is a relatively uncommon but powerful technique which involves measuring the intensity of characteristic emission lines of molecular and atomic fragments sputtered from the surface of materials. Its advantages as a surface technique lie in the ability to detect hydrogen (unlike ESCA or Auger spectroscopy) and neutral species (unlike SIMS). Using this technique Houser, et al., were able to determine that in silicate glass hydrated at 30° for one hour hydrogen had diffused inward from the surface for a distance of 2 μm , with accompanying depletion of sodium in this layer. Figure 3 shows the depth profile of hydrogen and sodium in a $\text{Na}_2\text{O}\cdot 3\text{SiO}_2$ glass under these conditions (22). The presence of a broad band in a thin film of hydrated silicate at 3360cm^{-1} was interpreted by Doremus (23) as indicating the presence of hydronium ions. He also observed in reflection spectra of hydrated silica glass a decrease of the 950 cm^{-1} band intensity, assigned to the Si-O M^+ stretching vibration and a major increase in the Si-O-Si stretch at $1050\text{--}1100\text{ cm}^{-1}$. He attributed these changes to the formation of a porous gel layer produced by hydrolysis of the surface layer.

It is likely that further applications of sophisticated instrumentation to analysis of silicates will appear in future literature. In addition to ESCA, SIPS, X-ray spectroscopy, laser Raman and dispersive infrared spectroscopy, newer techniques such as Fourier transform infrared and photoacoustic spectroscopy may be used as tools to characterize silicate structure.

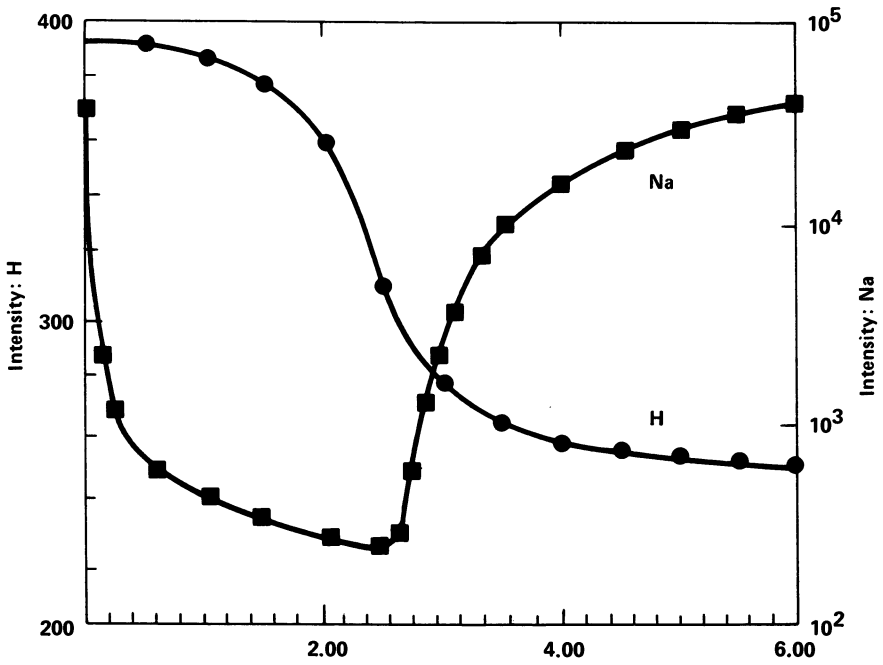


Figure 3. Depth profiles of H and Na in a $\text{Na}_2\text{O} \cdot 3\text{SiO}_2$ glass after hydration of 1 h at 30°C . The intensities of both H and Na are expressed in photon counts/s. (Reproduced, with permission, from Ref. 22. Copyright 1980, North-Holland Publishing Co.)

Literature Cited

1. Chemical and Engineering News, 54, May 4, 1981.
2. J. G. Vail, "Soluble Silicates", Vols. 1 and 2, Reinhold, New York (1952).
3. N. A. Tananaeff and A. K. Babko, Z. anal. Chem., 82, 145 (1930).
4. I. A. Voinovitch, J. Debras-Guedon and J. Louvrier; "The Analysis of Silicates", Herman; Paris (1965).
5. J. D. H. Strickland, JACS 74, 862 (1952).
6. S. W. Babulak and L. Gildenberg, JAOCs 50, 296 (1973).
7. R. K. Iler, "The Chemistry of Silica", John Wiley; New York (1979).
8. C. Manoliu, B. Tomi, A. Daescu and T. Petru, Rev. Chim., 24, 639 (1973).
9. K. Govindaraju, G. Mevelle and C. Chouard, Anal. Chem. 48, 1325 (1976).
10. W. W. Fletcher, Glass Technology, 17, 226 (1976).
11. H. Strauss and R. Rutkowski, Silikattechnik, 29, 339 (1978).
12. E. Van Dalen and L. G. Ward, Anal. Chem. 45, 2248 (1973).
13. L. Kovar, private communication (1979).
14. H. Small, T. S. Stevens and W. C. Bauman, Anal. Chem. 47, 1801 (1975).
15. H. Verweij, H. Van den Boom and R. E. Breemer, J. Am. Cer. Soc., 60, 529 (1977).
16. A. Marinangeli, M. A. Morelli, R. Simoni and A. Bertoluzza, Can. J. Spectroscopy 23, 173 (1978).
17. W. C. Beard, 3rd International Symposium on Molecular Sieves, 162 (1973).
18. J. S. Jen and M. R. Kalinowski, J. Non Cryst Solids, 38, 21 (1979).
19. R. Bruckner, H. W. Chun, H. Goretzki and M. Sammet, J. Non Cryst. Solids, 42, 49 (1980).
20. S. Sakka and A. Senga, J. Mat. Sci., 13, 505 (1978).
21. T. Maekawa, N. Kikuchi, S. Sumita and T. Yokokawa, Bull. Chem. Soc. Japan, 51, 780 (1978).
22. C. A. Houser, J. S. Herman, I. S. T. Tsong and W. B. White, J. Non Cryst. Solids, 41, 89 (1980).
23. R. H. Doremus, J. Non Cryst. Solids, 41, 145 (1980).

RECEIVED March 2, 1982.

Current Regulatory Status of Soluble Silicates

J. G. BLUMBERG and W. L. SCHLEYER

The PQ Corporation, Research and Development Center, Lafayette Hill, PA 19444

Federal agency promulgations authorizing or affecting the soluble silicates are compiled. Their safety has been extensively reviewed. For cautionary labeling, it is industry practice to group commercial soluble silicate products into three hazard classes. Occupational exposure limits vary similarly with alkalinity. The warning language for consumer products, notably household detergents, may be affected by the type and quantity of their soluble silicate content. Soluble silicates have both GRAS and additive regulation status for food uses. As inert ingredients, sodium silicate and metasilicate are exempt from the requirement of a pesticide residue tolerance. They are also classed as active pesticidal ingredients and thereby exposed to inappropriate generic regulation. Only highly alkaline forms of sodium silicate are regulated as hazardous materials for transportation purposes and, when discarded, are classified as hazardous waste. Except to that extent, soluble silicates are not hazardous substances under spill regulations. The proposed Preliminary Assessment Information Rule under TOSCA included soluble silicates. For inventory reporting purposes, currently available sodium silicates are three "chemical substances." The environmental-regulatory profile of soluble silicates provides incentive for their preference over more hazardous and more highly regulated alternate materials.

Safety Reviews

High tonnage production combined with consumer related uses in food and detergents have occasioned extensive reviews of the long-range safety of sodium silicate. Both in the environment and in the body, it degrades to silica which is indistinguish-

able from naturally occurring forms. Furthermore, it has a long history of production and safe use. Therefore, it is not surprising that little need has been seen to confirm the absence of chronic health effects by thorough laboratory studies. The recent commercialization of laundry detergent containing zeolite A has, in effect, added to the available information, because sodium silicate forms when zeolite A breaks down (1).

A comprehensive review of sodium and potassium silicate was conducted by the Select Committee on GRAS Substances of the Life Sciences Research Office, Federation of American Societies for Experimental Biology (FASEB) for the Food and Drug Administration. It was concluded that

"there is no evidence in the available information on ... potassium [and] sodium silicate that demonstrates or suggests reasonable grounds to suspect a hazard to the public when they are used at levels that are current or that might reasonably be expected in the future" (2).

The evaluation was based in part on a scientific literature review with 544 references, sponsored by the Food and Drug Administration (3).

The International Joint Commission (U.S.-Canada) under the Great Lakes Water Quality Agreement undertook a safety review of detergent builders which encompassed both human health and environmental aspects. The Task Force on the Health Effects of Non-NTA Detergent Builders of the IJC's Great Lakes Science Advisory Board concluded that "the use of sodium silicate in detergents poses no hazard to man" (4). A separate Task Force on the Ecological Effects of Phosphate Replacements has not yet issued a report, but it is understood to have concluded that there is no cause for concern (5).

Sodium and potassium silicate are the soluble silicates of commercial importance. For potassium silicate, not nearly as extensive data from the laboratory or from human experience are available. The assumption of its similarity to sodium silicate in health and environmental effects appears to be valid, for an equivalent mole ratio of SiO_2 to alkali metal oxide.

Although soluble silicates are produced from quartz sand, they do not contain detectable amounts of crystalline silica. All evidence points to the moderate to strong alkalinity of soluble silicates as the sole source of a potential hazard to human health or environment. The regulatory controls currently in effect stem either from this acute hazard or from their use in regulated applications. The entire regulatory spectrum is described here, insofar as it would concern processors or users of soluble silicates in the United States.

Workplace

Although chemical hazard communication has been of concern

to the Occupational Safety and Health Administration of the U.S. Department of Labor (OSHA) since its inception in 1972, cautionary labeling of industrial chemicals remains to this day a voluntary industrial practice. The most widely used system is set forth in ANSI Standard Z129.1-1976 (6). The standard defines hazard classes and specifies the applicable label language. By these criteria, the silicates constitute three different hazard classes because rising alkalinity increases the severity of the hazard. Since silicates are good buffers, their $\text{SiO}_2/\text{Na}_2\text{O}$ ratio is a far more important determinant of the degree of alkalinity than is their concentration level.

Commercial sodium silicate liquids of 2.0 ratio or greater and dry sodium silicate of at least 2.4 ratio constitute the least hazardous group: they cause eye and skin irritation. Sodium metasilicate, sodium orthosilicate and 1.6 ratio sodium silicate liquids fall into the class of highest hazard: they are corrosive, i.e., cause eye and skin burns. The intermediate hazard class consists of dry silicates and liquids between the other two classes in ratio, which are considered corrosive to the eye but not to the skin. Typical industrial labels for a representative sodium silicate product from each hazard class are shown in Figs. 1-3.

Since commercial potassium silicate products range in $\text{SiO}_2/\text{K}_2\text{O}$ mole ratio only from approximately 2.5 to 3.9, all fall into the lowest hazard class: they are eye and skin irritants.

Although OSHA Form 20 or one approved as essentially similar is mandatory only in the maritime trades (7), it has become customary throughout the chemical industry to obtain or prepare a material safety data sheet before a new chemical enters a workplace. For products in the same industrial hazard class the information provided on the material safety data sheet is the same, except as modified by differences in physical properties. For example, the spill removal instructions for liquids are different from those for solids. Figs. 4a and 4b show a material safety data sheet for a dry, powdered sodium silicate in the lowest hazard class.

Word processing equipment is very useful for maintaining and providing this information, as well as for recording and retrieving those who received it. It may be noted that the sheet contains more than occupational safety data. It includes spill response and TOSCA data as well. It is evolving into a safety and regulatory data sheet.

There are no specific OSHA exposure standards for sodium or potassium silicate. Depending on rate of solution and degree of alkalinity of airborne materials, a prudent industrial exposure standard could range from the permissible exposure limit (PEL) for inert or nuisance particulates up to nearly the PEL for sodium hydroxide.

WARNING!
CAUSES IRRITATION

Avoid contact with eyes, skin, and clothing.
Wash thoroughly after handling.
Wash contaminated clothing before re-use.

FIRST AID: In case of contact, immediately flush eyes with plenty of water for at least 15 minutes. Call a physician.
Flush skin with water.

SPILLAGE: Mop up and flush to sewer with plenty of water.

FOR INDUSTRIAL USE ONLY
COVER WHEN NOT IN USE
PROTECT FROM FREEZING

Figure 1. Sodium silicate cautionary label, least hazardous class.

DANGER!
CAUSES EYE AND SKIN BURNS

Do not get in eyes, on skin, on clothing.
Avoid breathing mist.
Keep container closed.
Use with adequate ventilation.
Wash thoroughly after handling.
Do not take internally.
When handling, wear goggles or face shield.
Wash contaminated clothing before re-use.

FIRST AID: In case of contact, immediately flush eyes or skin with plenty of water for at least 15 minutes while removing contaminated clothing and shoes. Call a physician.

ANTIDOTE: If swallowed, do NOT induce vomiting. Give large quantities of water. Give at least one ounce of vinegar in an equal amount of water. Never give anything by mouth to an unconscious person. Call a physician.

SPILLAGE: Mop up and flush to sewer with plenty of water.

Figure 2. Sodium silicate cautionary label, most hazardous class.

DANGER!
CAUSES EYE BURNS, CAUSES SKIN IRRITATION

Do not get in eyes, on skin, on clothing.
Avoid breathing mist.
Keep container closed.
Use with adequate ventilation.
Wash thoroughly after handling.
Do not take internally.
When handling, wear goggles or face shield.
Wash contaminated clothing before re-use.

FIRST AID: In case of contact, immediately flush eyes with plenty of water for at least 15 minutes. Call a physician. Flush skin with water.

ANTIDOTE: If swallowed, do NOT induce vomiting. Give large quantities of water. Give at least one ounce of vinegar in an equal amount of water. Never give anything by mouth to an unconscious person. Call a physician.

SPILLAGE: Mop up and flush to sewer with plenty of water.

Figure 3. Sodium silicate cautionary label, intermediate hazardous class.

SECTION 1. IDENTIFICATION OF PRODUCT

MANUFACTURER: PQ CORPORATION
ADDRESS: 11 EXECUTIVE MALL, P.O. BOX 840, VALLEY FORGE, PA 19482
EMERGENCY TELEPHONE NUMBER: (215) 293-7200
SALES NAME: BRITESIL C-24^B sodium silicate
CHEMICAL NAME: Silicic acid, sodium salt*
TOSCA CAS REGISTRY No.: 1344-09-8
DOT HAZARD CLASS: N.A.
DOT SHIPPING NAME: N.A.

SECTION 2. PHYSICAL DATA

APPEARANCE & ODOR: Aquamarine glassy lumps, white granules, or white powder.
 Odorless.
SPÉCIFIC GRAVITY (liquids only): N.A.
SOLUBILITY IN WATER: Complete.
VAPOR PRESSURE (mm Hg at °F, nonaqueous liquids only): N.A.
EVAPORATION RATE (Butyl acetate = 100, nonaqueous liquids only): N.A.
SOLIDS CONTENT (solutions dispersions, or pastes only): N.A.
BOILING POINT (°F, nonaqueous liquids only): N.A.
VAPOR DENSITY (nonaqueous liquids only): N.A.
pH (aqueous liquids only): N.A.

SECTION 3. FIRE AND EXPLOSION HAZARD DATA

FLASH POINT (°F): N.A.
FLAMMABLE LIMITS (vapor in air, Vol. %): N.A.
FIRE EXTINGUISHING MEDIA: N.A.
SPECIAL FIRE FIGHTING PROCEDURES: N.A.
UNUSUAL FIRE AND EXPLOSION HAZARDS: None

SECTION 4. REACTIVITY DATA

STABILITY: Stable
CONDITIONS TO AVOID: N.A.
INCOMPATIBILITY (Materials to Avoid): N.A.
HAZARDOUS DECOMPOSITION PRODUCTS: None

N.A. = Not Applicable

* Includes other hazard classes, to which different safety data sheets apply.

Figure 4a. Material safety data sheet; high ratio powders, side 1.

SECTION 5. SPILL OR LEAK PROCEDURES

SPILLAGE: Sweep, scoop, or vacuum discharged material. Flush residue with water. Observe environmental protection regulations.

WASTE DISPOSAL METHOD: Neutralize with dilute acid and landfill solids according to local, state, and federal regulations. Flush neutral liquid to sewer with plenty of water.

SECTION 6. HEALTH HAZARD DATA

EYE CONTACT Causes irritation.

SKIN CONTACT: Causes irritation.

INHALATION: Dust may irritate respiratory tract.

FIRST AID PROCEDURES: In case of contact, immediately flush eyes with plenty of water for at least 15 minutes. Call a physician. Flush skin with water. **MEDICAL EXAMINATIONS:** N.A.

SECTION 7. SPECIAL PROTECTION INFORMATION

RESPIRATORY PROTECTION: Use NIOSH approved dust respirator where dust occurs.

GLOVES: Rubber where contact likely.

EYE PROTECTION: Chemical goggles and/or face shield.

OTHER PROTECTIVE EQUIPMENT: Safety shower and eyewash fountain should be within direct access.

PERSONAL HYGIENE: Avoid contact with eyes, skin, and clothing. Wash thoroughly after handling. Wash contaminated clothing before re-use.

ENGINEERING CONTROL: N.A.

SECTION 8. SUBSTANCES FOR WHICH STANDARDS HAVE BEEN SET

SINGLE CHEMICAL SUBSTANCE: N.A. **COMPONENTS:** N.A.
Percent: N.A. Percent: N.A.

OSHA Exposure Limit: N.A. **OSHA Exposure Limit:** N.A.

EXPOSURE ANALYSIS METHODS: N.A.

SECTION 9. SOURCE OF INFORMATION

Walter L. Schleyer Gov't & Industry Relations Manager Date: 7/17/79

N.A. = Not Applicable

Figure 4b. Material safety data sheet; high ratio powders, side 2.

Publication Date: June 1, 1982 | doi: 10.1021/bk-1982-0194.ch003

Consumer Products

Years ago, sodium metasilicate was the only readily soluble sodium silicate available in dry form. It was used in dry blended home laundry detergents and in automatic dishwasher detergents. When low-phosphate and phosphate-free detergents first came on the market, some of them carried an increased metasilicate content, and concern arose about their safety in the home. Although sodium metasilicate is corrosive to biological tissue, this is not necessarily true of detergents in which it is an ingredient. Among determining factors are the amount used, its particle sizing, the processing method, and the modifying effect of other ingredients.

The Consumer Product Safety Commission has recognized this. It has established labeling criteria based on the results of biological testing, as specified under the Federal Hazardous Substances Act. If the product contains 15% sodium metasilicate or more and if no animal test data to the contrary are available, inspectors are instructed to require "DANGER! MAY CAUSE BURNS" on the label. Less severe warning language is specified for lower metasilicate content and less strongly alkaline types of silicate ingredients (8). Both the animal test methods (9) and the caution label language are currently under review within the agency and its Toxicological Advisory Board.

Readily soluble but less strongly alkaline hydrous sodium polysilicate materials have long since been available as ingredients of dry blended detergents. Unlike sodium metasilicate, these fall into the intermediate or lowest silicate label hazard class, depending on their $\text{SiO}_2/\text{Na}_2\text{O}$ ratio. The household hazard is correspondingly reduced. The bulk of household detergents is spray dried from slurries which comprise a sodium silicate solution. The finished product then consists of homogeneous beads, and not of discrete particles of its components, usually resulting in lesser hazard characteristics.

Food Uses

We begin with a glossary of the terms by which the regulatory status of food ingredients is defined. To be used in food, a chemical substance must be either a "food additive" or "Generally Recognized As Safe (GRAS)" or "prior sanctioned." Each food additive and its uses is described by an FDA regulation (10), issued in response to a food additive petition which was supported by full reports of investigations into its safety.

A GRAS substance is "generally recognized, among experts qualified by scientific training and experience to evaluate its safety, as having been adequately shown through scientific

procedures to be safe under the conditions of its intended use"(11).

A "prior sanctioned" substance is one which is used in accordance with a sanction or approval granted prior to enactment of the 1958 Food Additive Amendments to the Federal Food, Drug and Cosmetic Act (11).

Today the scientific evidence required to show GRAS status is equal in extent to the documentation which must be submitted in support of a food additive petition (12). However, there is a grandfather clause in the case of a substance used in food prior to January 1, 1958: safety may be shown either through scientific procedures or through experience based on common use in food (11).

In 1973 FDA embarked on its GRAS review process, under which chemicals "Generally Recognized As Safe" are being reexamined for safety. Those affirmed will be codified, that is, listed in Title 21 of the Code of Federal Regulations (13). Those not affirmed will no longer be considered GRAS by FDA, so that an approved food additive petition will be required for their use in food (14).

Examples of substances which are regarded as GRAS already appear in the Code (15), but many more are presently unpublished. Unpublished GRAS status can arise from an FDA opinion letter in response to an inquiry or from a determination by industry that a substance is GRAS. FDA bears the burden of proof that such a substance is not GRAS (16).

Specifications for food chemicals are to be found in the Food Chemicals Codex (17). This compendium is prepared by the Food and Nutrition Board of the National Research Council. It contains monographs of many food chemicals and is recognized by the Food and Drug Administration as defining their "appropriate food grade" within the meaning of FDA regulations (12,18).

The use of sodium silicate for preserving eggs apparently escaped government scrutiny by timely obsolescence. The use of sodium silicate as a corrosion inhibitor in drinking water was passed on affirmatively by the Surgeon General of the Public Health Service in 1937 (19). In the early 1960s FDA issued a series of opinion letters stating that sodium silicate up to 100 ppm would be "generally recognized as safe" in canned drinking water as well as in other potable water systems (2). Later its use was mandated by a federal military specification for canned emergency drinking water (20), since sodium silicate remained the only additive acceptable to the Food and Drug Administration.

Because of this unpublished GRAS status, sodium and potassium silicates were included in the GRAS Review process. In 1979 the Select Committee on GRAS Substances issued an affirmative report (2) [see Safety Reviews above] and industry submitted proposed food grade specifications, but the regulatory process has not yet reached Federal Register publication. Sodium and potassium silicate and sodium metasilicate monographs

have also been proposed for inclusion in the Food Chemicals Codex.

Sodium silicate has published GRAS status as a substance migrating to food from paper and paperboard products used in food packaging (21), and from cotton and cotton fabrics used in dry food packaging (22). These are indirect food uses.

Sodium silicate has regulation status as a boiler water additive in the preparation of steam that will contact food (23); in zinc-silicon dioxide matrix coatings (24); and as a constituent of cellophane used for packaging food (25).

Sodium metasilicate, although merely one species of sodium silicate, has a regulatory identity of its own, perhaps because of its crystalline form and stoichiometric nature. It has unpublished GRAS status for fruit and vegetable washing (26,29), as a refining agent for edible rendered fats (26); as a peeling solution for peaches (27); and as a component of sanitizing solutions intended for use on food contact surfaces (29). It entered GRAS review as a separate entity.

The Select Committee, in a 1977 tentative report (26), did not pass on its safety, feeling it had insufficient information. FDA then commissioned a literature review (28), and, in a 1981 final report, the Select Committee recommended Class I status for sodium metasilicate to the FDA. This was expressed in analogy to the statement on sodium and potassium silicates, quoted on page 2 (29). Codification, the final step in the GRAS affirmation process, could be another two years away.

Sodium metasilicate has food additive regulation status as boiler water additive in the preparation of steam that will contact food (23). In addition it is believed to be "prior sanctioned" under the Meat Inspection Act for hog scalding and tripe denuding.

The U.S. Department of Agriculture's Food Safety and Quality Service has original jurisdiction under the Federal Meat Inspection Act and the Poultry Products Inspection Act. It has approved sodium metasilicate as cooling and retort water treatment agent, as tripe denuding agent, and as hog scald agent (30). Sodium ortho and sesqui silicates are similarly approved.

Based on USDA's and FDA's regulatory schemes, the Meat and Poultry Inspection Program, Animal and Plant Health Inspection Service of the U.S. Department of Agriculture has approved specific sodium silicate and/or sodium metasilicate products as general cleaning agents for food contact surfaces, for treating boiler and cooling system water, as water conditioner, as wetting agent for use in poultry scald vats, in hog scalding and tripe denuding, and to wash fruit and vegetables that are to become ingredients of poultry, meat, rabbit and egg products (31). The difference in regulatory structure is that FDA and USDA rules set generic standards, whereas the Meat and Poultry Inspection Program must authorize every single commercial product of each supplier, including proprietary mixtures, before its admission to a federally inspected food packing plant.

Recently the Safe Drinking Water Act transferred jurisdiction for potable water, other than water used in food and bottled water, from the FDA to the Environmental Protection Agency. EPA is planning a control program for water treatment chemicals and, in a memorandum of agreement with FDA, announced (32) that it had contracted with the National Academy of Sciences to develop a compendium of approved substances and specifications, comparable to the Food Chemicals Codex. No chemicals have so far become known to have been selected for inclusion. Historically, the use of sodium silicate, and of activated silica sol prepared from sodium silicate, for treating public water supplies has been authorized by public health agencies on the state level.

The amount of soluble silicates consumed in regulated food uses is small compared to the tonnage consumed in the cleaning of food contact surfaces. Since it is considered that there is no residue of cleaning agents when the surfaces have been rinsed with potable water, the detergent uses are unregulated. Recognition of the safety of the soluble silicates in food is considered important because of the eventuality that utensil cleaning agents would some day be regulated as chemical food ingredients.

Pesticide Formulations

Sodium silicate and sodium metasilicate are exempt from the requirement of a residue tolerance in pesticide formulations applied to growing crops or to raw agricultural commodities after harvest (33).

The detergency builder and buffering characteristics of sodium silicate and metasilicate have led to their inclusion in about 480 EPA-registered detergent sanitizer products. Relying apparently on an historical master list of substances for which pesticidal activity had ever been claimed by any applicant for a pesticide registration, EPA regards the silicates as active ingredients whenever they are part of a pesticide formulation. In most if not all such formulations, silicate performs as an adjuvant and has no antimicrobial activity of its own at use concentration. Therefore it does not meet FIFRA (34) definition of a pesticide.

With pesticide regulation tightened in recent years, the presence of soluble silicates on EPA's pesticide actives master list threatens its indiscriminate regulation, along with many other common industrial chemicals of low hazard potential. A control program (35) directed at technical actives not hitherto subject to pesticide regulation, such as kepone, should not be purposely or inadvertently extended to multi-purpose commodity chemicals which are already regulated under the Toxic Substances Control Act (TOSCA). Examples of inappropriate uses of the

entire list for regulatory purposes are: a proposed scheme for recordkeeping, reporting and pesticide manufacturing establishment registration (36); and a possible generic OSHA standard for occupational exposure to pesticides during manufacture and formulation (37).

It has been reported in newsletters that EPA plans to remove at least 114 chemicals, including the soluble silicates, from active pesticidal ingredient status, but no official action has as yet been taken.

Transportation

Sodium silicate liquids of 1.6 $\text{SiO}_2/\text{Na}_2\text{O}$ ratio or less and sodium orthosilicate meet the criteria (38) for regulation as corrosive materials for purposes of transportation. As neither substance is listed specifically in the DOT Hazardous Materials Table (39), the proper shipping names are, respectively, alkaline (corrosive) liquid, n.o.s. and corrosive solid n.o.s. DOT regulations prescribe the proper manner of packaging (38), preparing shipping papers, marking, labeling (with the diamond-shaped label bearing the "corrosive" legend and symbols), and vehicle placarding (40).

"Limited quantities" in surface transportation are exempt from many of these requirements (41). More stringent rules apply to transportation by air (42), where a further distinction as to net quantity limit in a single package is made between passenger-carrying and cargo-only aircraft. Only the DOT rules which are generic to corrosive materials apply to those soluble silicates of very high degree of alkalinity. Hence, they are mentioned as being applicable, but not explained further.

As discussed in the next section, certain sodium silicate liquids which do not meet DOT criteria for a corrosive liquid are hazardous waste under RCRA when discarded. These are DOT-regulated as ORM-E (43). Similarly, the dry blends which are identified in the next Section as EPA hazardous substances because of their sodium hydroxide content are DOT-regulated as ORM-E, if they contain the reportable quantity of 1,000 lb. NaOH in a single package or bulk container.

Pollution and Waste Control

The effluent limitation guidelines governing users of soluble silicates are determined by their standard industry classification (SIC Number). It may be noted that the sodium silicate subcategory of the Inorganic Chemicals Manufacturing Industry has been excluded from further rulemaking under the National Resources Defense Council v. Costle consent decree because of the absence or virtual absence of 65 toxic pollutants from the industry's effluents (44). Because of high temperature manufacturing processes, aqueous media and high insolubility of

the silicates of most metals, the commercial soluble silicates are generally low in both organic and inorganic impurities. Typical values are shown in Table I.(45). Their range represents eleven producing points which are located throughout the United States and employ different manufacturing processes.

The soluble silicates are not designated as hazardous substances under Section 311 of the Federal Water Pollution Control Act, relating to discharges or spills into navigable waters (46). However, some commercial sodium orthosilicate products are actually physical blends of sodium hydroxide and sodium metasilicate particles. Such mixtures are EPA hazardous substances by virtue of their sodium hydroxide content, and their reportable quantity is the equivalent of 1,000 lbs of sodium hydroxide (47).

In terms of the Resource Conservation and Recovery Act of 1976 (RCRA) sodium silicate is not among certain chemicals which have been designated as rendering a waste hazardous (48). However, a waste is also classified as hazardous if it exhibits certain characteristics (49). One of these is corrosivity. On the alkaline side, corrosivity is defined by a pH equal to or greater than 12.5, provided the waste is aqueous (50).

We have measured the pH of various sodium silicate solutions by EPA's reference method. According to our results, sodium silicate solutions have a pH of 12.5 or greater when

- a. regardless of concentration, the $\text{SiO}_2/\text{Na}_2\text{O}$ weight ratio is less than 2.0; and
- b. the $\text{SiO}_2/\text{Na}_2\text{O}$ ratio is equal to 2.0 and the solids concentration is approximately 44% or greater.

Below that concentration and at all concentrations above 2.0 ratio the pH remained below 12.5.

On November 17, 1980, EPA proposed to grant a permit-by-rule to operators of "elementary neutralization units," defined as devices that are used for neutralizing wastes which are hazardous wastes only because they exhibit the corrosivity characteristics. Pending completion of this rulemaking, EPA has suspended its permit requirements for eligible operators. As a result, operators of "elementary neutralization units" no longer need RCRA permits on a case-by-case basis, only a registration number (51).

When sodium silicate solutions at or above pH 12.5 become wastes, they are "hazardous wastes only because they exhibit the corrosivity characteristic." Consequently, their dilution or neutralization in accordance with EPA's operating conditions does not require an individual RCRA permit provided, of course, they are not part of an industrial waste stream which has been designated as hazardous (52). It should be noted that, as of this writing, the permit requirement is only suspended, and the permit by rule is not yet in effect. Current EPA regulations should be reviewed concerning further developments and concerning all other applicable requirements.

If a highly alkaline sodium silicate waste is classified as a hazardous waste under RCRA, it is also a hazardous substance under the Comprehensive Environmental Response, Compensation and Liability Act of 1980 (CERCLA or Superfund Act). The law's reporting requirements would apply to any release into the environment. This is also true for the previously mentioned sodium orthosilicate products which are EPA hazardous substances, since they are physical mixtures containing sodium hydroxide. For sodium hydroxide the reportable quantity remains 1,000 lb. Until rules to implement the act are published, the reportable quantity of a corrosive waste is 1 lb.

Toxic Substances Control Act

Following Chemical Abstract Service terminology, the commercial soluble silicates were reported to the initial inventory of existing chemical substances as indicated in Table II.

Under the reporting rules (53), a hydrated chemical was to be regarded as a mixture, and the anhydrous substance was to be reported.

The only subsequent regulatory development thus far under TOSCA, directed specifically at soluble silicates, was a proposed rule (54) under Section 8(a) which would require manufacturers to keep certain records and report production and exposure related data on approximately 2300 chemicals to EPA. This information was held to be necessary to rank chemicals for investigation and to make preliminary risk assessments. Sodium silicate, potassium silicate, sodium metasilicate and sodium orthosilicate were included on the candidate list, presumably because reports to the initial inventory showed them to be manufactured in high tonnage volume.

It is now understood that the list has been pared down to about 300 chemicals. In view of the public availability of previous health hazard assessments by FDA, IJC and others, which has been pointed out to EPA in comments on its proposal, it is expected that the soluble silicates are among the chemicals which have been slated to be eliminated from the list.

Discussion

It has been seen that even relatively simple and familiar chemicals like the soluble silicates have become quite extensively involved in the various regulatory schemes designed to protect our health and environment. The reason is their high tonnage production and their broad distribution, ranging from industrial plants to the home.

The soluble silicates are truly recycled by man: they derive entirely from mineral deposits and are returned to the

Table I. Typical Impurity Levels in Commercial Sodium Silicates (ppm, ppb where noted)

F	6.7-9.5	Cl	130-1900	SO ₄	<160-1700
N	0.1-44	As	<1	Hg	<0.3-2.5ppb
Pb	0.2-0.6	Cu	<0.6-1.1	Cd	<10-21ppb
Fe	36-120	Mg	4-26	Ca	<1-76
Al	50-220	P	<18	V	<0.3-0.8
Cr	<0.3-10	Ni	<0.3	Co	<0.3
Zn	<0.6-2.8	Bi	<25	Sr	<0.2-1.5
Ba	<0.2-2.8	Mn	0.1-1.8	Sn	<60
Sb	<15	Se	<20		

Table II. Soluble Silicates as Reported to TOSCA Inventory

COMMON NAME	CAS Reg. No.	CAS INDEX NAME
Sodium Silicate	1344-09-8	Silicic acid, sodium salt
Sodium meta-silicate	6834-92-0	Silicic acid (H ₂ SiO ₃), disodium salt
Sodium sesqui-silicate	15,593-82-5	Silicic acid (H ₆ Si ₂ O ₇), hexasodium salt
Sodium ortho-silicate	13,472-30-5	Silicic acid (H ₄ SiO ₄), tetrasodium salt
Potassium silicate	1312-76-1	Silicic acid, potassium salt

natural cycles of their components. The principal deviation from common naturally occurring forms is a transitory rise in alkalinity, in order to increase the solubility of silica. This moderate to strong alkalinity constitutes an acute hazard potential and is their sole recognizable source of hazard.

These safety characteristics and the resulting comparatively low regulatory profile furnish incentives for preferring the soluble silicates over more hazardous and more highly regulated alternate materials.

LITERATURE CITED

1. Health Implications of Non-NTA Detergent Builders
International Joint Commission, 1980, 59.
2. Select Committee on GRAS Substances, Evaluation of the Health Aspects of Certain Silicates as Food Ingredients, SCOGS-61, NTIS Pb 301-402/AS, 1979
3. Scientific Literature Reviews on Generally Recognized as Safe (GRAS) Food Ingredients - Silicates, Tracor-Jitco, Inc., September 1973, National Technical Information Service, PB-228-554
4. International Joint Commission, Health Implications of Non-NTA Detergent Builders, 1981, 45
5. Private communication from the industry liaison member
6. American National Standard for the precautionary labeling of hazardous industrial chemicals. American National Standards Institute, Inc., 1430 Broadway, NY, NY 10018
7. 29 C.F.R. 1915.57
8. Consumer Product Safety Commission, Hazardous Substances Labeling Guide, Doc. #9010.125, November 15, 1975
9. 16 C.F.R. 1500.41 and 1500.42
10. 21 C.F.R. Parts 170-178
11. Federal Food, Drug & Cosmetic Act, as amended, 201(s)
12. 21 C.F.R. 170.30 (b)
13. 21 C.F.R. Part 184 for direct food substances and
21 C.F.R. Part 186 for indirect food substances
14. 21 C.F.R. 170.35
15. 21 C.F.R. Part 182
16. 21 C.F.R. 170.38
17. Food Chemicals Codex, 3rd Edition, National Academy Press, Washington, D.C., 1981
18. *Ibid*, p. xxiii
19. Soluble Silicates, Their Properties and Uses, Vol. 2, American Chemical Society Monograph Series #116, Reinhold Publishing Corp. New York, 1952, 597.
20. Federal Specification MIL-W-15117D dated December 11, 1967, and Amendment 3 dated January 22, 1975
21. 21 C.F.R. 182.90
22. 21 C.F.R. 182.70
23. 21 C.F.R. 173.310

24. 21 C.F.R. 175.390
25. 21 C.F.R. 177.1200
26. Tentative Evaluation of the Health Aspects of Certain Silicates as Food Ingredients. 1977. Life Sciences Research Office, Federation of American Societies for Experimental Biology, Bethesda, MD 20014
27. Chemicals Used in Food Processing, Publication 1274, Food Protection Committee, Food and Nutrition Board, National Academy of Sciences/National Research Council, Washington, D.C., 1965, p. 46
28. Monograph on Sodium Metasilicate, Informatics, Inc., May 1978, National Technical Information Service, PB-287,766
29. Evaluation of the Health Aspects of Sodium Metasilicate and Sodium Zinc Metasilicate as Food Ingredients. 1981. Life Sciences Research Office, Federation of American Societies for Experimental Biology, Bethesda, MD 20014.
30. 9 C.F.R. 318.7 (c)(4)
31. List of Chemical Compounds Authorized for Use Under USDA Meat, Poultry, Rabbit, and Egg Products Inspection Programs, Supt. of Documents, U.S. Govt. Printing Office, Washington, D.C. 20402
32. 44 F.R., 42,775-778, July 20, 1979
33. 40 C.F.R. 180.1001 (c)
34. Federal Insecticide, Fungicide and Rodenticide Act, as amended, Sect. 2(a)
35. Federal Pesticide Act of 1978, Public Law 95-396, amending Sect. 7 of FIFRA
36. 45 F.R. 46,100-03, July 9, 1980
37. 43 F.R. 54,955, November 24, 1978; 45 F.R. 77,827, November 24, 1980
38. 49 C.F.R. 173.240
39. 49 C.F.R. 172.101
40. 49 C.F.R. Part 172
41. 49 C.F.R. 173.244
42. 49 C.F.R. 173.6
43. 49 C.F.R. 173.1300
44. 46 F.R. 9,459, January 28, 1981
45. PQ Corporation unpublished data
46. 40 C.F.R. Part 116
47. 40 C.F.R. Part 117
48. 40 C.F.R. 261.33(e) and (f)
49. 40 C.F.R. 261.3
50. 40 C.F.R. 261.22
51. 45 F.R. 76,076ff, November 17, 1980
52. 40 C.F.R. 261.31 and .32
53. 40 C.F.R. Part 710
54. 45 F.R. 13,646ff, February 29, 1980

RECEIVED March 8, 1982.

American Chemical
Society Library
1155 16th St. N. W.
Washington, D. C. 20036

Health, Safety, and Environmental Aspects of Soluble Silicates

W. L. SCHLEYER and J. G. BLUMBERG

The PQ Corparation, Research and Development Center, Lafayette Hill, PA 19444

The alkalinity of soluble silicates is their primary hazard. Contact exposure effects can range from irritation to corrosion. Inhaled or ingested sodium silicates are rapidly eliminated in the urine. Trace quantities of dissolved silica are essential to nutrition, but if normal dietary amounts are exceeded, siliceous urinary calculi may result. Dissolved silica is a minor but ubiquitous constituent of the environment. When dissolved silica becomes depleted in natural waters, diatoms are displaced by species that accelerate eutrophication. Commercial soluble silicates rapidly depolymerize upon dilution to molecular species indistinguishable from natural dissolved silica.

Soluble silicates have been known since ancient times, but it was not until the middle of the 19th Century that soluble silicates were produced on a commercial scale. In 1877, a 46-page pamphlet(1) was sufficient to encompass most of the knowledge about soluble silicates then available. By 1928, over 400 pages were required for Vail's first American Chemical Society Monograph on the subject(2). This monograph contained information on the amelioration of the adverse environmental effects of emissions from the now abandoned sulfate process for soluble silicate production(3), the use of soluble silicates in aqueous effluent treatment(4), and a short chapter on the physiological effects of soluble silicates(5).

In recent years, there has been an increasing emphasis on biological testing for the quantitative determination of environmental and health effects of chemical products and processes. But since biological testing is both time consuming and expensive, those who fund this type of research, government, industry, labor or academic organizations, tend to give higher priority for testing to newer chemicals about which little is

known, rather than test established chemicals, such as soluble silicates, with which there has been over a century of human experience. Nevertheless, there has been a limited amount of biological testing conducted on soluble silicates by government, industry and academic scientists. There have also been several critical evaluations of the available information on soluble silicates by expert groups impaneled to assess to the environmental or health risks of various uses of these substances.

The objective of this review is to draw together and briefly discuss the available information on the health, safety and environmental aspects of the soluble silicates. The sources of information for this review include scientific publications, reports of regulatory bodies and government agencies, and the incidental records of a corporation which has manufactured soluble silicates for over 120 years(6).

HEALTH AND SAFETY ASPECTS

Ingestion

Oral LD₅₀, the dose level where 50% of an exposed population of rats will die within a specified time, is a useful expression of the approximate magnitude of toxicity of a substance. It also provides a standard measure of comparison among many substances. The LD₅₀ values for sodium silicates in Table I and Figure 1 were compiled from the results of a number of studies. It should be noted that these studies were conducted at different times, and vary somewhat in their test conditions such as, length of observation period, and strain, number and sex distribution of the animals. Nevertheless, we believe the comparison is useful for the purpose of illustrating, in a general way, the influence of silicate composition on acute oral toxicity. Even a very closely controlled LD₅₀ study would not yield data from which conclusions could be drawn with greater certainty unless a great number of animals were used. Thus, in the lethal range of sodium silicates, large doses are required, and the 95% confidence intervals are on the order of 0.5 g/kg.

The autopsy results from the reported studies, acute gastroenteritis, vascular congestion, mottled livers(8), were consistent with nonspecific causes of death, e.g., changes in pH of body fluids, shock, chemical irritation or corrosion of the viscera, etc. It appears that the SiO₂/Na₂O ratio of sodium silicates has a greater influence on their toxicity than their concentration. This relation is perhaps not unexpected when it is considered in light of the sodium silicate's property of yielding aqueous solutions of relatively constant pH over a range of concentrations, while at constant concentration, pH varies inversely with ratio (see Figures 2 and 3).

In an attempt to develop a more specific test for modeling ingestion hazard than oral LD₅₀, the FDA conducted a series of

**Table I. Median Lethal Dose (Oral, Rat)
Sodium Silicate**

SiO ₂ /Na ₂ O wt. ratio	CONCENTRATION wt. percent	LD-50 g/kg	REFERENCE
-	-	>3	7.
3.2	36	3.2	8.
3	-	1.6-8.6	9.
2	-	1.3-2.1	9.
2.0	81	1.5-2.2	10.
2.0	81	1.6	11.
1.6	51	2.0-2.5	10.
1.0	99	0.6	11.
1.0	50	0.8	11.
0.7	61	1.5	10.
0.7	61	1.0	11.
0.5	90	0.5	10.

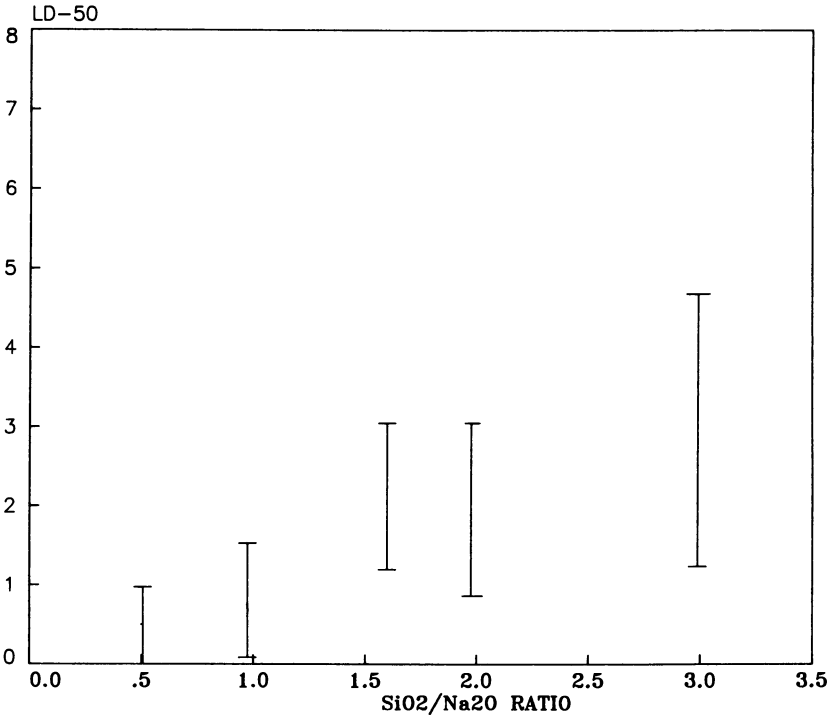


Figure 1. Ratio vs. LD₅₀ sodium silicate.

Publication Date: June 1, 1982 | doi: 10.1021/bk-1982-0194.ch004

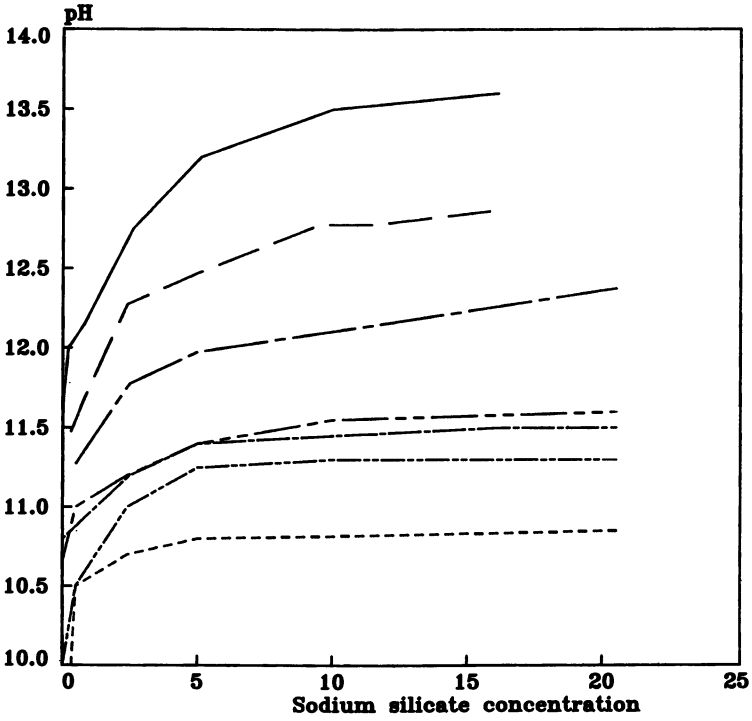


Figure 2. Concentration vs. pH. Key: ---, 3.7; - - - - - , 3.2; , 2.9; - . - . - , 2.5; - - - , 2.0; - - - - , 1.6; and ———, 1.0 ratio.

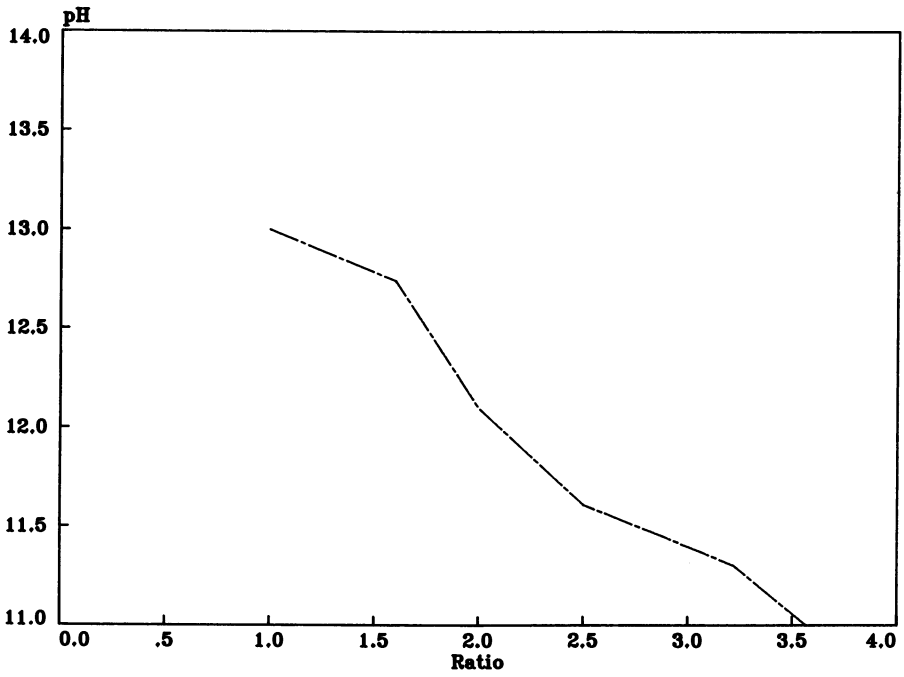


Figure 3. Ratio vs. pH.

tests using rabbits during the late 1960s and early 1970s. Initially a description of the findings upon macroscopic examination were the only results reported. Two samples of a 2.0 ratio sodium silicate powder (80% solids) and two samples of sodium metasilicate were tested at this time. "No lesions ..." and "submucosal edema" were noted in the animals exposed to 2.0 ratio sodium silicate, but "severe ulcer" and "active hyperemia" resulted from metasilicate exposure(12). In 1973, Bierbower,(13) reported on a series of similar tests, conducted under the auspices of the Consumer Product Safety Commission. Microscopic examination of the esophagus was used as the primary criterion for categorizing results as either "corrosive" or "negative." This data is summarized on Table II. The data indicate a correlation of hazard with ratio only at the extremes of ratio. In the intermediate range, the results for liquids vary with concentration (independent of pH which is virtually constant - see Figure 2), and the results for powders in this range are equivocal.

In man, the lethal oral dose of sodium silicates has been estimated as 0.5-5 g/kg(7). Ingestion of 200 ml of sodium silicate egg preserving solution (these solutions typically contain 5-36% of $3.2 \text{ SiO}_2/\text{Na}_2\text{O}$) caused severe vomiting, diarrhea and bleeding, elevated blood pressure, and renal damage, but was not fatal(14). In the past, sodium silicate has been administered orally for medicinal purposes in doses of 1 to 3 g/day without reported adverse effects(15), however, it is not presently known to be used as a drug.

In an early feeding study, King *et al.*(16) attempted to administer soluble silicates to dogs as 5% solutions, but found they had to preneutralize the solutions or the dogs invariably vomited them. Such soluble silica that was absorbed by the dogs from the neutralized solution was found to be quickly eliminated in the urine. The level of silica in the blood remained low, and it was suggested that these animals have a low renal threshold for dissolved silica. Newberne and Wilson(17) succeeded in feeding dogs and rats sodium silicate incorporated into an semisynthetic diet at levels equivalent to 0.8 g $\text{SiO}_2/\text{kg}/\text{day}$. The only untoward clinical signs observed were polydipsia, polyuria, and soft stools. Renal lesions were observed in the dogs upon histopathological examination. Similar effects were not observed in the rats. Smith(18) studied the effects of 3.22 ratio sodium silicate added to the drinking water of rats at levels of 600 and 1200 mg/l. Two trials were conducted. The first, with a nutritionally adequate diet, lasted 180 days. The second, in which a diet inadequate for normal growth was provided, lasted 84 days. The rats used in the second trial were the offspring of those used in the control group of the first trial. Nitrogen and phosphorus retention was measured by assaying the diet and wastes for these elements. Weight gain and reproductive ability were recorded. Consumption of the water was

**Table II. Esophageal Test (Oral, Rabbit)
Sodium Silicate**

SiO₂/Na₂O wt. ratio	CONCENTRATION	RESULTS + = corrosive
3.2	5% w/v	-
3.2	10% w/v	-, -
2.9	10% w/v	-
2.9	15% w/v	+
2.9	Neat liq.(43%)	+
2.4	10% v/v	-
2.4	15% v/v	+
2.4	Neat pwd.	+, -
2.0	5% v/v	-
2.0	10% v/v	+, +
2.0	Neat pwd.	+, -
1.0	10% w/v	+, +
0.7	10% w/v	+

only noted by casual observation, but it was reported to be similar for all groups.

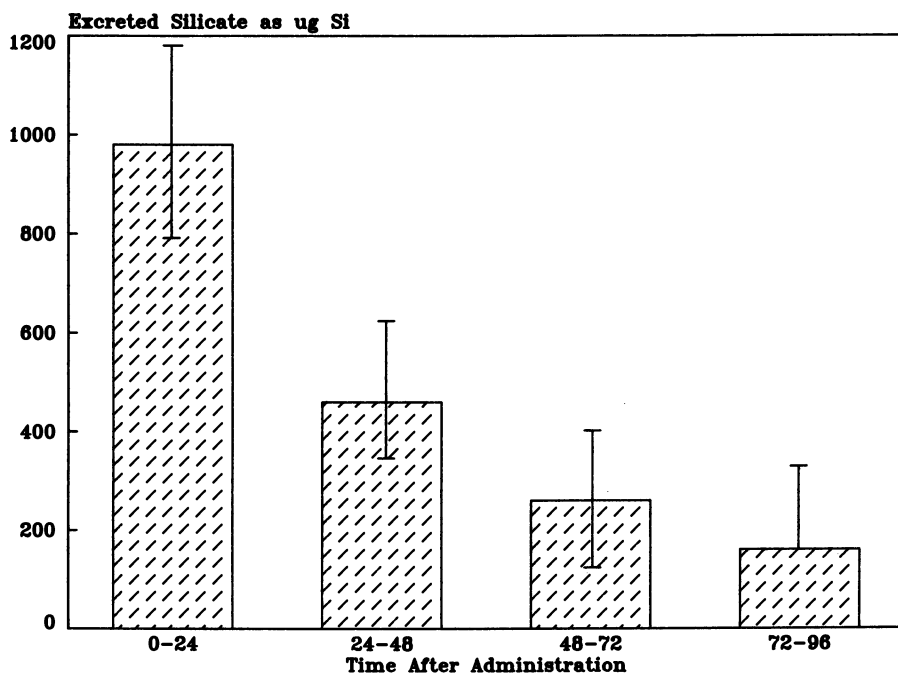
In the trial receiving an adequate diet, the male rats receiving sodium silicate at the 600 ppm SiO_2 level (about 790 ppm sodium silicate), experienced a 6% greater weight gain over controls receiving deionized H_2O . Females from this same group gained 5% less weight than the controls. At the higher level (about 1580 ppm sodium silicate) weight gains by both sexes did not differ significantly ($P = 0.05$) from controls. In the second trial, there was no significant difference in weight gain of the silicate treated versus the control animals at the lower level, although the males at the higher levels were 6% lighter than controls. The greatest variation in nitrogen retention was a 13% retention of urinary nitrogen in the first trial group at the lower level of silicate consumption - the same group that gained weight. The largest variation in phosphorus retention was a 9% increase in the second trial group that consumed silicate at the higher level, but it was not apparent whether this difference was due to the silicate treatment or the greater body size of these animals. The results of the study of the rats reproductive performance are given in Table III. It appears that of all the factors observed, the number of offspring to survive until weaning is the only one to consistently correlate with increased silicate consumption. In view of the high mortality of the control offspring (only 35% survived), any additional stress might have produced the same effect. The author concludes that "soluble silica ... exerts biologically important effects on growth and reproductive performance,"(19) but it is not clear from his data whether there is an effect, and if there is, whether it can be attributed to the dissolved silica or the alkalinity of the drinking water.

Ito *et al.*(20), fed rats drinking water containing from 200 to 1800 ppm sodium silicate for 3 months. They reported an increase in serum alkaline phosphatase activity at a concentration of 1800 ppm in males, and an increase of serum glutamic-pyruvic transaminase activity at 200 and 600 ppm sodium silicate in females. A decrease in leukocyte count occurred in both sexes at 600 ppm. No specific change in the rats due to the sodium silicate was observed upon histopathological examination.

Benke and Osborne(21) studied the rate and extent of urinary excretion of silicon in rats after oral administration of single doses of several silicates, including a 2.4 ratio sodium silicate, to rats. Two trials were conducted: in the first trial, a dose of 40 mg/kg was administered, in the second trial the dose was 1000 mg/kg. At the 40 mg/kg level, 18.9% of the administered silicate was excreted in the urine, and elevated levels of Si in the urine were observed only in the first 24 hours after the oral dose. At the 1000 mg/kg level, 2.8% of the total administered silicate was excreted in the urine, and the data in Figure 4 were obtained for the rate of excretion Benke

Table III. Reproductive Ability of Rats Fed Sodium Silicate in Drinking Water

	CONCENTRATION (as ppm SiO ₂)		
	0	600	1200
Matings	77	77	77
Litters	54	51	49
No. Born	517	346	414
No. Weaned	182	83	44
% Weaned	35	24	11
Difference as % of Controls			
Born		67	80
Weaned		46	24

*Figure 4. Urinary excretion of sodium silicate.*

and Osborne calculated the urinary excretion half-life for ingested sodium silicate to be 24 hours.

Sauer *et al.*(22), measured the total silica eliminated (i.e., urinary and fecal SiO_2) by guinea pigs after oral administration of 1) a single dose of sodium metasilicate pentahydrate, equivalent to 80 mg SiO_2 , and 2) four doses of sodium metasilicate pentahydrate, equivalent to 80 mg SiO_2 , at 48 hr. intervals. Within 8 days, 60% of the silica administered as a single dose and 96% of the silica administered as multiple doses was excreted.

Although there are no reports in the scientific literature of chronic testing or carcinogenicity of sodium silicates, a number of studies on zeolite type A, which rapidly decomposes to amorphous aluminates and sodium silicate in the stomach and tissues, were recently reported(23). Among these studies was a lifetime feeding study in rats which concluded that chronic feeding of high doses (.001, .01 and .1% in diet) of type A zeolite did not produce cancer or chronic organ toxicity in rodents(24). It is also relevant to note that sodium silicates have had a long history of safe use in numerous food-related applications(25). Sodium silicate and potassium silicate are considered GRAS (Generally Recognized as Safe) by the U.S. FDA for addition to canned drinking water as a corrosion preventative at concentrations up to 100 ppm(26).

Skin Contact

Tests for the effects of skin contact of sodium silicates have been undertaken by both industry and governmental agencies. Since many soluble silicates are not stoichiometric compounds, but rather can be prepared with variable $\text{SiO}_2/\text{Na}_2\text{O}$ ratios, tests have been conducted at various points on the continuum of possible ratios, usually at points within the specifications of commercial products.

Two similar experimental procedures have been used to quantify the skin contact effects of soluble silicates; both are based on the Draize method(27). The first is the protocol adopted by the U.S. Food and Drug Administration and Consumer Product Safety Commission for determining the contact hazard of substances under the Federal Hazardous Substances Act, and is specified in 16 C.F.R. §1500.41 *et seq.* The second, is the protocol adopted by the U.S. Department of Transportation for determining the contact hazard of substances under the Federal Hazardous Materials Transportation Act, and is specified in 49 C.F.R. §173.240.

In the FHSA test, 0.5 g or 0.5 ml of the test substance is moistened with physiological saline and applied to the intact and abraded skin of rabbits for 24 hours. The site of contact is examined after 24 and 72 hours and the extent of irritation is ranked on a scale (Primary Irritation Index) of increasing

severity of from 1 to 4. Corrosivity, i.e., nonreversible injury, is also noted. Tables IV. and V. list the values obtained for soluble silicates in a number of laboratories over the course of about 20 years. The PII values listed are the sum of intact and abraded scores unless otherwise noted. Too few determinations have been done to compute the standard error of the PII, but the subjective nature of the scaling system makes the inference reasonable that it is large enough to account for the otherwise anomalous values for 3.2 ratio at 80 and 36 percent, respectively.

It appears that the breakpoint between irritant and corrosive solid sodium silicates occurs between 2.0 and 2.4 ratio. Potassium silicates are evidently more irritating than sodium silicates of equivalent mole ratio. Perhaps this is the result of the greater aqueous solubility of potassium silicates.

Test Results

The DOT test differs from the FHSA test principally in that the exposure period is 4 hours instead of 24 hours, and dry substances are tested dry - they are not moistened with saline solution. Consequently, this test is less sensitive to small differences in the activity of compounds, but it provides a more realistic model of accidental human exposure. The data in Table VI. indicates that the breakpoint between irritant and corrosive liquid sodium silicates occurs between 1.6 and 1.8 ratio, but it is also probably influenced by the concentration of the solutions.

In industries using sodium silicates, dermatitis has been attributed to sodium silicate exposure(34). Where adequate protection of the hands is not undertaken, physical injury by projecting points of dried silicate is further aggravated by alkaline irritation(35). Workers within the soluble silicate industry have been reported to sustain burns from hot glass and dermatitis from alkaline materials.(36) In our experience, the most common type of accidents involve spilling or splashing silicates into shoes or getting it between the skin and clothing at the collar and cuffs where abrasion occurs.(37) Safety boots and gloves with gauntlets are recommended to avoid these types of exposure.

Eye Contact

The effects of eye contact with sodium silicates have been tested by industry and in government laboratories. The standard test for determining the hazard of eye contact is the FHSA Draize method specified in 16 C.F.R. §1500.42. The data in Table VII. indicates that at the ratios and concentrations tested, soluble silicates are irritating to the eyes, and severely irritating at high concentrations. A new test for assessment of eye contact effects is currently under development.

**Table IV. FHSA Skin Contact Data
Sodium Silicate**

SiO₂/Na₂O wt. ratio	CONC. wt.%	PII	CORROSIVITY + = corrosive	Ref.
3.2	99	4	-	28.
3.2	80	0	-	28.
3.2	36	3	-	28.
2.9	43	3	-	28.
2.5	37	3	-	28.
2.4	24	4	-	28.
2.0	99	8	+	28.
2.0	54	4	-	28.
2.0	8	>4*	-	29.
1.0	10	5.6*	+	29.
1.0	6	>8*	+	29.

* 2x average of intact and abraded score.

**Table V. FHSA Skin Contact Data
Potassium Silicate**

SiO₂/K₂O mol. ratio	CONC. wt.%	PII	CORROSIVITY + = corrosive	Ref.
3.45	29	0	-	28.
3.33	39	2	-	28.
2.5	85	8	-	30.

**Table VI. DOT Skin Contact Data
Sodium Silicate**

SiO ₂ /Na ₂ O wt. ratio	CONC. wt.%	PHI	CORROSIVITY + = corrosive	Ref.
2.9	43	3.3	-	31.
2.5	37	0	-	31.
2.4	47	4.2	-	31.
2.0	44	4.2	-	31.
2.0	54	4.7	-	32.
1.8	38	3.2	-	32.
1.6	51	*	+	33.
1.0	99	*	-	33.
0.7	61	*	-	33.
0.5	90	*	+	33.

* not reported.

**Table VII. FHSA Eye Contact Data
Soluble Silicates**

SiO ₂ /Na ₂ O wt. ratio	CONC. wt.%	IRRITATION	Ref.
3.2	36	-	37.
2.9	43	+(severe)	37.
2.0	8	+	37.
2.0	44	+(severe)	37.
1.0	10	+	37.
1.0	6	+	37.
1.0	5	+	37.
1.0	3	+	37.
0.7	6	+	37.
0.7	3	+	37.
2.5*	80	+(severe)	38.

* SiO₂/K₂O ratio

Inhalation

Michon, et al.(40), studied the silicon metabolism of rabbits after inhalation of a sodium silicate aerosol. They concluded that sodium silicate dissolves in the lungs and is rapidly eliminated in the urine.

Becking(41) summarized two inhalation studies of type A sodium zeolite which rapidly decomposes to sodium silicate and amorphous aluminates under physiological conditions. In the first study, hamsters were exposed to approximately 20 mg/m³ of type A zeolite 3 days per week, 5 hours per day for 52 weeks. In the second study, Cynomolgus monkeys were exposed to 1 and 6 mg/m² of type A zeolite for 24 months, and 50 mg/m³ type A zeolite for 12 months. No evidence of fibrosis was observed in the animals in either study.

ENVIRONMENTAL ASPECTS

Occurrence

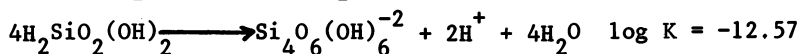
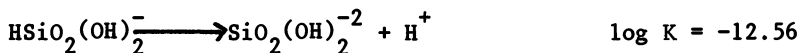
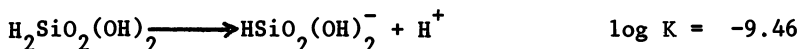
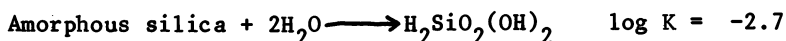
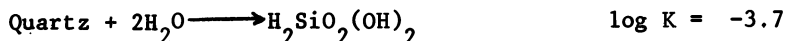
Compounds of silicon and oxygen are the primary constituents of earth's land masses. Dissolved silica is a minor but ubiquitous constituent of earth's hydrosphere. Ground waters contain the highest concentrations of dissolved silica: the median value in the U.S. is 17 ppm(42). Of earth's surface waters, streams and rivers contain the most dissolved silica. The median value for streams in the U.S. is 14 ppm(43). For rivers, the worldwide mean concentration is 13 ppm(44). Lakes are reported to contain about 4 ppm(45), while the mean concentration of dissolved silica in the oceans is about 6 ppm(46). The median value for dissolved silica in the public water supplies of the 100 largest U.S. cities is 7.1 ppm(47).

Earth's biomass also contains appreciable soluble silica. Relatively large amounts of silica are absorbed from solution, concentrated, and precipitated by the siliceous sponges (Hyalospongiae) and the protozoan orders Radiolaria and Heilozoa, while the majority of species in the Animal Kingdom only contain dissolved silica in the parts per million range.(48) The precise amount of soluble silica found in plants is determined by both species and soil factors. Lower plants, such as grasses (Gramineae) are very rich in silica, wet-land varieties usually containing the highest concentrations(49). In general, legumes and dicotyledonous plants contain less soluble silica than monocotyledons.(50)

Infrared absorption studies have shown that most biogenic silica is present as gel or dissolved silica. However, emission spectroscopy studies have indicated that some of the soluble silica found in animals is bound to organic molecules, such as glycosaminoglycans, whose structure has yet to be identified(51).

Environmental Chemistry

The solubility of silica can be characterized by the following equilibria at 25°C. Monosilicic acid has been written $\text{H}_2\text{SiO}_2(\text{OH})_2$, rather than $\text{Si}(\text{OH})_4$ or H_4SiO_4 in order to emphasize its diacidic character, and the tendency of silicon, like other metalloids, to coordinate with hydroxo and oxo ligands.



Stumm(52) used these equilibria to construct the diagram in Figure 5 which describes the speciation of silica in aqueous solution. His data indicate that at normal environmental pH values (pH 9) dissolved silica exists exclusively as monosilicic acid. This conclusion is supported by the finding that soluble silica has a diffusion coefficient of 0.53 indicating a molecular size about equivalent to monosilicic acid(53).

Below about pH = 9.4 the solubility of amorphous silica is about 120 ppm(54). Quartz has a solubility of only about 6 ppm, but its rate of crystallization is so slow at ordinary temperatures and pressures that the solubility of amorphous silica represents the upper limit of dissolved silica concentration in natural waters.

Dissolved silica is supplied to the environment by chemical and biochemical weathering processes which involve the transfer of energy from biological systems to silicate minerals as well as ion substitution and chelate forming reactions which remove mineral lattice cations(55). The concentration of dissolved silica in natural waters is controlled by a buffering mechanism which is thought to involve the sorption and desorption of dissolved silica by soil particles and sediments(56, 57). The average silica weathering rate of watersheds is 20 kg/ha/hr(58). The processes of the natural silica cycle are depicted in Figure 6. Any soluble silica input to this natural cycle as a result of the production or use of commercial soluble silicates would be a trivial amount in view of the high flux of the natural silica cycle. Dissolved silica from commercial soluble silicates is indistinguishable from natural dissolved silica since depolymerization of polysilicate anions to monomeric dissolved silica occurs very rapidly when

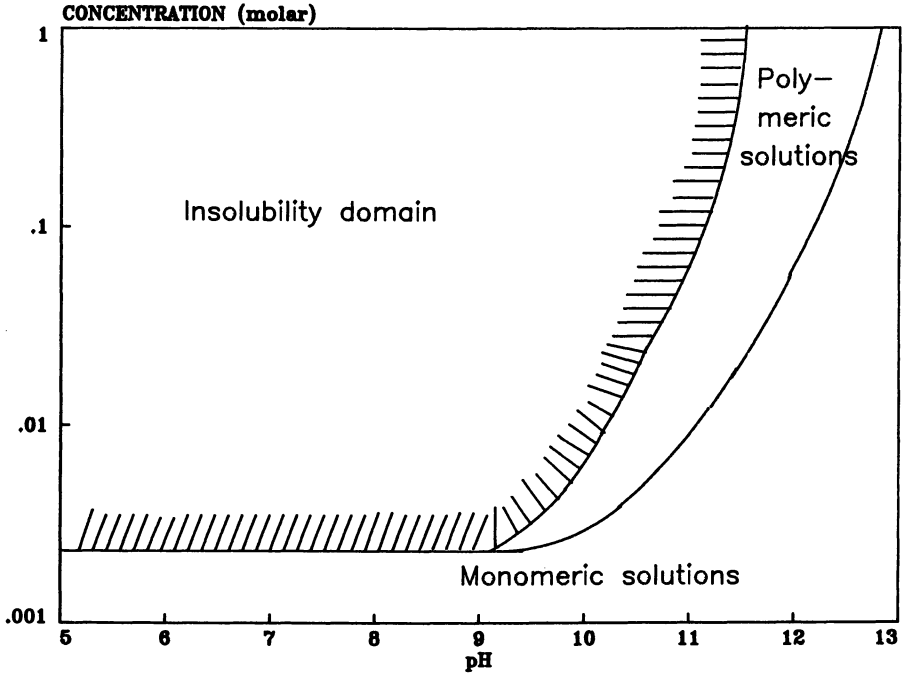


Figure 5. Soluble silicate speciation.

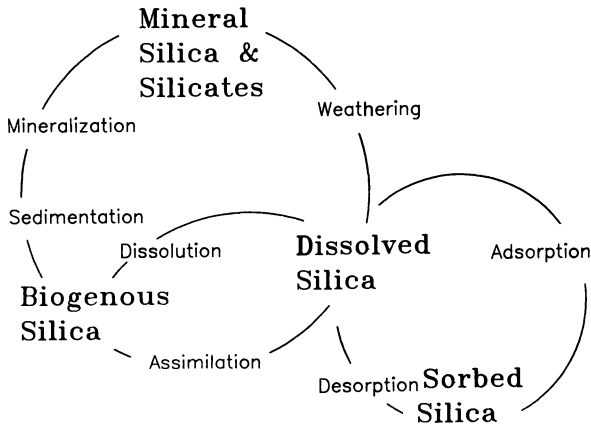


Figure 6. The natural silica cycle.

commercial soluble silicate solutions are diluted with water(59).

Aquatic Toxicity

Aquatic toxicity data is usually expressed in terms of the median tolerance limit. TL_m, which is defined as that concentration of a substance that it lethal to 50 percent of the test population in an arbitrary time period. Table VIII. lists the TL_m values obtained for sodium silicate.

Nutritional Aspects

The essential nature of silicon as a nutrient has long been recognized in primitive plant and animal species that utilize it in the form of silica as a structural material(60). Until recently, it had been thought that since the bone-cartilage system had evolved in animals and the cellulose-lignin system had evolved in plants silica had become obsolete; that the presence of silica in higher species was simply attributable to their contamination by the vast quantities of silica in the natural environment. In the past few years, however, a number of experiments have indicated that silicon is necessary, albeit in trace quantities, for the normal growth, development and functioning of a large variety of higher animals(61), and it is anticipated that silicon will become recognized as an essential nutrient for most if not all species.

The problems associated with "blooms" of algae which occur in eutrophic bodies of water have motivated much research into determining the limiting nutrients which control the growth of algal populations. It has been demonstrated that at concentrations of less than 0.1 ppm, silica is a limiting nutrient for diatoms(62), and a few other algal species(63). Thus, only in bodies of water which are orders of magnitude lower in silica concentration than normal environmental levels, could silica become a limiting factor to algal growth. The addition of excess soluble silica over the limiting concentration will not stimulate the growth of diatom populations; their growth rate is independent of silica concentration, once the limiting concentration is exceeded(64, 65).

It has been observed that when a body of water becomes eutrophic due to large inputs of phosphorus, diatom populations increase, and this results in a decline in the dissolved silica content of the water, especially the surface water(66). If this process continues until the available silica becomes depleted below the limiting concentration for diatoms, they are replaced by obnoxious green and blue-green algal species which have much lower requirements for silicon(67). Thus, it is beneficial to maintain an adequate supply of soluble silica in a phosphorus-rich body of water in order to promote diatoms as

**Table VIII. Aquatic Toxicity
Sodium Silicate**

Animal	Time	Dose	Ref.
Annelids			
<i>Negris grubei</i>	28days	250g-at/l.	68.
<i>Capitella capitata</i>	28days	210g-at/l.	68.
Mosquitofish			
<i>Gambusia affinis</i>	24hr.	3200ppm	69.
" "	48hr.	2400ppm	69.
" "	96hr.	2320ppm	69.
Water flea			
<i>Daphnia magna</i>	96hr.	247ppm	70.
Snail eggs			
<i>Lymnea</i>	96hr.	632ppm	70.
Amphipoda	96hr.	160ppm	70.

the dominant algae. Sodium silicate has been reported to inhibit the growth of a troublesome species of blue-green algae(68).

LITERATURE CITED

1. Zwick, H., Das Wasserglas, Fussli, Zurich, 1877.
2. Vail, J.G., Soluble Silicates, ACS Monograph (46), Chemical Catalog Co., NY, 1928.
3. Ibid., 95.
4. Ibid., 410-11.
5. Ibid., 413-14.
6. PQ Corporation, unpublished documents and records.
7. Joint FAO/WHO Expert Committee on Food Additives, WHO Food Additive Ser. (5), 21-30.
8. Gaskins, J.R., "Analytical Report," No. 016-2583, U.S. FDA, Div. Toxicological Evaluation, Bureau of Science, Washington, D.C., 1966, 2.
9. Calandra, J.C.; Fancher, O.E., The Soap and Detergent Association Scientific and Technical Report 1972, (5R), 24.
10. PQ Corporation, "Biological Study No. LH57085-1-4," 1961, 4.
11. Hehir, R.M., "Research Data on Silicates - Memorandum" E.W. Ligon/R.M. Hehir, U.S. FDA, Div. Toxicological Evaluation, Bureau of Science, Washington, D.C. 1967, 1.
12. Ibid., 9-10.
13. Burbower, G.W., "Experimental Data From Consumer Product Safety Commission Studies on the Provisional Rabbit Test," 1973, 5.
14. Eichhorst, H., Schweiz Med. Wochschr., 1920, 50, 1081.
15. Scheffler, L., Comptes Rendus, 1920, 171, 416-18.16.
- King, E.J.; Stantial, H.; Dolan, M., Biochem. J., 1933, 27, (4), 1002-6.
17. Newberne, P.M.; Wilson, R.B., Proceedings National Academy of Science U.S., 1970, 65, (4), 872-75.
18. Smith, G.S.; Neumann, A. L.; Gledhill, V. H.;; Arzola, C. A., J. Anim. Sci., 1973, 36, (2), 271-8.
19. Ibid., 876.
20. Ita, R., Toho Igakkai Zasshi, 22, (2), 223-7.
21. Benke, G.M.; Osborne, T.W., Fd. Cosmet. Toxicol., 1979, 17, 123-127.
22. Sauer, F.; Laughland, D. H.; Davidson, W. M., Can. J. Biochem. & Physio., 1959, 37, 183-91.
23. Becking, G.C., Report of the Task Force on the Health Effects of Non-NTA Detergent Builders to the International Joint Commission Great Lakes Advisory Board, Windsor, Ontario, 1981, 57-69.
24. Ibid., 64.
25. Blumberg, J.G.; Schleyer, W.L., "Current Regulatory Status of Soluble Silicates," American Chemical Society Symposium on Soluble Silicates, New York, 1981.

26. Select Committee on GRAS Substances, Evaluation of the Health Aspects of Certain Silicates as Food Ingredients, SCOGS-61, NTIS Pb 301-402/AS, 1979, 4.
27. Draize, J.H., J. Pharm. and Exp. Ther., 1944, 82, 337.
28. PQ Corporation, "Biological Study No. LH57393," 1961, 2-3.
29. Hehir, R.M., Op. cit., 2.
30. PQ Corporation, "Biological Study No. FDRL800573," 1980, 1.
31. PQ Corporation, "Biological Study No. HL790101," 1972, 2-4.
32. PQ Corporation, "Biological Study No. HL790104," 1973, 2-3.
33. PQ Corporation, "Biological Study No. HL790106," 1973, 1.
34. Arch. Ind. Hyg. Occ. Health, 7, 1953, 411-23.
35. White, R.P., The Dermatogoses or Occupational Affections of the Skin, Lewes, London 1934.
36. Schwartz, L.T.L., Birmingham, D.J., Occupational Diseases of the Skin, 3rd ed., Lea & Febiger, Philadelphia, 1957 248.
37. PQ Corporation, unpublished records.
38. Hehir, R.M., Op. cit., 5.
39. PQ Corporation, "Biological Study No. FDRL800573," 1980, 1.
40. Michon, R.; Sue, P.; Merinis, J., Comptes Rendus, 1956, 243, 2194-5.
41. Becking, G.C., Op. cit., 64.
42. Davis, S.N., American Journal of Science, 1964, 262, 870.
43. Ibid., 870.
44. Edwards, A.M.C.; Liss, P.S., Nature 1973, 243, 341.
45. Sutherland, J.C., Envt. Sci. Tech., 4, (10), 826.
46. Kido, K., Marine Chemistry, 1974, 2, (4), 277-86.
47. Anon., "Public Water Supplies of the 100 Largest Cities in the United States," U.S.G.S. Paper No. 1812, 1962.
48. Levier, R.R., Bioinorganic Chemistry, 1975, 4, (2), 109-16.
49. D'Hoore, J.; Coulter, J.K., Soils of the Humid Tropics Nat. Acad. Sci., Washington, D.C. 1972, 163-73,
50. Lewin, J.; Reimann, B.E.F., Annual Review of Plant Growth, 1969, 20, 289.
51. Schwarz, K., Trace Elements Metab. Anim., Proc. Int. Symp. 2nd, 1974, 355.
52. Stumm, W.; Morgan, J.J., Aquatic Chemistry, New York, Wiley, 1970.
53. Iler, R., The Colloid Chemistry of Silica and Silicates, 1955, Cornell U. Press, Ithaca, NY, 12.54.
- Alexander, G.B.; Heston, W.M.; Iler, R.K., J. Phys. Chem., 1954, 58, 453.
55. Boyle, J.R.; Voight, G.K., "Biological Weathering of Silicate Minerals," Plant Soil, 1973, 38, (1), 191-201.
56. Edwards, A.M.C.; Liss, P.S., Nature 1973, 243, 341.
57. Oehler, J.H., Biogeochemical Cycling of Mineral Forming Elements, Trudinger, P.A.; Swaine, D.J., eds., Elsevier Publ. Co., 1979, 467-483.

58. Soukup, M.A., "The Limnology of a Eutrophic Hardwater New England Lake, with Major Emphasis on the Biogeochemistry of Dissolved Silica," Xerox Univ. Microfilms, Ann Arbor, Michigan, Order No. 75-270527.
59. O'Connor, T.L., J. Phys. Chem., 1961, 65, (1), 1.
60. Carlisle, E., Trace Elem. Metab. Anim., Proc. Int. Symp. 2nd 1973(pub 1974), 407-423.
61. Schwarz, K., Op. cit., 357.
62. Kilham, P., Limnology and Oceanography, 1971, 16, (1), 10.
63. Klaveness, D.; Guillard, R.R.L., J. Phycol., 1975, 11, 3, 349-55.
64. Jorgensen, E.G., Dansk Botanisk Arkiv, 18, (1), 1957, 5.
65. Schwartz, A.M., Interim Report for Environmental Protection Agency Contract FWQA 14-12-875, 1972.
66. Schelske, C.L.; Stoermer, E.F., Science, 1971, 173, 423.
67. Kilham, P., Op. cit., 12.
68. Schwartz, A.M., Op. cit., 79.
69. Reish, D.J., Water Research, 1970, 4, 721.
70. Wallen, I.E.; Greet, W.C.; Lasater, R., Sewage and Industrial Wastes, June 1957, 695.
71. Dowden, B.F.; Bennett, H.J., J. Water Pollution Control Fed., 1965, 37, (9), p. 1308.

RECEIVED March 2, 1982.

Silicon NMR Studies on Dissolved Silicates

H. C. MARSMANN and M. VONGEHR

Universität Paderborn, Fachbereich Chemie, 4790 Paderborn,
Federal Republic of Germany

There are a number of possible ways to look at dissolved or liquid silicates. But if someone is studying this type of compounds in rather concentrated solutions typical of most commercial preparations, then it is useful to distinguish them by the occurrence of building units. In the first figure the schematic representations of such units, namely the neso, end, middle and two different types of branching units are depicted. Naturally occurring silicon contains 4.1 % of the isotope with 29 mass units. This isotope has a spin of $1/2$, a magnetic moment and can thus be used in magnetic resonance studies. The usefulness of Si magnetic resonance in resolving problems in silicate chemistry derives from the fact, that there is an up-field shift to approx 10 ppm if exchanging one R-group by another siloxane unit. This also corresponds to a change from one building unit to another (1). So in a ^{29}Si nmr spectrum of a silicate you see the neso unit on the left side and the end, middle, tri- and tetrafunctional branching units appearing in steps of approx 10 ppm from that to the high field direction. Due to strain effects building units of ring compounds very often do not follow these rules.

The Fig. 2 shows the ^{29}Si -spectrum of a sodium silicate dissolved in water (2). The composition of the silicate comes close to commercial water glass solutions. Under these circumstances it is not possible to distinguish individual molecules. But information about the incidence of the various building units can be obtained. Beginning from the right side the resonance lines of the tetra- and trifunctional branching moieties and of small amounts of middle and endgroups can be observed. From the area under the resonance lines it is possible to deduce the concentrations of the different structural entities within the mixture of polymers. It is obvious that the best way to describe the polymers is to think of rather ball shaped molecules consisting mostly of branching structures with a surface of hydrophilic end- and middle groups. The width of the resonance lines increases from that of the neso to that of the tetrafunctional branching groups. Individual mole-

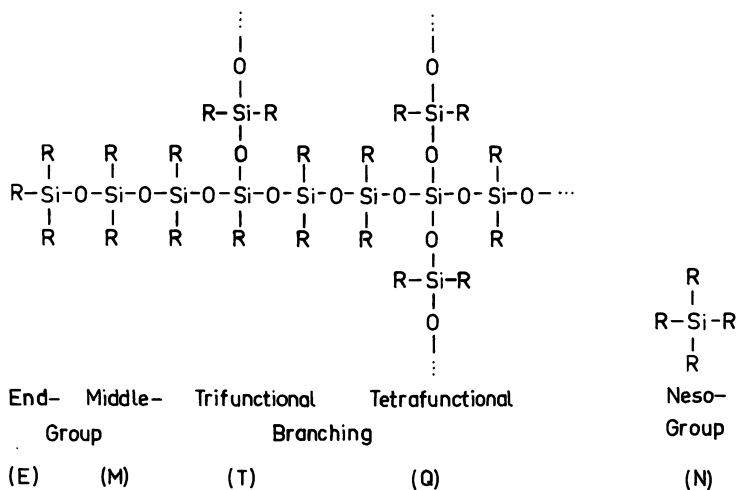


Figure 1. Principal structural building units of polymeric siloxane.

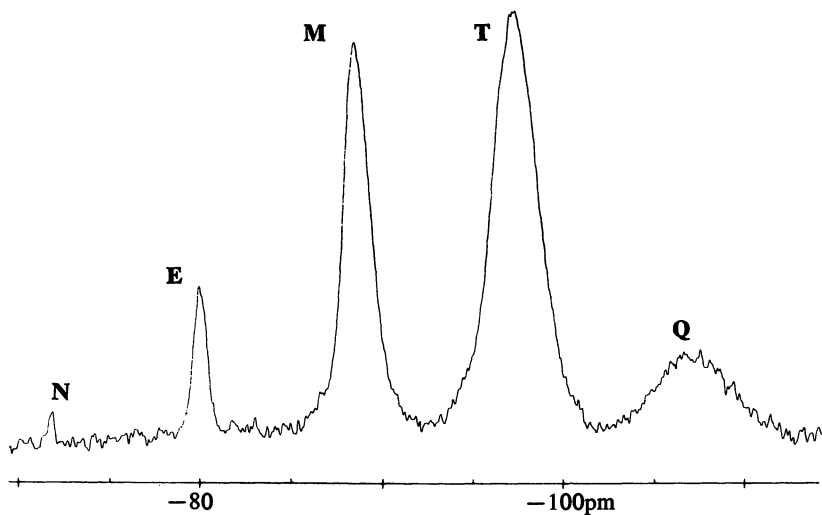


Figure 2. ^{29}Si NMR spectrum of a sodium silicate solution in D_2O with a ratio of $\text{R} = \text{Na}:\text{Si} = 0.14$. The spectrum shows the resonance of the principal building units of a polysilicate. This and all of the other spectra were run on a Bruker WM 250. Conditions: measuring time 1 h; 8-s pulse length; 0.8-s acquisition time.

cules can only be detected after addition of sodium hydroxide (fig.3). Appearing now are the lines of some other oligomeric species, mainly small rings and cages. The resonance lines of them are noted by asterisks between the bands of lines belonging to the normal kind of building units. It is probably not the best proposition to study the nature of such molecules in concentrated equilibrium mixtures, but you will hear more about them by the next speaker Prof. Harris. There are however two more points to be mentioned. First of all: equilibria between structural units in solutions are rather slow. Secondly, compared to fig. 2 the resonance lines are moderately narrow in fig. 3. There are several reasons for line broadening. But this sequence is explained best by the assumption, that the number of possible environments increases from neso, end and middle groups to the different branching types. All of them display slightly different chemical shifts, which can not be resolved into separated lines.

But there are other causes for line broadening as well. This can be shown by the situation as found in the methyl siliconates. Here one position around the silicon atom is now fixed by a methyl group and is therefore not susceptible to an equilibrium. A trifunctional branching group is now the highest degree of connectivity available. But due to the low solubility of methyl siliconates in water, short chains are observed only. Again these are changes caused by increasing alkalinity of the aqueous solution (fig. 4). The lines of neso, end and middle groups are recognizable, appearing as rather broad lines. Narrow are two lines only due to rings possibly the trimer and the tetramer. Except for those rings, line widths are increasing with greater alkalinity pointing to another cause of line broadening. In this case it is probably the influence of paramagnetic impurities because the argument of very different environments is no longer true for short chain molecules. But the position of the lines is varying with the pH-value also. This is a common feature for ionic species and due to the very fast equilibrium between protonated and unprotonated forms of the molecules. This fact makes the assignment of lines sometimes rather difficult. To get around this problem we studied the alkyl esters of the polysilicic acid. Most useful are the ethyl silicates. They are usually liquids. Individual members can be obtained by distillation on the low end and by gel chromatography on high side of the molecular weight distribution. For experimental details see (3). A typical spectrum of a mixture of ethyl silicates is depicted in fig. 5. A number of resonance lines could be assigned with the help of isolated oligomeric ethyl silicates. The chemical shifts of the different building units in the ethyl silicate system are closely related to those of the aqueous solutions of the polymeric silicic acid salts. The different building units are symbolized by capital letters, but those of subunits characterized by small letters. Tetrafunctional branching moieties are probably present in the

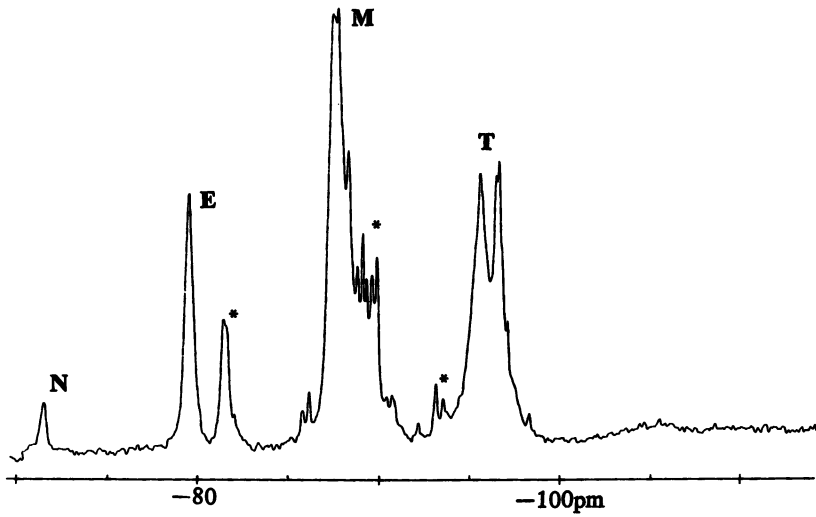


Figure 3. ^{29}Si NMR spectrum of a sodium silicate with a ratio of $R = \text{Na}:\text{Si} = 0.25$. The lines due to small rings and cages are marked by asterisks and are next to the bands of the principal building units.

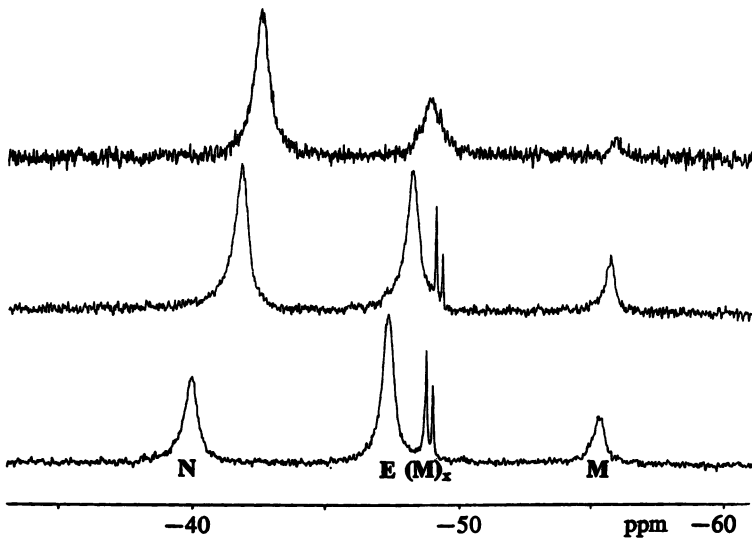


Figure 4. ^{29}Si NMR spectrum of methyl siliconates. Conditions: 10-s pulses; 20-s waiting period; 0.8-s acquisition time; and broad-band proton decoupling.

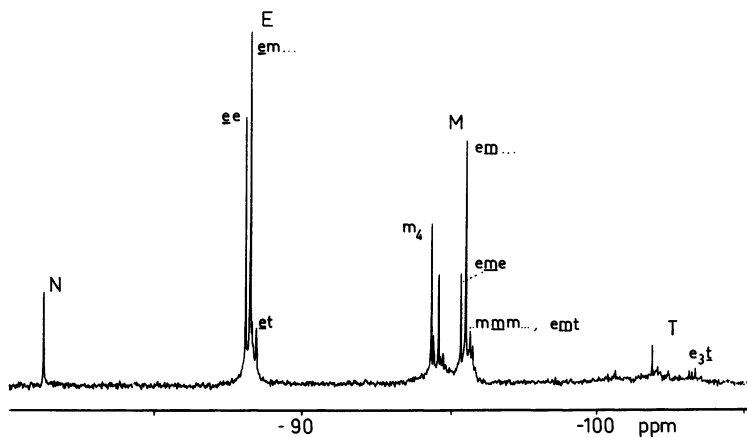


Figure 5. ^{29}Si NMR spectrum of mixture of ethyl esters of polysilicic acids. Conditions: 10-s pulses; 20-s waiting period; 0.8-s acquisition time; and broad-band proton decoupling.

equilibrium mixtures but due to the low sensitivity of the ^{29}Si experiment resonance of this entity, it could not be detected in such mixtures. After keeping the samples at temperatures close to 100°C for a longer period of time (several weeks in case of the water glass solutions, 24h for the silicic acid esters (2,3) no further change in the line intensities could be observed. It is then assumed, that some equilibrium state is obtained. Equilibrium constants for the reaction between building units are calculated, using the integral over their resp. resonance lines. The results for water glass solutions and silicic acid esters seem comparable but different from the silicates. (See Table I)

Table I. Equilibrium between building units in soluble silicates

R	$K_1 = \frac{[\text{N}] : [\text{M}]}{[\text{E}]^2}$	$K_2 = \frac{[\text{E}] : [\text{T}]}{[\text{M}]^2}$	$K_3 = \frac{[\text{M}] : [\text{O}]}{[\text{T}]^2}$
$-\text{O}^-$ (2)	0.19 + 0.07	0.39 + 0.05	0.06+ 0.2
OEt	0.26 + 0.10	0.39 + 0.10	--
$\text{CH}_3/-\text{O}^-$	0.5 + 0.1	--	--

Data for silicate solutions from (2).

Literature Cited

1. Marsmann, H. ^{29}Si -NMR Spectroscopic Results'; Diehl, P., Fluck, E., Kosfeld, R., Ed. Springer, 1981
2. Marsmann, H.C., Z. Naturforsch. 1974, 29b, 495-99
3. Marsmann, H.C., Meyer, E., Vongehr, M., Weber, F., Die makromolekulare Chemie, in prep.

RECEIVED March 2, 1982.

NMR Studies of the Chemical Structure of Silicates in Solution

ROBIN K. HARRIS¹ and CHRISTOPHER T. G. KNIGHT

University of East Anglia, School of Chemical Sciences, Norwich NR4 7TJ, England

WILLIAM E. HULL

Bruker Analytische Messtechnik GmbH, Silberstreifen, Federal Republic of Germany

The use of ^{29}Si NMR to obtain definitive information about the chemical structure and kinetics of aqueous silicate solutions is discussed. Special techniques such as enrichment in ^{29}Si are required. Some typical spectra are shown and results presented. Twelve species have been positively identified in a particular potassium silicate solution.

19 DOWN: "It sounds foolish to study this element"

"The Times" crossword puzzle no. 13321.

Silica dissolves readily in aqueous solutions of alkali metal hydroxides, but for many years the precise nature of the species present has been a matter of speculation rather than proof. It has been clear that there is a dynamic equilibrium between a range of silicate ions of varying molecular weight, and that the exchange rate between the species is sufficiently rapid that their chemical separation is not feasible. Indirect methods of analysis, such as phosphomolybdate formation and trimethylsilylation, involve an acidification stage which renders the results liable to controversy.

As discussed in the preceding article, it was shown in 1973 (1) that ^{29}Si NMR might contribute greatly to the knowledge of aqueous alkaline silicate solutions, since the rate of exchange between the species is slow on the NMR timescale. Figure 1 shows a typical spectrum, and bands labelled (2) A, B, C, D, and E may be observed. Under suitable conditions, two further bands, F and G, occur to low frequency of those in Figure 1. The assignment of these bands in terms of the silicate structural units Q^i , where

¹ Author to whom correspondence should be addressed.

i is the number of attached siloxane bridges and the state of protonation is ignored (3), has been assumed (2) to be as follows:

band	A	B	D	F	G
assignment	Q^0	Q^1	Q^2	Q^3	Q^4

Bands C and E have been subject to controversy (3-6) but the assignments which are supported by our own work (6, 7) are to Q^2 and Q^3 units in "three-membered rings", i.e. rings involving $(SiO)_3$.

However, Figure 1 shows that all bands except A have fine structure, indicating overlapping resonances from a variety of silicon environments, and the question which arises is: how can detailed assignments of individual resonances to particular silicate species be made? Until the work described herein progress was very slow, for the simple reason that ^{29}Si is a "rare" nucleus (4.7% natural abundance) and proton exchange is rapid on the NMR timescale, so that neither (Si,Si) nor (Si,H) spin-spin couplings affect the observed spectra. Consequently the only arguments which can be used to deduce assignment involve chemical shift considerations, relative intensities for different silicons supposed to be in the same species, and speculations based on the effects of dilution. None of these arguments are definitive, although assignments to monomer, Q^0 , and dimer, Q^1 , have been clearly made (3, 5, 8) and speculations put forward regarding a handful of other species.

It has seemed, therefore, that the author of "The Times" crossword clue quoted at the beginning of this article was more accurate than he realised!

Methodology

The advances reported here in our knowledge of the species present in aqueous silicate solutions at high pH were made by combining four techniques, viz:-

- (i) Use of the highest feasible applied magnetic field, B_0 .
- (ii) Use of samples enriched in ^{29}Si .
- (iii) Homonuclear Si - {Si} decoupling.
- (iv) Spectral analysis.

None of these techniques is novel in concept, yet none had been adopted for ^{29}Si studies before our work (7, 8, 9). Use of a very high B_0 (in our case 11.75 T) is essential to achieve maximum dispersion, since otherwise spectral overlap is a problem for all solutions except those at very high pH and/or very low concentration. Enrichment in ^{29}Si not only improves the S/N, but also introduces splittings in the spectrum for many silicon environments due to (Si, Si) spin-spin coupling. Homonuclear decoupling then enables bands due to nuclei in the same chemical species to be

located. Finally, observation of the spectral patterns (in some cases first-order, in others second-order) gives information on the spin system involved, and hence on the chemical species. The spectral analyses were, in fact, carried out (7, 10) under the assumption that only two-bond couplings need to be considered.

Results and Discussion

Figure 2, which is of a spectrum obtained at 99.4 MHz ($B_0 = 11.75$ T) illustrates the significant gains achieved by high-field work (compare Figure 1). We first (8) used enrichment in ^{29}Si to determine the lower limit of detection for silicates by NMR, and obtained acceptable spectra for a solution ca. 0.01 M in SiO_2 , under conditions where only monomer could be detected. However, the spectra (see ref. (8)) were obtained at a relatively low magnetic field, and it is likely that an order-of-magnitude lower concentration could be detected with a high-field spectrometer. At higher concentrations, where condensed species are present, a simple principle may be used to obtain preliminary structural information. This principle states that coupling between equivalent nuclei does not affect NMR spectra. As a corollary, all peaks in a natural-abundance spectrum which do not split when enriched silica is used must be assigned to species in which all the silicon atoms are chemically equivalent. Figure 3 indicates how this principle is applied, and Table I lists the shifts of such peaks for a ^{29}Si -enriched potassium silicate solution, together with the assignments.

Table I: Species giving singlet ^{29}Si NMR resonances for an alkaline aqueous silicate solution (K:Si = 1.0; concentration $\sim 0.65\text{M}$ in Si) enriched in ^{29}Si to 95.3%

		$\Delta\delta_{\text{Si}}/\text{ppm}^a$
I	Monomer, Q^0	0.00
II	Dimer, Q_2^1	-8.62
III	Cyclic trimer, Q_3^2	-10.19
IV	Cyclic tetramer, Q_4^2	-16.10
V	Prismatic hexamer, Q_6^3	-17.21
VI	Unknown	-25.60
VII	Cubic octamer, Q_8^3	-27.55 ^b

^aRelative to the signal of the monomer, using the high-frequency positive convention. Values taken from ref. (7), except for VII.

^bFor a solution with K:Si = 1.5 and concentration 0.6M in Si.

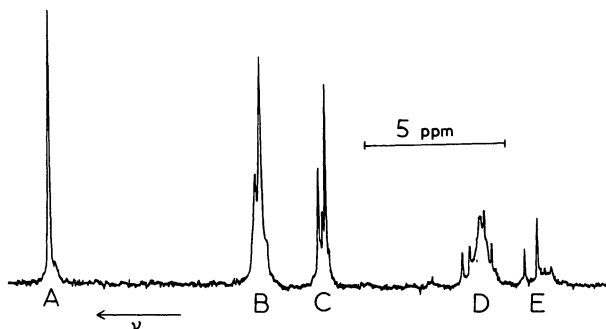


Figure 1. Natural-abundance ^{29}Si NMR spectrum at 19.87 MHz of aqueous alkaline potassium silicate solution with atomic ratio $\text{K}:\text{Si} = 1.5$ and concentration 5 mol/kg in Si (8). Bands A to E are indicated (see text). (Reproduced, with permission, from Ref. 8. Copyright 1980, Elsevier Publishing Co.)

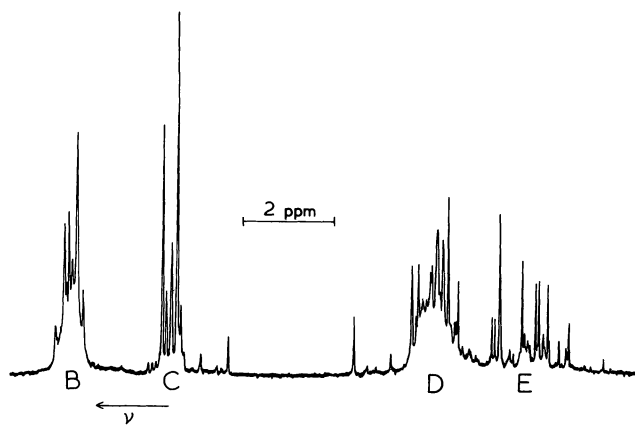


Figure 2. High-field (11.75 T) natural-abundance ^{29}Si NMR spectrum of aqueous alkaline potassium silicate solution with atomic ratio $\text{K}:\text{Si} \sim 1.3$ and concentration ca. 5 mol/kg in Si. Only bands B, C, D, and E are shown. Irradiation frequency increases to the left.

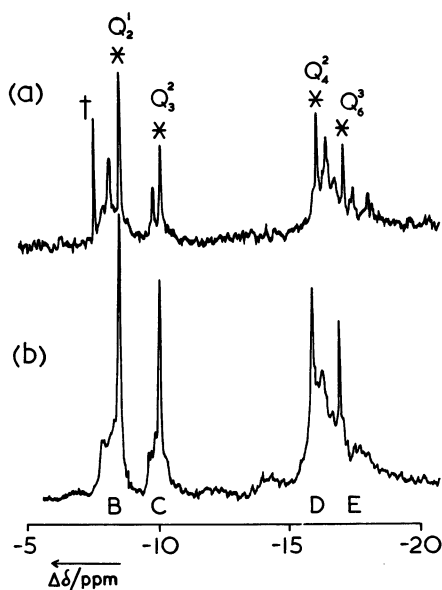


Figure 3. ^{29}Si NMR spectra of aqueous alkaline sodium silicate solutions with atomic ratios $\text{Na}:\text{Si} = 1.0$ and concentrations ~ 0.65 M in Si (8). Only bands B, C, D and E are shown, although bands D and E are not well separated for this solution. Key: natural abundance ^{29}Si , 49.7 MHz spectrum (a); ^{29}Si enriched to 95.3%, 15.7 MHz spectrum (b). Conditions: peaks unsplit for enriched sample (*), assignments are given; peak is spurious (†); chemical shift scale given with respect to signal for monomer, Q^0 ; high-frequency-positive convention is used. Irradiation frequency increases to the left.

Evidence for the assignments (7, 10) is, of course, indirect, and involves (i) chemical shift considerations, (ii) relationship to substituted species of clearly established structure, and, more recently, (iii) evidence from high-resolution ^{29}Si NMR of solid silicates (11). The third of these methods is likely to be of increasing value. The high-resolution NMR technique for solids involves magic-angle rotation and high-power proton decoupling. Some relevant data (11) are given in Table II.

Table II: Data from high-resolution silicon-29 NMR of simple solid silicates (ref. (11))

Compound	Unit	$\delta_{\text{Si}}/\text{ppm}^{\text{a}}$
NaH_3SiO_4	monomer	-66.4
$\text{Zn}_4(\text{OH})_2[\text{Si}_2\text{O}_7]\cdot\text{H}_2\text{O}$	dimer	-77.9
$\text{K}_4\text{H}_4[\text{Si}_4\text{O}_{12}]$	cyclic tetramer	-87.5
$(\text{Et}_4\text{N})_6[\text{Si}_6\text{O}_{15}]$	prismatic hexamer	-90.4
$(\text{Me}_4\text{N})_8[\text{Si}_8\text{O}_{20}]$	cubic octamer	-99.3
low cristabolite	six-rings	-109.9

^a Relative to the signal for Me_4Si , using the high-frequency-positive convention

One of the entries in Table II enabled an initial assignment error in ref. (7) (for the cubic octamer) to be corrected in Table I, leaving one unassigned unsplit line at $\Delta\delta_{\text{Si}} = -25.60$ ppm. It is possible that this peak is due to a 5- or 6-membered ring, or to a double -5- or double -6- membered cage (12), but chemical shift considerations make all these possibilities seem somewhat unlikely.

Further analysis of spectra for enriched solutions relies on observation of splitting patterns. Figure 4 shows the dramatic increase in information content available in the high-field spectrum of the potassium silicate solution enriched in ^{29}Si (compared with Figure 1 or Figure 3). Homonuclear double resonance links the bands indicated, and spectral analysis follows. As an example, consider Figure 5, which shows on expanded scale a doublet in the Q^1 region and a triplet in the Q^2 region. These multiplets have the same splitting magnitude, and mutual homonuclear decoupling experiments reduce them to singlets. It is clear that they represent a first-order AX_2 spin system and assignment to the linear trimer, $Q^1Q^2Q^1$ (VIII), is indicated. Figure 6 also shows a first-order pattern, which is attributed to a substituted cyclic trimer, IX (see Figure 7), the existence of which had

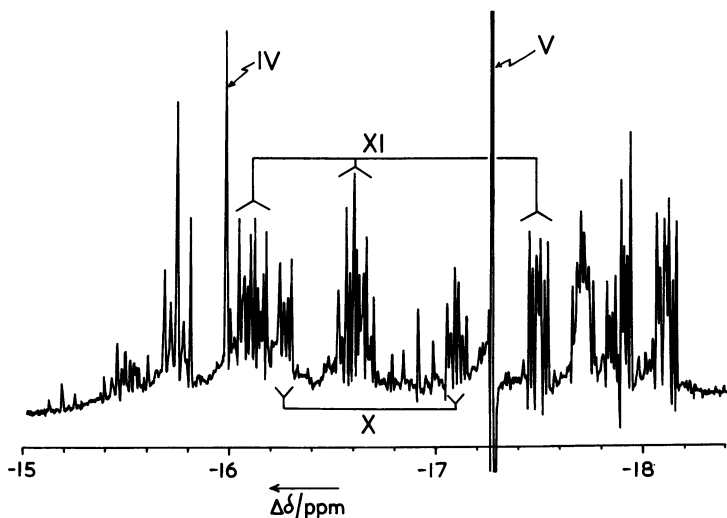


Figure 4. High-field (11.75 T) ^{29}Si NMR spectrum of alkaline aqueous potassium silicate solution with atomic ratio $\text{K}:\text{Si} = 1.0$ and concentration ~ 1.4 M in Si using sample enriched in ^{29}Si to 95.3%. Only D and E regions are shown. Resolution enhancement by computation was used. Strongest peak, due to species V, is not taken to its full height. Assignments to species mentioned in text are given; bands due to Si sites in same molecule were linked by double-resonance experiments. Conditions are the same as Fig. 3. Irradiation frequency increases to the left.

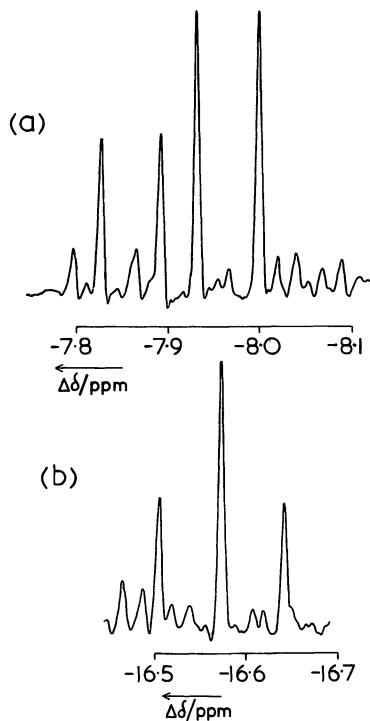


Figure 5. Scale expansions for parts of bands B and D for spectrum of sample discussed in Ref. 7, showing peaks due to linear trimer, VIII. Key: end group (Q^1) region (band B) (a); and middle group (Q^2) region (band D) (b). The most intense doublet is assigned to VIII in (a). Coupling constant is 6.9 Hz. Conditions are the same as Fig. 3. Irradiation frequency increases to the left.

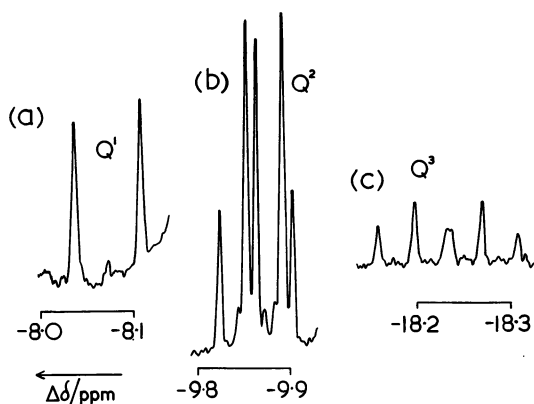


Figure 6. Scale expansions for parts of bands B, C and E of sample discussed in Ref. 7, showing the first-order pattern of peaks due to substituted cyclic trimer, IX. Key: band B (a); band C (b); band E (c). The intense doublet is assigned to IX in (b). Conditions are the same as Fig. 3. Irradiation frequency increases to the left.

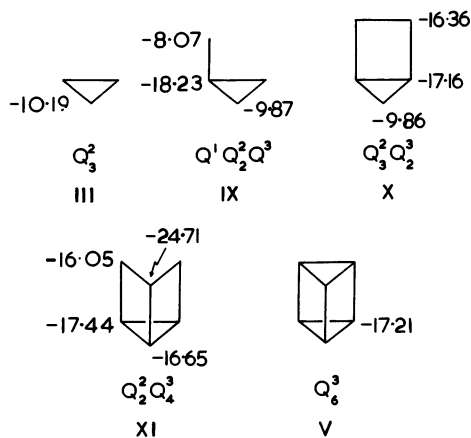
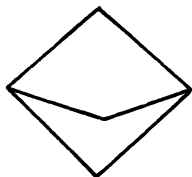


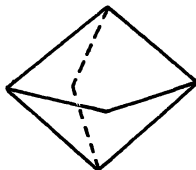
Figure 7. Identified series of species containing three-membered rings in solution giving spectrum of Fig. 4. Vertices in diagrams indicate positions of silicon atoms, which are bridged by oxygens. Additional oxygens (or OH groups) are present as required for valency fulfillment. Chemical shifts are given in ppm with respect to signal due to monomer resonance on high-frequency-positive convention, as obtained (7) for solution of alkaline aqueous potassium silicate with atomic ratio $K:Si = 1.0$ and concentration 0.65 M in Si.

been tentatively suggested earlier (6). The suggestion had been greeted sceptically by some silicate chemists on the grounds (i) that the cyclic trimer itself was thought (13, 14) to be unstable, and (ii) stable species were expected (15) to contain similar units (as opposed to the mixture of Q^1 , Q^2 and Q^3 in IX). The confirmation of the existence of IX is therefore important, particularly because it enables the unsplit line at $\Delta\delta = -10.19$ ppm to be assigned with confidence to the cyclic trimer itself on the grounds of its proximity to the peak due to the Q^2 units of IX. Our studies (7, 10) enable us to identify two further species, X and XI, containing three-membered rings. These two structures give rise to second-order spectra, and details of the spectral analysis will be given elsewhere. Moreover, the shifts for Q^3 units in the three-membered rings of X and XI enable us to suggest that the species giving rise to the singlet at $\Delta\delta = -17.21$ ppm for the enriched solution is due to the prismatic hexamer V. A connected series of species involving three-membered rings, shown in Figure 7, is therefore established.

Two novel species, XII and XIII, have also been identified in the ^{29}Si -enriched potassium silicate solution, as described in ref. (7). The chemical shifts of these species are unusual, probably indicating structural strains.



XII



XIII

Altogether, then, we believe we have positively identified twelve silicate ion species in KOH/SiO_2 solution. The particular sample was 0.65 M in SiO_2 with a ratio $\text{K}:\text{Si} = 1:1$. We cannot be absolutely certain of the existence of some of these species, but our confidence is at least at the 80% level. There are also a number of species for which we believe our spectra show some evidence, though there are either possible anomalies (of relative intensity or chemical shift), or the available sensitivity or resolution is not quite adequate for positive assignment. In spite of our lack of definitive evidence, we list these "possible" species in Figure 8.

The nature of the twelve species positively identified indicates a predilection for rings and cages, especially those involving three- and four-membered rings (whether in cages or not). We have not found any of the cages which may be considered as basic building blocks of zeolites, except for the cubic octamer, but we

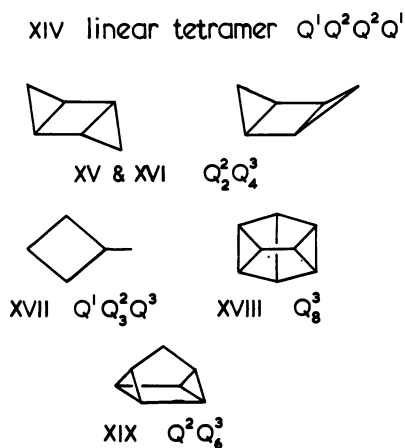


Figure 8. Additional species which may be present in solution giving spectrum of Fig. 4. Evidence for existence of these species is not definitive.

cannot exclude the existence of such species in our sample, because a number of bands are still unidentified.

Of course, once species are positively identified for one ^{29}Si -enriched solution, variations in their shifts and/or intensities can in principle be followed when parameters such as cation, pH, concentration and temperature are varied, though this procedure is not always easy in practice because of the difficulty of obtaining reproducibility of solution conditions for silicates. Experiments have been carried out on tetraalkylammonium silicates (9, 11, 12), and Figure 9 shows a spectrum of a $\text{Me}_4\text{NOH}/\text{SiO}_2$ solution using enriched ^{29}Si . It can be seen that the distribution of species is very different from that for the KOH/SiO_2 solution described above. For the tetramethylammonium case, the cubic octamer gives easily the most prominent peak in the spectrum, which is consistent with the fact that this species can be crystallised from such solutions (16).

Before concluding this article, it is worth mentioning very briefly the information available from ^{29}Si NMR on silicate solutions at low pH. The work described so far relates to highly alkaline solutions, where oligomeric species exist in equilibrium. At low pH, in contrast, oligomeric species condense to form gels, but the rate of this process is sufficiently slow (10, 17-20) that the kinetics can be followed by ^{29}Si NMR. The procedure is to form moderate initial concentrations of oligomers, usually by hydrolysis of a suitable compound, typically an alkoxy system. Figure 10 shows three typical spectra formed by the hydrolysis of tetramethoxysilane, and Figure 11 shows a plot of the second-order rate constants for dimerisation, deduced from initial changes in monomer concentration, as a function of the concentration of added HCl. The monomer stability is greatest below $[\text{HCl}] = 10^{-3.5}$ mol dm^{-3} , but as Dent Glasser et al. have shown (21) this does not correlate with the stability of the solution against gel formation.

Conclusions

In spite of the low inherent sensitivity of ^{29}Si NMR, it is a very valuable tool for the study of the species present in aqueous silicate solutions. Firm deductions about the chemical structure of such species can only be made using systems enriched in ^{29}Si . With the methodology described above, we have positively identified twelve species in an alkaline potassium silicate solution. Kinetic information is available in acid silicate solutions. Our experimental procedures are outlined in references (6-9, 20). This article is not intended as a comprehensive review of the area, but the list of references, including ref. (22) (hitherto unmentioned), covers all currently published work.

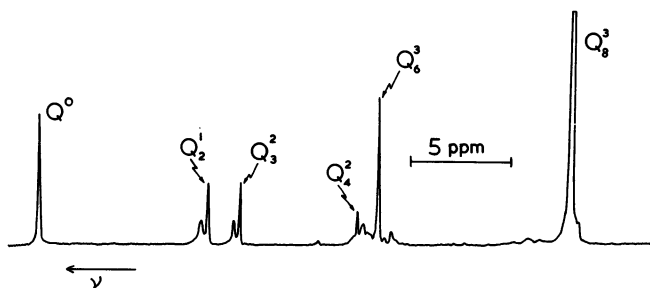


Figure 9. ^{29}Si NMR at 79.5 MHz and 5°C of alkaline aqueous tetramethylammonium silicate solution (9) with atomic ratio $\text{N}:\text{Si} = 1.0$ and concentration $\sim 2\text{ M}$ in Si . Sample was enriched in ^{29}Si to 95.3%. Peak assignments are indicated. Peak due to cubic octamer is not taken to its full height. Measurements show this peak is ca. 12 times as intense as that of monomer. (Reproduced, with permission, from Ref. 9. Copyright 1981.)

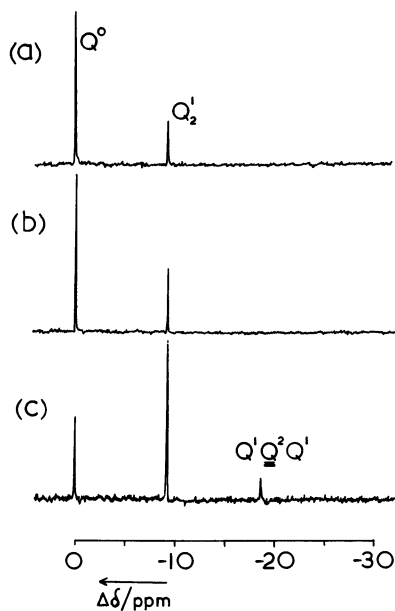


Figure 10. ^{29}Si NMR spectra at 19.87 MHz of acid aqueous methanolic solution of silicic acids (1.5 M in Si), obtained from hydrolysis of $\text{Si}(\text{OMe})_4$. Hydrochloric acid was incorporated to a concentration of 10^{-3} mol/dm^3 . Times in minutes between hydrolysis and end of spectral accumulation are 32 (a), 64 (b), 395 (c). Accumulation times were 10, 14, and 20 min respectively. Solution was maintained at -13°C throughout the experiment. Conditions are the same as Fig. 3. Irradiation frequency increases to the left.

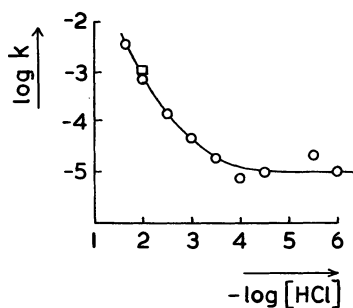


Figure 11. Second-order rate constant for dimerization of monosilicic acid under conditions typified by solution giving spectra shown in Fig. 10 as function of hydrochloric acid concentration. Result (\square) due to Engelhardt et al. (17). Solutions are effectively buffered below $[\text{HCl}] = 10^{-3.5} \text{ mol/dm}^3$.

Acknowledgments

We are grateful to Unilever Research Ltd. for financial support in the form of a Research Studentship for one of us (CTGK), and to the U.K. Science and Engineering Research Council for funds to purchase the ^{29}Si -enriched material.

Literature Cited

1. Marsmann, H.C., *Chemiker-Zeitung* 1973, 97, 128.
2. Marsmann, H.C., *Z. Naturforsch.* 1974, 29b, 495-9.
3. Engelhardt, G.; Jancke, H.; Hoebbel, D.; Wieker, W., *Z. Chem.* 1974, 14, 109-110.
4. Gould, R.O.; Lowe, B.M.; MacGilp, N.A., *J.C.S. Chem. Comm.* 1974, 720-1.
5. Engelhardt, G.; Zeigan, D.; Jancke, H.; Hoebbel, D.; Wieker, W., *Z. anorg. allg. Chem.* 1975, 418, 17-28.
6. Harris, R.K.; Newman, R.H., *J.C.S. Faraday II* 1977, 73, 1204-15.
7. Harris, R.K.; Knight, C.T.G.; Hull, W.E., *J. Am. Chem. Soc.* 1981, 103, 1577-8.
8. Harris, R.K.; Jones, J.; Knight, C.T.G.; Pawson, D., *J. Mol. Struct.* 1980, 69, 95-103.
9. Harris, R.K.; Knight, C.T.G., *J. Mol. Struct.*, to be published (1981).
10. Knight, C.T.G., Ph.D. thesis, University of East Anglia 1982.
11. Lippmaa, E.; Mägi, M.; Samoson, A.; Engelhardt, G.; Grimmer, A.-R., *J. Am. Chem. Soc.* 1980, 102, 4889-93.
12. Hoebbel, D.; Garzó, G.; Engelhardt, G.; Ebert, R.; Lippmaa, E.; Alla, M., *Z. anorg. allg. Chem.* 1980, 465, 15-33.
13. Iler, R.K., "The Chemistry of Silica", John Wiley & Sons, New York 1979, page 216.
14. Glidewell, C., *Inorg. Chim. Acta* 1977, 25, 77.
15. Dent-Glasser, L.S.; Lachowski, E.F., *J.C.S. Dalton* 1980, 399-402.
16. Hoebbel, D.; Wieker, W., *Z. anorg. allg. Chem.* 1971, 384, 43-52.
17. Engelhardt, G.; Altenburg, W.; Hoebbel, D.; Wieker, W., *Z. anorg. allg. Chem.* 1977, 428, 43-52.
18. Engelhardt, G.; Altenburg, W.; Hoebbel, D.; Wieker, W., *Z. anorg. allg. Chem.* 1977, 437, 249-52.
19. Hoebbel, D.; Garzó, G.; Engelhardt, G.; Till, A., *Z. anorg. allg. Chem.* 1979, 450, 5-20.
20. Harris, R.K.; Knight, C.T.G.; Smith, D.N., *J.C.S. Chem. Comm.* 1980, 726-7.
21. Dent-Glasser, L.S.; Smith, D.N., *J.C.S. Chem. Comm.* 1980, 727-8.
22. Engelhardt, G., *Z. Chem.* 1975, 15, 495-6.

RECEIVED March 2, 1982.

Colloidal Components in Solutions of Sodium Silicate

RALPH K. ILER

Wilmington, DE 19809

In concentrated solutions of sodium silicate with $\text{SiO}_2:\text{Na}_2\text{O}$ ratios ranging from 2:1 to 4:1, about 75% of the silica is present as extremely small particles which increase from 1 to 2 nm in diameter with increasing ratio. It is suggested that the ionized surface of the particles is covered with an adsorbed monolayer of hydrated sodium ions. The alkali thus limits the specific surface area and determines the size. These colloidal particles are in equilibrium with monomeric and oligomeric silicate ions containing up to about 8 silicon atoms. When the solutions are diluted, there is instant partial depolymerization and rearrangement. These conclusions are based on a study of the corresponding silicic acids liberated in dilute solution at pH 1.7 by sudden acidification of the silicate. Characterization involved measuring the rates of reaction with molybdic acid. In one sample the particle size was confirmed by ultrafiltration. The colloidal particles were separated from monomer and oligomers by extraction into tetrahydrofuran which was salted out of the sol.

In solutions of sodium silicates, as the molecular or weight ratio of $\text{SiO}_2:\text{Na}_2\text{O}$ increases from 2:1 to 4:1, there is a corresponding increase in the proportion of silica present as highly "polymeric" or "colloidal", negatively charged species (1). Similar conclusions by numerous investigators were summarized by Iler (2). In equilibrium with monomeric and higher polymeric colloidal species, there are oligomers containing 2 to 10 silicon atoms (3,4) which have been characterized by NMR (5,6). By ultracentrifuging silicate solutions of different ratios Aveston (4) found degrees of

polymerization, (DP), up to 27. For 3.3 ratio, a DP of 10 corresponds to SiO_2 particles 1.2 nm in diameter.

The rate of reaction with molybdcic acid has been used as a way to characterize soluble silicates (7). Only monomeric silicic acid, $\text{Si}(\text{OH})_4$, reacts with molybdcic acid to form the yellow silicomolybdcic acid. Oligomers and colloid must first depolymerize or dissolve. This occurs slowly enough at pH about 1.5 to permit the rate of development of the color to be recorded. Hoebbel and Wieker (8) have related the reaction rate constant to the molecular weight of the polysilicic acid; Iler (9) reviewed the method and results and related the molecular weight to the particle size (10). O'Connor (11) related the reaction rate to the molecular weight by light scattering. Electron Micrographs by McGarry and Hazel (15) showed the presence of 1 to 2 nm particles in freshly diluted silicates which grew slowly in size. From pH and concentration data on 3.36 ratio sodium silicate solutions reported by Bacon and Wills (12, 13) Iler (14) calculated the concentration of monomer to be 474 ppm as SiO_2 which corresponds to the solubility of amorphous silica particles about 2 nm in diameter.

The proportions of different silicate species change when the solution is diluted (11, 16). Most studies have involved dilution and concentrated solutions have received little attention.

EXPERIMENTAL

Both concentrated and somewhat diluted solutions of sodium silicates of different ratios were examined by suddenly injecting samples into rapidly stirred dilute H_2SO_4 to convert the ionized species to the corresponding silicic acids. These were at once characterized by reaction with molybdcic acid. Also colloidal species were separated from monomer and oligomers by extraction into tetrahydrofuran (THF).

The term "colloid" is defined as matter in a state of subdivision from 1 to 100 nm in diameter (17). Silicic acid oligomers are linear and cyclic structures generally smaller than 1 nm. The smallest three-dimensional polymers having internal siloxane bonds and exterior silanol groups are about 1 nm in diameter (18) and are thus the smallest possible colloidal particles.

The term "polymer" includes oligomers as well as particulate colloidal species and excludes only the monomer.

Materials: Commercial silicates obtained from the PQ Corp. and E. I. DuPont de Nemours and Co. are listed in Table I. These were diluted to have a uniform viscosity of about 100 cps. and aged 3 months at 25°C. In some cases these were also diluted to about 1.0 M SiO_2 (60 g l^{-1}) and aged.

Table I
Commerical solutions of sodium silicate

SiO ₂ :Na ₂ O (by weight)	SiO ₂ Original Conc.		SiO ₂ Final Conc.
	%	g l ⁻¹	g l ⁻¹
3.75	25.3	331	314
3.22	28.7	396	365
2.88	31.7	466	374
2.40	33.2	514	378
2.00	29.4	450	371
1.60	31.5	526	331

Conversion to silicic acids: The general method has been described (10, 19). The sample of concentrated silicate solution (about 5 M SiO₂) in a syringe was injected suddenly into the vortex of a cooled (0-5°C) dilute solution of H₂SO₄ in a blender. The volume and concentration of acid was such as to result in a sol at pH 1.7 and at a concentration of not over 100 mM SiO₂ (6000 ppm). This requires enough acid to convert the alkali to NaHSO₄ and leave 0.02 N free acid. Unlike monomer which is most stable at about pH 3, silicic acid from these commerical silicates polymerizes least rapidly at pH 1.7 - 1.8 since colloidal nuclei are already present.

Reaction with molybdic acid: This reagent is prepared as follows: A stable stock solution of ammonium molybdate is prepared containing 100 g l⁻¹ of (NH₄)₆Mo₇O₂₄·4H₂O and 47 ml l⁻¹ of ammonium hydroxide (28% NH₃). The molybdic acid reagent is made by mixing 100 ml of the stock solution, 500 ml of distilled water and 200 ml of 1.5 N H₂SO₄. To 20 ml of this reagent is added no more than 5 ml of sample solution containing from 0.01 to 1.0 mg of SiO₂. The volume is diluted to 25 ml and the color measured at 410 nm. A standard containing 1.0 g l⁻¹ of monomeric silica is used (20). The reagent begins to deteriorate after about 3 days. The data are plotted as log₁₀ percent of unreacted silica versus minutes at 25°C.

Typical data graphs are shown in Figure 1. Calculation of the first order rate constant, k , has been described (10, 21).

O'Connor pointed out that the yellow color slowly fades. In current work, in reactions that were followed for more than 50 minutes a correction of 3.5% per hour was added for up to 2 hours.

Rough estimates of the distribution of silica among monomer, oligomers and colloid can be made from the reaction curves as in Figure 2. Monomer reacts in 2 minutes; polymer is estimated by extrapolating the later straight portion of the

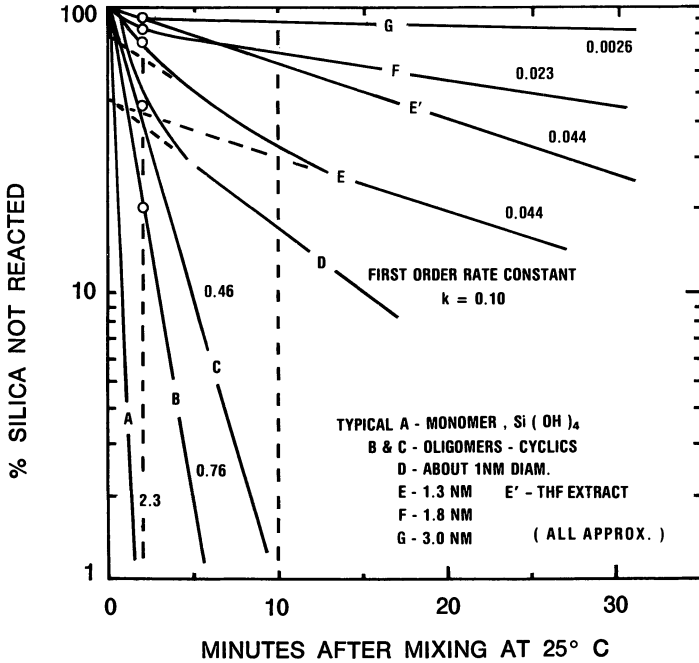


Figure 1. Typical data graphs for reaction of molybdic acid with silicic acid monomer, oligomers, and small colloidal particles. Line E' for polymer that was extracted from sol E extrapolates through 100% untreated silica, thus indicating no monomer is present. Slope of E' is the same as that of E after 20 min, showing that the polymer reacts the same as before being extracted. Particle diameter of the colloid is estimated from k, assuming anhydrous SiO₂ particles. (Reproduced, with permission, from Ref. 10. Copyright 1980, Academic Press.)

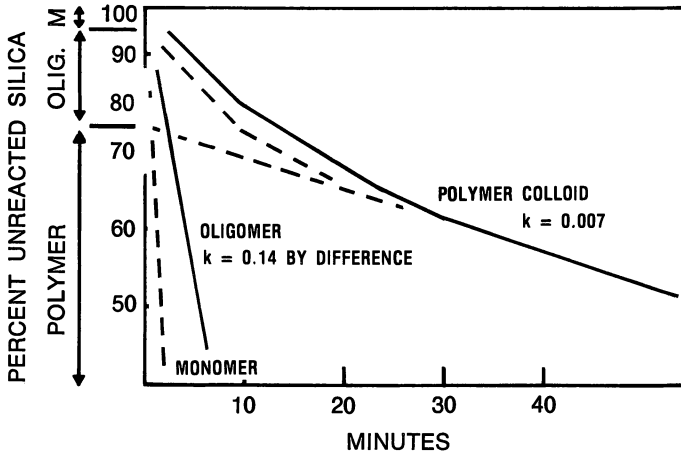


Figure 2. Silicomolybdate reaction: estimation of monomer, oligomer, and polymer colloid and first order reaction constant k.

line to zero minutes. The difference is oligomer. The percentage of the oligomer that remains unreacted is plotted as a second line. The values of k are estimated from the slope.

The relation between k and the calculated particle diameter, d , is shown in Figure 3 (10, 22).

$$\log_{10}d = -0.250 - 0.257 \log_{10}k$$

Aging of silicic acid sols: To characterize the silicate species in sodium silicate solutions, the silicic acid liberated therefrom must be examined promptly. At a silica concentration of 100mM SiO₂ at pH 1.7, 25°C, measurable change begins in about 30 minutes. The sol must be examined within this time.

In such dilute solutions, changes involve the dissolution and desposition of soluble silica, i.e. monomer, Si(OH)₄, until a temporary solubility equilibrium is reached with the solid phase, i.e. the colloidal particles.

Solubility increases rapidly with decreasing particle diameter (Figure 4). This fact plays a key role in the behavior of this system.

The colloidal silicic acid from the corresponding species in the silicate solution is in the size range of 1 to 2 nm and there is undoubtedly some distribution about an average size. This is accompanied by some monomer and oligomers. When the acid sol is formed at pH 1.7 several things can happen: (a) If the monomer concentration exceeds the solubility of the particles they grow in size and monomer is consumed. (b) If monomer concentration is less than this solubility, the particles dissolve, starting with the smaller ones; it should be noted that once a particle begins to dissolve it becomes smaller and thus ever more soluble and quickly disappears. (c) Larger particles continually grow at the expense of monomer, oligomers and smaller particles.

At higher concentrations and lower or higher pH, particles begin to aggregate and eventually form a precipitate or gel. This further complicates the study of this system by present methods. However, under the conditions of this study aggregation did not occur.

As solubility equilibrium is approached, the monomer concentration rises to the solubility of the colloidal particles. Since the reaction rate with molybdic acid, expressed as k , is related to the particle size, then in aged sols there arises a relation between k and the concentration of monomer. Iler has shown a linear relation between $\log k$ and \log monomer concentration, providing equilibrium has been approached (23).

Extraction of colloidal polymer into THF This technique has been described (10) and the theory reviewed by Iler (24). The

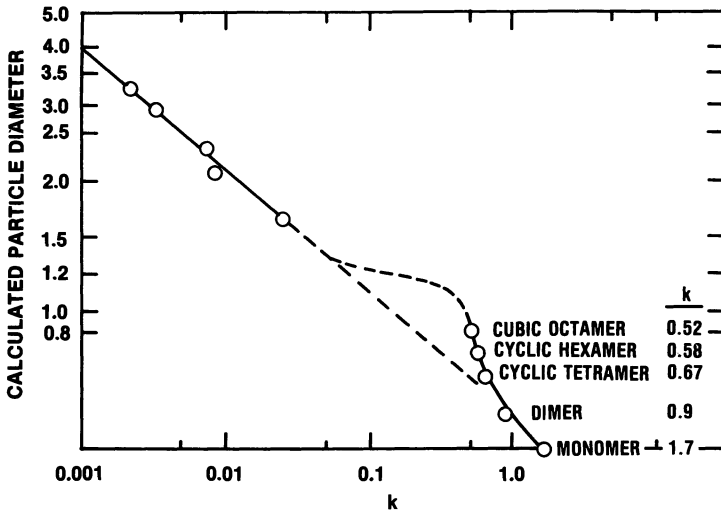


Figure 3. Particle diameter in nanometers, assuming anhydrous SiO_2 spherical particles, calculated by Iler from data relating molecular weight and the silicomolybdate first order reaction rate constant, k , by Hoebbel and Wieker (5).

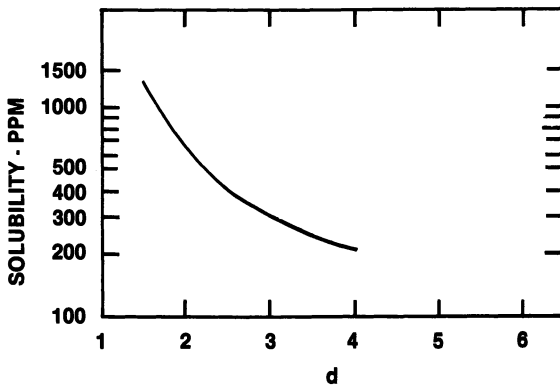


Figure 4. Solubility S_d of amorphous silica in water vs. particle size. Key: d , particle diameter in nanometers; S_i , solubility of particle of infinite diameter, assumed to be 70 ppm; E , ergs/cm²; 298 K; and $\log_{10}(S_d/S_i) = 5.7 E/Td$.

sol sample is mixed with an equal volume of THF and the clear solution saturated with fine sodium chloride. A second upper liquid layer of THF separates at once. After standing for 10 minutes (or centrifuging) the THF layer is recovered, analyzed for SiO_2 and samples reacted with molybdic acid. The silica is much more stable in THF than in water.

Ultrafiltration: This was tried with only one sol; more work is planned. A 200 ml Amicon magnetically stirred ultrafilter was used with 25 psi air pressure. The membranes were 62 mm diameter with reported pore diameters as follows: Nucleopore Corp., Pleasanton, Calif: - Type 1C7452, C-500, 0.9 nm; Type 1C7453, C-1000, 1.3 nm; Type 1C7457, C-20,000, 2.0 nm. Amicon Corp. Lexington, Mass.: Type UM 10, 1.5 nm.

Ultrafiltrations were conducted at about 5°C over periods of up to an hour. The filtrates and concentrates in the filter were analysed and silicomolybdate curves run at once.

Results

Effects of diluting silicate solutions: Before proceeding to the main experiments involving silicic acid solutions made from silicates by methods already described, some preliminary tests were made by injecting samples of the higher ratio silicates directly into the molybdic acid reagent. In this case very small samples of one to ten microliter volumes were injected suddenly into rapidly stirred molybdic acid solution and the development of the yellow color recorded.

By this method concentrated silicate solutions (6 M SiO_2) were compared with the same silicates that had been diluted with water at 0°C to silica concentrations of 0.33 and 0.6 M within 5 minutes before being added to the molybdic acid.

A major difference was noted in the monomer content, i.e. the percent of silica that reacted in two minutes. The concentrated silicates with $\text{SiO}_2:\text{Na}_2\text{O}$ ratios of 3.2 and 3.75 contained 11±2% monomer. The freshly diluted silicates contained about 23% monomer. For comparison, samples of the diluted silicates were also converted to dilute silicic acids, as previously described, and were also found to contain about 23% monomer.

It is clear that when concentrated solutions of silicates are diluted, more monomer is released almost instantly into the solution. Thus the nature of silica in concentrated silicate solutions cannot be determined from diluted samples.

This direct injection method was abandoned because such small volumes of concentrated, viscous silicate solutions were difficult to measure and dilute reproducibly into the molybdic acid. Also samples of the corresponding silicic acids were needed for the extractions into THF and for ultrafiltration studies.

Silicic acid solutions prepared from silicates

It is believed that the fresh dilute silicic acid solution at pH 1.7, prepared by the described method, represents the silicate species found in the silicate solution from which it was made. In the following experiments concentrated silicate solutions were compared with diluted and aged solutions as sources of silicic acids. Also silicic acids prepared at two different concentrations were compared. As a matter of side interest, the changes that were observed in silicic acid solutions as they were aged at 25° C were also noted.

Dilute silicic acids (16.6 mM SiO₂) from concentrated silicates (5M Si)₂

Results are shown in Figures 5, 6 and 7 and Table II. In Figure 5 data are shown only for silicic acids from only the three highest ratio silicates. In Figures 6 and 7, data are given from all six ratios of silicates.

In the freshly made solutions the state of polymerization of silicic acid corresponds to that in the silicate used and led to the following conclusions:

- (a) The colloid fraction, estimated by extrapolating the linear portions of the curves to zero time, was about 75% of the total silica in all ratios of silicates. (Figure 7, line A)
- (b) The concentration of monomer increased with increasing alkalinity, in silicate ratios less than 3.0 (Figure 6, line A)
- (c) The calculated diameter of the colloidal particles decreased from 2.3 to 1.7 nm with increasing alkalinity or lower ratio. (Table II)

Aged solutions of the silicic acids no longer reveal the nature of the silicate from which they were made. The characteristics of sols aged at 25° C for 10 days are shown in Figures 5, 6 and 7. The concentrations of monomer increased greatly (Figure 6). The particle size of the colloid increased as shown by the lower slopes of the lines in Figure 5. However in Figure 7 the percentage of colloid decreased as smaller particles dissolved and larger ones increased in size.

The concentrations of monomer in these aged sols appear to correspond to the solubility of the colloidal particles. Values of k , calculated from the slopes of lines B, D, and F in Figure 5, give particle diameters from Figure 6 from which the solubilities can be estimated from Figure 4. The calculated solubilities were found to be in the same range as the concentrations of monomer shown by line B of Figure 6.

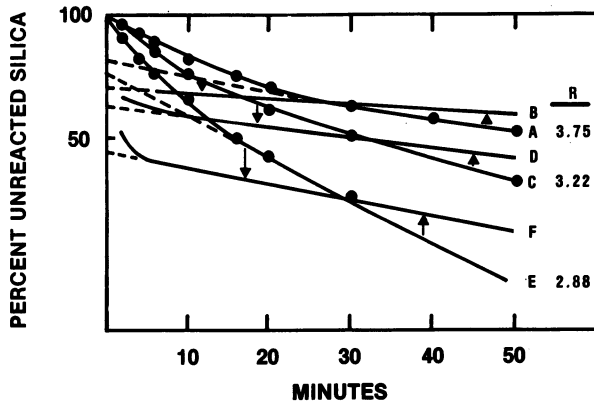


Figure 5. Silicomolybdate reaction data for silicic acids, 16.6 mM SiO_2 ; pH 1.7; 25°C, made from sodium silicates, 5 M SiO_2 ; ratios (R) indicated; A, C, and E sols aged 1 min; and B, D, and F aged 10 d at 25°C.

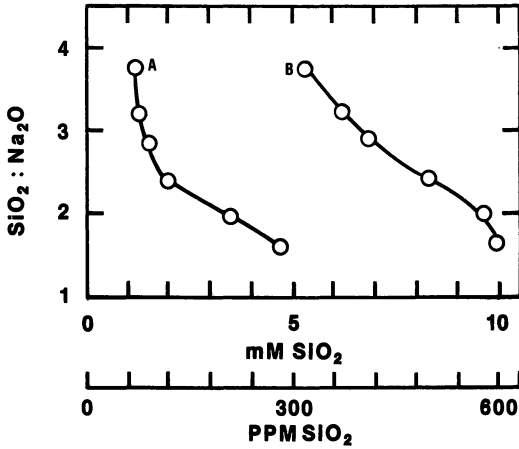


Figure 6. Monosilicic acid, reacted with molybdic acid in 2 min, in silicic acid sols made from concentrated (5 M SiO₂) sodium silicate solutions. Conditions: pH 1.7; 116.6 mM SiO₂ aged 5 min (A) and 10 d (B). Silicate ratios indicated.

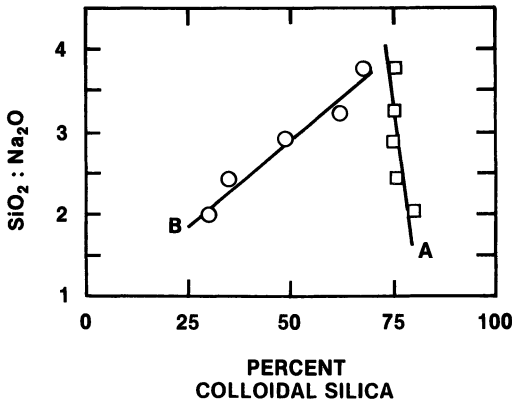


Figure 7. Colloidal silica contents of silicic acid sols determined by extrapolating the linear portion of silicomolybdate reaction curve to zero time. Sol made from concentrated (5 M SiO₂) sodium silicate. Conditions: pH 1.7; and 16.6 mM SiO₂ aged 5 min (A) and 10 d (B).

Dilute silicic acids (16.6 mM SiO₂) from diluted silicates (1.0 M)

For comparison with the above silicic acids from concentrated silicates, samples of the same silicates were diluted from 5 M to 1.0 M and aged at 25° C for 3 months. Then dilute sols of silicic acids were prepared from these and examined with results shown in Figures 8, 9 and 10.

The reaction data curves A, B and C in Figure 8 for the sols from diluted silicates are entirely different from the counterpart curves A, C and E in Figure 5 for sols made from concentrated silicates. Obviously the silicic acids from diluted silicates reacted much more rapidly with molybdc acid and thus consist of smaller particles.

Comparison of concentrated and diluted silicate solutions

In Table II the percent of silica present as colloid was determined by extrapolating the linear portions of the reaction data curves of Figures 5 and 8 to zero time as demonstrated in Figure 2. The values of k were calculated from the slopes of these lines and the particle size estimated from k according to Figure 3.

In these three silicates of highest ratios, the percentage of silica present as colloid appeared to be somewhat higher in the dilute solutions. However the particles are smaller than those in the concentrated solutions and some oligomers may have been included in the estimated colloids.

Table II

Silicic acids from
concentrated and diluted silicate solutions.

SiO ₂ :Na ₂ O Ratio	<u>Figures 5,6,7</u>			<u>Figures 8,9,10</u>		
	Silica from Concent. Silicate (5M SiO ₂)			Silica from Diluted Silicate (1.0 M SiO ₂)		
<u>w/w</u>	<u>% colloid</u>	<u>k of colloid</u>	<u>d nm calc.</u>	<u>% colloid</u>	<u>k of colloid</u>	<u>d nm calc.</u>
3.75	76±2	0.007	2.3	83±2	0.050	1.3
3.22	77	0.014	1.9	85	0.071	1.25
2.88	76	0.025	1.7	85	0.095	1.2

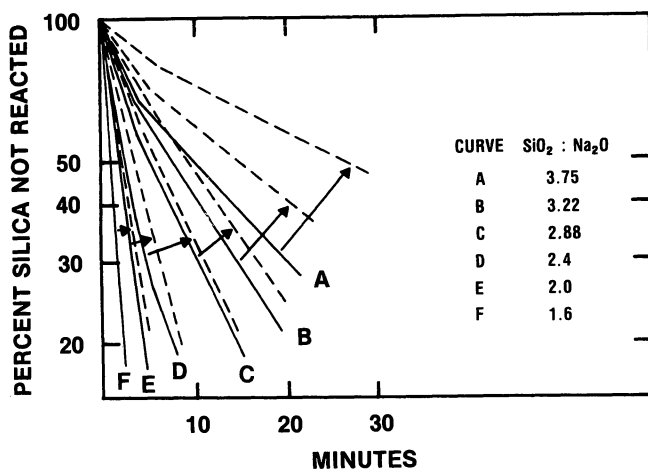


Figure 8. Silicomolybdate reaction data for silicic acid sols made from diluted silicate solutions. Silicic acids of 16.6 mM SiO₂; pH 1.7; 25°C; aged less than 15 min. Silicate solutions diluted from 5–1 M SiO₂, aged 3 mo at 25°C. Dashed lines are for polymeric silica extracted into THF within 15 min.

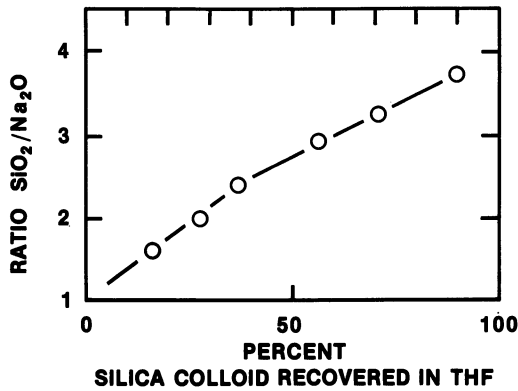


Figure 9. Percent of silica recovered in THF from sols of Fig. 8, aged 5 to 10 min.

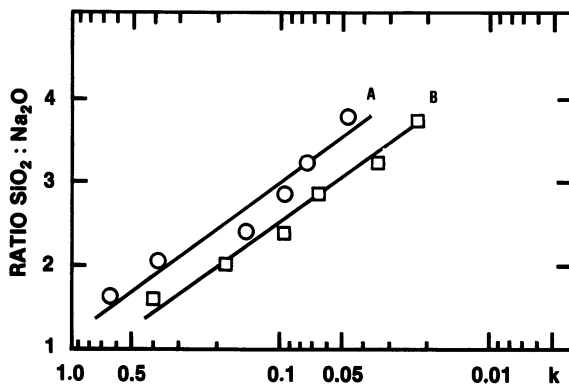


Figure 10. Silicomolybdate reaction rate constant k vs. $\text{SiO}_2:\text{Na}_2\text{O}$ ratio of silicates used. Key: A, silicic acid, 16.6 mM SiO_2 , pH 1.7, aged 1 min at 25°C, made from sodium silicate solutions diluted from 5-1 M SiO_2 , aged 3 mo at 25°C; and B, colloidal silica in THF extracted from A.

More concentrated silicic acids (100 mM SiO₂) from concentrated (5-7 M SiO₂) silicate: Figures 11 and 12 supplement and extend the data of Figures 5 to 7, also from concentrated silicates, but in this case the silicic acids are six times as concentrated. Nevertheless the fresh silicic acids are quite similar as shown by comparing sols from the three highest silicate ratios:

SiO ₂ :Na ₂ O Ratio	Sol Conc. 16.6 mM SiO ₂		Sol Conc. 100 mM SiO ₂	
	w/w	k of colloid d nm	k of colloid	d nm
3.75	0.007	2.3	0.012	2.0
3.22	0.014	1.9	0.020	1.7
2.88	0.025	1.6	0.037	1.4

The slightly larger particle sizes in the more dilute sols is probably not significant.

No data are given for these more concentrated sols after they have aged because aggregation and incipient gel formation begins more quickly than in the dilute sols and the characterization methods do not apply.

Extraction of colloidal silica into THF

Extraction experiments were carried out on (a) the dilute silicic acid sols (16.6 mM SiO₂) made from diluted silicates (Figures 8, 9, 10) and on (b) the more concentrated sols (100 mM SiO₂) made from concentrated silicates (Figures 11, 12).

(a) In the sols from diluted silicates the percentage of silica extracted into THF (Figure 9) increased almost linearly from zero percent at a ratio of 1.0, by extrapolation, to 100% at ratio of 4.0, the highest ratio at which concentrated solutions of sodium silicate are stable. Thus the monosilicic acid from metasilicate was not extracted while all the silica at 4.0 ratio would be colloidal and extractable.

The value of k of the extracted silica, by extrapolation, (Figure 10, line B) ranged from 0.3 at ratio 1.0 where silica just begins to be extracted, to about 0.018 at ratio 4.0 where theoretically all of the silica should be extractable. These k values, according to Figure 3, correspond to a minimum particle size of about 0.8 nm up to 1.7 nm.

Thus as the ratio exceeds 1.0, there is an increasing proportion of silica present as colloidal particles of increasing size.

(b) In the silicic acid sols made from concentrated silicates, the colloidal silica particles are larger than those

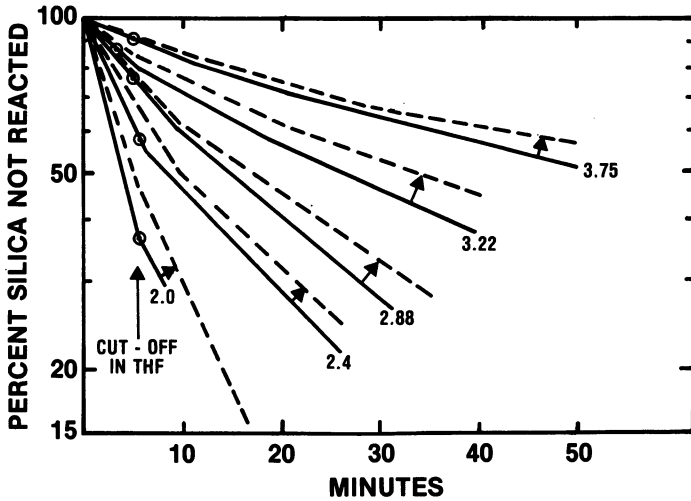


Figure 11. Silicomolybdate reaction data for silicic acid sols made from sodium silicate solutions of different indicated $\text{SiO}_2:\text{Na}_2\text{O}$ ratios. Silicic acids 100 mM SiO_2 , pH 1.7, aged 1 min at 25°C, made from concentrated sodium silicate solutions (5–7 M SiO_2), aged 3 mo at 25°C. Key: ---, reaction data for polymeric silica extracted into THF within 15 min; and O, percent of silica extracted into THF.

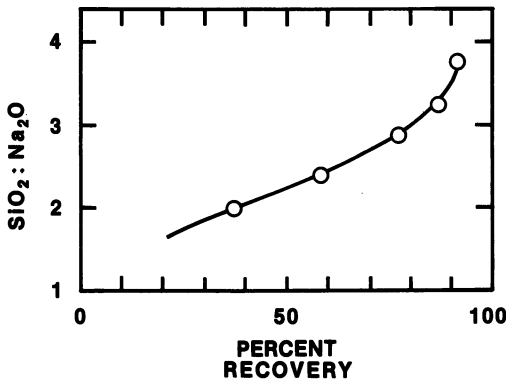


Figure 12. Recovery of silica in THF from silicic acid aged 1 min, 100 mM SiO_2 , pH 1.7, 25°C, prepared from concentrated 5–7 M SiO_2 , aged 3 mo at 25°C. Ratios of $\text{SiO}_2:\text{Na}_2\text{O}$ indicated.

from diluted silicates (Table II). The percentage of silica extracted into THF is higher as can be seen by comparing Figures 12 and 9. Also there is less difference between the k values of colloid in the sol and that extracted into the THF, as observed by comparing the differences between the dashed and solid lines of Figures 8 and 11. The data are as follows:

<u>SiO₂:Na₂O</u>	<u>SiO₂ recov. in THF</u>			<u>Colloid in sol (Fig. 11)</u>		
<u>Ratio</u>	<u>%</u>	<u>k</u>	<u>d nm</u>	<u>%</u>	<u>k</u>	<u>d nm</u>
3.75	92	0.008	2.2	92	0.012	2.0
3.22	87	0.016	1.8	87	0.020	1.7
2.88	83	0.032	1.5	77	0.037	1.4
2.4	75	0.042	1.4	48	0.048	1.3
2.0	37	0.080	1.2	-	-	-

The estimated percent colloid in the sols was based on extrapolation of the linear portions of the curves of Figure 11. For the lower ratios this extrapolation excluded smaller particles that are extractable into THF. Thus the value of 48% colloid shown for 2.4 ratio, is low.

Minimum particle size extracted by THF: When the percent of silica extractable into THF was marked by circles on the curves of Figure 11, they mostly fell on the abscissa at 6 minutes.

If 95% of the silica reacts in 6 minutes the corresponding value of k is about 0.5. According to Figure 3, this is close to the value for the cubic octamer, Si₈O₈(OH)₈. This suggests that silica that reacts in less than six minutes and is not extractable, consists of monomer and oligomers.

It should be noted that the cubic octamer is the smallest relatively stable three dimensional structure of polysilicic acid in which only one OH group is attached to each silicon atom on the surface. Such O₃SiOH groups are more acidic than the O₂Si(OH)₂ groups in the oligomers and thus more readily form hydrogen bonds with THF (25). Larger particles have a O₃SiOH surface and have additional SiO₂ in the interior.

Ultrafiltration: Tests have thus far been carried out only on one type of freshly prepared sols made from 3.25 ratio silicate by initially diluting the SiO₂ concentration from 5.9 to 0.59 M (350 to 59 g l⁻¹) at 0° C and at once adding this to enough dilute H₂SO₄ and ice in a blender to obtain a sol at 0° C, pH 1.7, 16.6 mM (1000 ppm) SiO₂. This was at once ultrafiltered through a membrane of selected pore diameter while the ultrafilter was surrounded by ice.

Depending on pore diameter and volume of sample, up to an hour was required in some cases to obtain sufficient filtrate to rinse the filtrate compartment and obtain samples for analysis yet leave sufficient sample on the filter for analysis containing under 4000 ppm SiO_2 to insure stability.

Silicomolybdate reaction curves are shown in Figure 13. In all cases water passed more rapidly than particles did, even when the pores were larger than the diameter of the particles. However when the pores were smaller than the size of most of the colloidal particles, the rate constants of the silica retained on the filter became smaller than the constants of the silica in the filtrate. This indicated that larger particles were being retained on the filter and that these were larger than the pores.

When filtration was stopped it might be assumed that the concentration of the undersized silica in the filtrate is about the same as in the sol remaining on the filter. If so, the fraction of oversize silica in the total sample may be calculated as shown below where C_F is the silica concentration in the filtrate, C_R in the sol still on the filter and R is the percentage of total silica that remains on the filter.

Ultrafiltration Data

UF PORE DIAM	ULTRAFILTRATE			CONCENTRATION ON FILTER			
	SiO_2 PPM C_F	% SiO_2 PASSED	RATE CONST k	SiO_2 PPM CR	% RET R	% OVER SIZE	RATE CONST k
0.9	225	--	0.12	1880	--	--	0.038
1.3	370	12	0.12	3600	88	81	0.047
1.5	690	56	0.065	1600	44	25	0.065
2.0	900	60	0.065	1250	40	11	0.065

$$\% \text{ OVERSIZE} = (C_R - C_F) (C_R)^{-1} R$$

Discussion

It may be possible to relate the size of the colloidal species in concentrated silicate solution to the $\text{SiO}_2:\text{Na}_2\text{O}$ ratio and the observed relative proportions of monomer, oligomer and three-dimensional colloidal species. It may be assumed that in concentrated solution:

(a) All of the sodium ions are combined with monomer, oligomer and the surface of colloid species.

(b) Sodium ions, $\text{Na}(\text{H}_2\text{O})_6^+$, exchange some of the H_2O for the oxygens of SiO^- and SiOH , and are thus held by coordination to the silicate species as ion pairs. (only in high concentrations).

(c) At the pH in 3.22 ratio silicate, only one Na^+ combines per Si atom in monomer and oligomers.

(d) On the surface of three dimensional polymers or colloids, the average population of Na^+ is 3.5 per nm^2 . (26)

On the basis of these assumptions the particle size of the colloidal species can be estimated:

From Table II, 3.22 ratio silicate contains 5.0 M SiO_2 and 3.0 N base or Na^+ . From the observed percentages of monomer, oligomer and colloid, the following concentrations are estimated: monomer- 0.4 M; oligomer- 0.75 M; colloid- 3.85 M (as SiO_2).

Of the 3.0 N Na^+ , 1.15 is combined with monomer and oligomer, leaving 1.85 N covering the colloid surface. This amount of Na^+ creates 11.1×10^{23} charge sites. Assuming 3.5 sites per nm^2 the area is $3.17 \times 10^{23} \text{ nm}^2$ or $3.17 \times 10^5 \text{ m}^2$. The weight of colloid is 3.85 M or $3.85 \times 60 \text{ g}$ so that the specific area is $1372 \text{ m}^2 \text{ g}^{-1}$. The corresponding diameter of SiO_2 particles is 2 nm. In Table II the diameter calculated from the rate constant k is 1.9 nm.

For 2.88 ratio silicate a corresponding calculation gives a diameter of 1.9 nm while the value from k was 1.7 nm.

These agreements are probably fortuitous but indicate at least the right order of magnitude for the size of the colloid. In the following section the size of the colloid in 3.25 ratio silicate appears to be 1.4 nm.

The equilibrium distribution of monomer, oligomers and colloid species in different ratios in concentrated solutions remains to be explained.

Particle size by ultrafiltration As shown by data in Figure 13, the particle size of the colloid in 3.25 ratio silicate (presumably the same as in 3.22 ratio) is about 1.4 nm. However the dependability of the stated values for the pore diameters is not known. On the other hand the rate constant for the particles that passed the filter was 0.12, corresponding to a diameter of 1.15 nm, while that of particles that did not pass was 0.038 and 0.047, corresponding to 1.4 and 1.35 nm. The agreement between a particle size of 1.4 nm from the pore diameters of the filters and about 1.15 to 1.4 nm from the reaction rate constants, is probably fortuitous.

Conclusion

In concentrated sodium silicate solutions with $\text{SiO}_2:\text{NaO}_2$ ratios from 2 to 4, about 75% of the silica is in the form of particles from 0.8 to 2.0 nm in diameter. The surface of the particles is probably saturated with adsorbed sodium ions. The particles are in equilibrium with smaller proportions of monomeric and oligomeric silicate ions which are also combined with sodium ions.

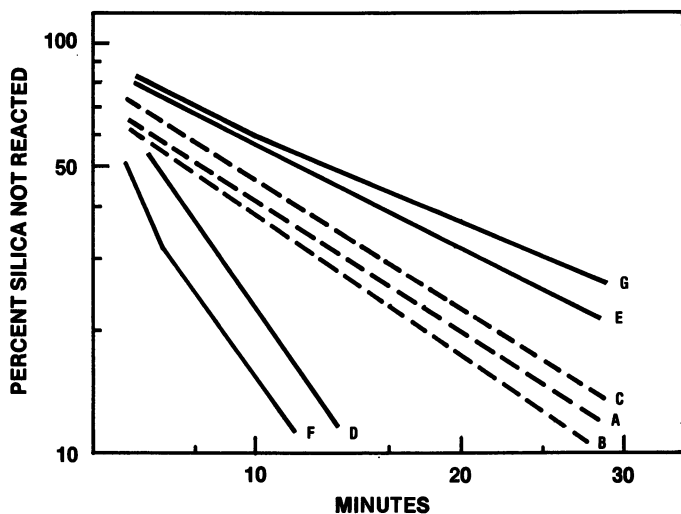


Figure 13. Silicomolybdate reaction data for silica in ultrafiltrates and concentrates using filters of known pore diameters. Sol 16.6 mM SiO_2 , made from concentrated sodium silicate (5 M SiO_2), pH 1.7 at 5°C, aged 5 min. Key: A, starting sol; B, filtrate; C, concentrate using 1.5 and 2.0-nm pore diameters; D, filtrate; E, concentrate using 1.3-nm pore diameter; F, filtrate; and G, concentrate using 0.9-nm pore diameter.

The ionized surface of the particles is possibly associated with the sodium ions as ion pairs. The amount of alkali thus determines the specific surface area and thus limits the particle diameter which varies inversely with $\text{SiO}_2:\text{Na}_2\text{O}$ ratio.

Literature Cited

1. Nauman, R.V.; Debye, P. J. Phys. Chem., 1957, 55, 1.
2. Iler, R.K. "The Chemistry of Silica". John Wiley and Sons; New York, 1979, pp 126-131.
3. Dent-Glasser, L.S.; Lachowski, E.E. J. Chem. Soc. Dalton, 1980, 393-8.
4. Aveston, J. J. Chem. Soc., 1965, 4444-8.
5. Engelhardt, G.; Altenburg, W.; Hoebbel, D.; Wieker, W. Z. anorg. allgem. Chemie 1977, 428, 43-52.
6. Harris, R.K.; Newman, R.H.; J. Chem. Soc., Farady II 1977, 1204.
7. Iler, R.K. "The Chemistry of Silica"; John Wiley and Sons: New York, 1979, pp 138-142.
8. Hoebbel, D.; Wieker, W. Z. Chem. anorg. allgem. Chemie, 1973, 400, 148-160, Figure 6.
9. Iler, R.K. "The Chemistry of Silica"; John Wiley and Sons: New York, 1979, 138-140; 262-8.
10. Iler, R.K. J. Colloid Interface Sci. 1980, 75, 138.
11. O'Connor, T.L. J. Phys. Chem., 1961, 65, 1-5.
12. Bacon, L.R.,; Wills, J.H. J. Franklin Inst. 1954, 258, 347.
13. Bacon, L.R.,; Wills, J.H. Soap Chem. Spec. 1954, 30, 85.
14. Iler, R.K. "The Chemistry of Silica" John Wiley and Sons: New York, 1979, pp 128-130.
15. McGarry, M.A.; Hazel, J.E. J. Colloid Sci. 1965, 20, 72.
16. Iler, R.K. "The Chemistry of Silica"; John Wiley and Sons: New York, 1979, pp 134-5, 139.
17. Hackh's Chemical Dictionary, 4th Edn. Julius Grant, Ed; McGraw Hill: New York, 1969.
18. Iler, R.K. "The Chemistry of Silica"; John Wiley and Sons: New York, 1979, pp 8, 217.
19. ibid p 137.
20. ibid p 101.
21. ibid pp 197-201.
22. ibid pp 265-8.
23. Iler, R.K. J. Colloid Interface Sci. 1980, 75, Figure 3.
24. Iler, R.K. "The Chemistry of Silica"; John Wiley and Sons: New York, 1979, pp 289-292, 653-658.
25. ibid p 182.
26. ibid p 360.

RECEIVED March 2, 1982.

Polymerization and Colloid Formation in Silicate Solutions

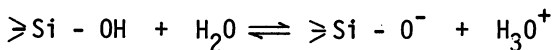
KJELL R. ANDERSSON¹, LESLEY S. DENT GLASSER,
and DOUGLAS N. SMITH

University of Aberdeen, Department of Chemistry, Old Aberdeen AB9 2UE, Scotland

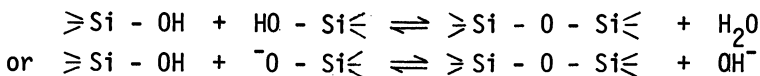
The relationship between polymerisation-depolymerisation reactions and the formation of colloids has been studied for silicate solutions lying in that area of the pH-concentration diagram commonly referred to as the instability region. Changes in both acidic and basic solutions have been followed by a variety of techniques, including pH measurements, trimethylsilylation, classic and dynamic light scattering, ultra-filtration and laser-Raman spectroscopy. In acid solution, kinetic studies showed that there is no direct correlation between the rate of disappearance of monomer and the rate of gelation. Similar results were found in more alkaline conditions: diluted silica-rich solutions showed slow changes in which colloidal particles grew, apparently at the expense of species of intermediate size, while the concentration of very small species remained constant or slightly increased. The colloid particles could be removed by ultrafiltration and the concentration of the remaining solution determined. It appears that the boundary of the instability region is in effect a form of solubility curve.

The behaviour of silicates in solution is governed by two interdependent sets of equilibria:

acid base -



and polymerisation - depolymerisation -



¹ Current address: EKA AB, Fack, S-445 01 Surte, Sweden.

The species in solution thus have to be considered in relation to pH and concentration, and Figure 1, modified from a diagram originally presented by Stumm, Huper and Champlin (1), provides a suitable starting point.

The heavy line on this diagram effectively represents the solubility of amorphous silica. It is by now fairly generally accepted that in the region below and to the right of this line, the silicate species are in true solution. In very dilute or very alkaline solutions, the silicate is present mainly as monomeric units (H_4SiO_4 - $HSiO_4^{3-}$, depending on pH). As the right-hand branch of the solubility curve is approached, polymeric species form in equilibrium with the monomer. The structure of these polymeric species has been extensively investigated over the past few years (2,3,4), and is described elsewhere in this symposium. There is evidence that the species encountered may depend on the cation present (5), although there seems to be little or no difference between sodium and potassium silicate solutions. Earlier findings are well summarized in a recent review (6).

The species encountered in the region of true solution appear to be labile, and changes in pH or concentration are followed by rapid re-establishment of equilibrium between species. The situation in the so-called "instability region" (7), which is to be discussed here, is quite different. In this region, all 'solutions' are metastable with respect to eventual precipitation of amorphous silica, but changes may be quite slow. Some apparently clear liquids, that in fact contain particles of colloidal dimensions, persist virtually unchanged for months or years. Hence our use of quotes in referring to 'solutions'. However, for convenience in the following account we shall refer to such liquids as solutions, although we are aware that this is formally incorrect: when we mean 'true solution' we shall say so.

Our studies have been directed at determining the connexion, if any, between polymerisation - depolymerisation equilibria among the smaller species and the formation of colloids, including gels. We summarize here our major findings; fuller details of the experimental techniques will be published elsewhere.

Gel and Colloid Formation in the Instability Region

It is well-known that neutralisation of a reasonably concentrated ($\geq 0.1M$ Si) alkali silicate solution normally results in a solid silica gel, which may contain well over 90% of its weight as water. Gelation is most rapid around pH 5-6, becoming slower as the pH is reduced further. It is slowest at pH 1-2, becoming more rapid again as the pH drops yet lower. Treatment of alkaline silicate solutions with acid ion-exchange resin are reported to give true (albeit metastable) solutions of silicic acids at pH 1-2 (8,9), and this seems to suggest that the rate of polymerization of silicic acid is at a minimum here, and would increase with increasing pH. However, there is no real

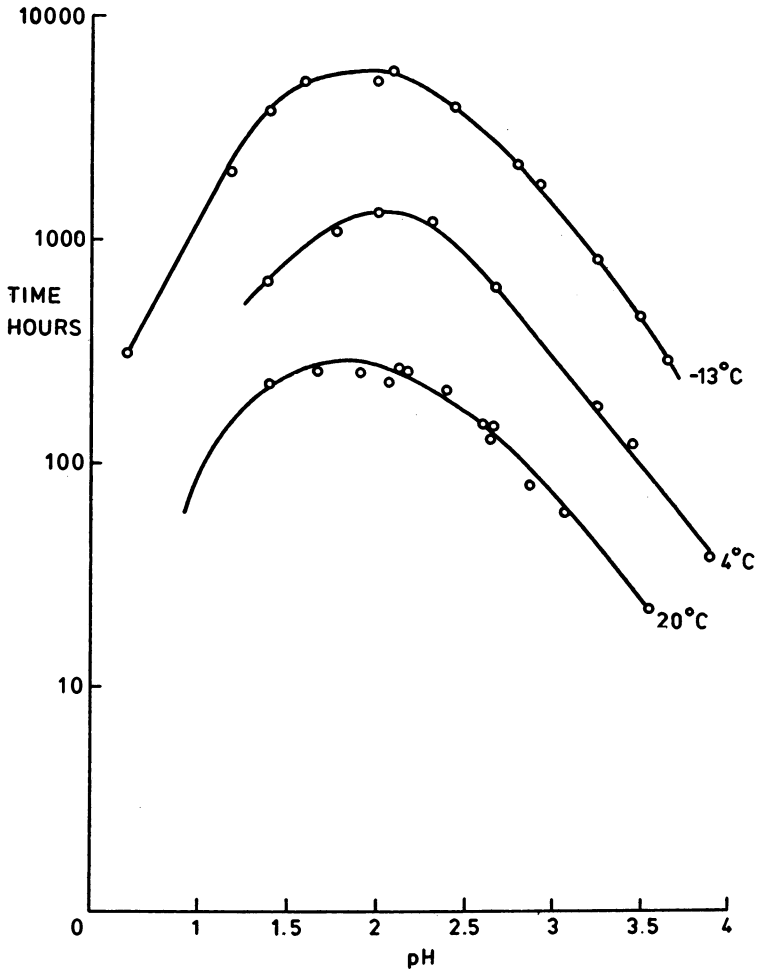


Figure 1. Behavior of silicate solutions at different pH values and concentrations. Solid line represents solubility of amorphous silica.

evidence that the two processes - polymerization and gelation - are directly connected, forming part of a continuous process analogous to a typical organic polymerization. Rather, as various workers have pointed out, the process may be stepwise. Iler (10) recognises three stages:

1. Polymerisation of monomer to form polymer
2. Growth of particles
3. Linking of particles together into branched chains, then networks, finally to a gel."

Reduction of the pH of alkaline solutions to bring them just inside the boundary of the instability region results in very rapid and quite reproducible changes in the concentration of small silicate species (11), but the form of the colloidal species is highly dependent on the method of preparation. Here also, then, is the suggestion that polymerisation and colloid formation may not be part of the same continuous process.

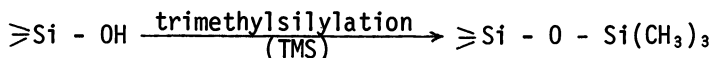
In the present work we have tried to characterise both the colloids and the silica in true solution. The studies fall into two main sections: runs in acid solutions of pH 1-4, and runs in alkaline solutions just inside the instability region. These will be considered separately after a brief review of experimental techniques common to both.

Experimental

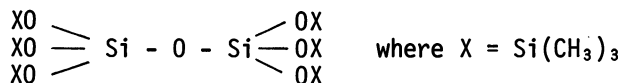
True Solutions were analysed for sodium and silicon by atomic adsorption spectroscopy; pH measurements used a Radiometer Type G202B glass electrode, which was corrected for the (low) sodium-ion error.

Colloids were routinely studied by classic light scattering. For the alkaline runs, additional information on their size was obtained by dynamic light scattering and electron microscopy, and on their composition by ultrafiltration.

The Distribution of Species was studied by trimethylsilylation, using essentially the method originally described by Lentz (12). In this technique, labile silanol groups are rendered unreactive by 'capping' with trimethylsilyl (TMS) groups :



Under ideal conditions, molecules should be produced whose structure reflects that of the parent silicate group. Thus, for example, the pyrosilicate group, $\text{Si}_2\text{O}_7^{6-}$, which exists in solution in a more-or-less protonated form depending on pH, should react with the acid trimethylsilylating reagents to give :



Unfortunately it is always possible that the necessary acidification may change the nature of the silicate species present before capping is complete. The risk is minimised by adding the silicate solution slowly to a vigorously stirred excess of reagent; nevertheless the results have to be interpreted with caution. However, comparison with other methods such as laser-Raman and ^{29}Si NMR spectroscopy suggest that although the TMS method can give misleading results about some individual structures, it does give a reasonably good picture of the overall degree of condensation of the system. It has the advantage over the spectroscopic techniques of being rapid, usable in dilute solution and of giving more detail about the larger species.

The TMS derivatives produced can be characterised by the normal techniques of organic and polymer chemistry. Small species, corresponding to up to about six silicon atoms in the parent silicate (the exact number depends on its structure), can be characterised quite precisely by conventional gas-liquid chromatography. Larger silicate species yield derivatives that are greases or waxes which are not volatile enough to be characterised by g.l.c. This material, collectively referred to as 'polysilicate derivatives' is soluble in organic solvents, and, if available in sufficiently large amount, can be studied by gel permeation chromatography; C and H analysis enables the extent of capping to be determined and from this the connectivity (\bar{Q}), or mean number of shared corners per tetrahedron in the original silicate, can be calculated.

Still larger silicate species give rise to an insoluble solid material that is readily detected but difficult to quantify because it tends to stick to the surface of the reaction vessel. Its presence reduces the total yield of detectable species, and the amount usually has to be determined by difference.

These broad categories are summarised in Table 1; the first undoubtedly arises from small species in true solution and the

Table 1

Characterisation of Silicate Species.

TMS derivative	Corresponding silicate
gas or mobile liquid - g.l.c. volatile	small species in true solution
soluble grease or wax	polysilicate - larger species up to colloidal size
insoluble solid	colloid particles

last from colloidal species. The nature of the polysilicate fraction is less certain; it covers a large range of molecular weights and might derive either from large species in true

solution or small colloids or a mixture of both, if indeed there is any sharp distinction to be made.

Polymerisation in Acid Solution

The polymerisation of silicic acid was studied at low pH (1-4). The silicic acid used was prepared either by hydrolysis of tetramethoxysilane or by acid ion-exchange of pure $\text{Na}_2\text{H}_2\text{SiO}_4 \cdot 8\text{H}_2\text{O}$ at about 0°C . Neither technique gives a pure solution of H_4SiO_4 . The first method gives a solution that contains a mineral acid and substantial quantities of methanol; the second also gives a solution that contains some mineral acid and moreover, because a finite time is needed for the ion-exchange process, some polymerisation may have occurred before the preparation is complete.

Figure 2 shows the gel time as a function of pH for the solutions produced by hydrolysis of tetramethoxysilane. The overall pattern, with a maximum between pH 1 and 2, does not appear to be affected by the presence of methanol; however comparison of ion-exchanged solutions with and without added methanol showed that the presence of methanol does increase individual gel times by 50% or more.

Observation using ^{29}Si NMR (13) showed that monosilicic acid was, rather surprisingly, more persistent at pH 3-4 than at pH 1-2. This is of course the reverse of what would be expected if polymerisation is a continuous process analogous to, say, the formation of polyethylene. Changes in the concentration of the various species with time were therefore followed by the TMS method.

Figure 3 shows how the concentration of monosilicic acid changed with time for different initial pH values (pH changes slightly during the polymerisation process). The results confirm the NMR conclusions: monomer is more persistent at the higher pH values. These particular runs were made at -13°C , the same temperature as the NMR experiment; runs at higher temperatures showed the same pattern, although loss of monomer was then more rapid at all pH values.

Figure 4 shows how the concentration of each of the g.l.c. volatile species changes with time, at -13°C and an initial pH of 3.5; similar patterns of change are observed at other temperatures at this pH. Monomer decreases monotonically but the large species increase to a maximum and then decay. The overall pattern for all species, including polysilicate, for these conditions is compared in Figure 5 with that found at a lower pH (1.85). In neither case is insoluble material formed; therefore the colloids formed must be small enough to be included in the polysilicate fraction. Although virtually the whole of the low molecular weight species have vanished from the sample at pH 1.85 by 336 hrs., gelation does not occur until 1500 hrs.; at pH 3.5 gelation occurs at 500 hrs., and monomer is still detectable at that point.

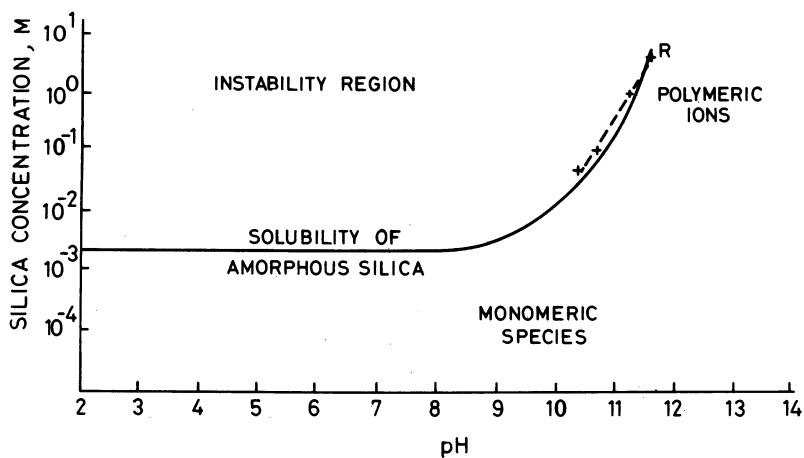


Figure 2. Variation of gel time with pH at three different temperatures. Starting solution contained 1.5 M monosilicic acid produced by hydrolysis of tetramethoxysilane.

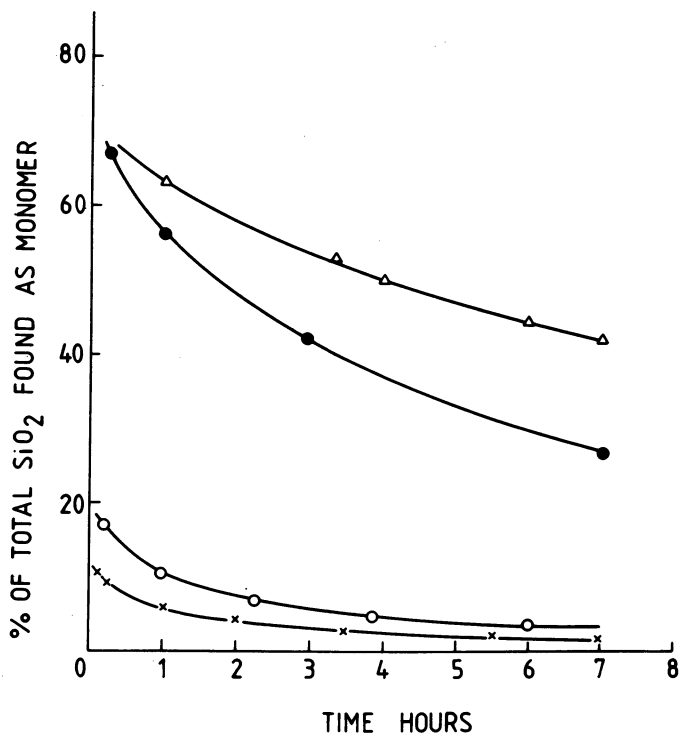


Figure 3. Disappearance of monosilicic acid from 1.5 M solution at 13°C with time for various initial pH values. Key: pH 1.85, X; 2.1, O; 3.0, ●; and 3.5, Δ.

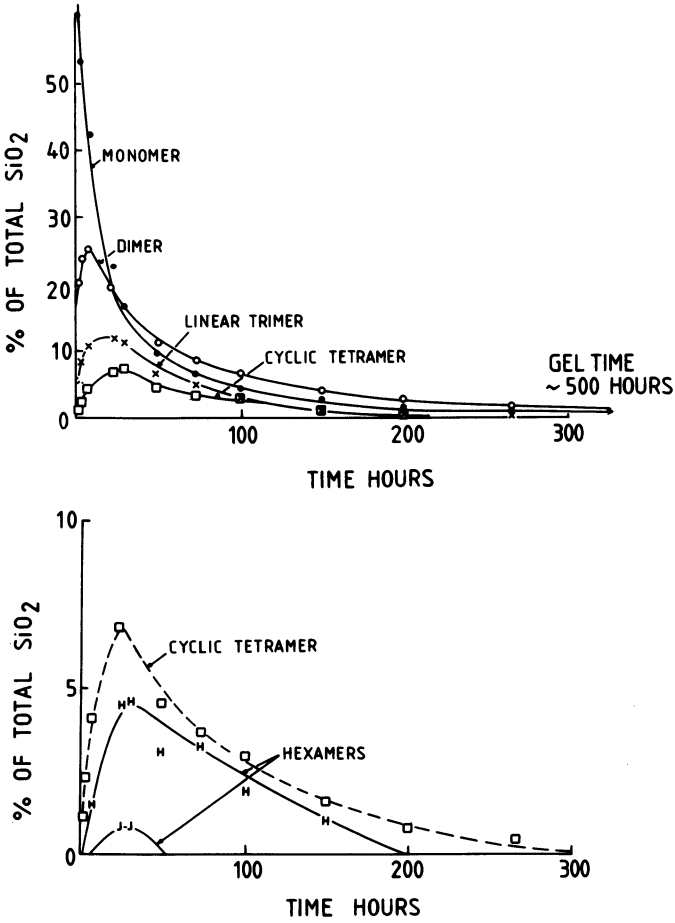


Figure 4. Variation with time of concentration of individual species during polymerization of 1.5 M monosilicic acid at -13°C , initial pH 3.5. Vertical scale of lower part of figure is expanded five times to show changes in the less abundant species. Curve for cyclic tetramer is included in both parts of diagram.

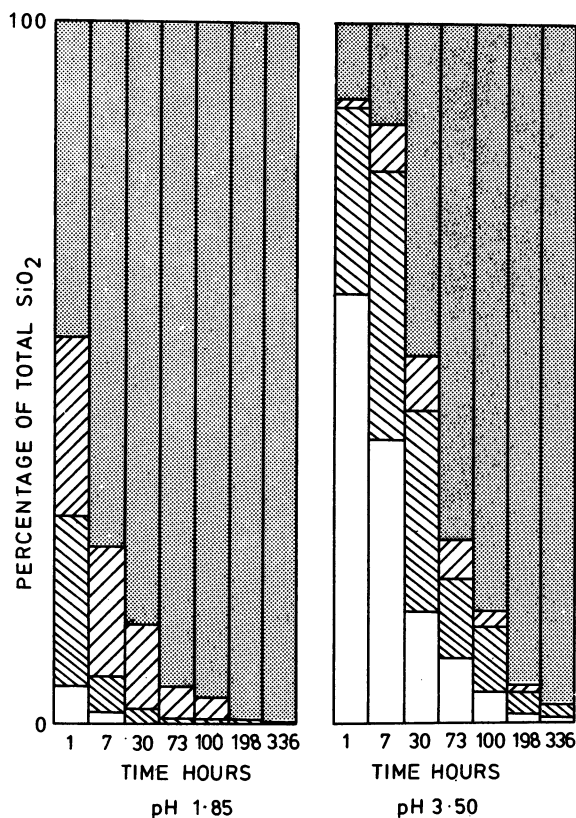


Figure 5. Distribution of species during polymerization at two different pH values; 1.5 M monosilicic acid at -13°C . Key: \square , monomer; ▨ , g.l.c. volatile material (lower block represents species with 2-4 silicate units); ▩ , polysilicate.

This difference in behaviour seems to be a result of differences in the nature of the larger silicate species. Figure 6a compares the connectivity, \bar{Q} , of the polysilicate formed. A \bar{Q} value of 2 corresponds to rings or infinite chains of tetrahedra, a value of 3 to closed cages or infinite sheets; in solution the former, finite, species are present. A \bar{Q} value of 3.5 is about the limiting value for colloidal species suggested in earlier studies (3); values much above 3 suggest rather high molecular weights. The difference in \bar{Q} is reflected in the physical properties of the polysilicate; the low pH sample was a soft gummy substance, while the high pH sample was hard and glassy.

Using the empirical relationship between \bar{Q} and n (degree of polymerisation, or number of silicate units)

$$\bar{Q} = \frac{7(n - 1)}{2n + 3}$$

derived in (3), approximate values of n corresponding to \bar{Q} were calculated and are plotted in Figure 6b. This shows clearly the very rapid increase in molecular weight of the polysilicate fraction at the higher pH. In other words, the medium molecular weight material, once formed, is reasonably persistent at pH 1.85, but at pH 3.5 is rapidly converted to material of still higher molecular weight.

This conclusion is borne out by the results of classic light scattering measurements, shown in Figure 7. Although these curves refer to a higher temperature (20°C) the general similarity in shape to Figure 6b is striking. In both figures, increase is initially slower at the higher pH, but as the larger species build up at the expense of the intermediate ones, the curves cross over.

The general picture is thus that at low pH species of intermediate size are relatively stabilised; at higher pH very large species rapidly form at the expense of the intermediate ones, so that, although monosilicic acid is relatively persistent, gelation occurs much sooner than at low pH. Studies using other techniques, such as laser-Raman spectroscopy and NMR, are in general accord with these ideas.

Formation of Colloids Under Alkaline Conditions

The pH and concentration of commercial high-ratio silicate solutions commonly lie at points such as R in Figure 1; that is they are very close to the boundary of the instability region. On dilution, the pH falls almost linearly with $\log[\text{SiO}_2]$ (dashed line, Figure 1), bringing them into the instability region. When such diluted solutions are stored at room temperature under rigorously CO_2 -free conditions, there is a slow, steady rise in pH and at the same time the intensity of scattered light increases (Figure 8); these phenomena were observed by Debye and Nauman (14).

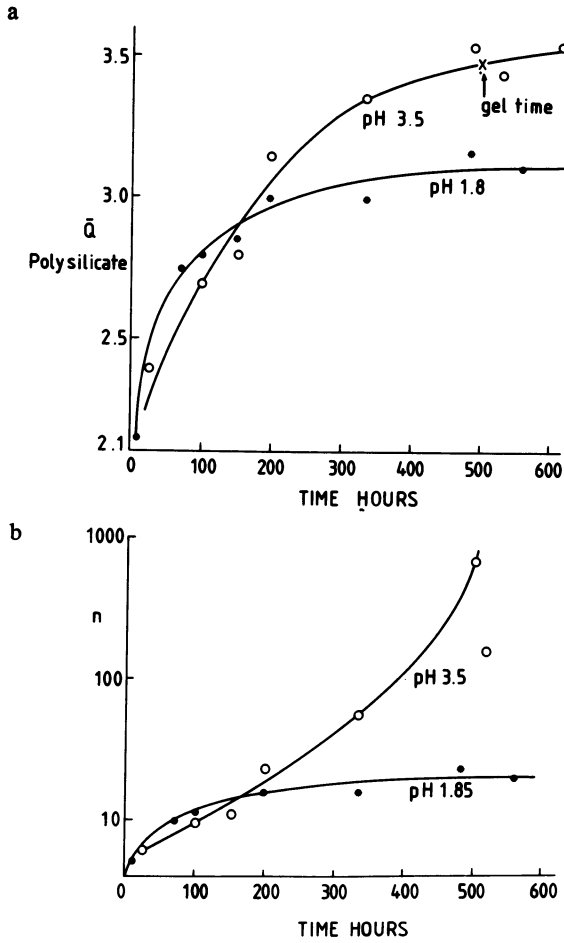


Figure 6. (a) Connectivity (\bar{Q}) for polysilicate formed at pH 1.85 and 3.5. (b) Degree of polymerization calculated from \bar{Q} using the relationship (3):

$$\bar{Q} = \frac{7(n-1)}{2n+3}$$

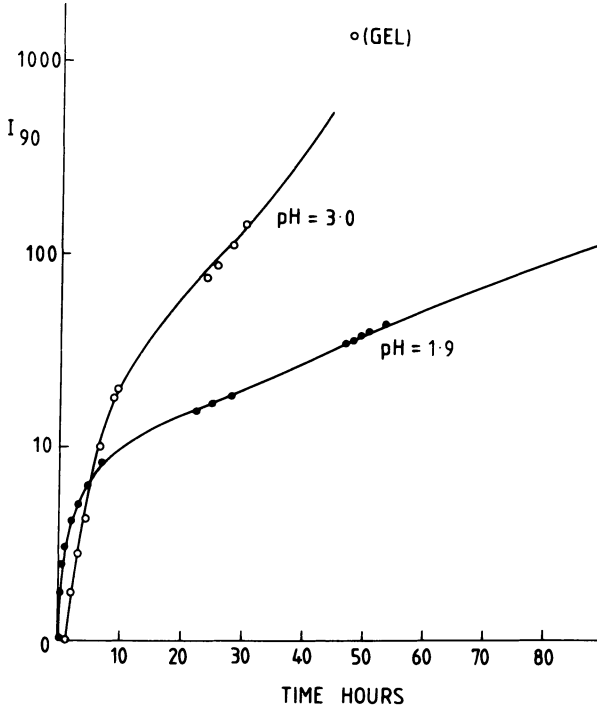


Figure 7. Classic light scattering results: I_{90} against time (h) for a 1.5 M monosilicic acid solution at 20°C.

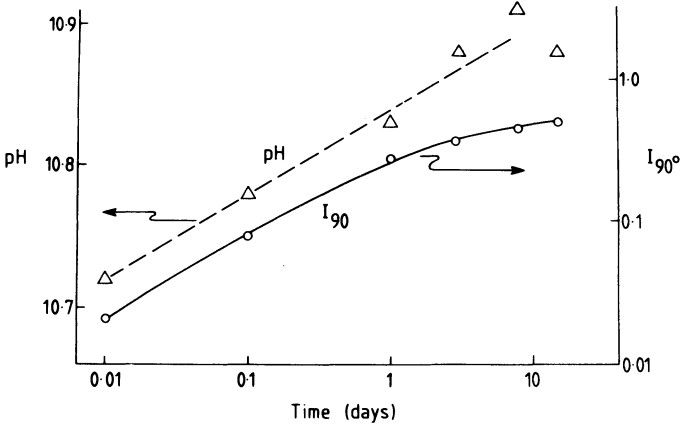


Figure 8. Change in pH and intensity of scattered light (I_{90}) for a sodium silicate solution ($Na_2:SiO_2 = 1:3.39$) diluted to 0.1 M Si and stored at 20°C under CO_2 -free conditions.

Comparison of the pH of a freshly diluted solution with the value after 30 days storage provides a useful criterion of stability. Figure 9 shows results for a number of solutions at or near the stability boundary. Solutions for which a rise of less than 0.1 of a pH unit is found are assumed to be stable. Note that in this diagram the concentration of silica is the total present, whether in true solution or as colloidal species; we shall return to this point later.

By analogy with other oxyacids, such as phosphoric, one would expect the acidity of individual silanol groups to increase with the connectivity of the group to which they are attached; the accepted values of the few known dissociation constants support this idea. (For orthosilicic acid, $pK_1 \approx 9.5$, $pK_2 \approx 12.6$ (7, 15); for silanol groups on silica gel, $pK \approx 7$ (16).) However, this is more than compensated by the fact that in the course of polymerisation the total number of silanol groups is greatly reduced, so that despite the pK values just quoted the overall result is a reduction in acidity, and a consequent rise in pH.

The concentration of species in the solutions during the course of polymerisation was monitored, as before, by the TMS technique. The most striking result was that the concentration of the smaller species, mainly monomeric and dimeric silicate units, did not decrease with time, as might have been expected in view of the increase in the amount of colloidal material. Instead the concentration of small species remained virtually constant, if anything appearing to increase slightly.

Full analysis of some solutions, including polysilicate and insoluble solid, are shown in Figure 10. In contrast to the results in acid solution (Figure 5) a considerable amount of insoluble solid is found: it is possible that this may be an artefact resulting from the acidification during the TMS process, but it seems more likely to be a function of the large size of the colloidal particles. This fraction increases markedly both during storage and on heating, and it does so at the expense of the soluble polysilicate fraction, not at the expense of the small species. The amount of monomer and dimer present in a solution is therefore not a good indicator of the overall degree of condensation.

Dynamic light scattering indicated that the colloids were monodisperse, and that their size increased steadily with storage time; after about 30 days they appeared to be roughly 80 Å in diameter. After heating to 95°C the particle size increased to over 100 Å. Both the size and the spherical nature of the particles were confirmed by electron microscopy. These unstable alkaline solutions thus contain a relatively constant proportion of small species in true solution, and a large colloidal fraction that increases in size at the expense of the intermediate polysilicate fraction. This seems to suggest that possibly the colloidal material should be considered as a separate phase, in the same way as a precipitate would be.

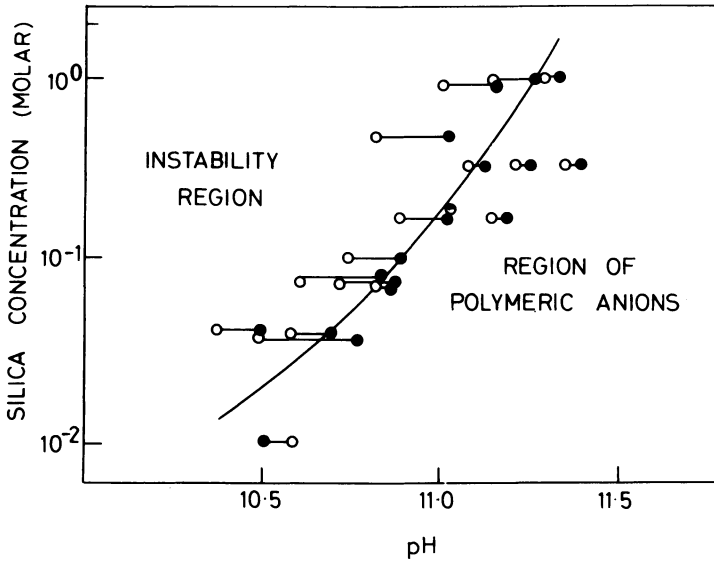


Figure 9. Stability boundary and pH changes. Key: ○, initial pH measurements; ●, pH of the same solution after storing at 20°C for 30 d.

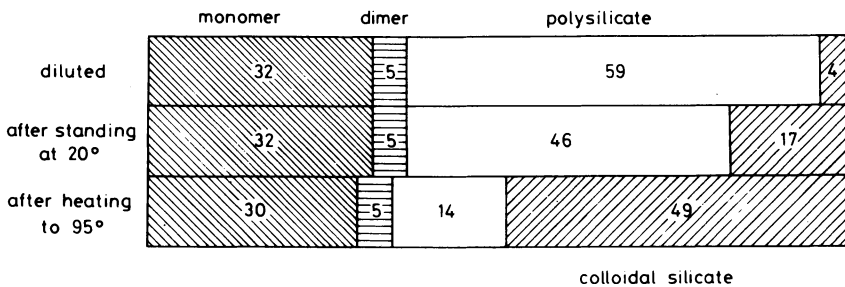


Figure 10. Distribution of species in a 1:3.39 sodium silicate solution immediately after dilution to 0.1 M Si; after standing at 20°C for 30 d; and after heating to 95°C for 1 d.

The results of ultrafiltration of solutions that had been allowed to precipitate reinforced this point. In each case the filtrate, which could be shown by light scattering to be free of colloids, had a higher ratio of sodium to silica than the original solution, whereas the colloids were relatively silica-rich. These results are summarised in Table II. When the filtrate composition is plotted on a diagram such as Figure 1 or Figure 9 it is

Table II

Results of ultrafiltration of colloidal solutions

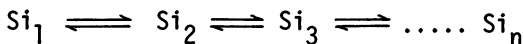
Original solution		Filtrate	Colloids
conc. (M. SiO ₂)	Rm($\frac{\text{SiO}_2}{\text{Na}_2\text{O}}$)	Rm	Rm
0.1	3.26	2.20	22.1
0.5	3.44	3.14	8.3

seen that the formation of the colloid has altered the composition of the true solution in such a way as to bring it down to the solubility curve. The analogy with precipitation is obvious.

The reason why the concentrations of monomeric and dimeric species remain constant or increase slightly during colloid formation is now apparent. So far as the species in true solution are concerned, the solution has become more alkaline, and this is reflected in the slight increase in pH; the concentration of silica in true solution has diminished. Consequently it is to be expected that the proportion of monomeric species, and perhaps also dimeric ones, should increase.

Conclusions

Studies both on acidic and basic solutions suggest that it is misleading to regard colloidal silica simply as the end member of a series of equilibria of the type:



the subscript representing the number of silicate units. Colloid formation seems rather to be a separate step, perhaps involving coagulation of species that are already rather large. The results indeed fit the scheme outlined in the introduction, if step 1 is visualised as the production of the medium weight species, and step 2 as the aggregation of these species into colloidal particles. Under some conditions, step 3 never occurs; colloidal solutions may remain indefinitely as sols, or they may gel, or they may coagulate in a different manner to produce amorphous hydrous silica as an obviously separate phase. Which path is followed appears to depend on a number of factors, including pH, temperature, and the presence of other solutes.

Finally, it is tempting to speculate that the boundary between stable and unstable solutions has a structural significance. The evidence from ^{29}Si NMR is that the many species encountered in concentrated alkaline solutions are based on rings of three tetrahedra whereas the evidence of trimethylsilylation suggests that rings of four or more tetrahedra are more common. This difference may be reconciled if rearrangement takes place during the acidification step of the TMS technique. The ring of three tetrahedra is known to be unstable in acid solution, so that cyclic trimer, for example, appears as linear trimer in the TMS extract. A crude electrostatic model shows, indeed, that cyclic trimer is stabilised by deprotonation of the non-bridging oxygen atoms - i.e. in alkaline conditions. As the oxygen atoms are protonated, the cyclic trimer becomes destabilised with respect to the cyclic tetramer (17) at roughly the pH at which solutions sufficiently concentrated to contain these species enter the instability region. The labile species in true solution could thus be equated with species based on rings of three tetrahedra, whereas colloidal species are based on rings of four or more. This would be consistent with what is known of crystalline silicates: rings of three tetrahedra are only very rarely encountered in extended structures such as networks, and have so far never been found in frameworks.

Acknowledgments

We would like to thank the S.E.R.C. and Unilever Research for support for one of us (DNS); Unilever Research also provided access to ^{29}Si NMR and laser Raman spectrometers. We thank EKA AB, Surte, Sweden, for financial support for another of us (KRA) and for help with the ultrafiltration experiments. We are also very grateful to Mr. Kenneth Rosenquist of the Swedish Institute for Surface Chemistry, Stockholm, for his assistance in applying the dynamic light scattering technique. Finally we are grateful to the PQ Corporation for making it possible for this paper to be presented at New York.

Literature Cited

1. Stumm, W.; Hüper, H.; Champlin, R.L. Environmental Science and Technology 1967, 1, 221.
2. Harris, R.K.; Newman, R.H. J.C.S. Faraday II 1977, 1204.
3. Dent Glasser, L.S.; Lachowski, E.E. J.C.S. Dalton 1980, 399.
4. Harris, R.K.; Knight, C.T.G.; Hull, W.E. J. Am. Chem. Soc. 1981, 103, 1577.
5. Hoebbel, D.; Garzó, G.; Engelhardt, G.; Ebert, R.; Lipmaa, E.; Alla, M. Z. anorg. allg. Chem. 1980, 465, 15.

6. Barby, D.; Griffiths, T.; Jacques, A.R.; Pawson, D. "The Modern Inorganic Chemicals Industry"; Thomson, R., Ed.; Chemical Society: London, 1977.
7. Lagerström, G. Acta Chem. Scand. 1959, 13, 722.
8. Alexander, G.B. J. Am. Chem. Soc. 1953, 75, 2887.
9. Iler, R.K. J. Phys. Chem. 1953, 57, 654.
10. Iler, R.K. "The Chemistry of Silica"; Wiley Interscience: 1979, p. 173.
11. Dent Glasser, L.S.; Lachowski, E.E. J.C.S. Dalton 1980, 393.
12. Lentz, C.W. Inorg. Chem. 1964, 3, 574.
13. Harris, R.K.; Knight, C.T.G.; Smith, D.N. J.C.S. Chem. Commun. 1980, 725.
14. Debye, P.; Nauman, R.V. J. Phys. Chem. 1961, 65, 5.
15. Bilinski, H.; Ingri, N. Acta Chem. Scand. 1967, 21, 2503.
16. Schindler, P.W.; Kamber, H.R. Helv. Chim. Acta 1968, 51, 1781.
17. Dent Glasser, L.S. Unpublished work presented at the Chemical Society Autumn Meeting, Cardiff 1980.

RECEIVED March 2, 1982.

The Effect of Degree of Polymerization of Silicates on Their Interactions with Cations in Solution

JAMES S. FALCONE, JR.

The PQ Corporation, Research and Development Center, Lafayette Hill, PA 19444

The development of a better understanding of the role soluble silicates play in detergency, mineral beneficiation, enhanced oil recovery, etc., has led us to look carefully at the interactions of soluble silicate species with metal ions in solution. The acidity of $\equiv\text{Si-OH}$ increases as the complexity of the silica species increases, e.g., pK_a for $\text{Si(OH)}_2\text{O}_2^-$ is 9.91 ± 0.04 whereas $\equiv\text{Si-OH}$ on silica gel has a $\text{pK}_a = 6.8 \pm 0.2$. Viewing the interaction of metal ions in solution with a soluble silica surface as an ion exchange process, one might expect differences dependent on the degree of polymerization of the silicate anion. Our results indicate that metal ion activities in solution are sensitive to factors related to the anion structure and pH value. The results support Iler's observation that silicate solution begins to absorb multivalent metal ions in solution at pH values roughly two units below the pH at which the metal hydroxide is precipitated

The water soluble glasses in the family $\text{Na}_2\text{O}:\text{mSiO}_2$ where m (referred to as the ratio or modulus of the silicate) varies between approximately 0.5 and 4.0 on a molar basis are a significant commodity chemical in world commerce. These materials find use in a wide variety of industries. They are valued as active sources of building block SiO_2 for the manufacture of synthetic clays, gels and sols useful as catalysts, desiccants, ion exchangers, anti-slip agents, silica wafer polishing chemicals and beer clarifiers, to name a few.(1) However they are also valued in other markets for their ability to provide a variety of solution and surface chemistry properties. They find use in essential technologies such as detergency(2), water treatment(3), mineral beneficiation(4) and oil recovery(5). These uses are generally dependent on the

interaction of the anionic silicate species in solutions with metal ions leading to a reduction in their activity and/or the interaction of silicate anions with surfaces (usually oxides). These interactions can influence the dispersion of particles, the effectiveness of surfactants, the wettability of clays and the corrosion of metals among other effects.

In many of these processes it has been observed that the effectiveness of silicates can vary as the ratio changes.

Some Early Studies of Silicate Metal Ion Interaction

In an early fundamental study of the effect of sodium silicates on iron oxide surfaces Hazel(6) concluded that "at a given hydrogen ion activity and a given silica concentration, the effectiveness of the silica in discharging and recharging iron oxide surfaces increased with silica ratio of the original sample." He attributed the differences observed to the silicate species variations suggested by Harman (7) in the 1920's. Harman showed through the analysis of the colligative properties of solutions with various ratios of $\text{SiO}_2/\text{Na}_2\text{O}$, that the silicate solutions contain colloidal species and what he called "crystalloidal" silica. This "crystalloidal" silica was considered to be analogous to the simple species then thought to be the components of the known crystalline sodium silicates, charged aggregates of these unit structures and silica (ionic micelles), or definite complex silicate ions.

Hazel specifically attributed the recharging behavior of alkaline (lower) ratio silicates to hydroxide or ionic "crystalloidal" silicate species, whereas the behavior of the higher ratio silicates was attributed to ionic micelles or aggregated "colloidal forms". In a subsequent paper Hazel, McNabb and Machemer(8) studied the interaction of zinc salts with silicates and suggested that the presence of silicate enhanced the hydrolysis of Zn^{++} . A mutual adsorption of $\text{Zn}(\text{OH})_2$ and colloidal silica was suggested as part of the interaction. Silicates with high proportions of SiO_2 reacted with zinc ions without the formation of precipitates.

A significant literature has developed in the last 30 years concerning the interaction of silica surfaces with metal ions. It is summarized in "The Chemistry of Silica" by Iler(9) who mentions that many ions are held irreversibly on silica surfaces by forces still poorly understood in addition to ionic attraction. Most of the studies summarized by Iler deal with the surface of hydroxylated silica or silica gel. For our purposes we are interested in these results as they relate to the understanding of the effect that "soluble" silicate species have on metal ion activities.

Polymers in Silicate Solution

Up until the mid-1970's, various indirect methods of studying the silicate species in solution, recently summarized by Dent Glasser and Lachowski(10), indicated that these solutions are indeed complex mixtures of silicate anions, with varying degrees of polymerization, in a dynamic equilibrium.

The use of FT-NMR spectroscopy in studying complex silicate structures in solutions which is summarized in a preceding paper(11) has been perfected over the last decade. The results of NMR studies have provided a somewhat clearer picture of the speciation in silicate solutions. Andersson, Dent Glasser and Smith(12) in the preceding paper indicate that the large colloidal species observed in alkaline silicate solutions (in the commercial range) might be thought of as a separate phase. One might think of these solutions as colloidal size "silica gel" - like particles dispersed in a true solution of ionic silicate species.

The Relative Acidity of "Dissolved" Silicate Species

The pK_a value of monosilicic acid is 9.91 ± 0.04 (13) and Belyakov(14) has shown that the pK_a value decreases to 6.5 for high polymers. Schindler and Kamber(15) have reported a pK_a value of 6.8 ± 0.2 for surface silanol groups of silica gel. Maatman, et. al.,(16) and Schindler, et. al.,(17) have shown that multivalent metal ions associate with a silica gel surface in a manner that indicates a linear correlation between the ligand properties of the surface silanol groups and metal ion hydrolysis. For Cu^{+2} , Fe^{+3} , Cd^{+2} and Pb^{+2} , Schindler observed that the log of the stability constant of surface complex on silica gel was roughly 60% of the log of the metal ions hydrolysis constant.

He also observed that this relationship did not hold for Ca^{++} and Mg^{++} and that the association was distinctly dependent on the surface charge and pH value.

James and Healy(18) looked at the adsorption of hydrolyzable metal ions on SiO_2 from the point of view of competition between ion-solvent and ion-surface interactions. They suggested that metal ion adsorption is initiated at a pH value corresponding to surface nucleation, which seems to relate to the reduction of cation-solvent interactions, as a result of hydrolysis or ligand complex formation, leading to conditions favorable to the adsorption of hydrated metal ions from solution. Their model suggests that metal ion hydrolysis enhances adsorption on SiO_2 , whereas Schindler proposes direct participation by unhydrated ions.

Based on the similarity of high polymer silicate pK_a values to that of silica gel one might expect these species to interact with metal ion in solution in a manner analogous to

silica gel. It might also be expected that as the degree of polymerization decreases, these silicates species would exhibit reduced interaction with the metal ions.

In order to test this hypothesis and develop a better understanding of the magnitude of the effects, three silicate solutions were chosen based on the knowledge that they span the distribution known to be present from structure studies on concentrated solution, that is:

- m = 0.5 predominantly monomer "ionic species"
at any concentration
- m = 2.0 predominantly multimeric "ionic species"
except at low concentrations (below Ca 100ppm)
- m = 3.8 a concentration dependent mixture of multi-
meric and larger colloidal species.

The influence of these solutions on the activities of Ca^{++} , Mg^{++} and Cu^{++} were carefully measured using commercial ion selective electrodes and compared to results for NaOH.

Experimental

The Preparation of Solutions

The water used in making all solutions was prepared using 10 MOhm water. Stock solutions of sodium silicates were made from carefully assayed commercially available solutions for ratio (w/w) values of 2.0 and 3.8 and from sodium metasilicate and NaOH for the 0.5 ratio solution.

Stock solutions of MgCl_2 , CaCl_2 and $\text{Cu}(\text{ClO}_4)_2$ were prepared from reagent grade salts without recrystallization. Concentrations of Mg^{++} and Ca^{++} were determined using EDTA. Copper concentrations were determined using atomic absorption (AA). The Ca^{++} and Mg^{++} solutions were used without the adjustment of their pH values, whereas Cu^{++} solutions were initially adjusted to a pH value of 4.0 using HCl.

The Ion Selective Electrodes

The electrodes used were purchased from ORION and they were as shown in TABLE I.

TABLE I
Equipment Specifications for Electrodes

<u>Specifications</u>	<u>Metal Ions</u>		
	<u>Calcium</u>	<u>Magnesium</u>	<u>Copper</u>
Electrode Model #	93-20	93-32	94-29
Reference Electrode #	90-01	90-01	90-01
pH Range	5.5-11.0	5.5-10.0	6
Concentration range, ppm	8-2000	5-2000	5-1000

The ORION 701/Digital pH meter was used for all ion selective electrode measurements in order to employ an expanded scale, whereas pH measurements were recorded on an ORION 601/digital ionalyzer. The Model 476050 Corning single pH reference combination glass electrode was used for the measurement of the hydrogen ion activity.

The Experimental Procedure

In order to minimize uncertainties that could arise from variations in polymerization equilibria due to dilution and other sources of error due to unsystematic sampling procedures, we adopted, after some trial and error, the following procedure:

- Prepare and analyze a 2000 ppm concentration metal ion stock solution.
- Prepare solutions from the above in the working range of 5 to 2000 ppm and check by EDTA or AA.
- Measure 100 cm³ of a given concentration metal ion solution into a sample bottle measuring cell using a 50 cm³ syringe.
- Record the value of the emf and pH associated with the above solution.
- Inject into the metal ion solution a 1 cm³ volume of silicate or hydroxide solution (yielding a predetermined SiO₂ content from 25 to 500ppm or pH value.)
- After one minute record the new emf and pH value of the combined solutions.
- Store the resultant solution in the airtight plastic sample bottle.
- Repeat this measurement procedure with a new SiO₂ and/or metal ion concentration.
- Periodically measure the emf and pH value of a fresh standard metal ion solution in order to assure internal consistency in the results.

All measurements in this study were carried out at room temperature which was maintained at 21.0 \pm 0.5°C.

RESULTS

The Electrode Response Data

The emf data collected for each concentration of a metal ion solution (approximately 13 replicates) before the addition of hydroxide or silicate solution were averaged and the mean value used to calculate a Nernst response curve. Metal concentrations in ppm were converted to mols/dm³ and the Davies equation (19) was used to estimate the values of the mean molar activity coefficients of the metal ions in

solution. Least squares regression of the mean emf value vs molar ion activity yielded the following Nernst response curves:

$$E_{Ca^{++}} = 75.8(14)^* + 26.9(5) \log [Ca^{++}]$$

$$E_{Mg^{++}} = 70.9(6) + 27.9(3) \log [Mg^{++}]$$

$$E_{Cu^{++}} = 140.1(38) + 32.6(14) \log [Cu^{++}]$$

*Values in parenthesis are the 95% confidence limits of the last digits.

These equations were used in all subsequent calculations of the values of metal ion activities.

The Calcium Results

Figure 1 represents a summary of the results observed where sodium hydroxide and the three silicate solutions are added to the various $CaCl_2$ solutions. The values for 3.8 and 2.0 ratio silicates are plotted, the individual 2.0 ratio silicates points are not shown, only the least square fit data and the 95% confidence prediction limits of the regression. These limits give an estimate of the precision of the metal ion activity results predicted from the experimental data which is useful when one wishes to compare entire regression lines. The highest values of pH obtained upon addition of 0.5 ratio silicate are also shown. No significant drop in pCa was shown for OH^- or orthosilicate in the pH range studied. It was not possible to study the effect of OH^- (that is, reproduce the literature value shown in Fig. 1) or orthosilicate ratio at higher pH values due to the loss of accurate response of the electrode. The results suggest that the activity of Ca^{++} in solutions at constant pH value is influenced by the nature of the silicate solutions used to attain said pH value. The 3.8 ratio silicate yielded a greater activity reduction at an equivalent pH value than did the 2.0 ratio silicate. However, due to its lower base strength the 3.8 ratio system contains more SiO_2 when the solution pH values are equivalent. The solutions when aged for several weeks and remeasured show an even greater reduction in pCa and less distinction between the 3.8 and 2.0 ratio silicate.

The Magnesium Results

The results for magnesium ion are presented graphically in Figure 2. In this case all solutions could be studied completely and intercompared as well as compared to the phase boundary for the active and brucite form of $Mg(OH)_2$. Only the least squares representations are shown with the regression limits for the 3.8 ratio and the NaOH experimental lines. The limits for the representations for the 2.0 ratio and 0.5 ratio are similar to

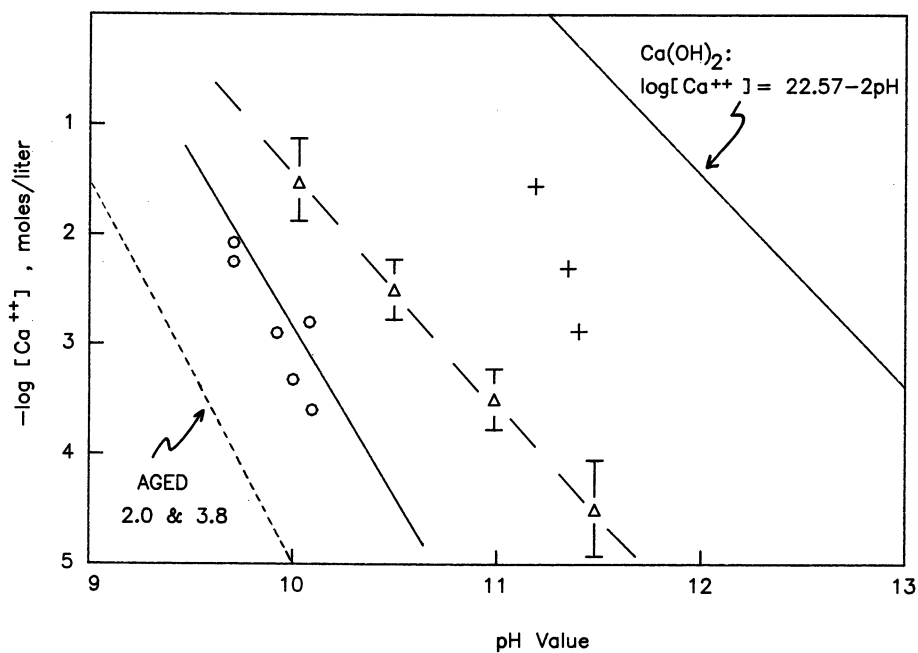


Figure 1. Calcium ion activity in solution vs. pH value for freshly prepared and aged solutions of CaCl₂. The pH value has been adjusted by a sodium silicate solution with the indicated ratio of SiO₂:Na₂O. Key: +, 0.5; Δ, 2.0; O, 3.8 ratios.

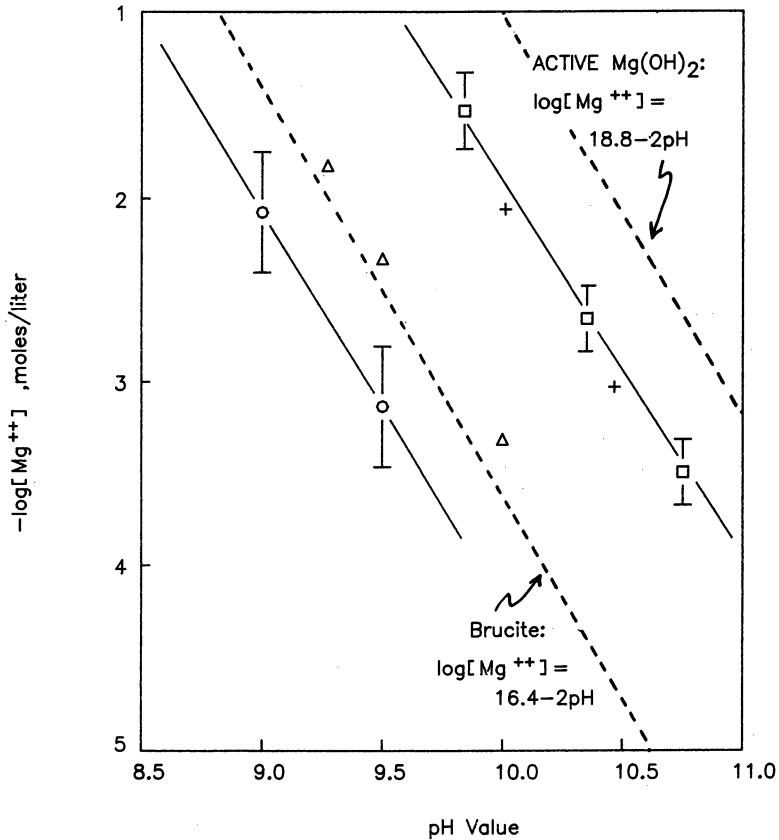
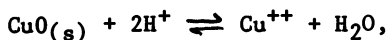


Figure 2. Magnesium ion activity in solution vs. pH value for freshly prepared solutions of MgCl₂. The pH values were adjusted by NaOH and sodium silicate solutions with the indicated ratios of SiO₂:Na₂O. Key: □, NaOH; +, 0.5; Δ, 2.0; ○, 3.8 ratios.

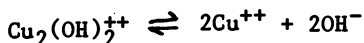
those shown for the adjacent lines. It is apparent that the results for sodium hydroxide and the 0.5 ratio silica are indistinguishable and significantly different from those observed for the higher ratio silicates. Comparison of the higher ratio results suggests a greater reduction as the ratio is increased, but this difference is not statistically significant at the 95% confidence level. It is also interesting to note that the results for the high ratio solutions are similar to the results expected if the more stable brucite form of $\text{Mg}(\text{OH})_2$ were being formed. These results suggests that higher ratio solutions nucleate the crystallization of this form of $\text{Mg}(\text{OH})_2$.

The Copper Results

The results for Cu^{++} are represented graphically in Figure 3 in the same manner as for Ca^{++} and Mg^{++} and we see again a statistically different interaction of Cu^{++} with the species present in higher ratio silicate solution when compared to the lower ratio solution and hydroxide. Also, of interest, is the fact that the values of Cu^{++} activity are somewhat higher in all cases than the values one would predict from the equilibrium:



but lower than those expected from:



There was also a greater drift in the emf data (towards reduced activity) immediately after addition of titrant making the measurement of a meaningful "active" equilibrium very difficult. A much greater stability was seen in the Ca^{++} and Mg^{++} data. Since the literature values indicate that in time the copper activity should decrease we measured the values of pH and pCu for the copper-silicate solutions at a later date and observed the results presented in Figure 4. In this Figure we see that all of the activities are reduced as expected based on the literature information, however, what is truly interesting is the nature of the precipitates formed with time in the various solutions. In the Ca^{++} and Mg^{++} ion studies precipitates, when observed, were seen immediately. For the copper solutions no precipitation was noted immediately after addition of complexing species; however, the aged solutions do show the presence of precipitates which differed in color as one varied the ratio of the silicate. The qualitative observations of the colors of the precipitates are:

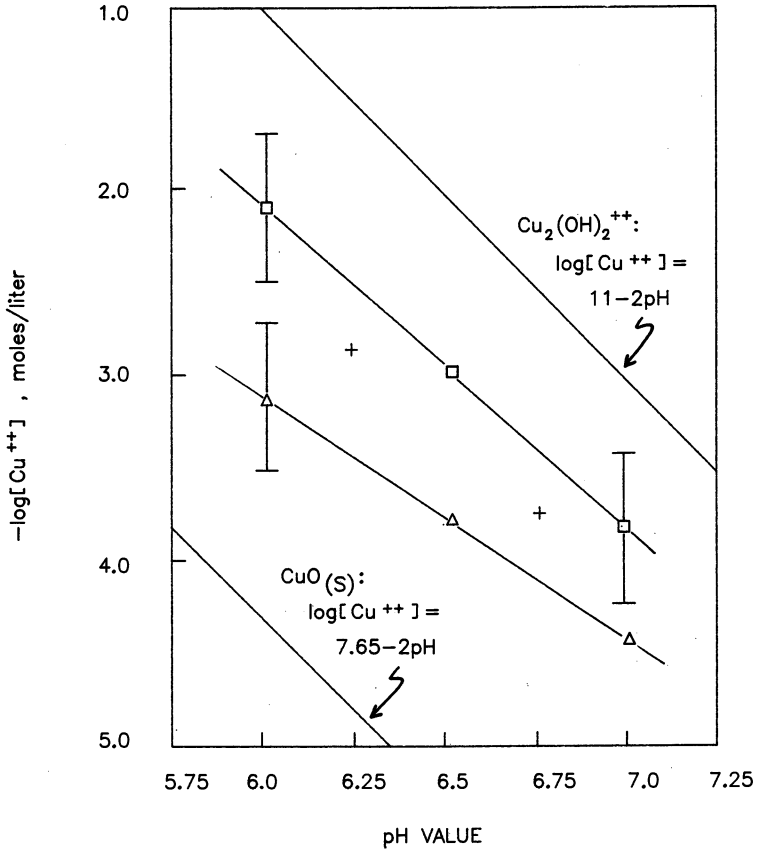


Figure 3. Copper ion activity in solution vs. pH value for freshly prepared solutions of $\text{Cu}(\text{ClO}_4)_2$ adjusted to initial pH 4.0. The pH values were further adjusted by NaOH and sodium silicate solution with the indicated ratios of $\text{SiO}_2\text{:Na}_2\text{O}$. Key: □, NaOH; +, 0.5; and △, 2.0 and 3.8 ratios.

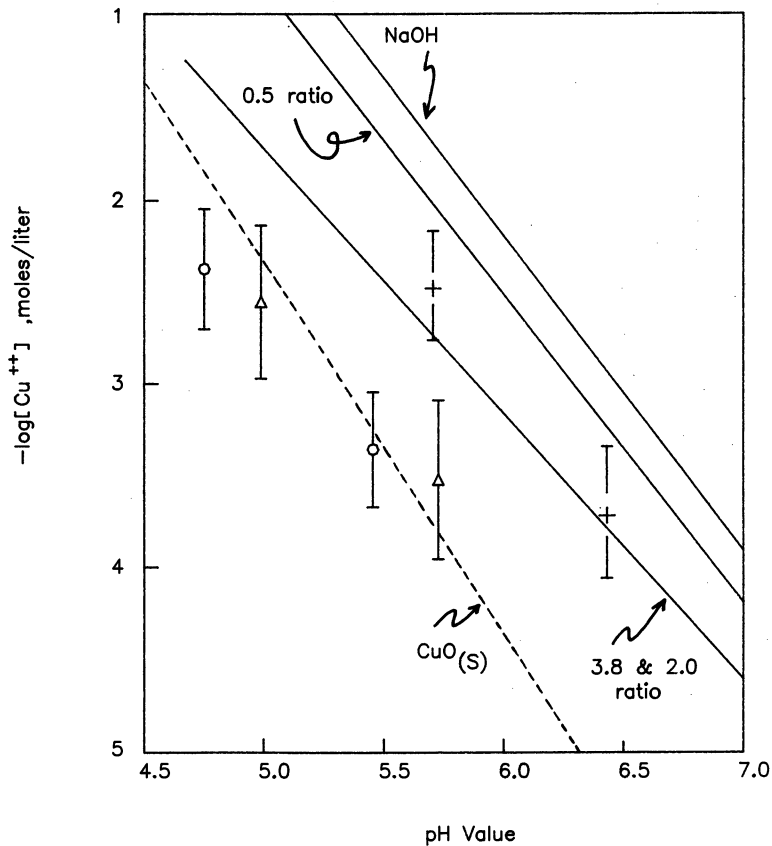


Figure 4. Copper ion activities vs. pH value for solutions shown in Fig. 3 after aging approximately 1 mo compared to the initial values shown as marked solid lines. Key: +, 0.5; Δ , 2.0; and \circ , 3.8 ratios of aged solutions.

<u>Material</u>	<u>Color</u>
NaOH	black-brown
0.5 ratio	brilliant blue
2.0 ratio	pale blue
3.8 ratio	white

These results suggest strongly that different structures exist in the solid phases for different ratios.

Discussion

The use of sodium silicate as a modifier of divalent ion solution activity could be studied using ion selective electrodes. It appears based on the results for Mg^{++} and Cu^{++} that the reduction in metal ion activities observed for the solutions of sodium orthosilicate are statistically indistinguishable from those observed when NaOH was used; however, for Cu^{++} different color precipitates are observed. No activity reduction as a result of base addition could be measured in the $CaCl_2$ solutions with 0.5 ratio silicate or NaOH; however, activity reductions were clearly observed with silicate solutions at m values of 2.0 and 3.8. This indicates some enhanced interaction of silanol with Ca^{++} ions. The most meaningful system was $MgCl_2$ in that the electrode was stable in all pMg-pH regions studied and the emf values were more stable than those observed for Cu^{++} . For this system a clear distinction could be made between the results seen for the higher ratio silicates and the more alkaline solutions. This effect is also seen for Cu^{++} , but the uncertainty in the emf data cloud the results.

Looking at all of the results together it appears that there is a significant difference between higher and lower ratio silicates in their interaction with the metal ions chosen. Iler has observed that:

"Silica suspended in a solution of most polyvalent metal salts begins to adsorb metal ions when the pH is raised to within 1-2 pH units below the pH at which the polyvalent metal hydroxide is precipitated."

This observation from results using silica sols is consistent with the experimental results observed here for the higher ratio solutions. Thus, it is most probable that the same mechanisms associated with surface complex formation with deprotonated silica, are operating here.

The results for Mg^{++} and Ca^{++} suggest that $Mg(OH)_2$ and $Ca(OH)_2$ species are being formed since the pH-pMe lines all have slopes of -2.0 within the error (see Table II) disregarding the erratic results for Ca^{++} at m = 3.8.

The Cu^{++} results suggest a mixture of $\text{Cu}(\text{OH})_2$ and $\text{Cu}_2(\text{OH})_2^{++}$. However, since no analyses were carried out of the solid phases formed in this study, we can not rule out the possibility of the formation of precursors to (or actual) mineral silicates and other basic precipitates due to the presence of ClO_4^- and Cl^- . Studies are currently under way in our laboratory to look at the solid phases formed in dilute silicate and metal ion solutions.

TABLE II
Slopes of pH-pMe lines

Silicate ratio	pH-pMe slopes		
	Ca^{++}	Mg^{++}	Cu^{++}
0.0(NaOH)	---	-2.02(10)*	-1.76(34)
0.5	---	-1.82(30)	-1.68(20)
2.0	-1.97(39)	-2.00(26)	-1.43(14)
3.8	-3.47(172)	-2.10(21)	-1.43(16)

*Values in parentheses are 95% CL values of last digits.

So far in our discussion we have just looked at the activities of the ions versus hydrogen ion activity. In Figure 5 the results for magnesium solutions with initial pMg values of 3.47 and 2.49 are shown versus varying SiO_2 concentration level. In this Figure we see that the 0.5 ratio solutions cause little pMg reduction compared to that seen for the 2.0 ratio silicate at constant values of SiO_2 content in solution; however, we also observe that the 3.8 ratio solutions are not as effective as the 2.0 silicate ratio when compared on this basis. These results suggest that at least for Mg^{++} significant activity reduction in the presence of colloidal silica species is dependent on some other factors, e.g. critical pH value, the presence of small ionic silicate species, a change in the solid species present, or some degree of surface Si-O^- sites, as well as having a polymerized form of SiO_2 available in solution. There was insufficient data to look at this effect for Ca^{++} and Cu^{++} .

It would appear that the most probable explanation of the results is that in higher ratio solutions the presence of colloidal size silicate anions with more acidic surface silanol groups readily adsorb nucleating metal ion hydroxides thus enhancing the reduction of pMe. This adsorption might be enhanced by the presence of OH^- , or increased Si-O^- sites on the colloidal sized silica surfaces at higher pH values. There is also the possibility that intermediate sized silicate species are capable of forming ligand complexes with metal ions due to their increased silanol acidity and structure. The

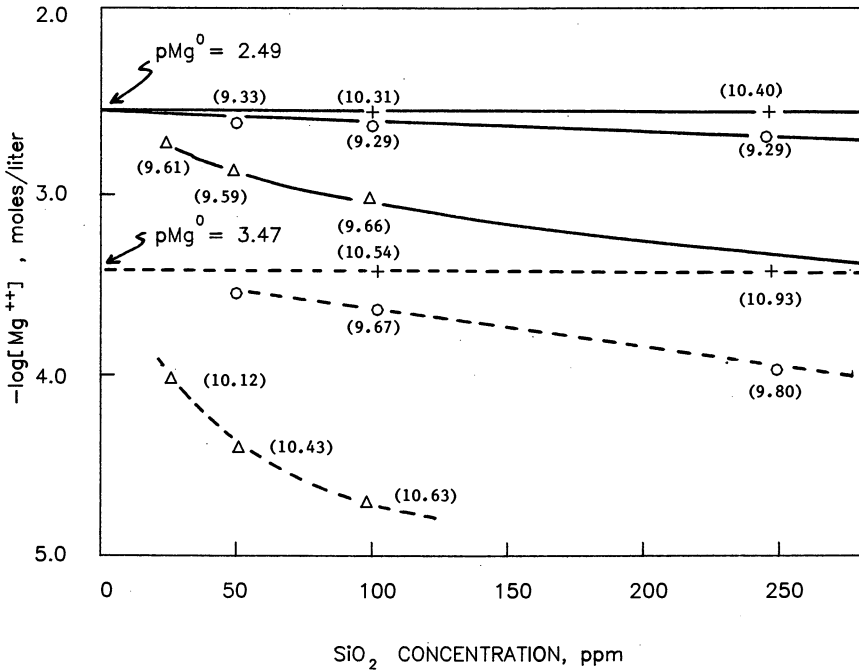


Figure 5. Reduction in magnesium ion activity vs. silica concentration for sodium silicate solutions with $SiO_2:Na_2O$ ratio values of 0.5 (+), 2.0 (Δ), and 3.8 (○). The pH values are shown in parentheses.

behavior of these solutions might be predicted using a model employing an analogy to silica gel surface-metal ion interactions.

The species present in the very alkaline lower ratio silicate solutions do not possess the capability of competing with OH^- as a ligand or of adsorbing these nucleating hydroxide species thus they do not enhance nucleation and their behavior is essentially predictable from metal ion hydrolysis constants.

Further experiments are planned to look at the above possibilities more carefully.

Literature Cited

1. Falcone, J.S., Jr. *Silicon Compounds, Synthetic Inorganic Silicates*, ECT, 20, 3rd ed. to be issued Dec. 1982.
2. Campbell, T.C.; Falcone, J.S., Jr.; Schweiker, G.C. HAPPI 1978, 15, 33.
3. Stumm, W.; Huper, H.; Champlin, R.L. Envi. Sci. Tech. 1967, 1, 221.
4. Falcone, J.S., Jr. "Recent Advances in the Chemistry of Sodium Silicates: Implications for Ore Beneficiation" presented at Fall Meeting SME-AIME, Denver, CO, Nov. 19, 1981.
5. Krumrine, P.H.; Ailin-Pyzik, I.B.; Falcone, J.S., Jr.; Campbell, T.C. "Surfactant Flooding III: The Effect of Alkaline Chemicals on the Adsorption of Anionic Surfactants by Clays", presented at the "ACS Symposium on the Chemistry of Enhanced Oil Recovery", Atlanta, GA, April 2, 1981.
6. Hazel, J.F. J. Phys. Chem. 1945, 49, 520.
7. Harman, R.W. J. Phys. Chem. 1928, 32, 44.
8. Hazel, J.F.; McNabb, W.M.; Macherer, P.E. J. Electrochem Soc. 1952, 99, 301.
9. Iler, R.K. "The Chemistry of Silica"; John Wiley & Sons: NY 1979, Chapter 6.
10. Dent Glasser, L.S.; Lachowski, E.E. JCS Dalton 1980, 393.
11. Harris, R.K.; Knight, C.T.G.; Hull, W.E. "NMR Studies of the Chemical Structure of Silicates in Solution", in this volume.
12. Anderson, K.R.; Dent Glasser, L.S.; Smith, D.N. "Polymerization and Colloid Formation in Silicate Solutions", the preceding paper.
13. Schwartz, R.; Müller, W.D. Z. Anorg. Allg. Chem. 1958, 296, 273.
14. Belyakov, V.N.; Soltiuskii, N.M.; Strazhesko, D.N.; Strelko, V.V. Ukr. Khim. Zh. (Russ. ed) 1974, 40, 236.
15. Schindler, P.W.; Kamber, H.R. Helv. Chim. 1968, 51, 1781.
16. Maatman, R.W.; Dugger, D.L.; Stanton, J.H.; Irby, B.N.; McConnell, B.L.; Cummings, W.W. J. Phys. Chem 1964, 68, 757.

American Chemical
Society Library
1155 16th St. N. W.
Washington, D. C. 20036

17. Schindler, P.W.; Furst, B.; Dick, R.; Wolf, P.U. J. Colloid and Interface Sci. 1976, 55, 469.
18. James, R.O.; Healey, T.W. J. Colloid and Interface Sci. 1972, 40, 65.
19. Robinson, R.A.; Stokes, R.H. "Electrolyte Solutions"; 2nd Ed., Butterworths: London, 1959, p 232.

RECEIVED March 2, 1982.

Aging of Amorphous Silica in Salt Water Solutions

JOAN D. WILLEY

University of North Carolina at Wilmington, Department of Chemistry,
Wilmington, NC 28406

Attempts to determine the solubility of amorphous silica in salt water solutions at near neutral pH and 0 to 5°C or 22 to 25°C have yielded a wide range of values, which results in part from aging of the silica surface in contact with solution. This makes determination of an initial solubility for silica difficult. Low temperature aging in salt water solutions or seawater causes a decrease in surface area, in specific pore volume, and in solubility. Solubilities determined at pressures to 1000 atmospheres (1×10^8 pascals) indicate that aging causes an increase in density of the surface silica; this data also allows calculation of the partial molal volume of dissolved silica. Identification of specific processes involved with aging of an amorphous surface are necessary for understanding silica solubility.

The solubility of amorphous silica in salt water solutions at 0 to 25°C has been the subject of much study in recent years, and it is interesting that determination of such an apparently simple number can yield such a wide range of results (Table I). As an illustration of the problem, Willey (1) showed a plot of the solubility of amorphous silica in seawater at 0°C and at pressures from 1 to 1000 atmospheres pressure. A later study using the same experimental apparatus (2) reproduced the same plot. However, two months later during the next experiment with the same equipment and the same silica, a solubility decrease occurred at all pressures, and the pressure dependence became slightly different than in both previous studies. This aging effect caused a solubility decrease of approximately 20%. Two other pressure studies (3, 4), which used different experimental techniques, reported results which agreed with the latter study after aging of the solid silica (Table II and Figure 1).

Table I. Reported solubilities for amorphous silica in seawater and in aqueous salt water solutions similar to seawater. The solid phase description comes from the primary reference. "sw" refers to seawater; "tris" refers to tris buffer. Temperature is indicated by T. The dissolved silica concentration, [Si], is reported as ppm Si and μm .

Reference	Solid Phase	Solution	T °C	[Si] ppm	μm
Krauskopf, 1956	Silica gel	Artificial sw	25	49.0	1750
	Silica gel	Natural sw	25	49.4	1760
	Amorphous silica	Natural sw	0	32.7	1160
Kitahara, 1960	Amorphous silica	Natural sw	2	32.7	1160
Lewin, 1961	Acid-cleaned	Natural sw	19	43	1500
	Biogenic silica	2.5% NaCl + tris	19	48	1700
Siever, 1962	Silica gel	Artificial sw	25	64.1	2290
	Synthetic opal	Artificial sw	25	56.0	1990
Stöber, 1967	Vitreous silica	0.9% NaCl + 0.1% NaHCO ₃	25	51.5	1830
Jorgensen, 1968	Precipitated amorphous SiO ₂	1M NaClO ₄	25	36.3	1290
Kato, et al., 1968	Silica gel	Artificial sw	20	39.7	1410
Hurd, 1972	Acid-cleaned	Natural sw	3	29.5	1050
	Biogenic opal	Natural sw	25	43.6	1550

Table I. continued.

Reference	Solid Phase	Solution	T °C	T ppm	[Si] μm
Hurd, 1973	Acid-cleaned	Natural sw + tris	23	44	1600
	Biogenic opal	0.7 M NaCl + tris	23	44	1600
		Natural sw + tris	3	26	930
		0.7 M NaCl + tris	3	25	890
Iler, 1973	Colloidal silica	0.015 N NaCl	25	45	1600
Jones, et al., 1973	Silica gel	Artificial sw	2	26.3	936
Willey, 1974	Amorphous silica	Natural sw	0	30.5	1090
Marshall, 1980	Silica gel	1 M NaCl*	25	54.3	1930
Willey, 1980	Amorphous silica	0.9% NaCl + 0.1% NaHCO ₃	2	31.0	1100
	Aged amorphous	0.9% NaCl + 0.1% NaHCO ₃	22	46.6	1660
			2	26.6	947
Griffin, et al., 1981	Amorphous silica	0.7 M NaCl	22	36.8	1310
			2	24.7	879

* Many other solutions reported also.

Table II. Experimental Conditions and References for Figure 1.
 ND indicates no data available.

Figure 1 Symbol	Reference	Solid Phase	Solid Pretreatment	Solution	Initial pH	Final pH
■	Jones and Pytkowicz, 1973	Matheson, Coleman and Bell Chromatographic Absorbent Silica Gel	wash with 0.10 N NaOH and distilled water	Artificial seawater	ND	ND
+	Willey, 1974	Baker Silicic Acid	none	Natural seawater, filtered 0.8 μ	8.1	7.0 ± 0.5
X	Willey, 1975	Baker Silicic Acid	none	0.6 N NaCl	8	ND
□	Willey, 1975	Baker Silicic Acid	none	0.6 N KCl	8	ND
●	Willey, 1980	Baker Silicic Acid	size fractionate to remove <5 μ, heat to 1000°C for 1 hour	0.9% NaCl + 0.1% NaHCO ₃	8.2	7.7 ± 0.1
○	Willey, 1980	Baker Silicic Acid	size fractionate to remove <5 μ, heat to 1000°C for 1 hour	0.9% NaCl + 0.1% NaHCO ₃	8.2	7.7 ± 0.1
△	Griffin, et al., 1981	Baker Silicic Acid	none	0.7 M NaCl	8.1	8.1 ± 0.2

Table II. continued.

Figure 1 Symbol	% H ₂ O in Solid	Solid Density, g/cm ³	Solid Surface Area, m ² /g	Experimental Temperature °C	Solid Aging Time
■	ND	ND	ND	2	>66 days
+	9.0	1.85	320	0	<14 days
x	9.0	1.85	320	0	< 7 days
□	9.0	1.85	320	0	< 7 days
●	0.0	2.15	110	2.3 ± 0.4	<20 days
○	0.0	2.15	64	2.3 ± 0.4	>60 days
△	9.3	1.86	350	2 ± 1	21 days

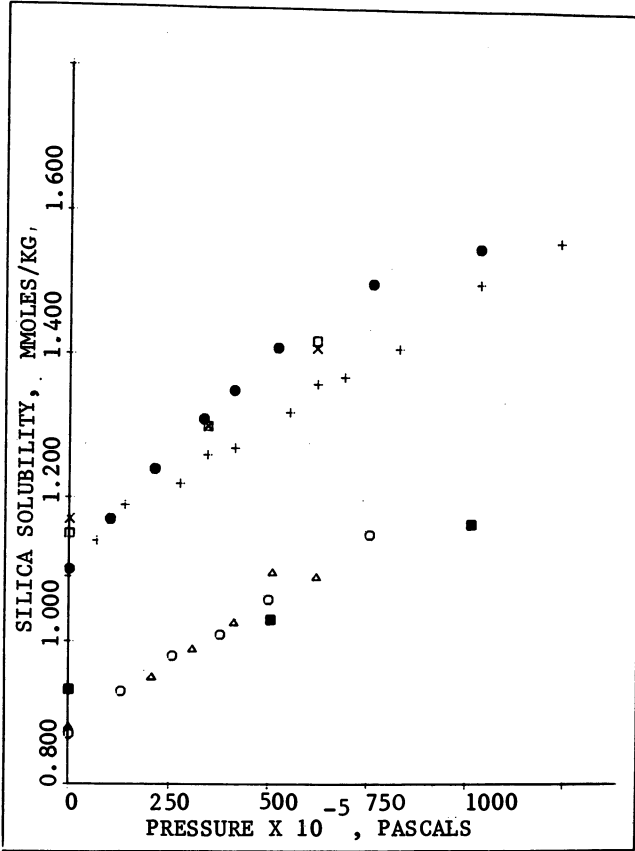
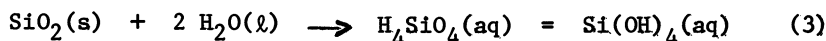
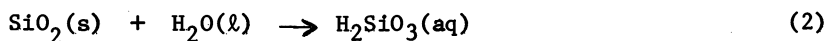


Figure 1. Solubility of amorphous silica in salt water solution or seawater at 0–2°C in mmol/kg as a function of pressure in Pa (1 bar = 10⁵ Pa). Symbols and experimental conditions are defined in Table II.

The reaction of interest is the dissolution of amorphous silica in aqueous solution in the temperature range from 0 to 25°C, the pressure range from one to 1000 atmospheres, and the pH range from 6 to 8.5. In this pH region, dissolved silica occurs primarily as undissociated silicic acid (5); above this pH range, the solubility increases due to the increased dissociation of silicic acid. The dissolution can be written several ways, depending upon how water is indicated, as follows:



Pressure is of interest as a variable both because it is a factor in many geochemical reactions and because information about a pressure dependency allows calculation of the volume change for a reaction. The relevant equations are given below. Equation 4 is the fundamental relationship for pressure dependency from thermodynamics; Equation 5 is this equation as solved by Owen and Brinkley (6); Equation 6 is a useful rearrangement of Equation 5; and Equation 7 defines the volume change for this dissolution of amorphous silica as written in Equation 3.

$$\partial \ln K / \partial P = - \Delta \bar{V} / RT \quad (4)$$

$$RT \ln(K_P / K_1) = - \Delta \bar{V}_1 P + \frac{1}{2} \Delta \bar{k}_1 P^2 \quad (5)$$

$$(RT/P) \ln(K_P / K_1) = - \Delta \bar{V}_1 + \frac{1}{2} \Delta \bar{k}_1 P \quad (6)$$

$$\Delta \bar{V}_1 = \bar{V}_{\text{Si}(\text{OH})_4(\text{aq})} - \bar{V}_{\text{SiO}_2(\text{s})} - 2 \bar{V}_{\text{H}_2\text{O}(\ell)} \quad (7)$$

In these equations, K is the equilibrium constant (for the dissolution of amorphous silica the solubility \underline{c} can be used in place of K (7)), P is pressure in atmospheres, $\Delta \bar{V}$ is the change in volume caused by the reaction, R is the universal gas constant, T is temperature, $\Delta \bar{k}_1$ is the change in compressibility caused by the reaction, \bar{V} indicates partial molal volume, and subscripts refer to pressure in atmospheres. Determination of $\Delta \bar{V}_1$ would allow calculation of $\bar{V}_{\text{Si}(\text{OH})_4(\text{aq})}$, a quantity necessary for predicting the direction of the pressure effect for several geochemical reactions which are difficult to investigate experimentally, for example, mineral formation at sea floor conditions. However, this calculation demands accuracy in knowledge of the atmospheric pressure solubility, and confidence in the reproducibility of the pressure versus solubility plots.

Therefore, the causes of the variation in published solubilities and pressure dependencies of the solubility must be understood, and that is the intention of the present study.

Experimental Methods

Important experimental conditions used to obtain the data considered in this paper are given in Tables I and II. The various methods used to determine silica solubility are described in detail in the primary references. The surface area measurements were made using nitrogen adsorption; two measurements were made for comparison using a Sears titration with 0.1 N NaOH. Other surface measurements were made using nitrogen adsorption studies.

Results and Discussion

When solid amorphous silica is placed in contact with salt water, the solid silica surface undergoes significant changes which can affect experimental results. The amount of time required for changes to be observed is not clearly established, however, the necessary duration of contact with solution is probably in the range from days (8) to months (2) at temperatures below approximately 25°C. Several studies of amorphous silica exposed to aqueous solution have reported a decrease in surface area with time (8-12). Willey (2) reported a decrease in surface area of amorphous silica which occurred along with a solubility decrease. Additional analyses of the silica sample used in Willey's (2) study show that the surface area decrease and solubility decrease occurred along with a decrease in specific pore volume (Table III). The agreement between the results of the BET surface area determinations and the two Sears titrations shows that the experimental silica did not have a significant proportion of pores smaller than the nitrogen molecules. No clear trend was observed for mean pore diameter of the solid silica, although logically this should increase with decreasing surface area. These data are presented in Table III along with information about biogenic silica (11, 12) for comparison. The similarity in trends and numbers for the chemically pure amorphous silica compared with the biogenic silica suggests that this initial aging step may be part of the process that occurs in nature as biogenic silica changes with time in sediments.

Indirect evidence suggests that the density of the silica surface also increases as a result of aging although the density of the bulk silica does not change (Table II). Willey (2) calculated $\Delta \bar{V}_1$ for aged and fresh silica based on pressure studies and found a change to a less negative number. Since the other parts of the reaction (water and dissolved silica) cannot have changed in volume, this is interpreted to indicate a change in

Table III. Surface characteristics and solubilities for amorphous silica before and after aging in salt water, and for recent and 40 million year old biogenic silica.

	Surface Area $m^2 g^{-1}$	Specific Pore Volume $cm^3 g^{-1}$	Mean Pore Diameter nm	Solubility $mmol kg^{-1}$ 0-30°C
Hydrated silica in seawater				
Initial	320	0.51	4	1.09
Aged 3 years	90	0.46	20	0.88
Dehydrated silica in 0.9% NaCl + 0.1% NaHCO ₃ solution				
Initial	110*	0.43	17	1.10
Aged > 60 days	64**	0.26	17	0.87
Biogenic silica in seawater***				
Recent	250	0.45	7	1.0
Aged 40 million years	2-20	0.00	7	0.1 - 0.8

* Sears titration $110 m^2 g^{-1}$

** Sears titration $80 m^2 g^{-1}$

*** data from Hurd and Theyer (11) and Hurd, Wenkam, Pankratz, and Fugate (12)

the silica surface to a higher density phase. Additional evidence has been obtained by measuring the rate of dissolution of aged versus fresh silica and this rate was found to be slower for the aged silica. In an experiment similar to that described by Stöber (13) and using a surface area to volume ratio of $0.1 \text{ m}^2 \text{ cm}^{-3}$ in a solution of 0.9% NaCl + 0.1% NaHCO_3 in water, the rate of dissolution was found to be $2600 \mu\text{g m}^{-2} \text{ day}^{-1}$ for fresh silica and $1400 \mu\text{g m}^{-2} \text{ day}^{-1}$ for aged silica. The fresh sample rate is higher than that reported by Stöber (13) for vitreous silica ($2000 \mu\text{g m}^{-2} \text{ day}^{-1}$), probably because Stöber used a time interval of one day and the present study used a time interval of one hour. The rate constants obtained from the present study (2×10^{-8} to $7 \times 10^{-8} \text{ cm sec}^{-1}$) are similar to those reported by Hurd (14) for acid cleaned biogenic silica, using similar experimental conditions. Stöber (13) found that the daily release of silicic acid from silica polymorphs decreased in the order: vitreous silica, stishovite, cristobalite, tridymite, quartz, coesite. The order is from low to high density with the exception of stishovite which has a high density but also a higher solubility and a different coordination number than the other crystalline polymorphs. The decrease in the rate of silica dissolution in the present study may therefore reflect an increase in order or density at least on the silica surface. The trends observed for the aging of amorphous silica in salt water solution are summarized in Table IV. Biogenic silica exhibits similar trends except that the rate of dissolution does not clearly change; in addition, with biogenic silica the water content decreases and crystallinity increases with time (11, 12).

Table IV. Trends in Aging of Amorphous Silica in Contact with Salt Water

<u>Decrease</u>	<u>Increase</u>
Specific Surface Area	Density
Specific Pore Volume	
Solubility	
Rate of Dissolution	

These trends indicate that the solid silica surface in contact with solution is changing with time. Small particles or areas with high positive radius of curvature are dissolving, and more dense and more ordered silica is precipitating to give a flatter surface with a lower solubility and lower surface area (15). This process takes time. It occurs with many different kinds of silica including biogenic silica. The result is to reduce differences in the solubilities of various silica solids because the surface precipitated from a given solution is at least partly a function of the solution and not totally dependent on the

solid amorphous silica. This interpretation is consistent with ideas presented by Okkerse and de Boer (9, 10), Stöber (13), Jorgensen (16), Sheinfain and Neimark (8), Vysotskii, et al. (17), and Iler (15).

These ideas can be used to interpret some of the variation in the pressure studies mentioned earlier. In one of the initial studies (Willey (1), and indicated by + on Figure 1) the solubility was determined several times at a pressure, and then the pressure was increased. This process continued, with some lower pressure determinations in the middle of the experiment, until the highest pressure was attained, at which point the internal silica columns ruptured which prevented a rechecking of the atmospheric pressure solubility. It is proposed that the solid silica was aging during the experiment, which causes the deflection to slightly lower than expected solubilities as the experiment progressed to higher pressures. The separation of points into two groups on Figure 1 also is a result of aging with the aged silica solubilities (■, 0, and Δ on Figure 1) falling into the lower solubility group. The magnitude of this aging process is significant (approximately 20%), and it contributes to the scatter in the published solubility values (2). Because of this aging, it is difficult to determine the solubility for amorphous silica in water after a short time period.

Not all investigators have observed a decrease in silica solubility with time (13, 18-23). Some evidence for aging (either a decrease in solubility or a change in surface characteristics) has been observed in several other studies (1, 2, 11, 16, 19, 24). Several studies (3, 4, 23, 25) obtained solubility values characteristic of aged silica, but no solubility change was observed. One experimental parameter which is different in the group which observed aging and the group that did not was the ratio of solid silica surface area to solution volume. Because of insufficient information, this could not be evaluated in all studies; however, estimation (based on product literature from several companies that manufacture amorphous silica) of a specific surface area for silica gel of $300 \text{ m}^2\text{g}^{-1}$ and of $100 \text{ m}^2\text{g}^{-1}$ for distilled water washed silica gel allows estimation of this ratio in most of the experiments listed above. In all the studies in which aging was indicated, the surface area to solution volume ratio was greater than $0.1 \text{ m}^2\text{cm}^{-3}$; in those which did not observe aging this ratio was less than $0.1 \text{ m}^2\text{cm}^{-3}$ or the experimental time period was less than 60 days. Apparently the higher surface area to volume ratio enhances the silica precipitation that occurs during aging. The silica surface that results from the precipitation has a lower solubility than the original surface. It is interesting to note that the lower solid surface area to solution volume ratio (which often is also a smaller mass of silica in contact with a specific volume of solution) produces a higher solubility value.

Identification of aging as a factor in silica solubility allows use of appropriate data for calculation of ΔV_1 , using Equation 6. For this calculation, only data for aged silica (including the atmospheric pressure solubility) was used (2, 3, 4). This calculation gives $\Delta V_1 = -9.9 \text{ cm}^3 \text{ mol}^{-1}$ and hence from Equation 7, $V_{\text{Si(OH)}_4(\text{aq})} = 55 \text{ cm}^3 \text{ mol}^{-1}$. The statistics of this calculation are discussed elsewhere (26).

Several other possible explanations in addition to short term aging were considered to explain the variation in published data (Figure 1) for the solubility of amorphous silica at elevated pressures:

1. Effect of hydration of the solid phase.

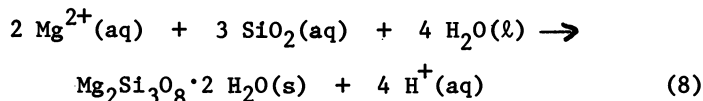
Comparison of the solubility behavior of unaged dehydrated silica (2, ● in Figure 1) with unaged hydrated silica (27, x or □ in Figure 1) shows no difference. Similar comparison of aged dehydrated silica (2, 0 in Figure 1) with aged hydrated silica (4, Δ in Figure 1) also shows no difference. Therefore, hydration of the solid phase does not affect the pressure dependence of silica solubility in the pressure range to 1000 atmospheres.

2. Seawater effect.

The solubility data points in Figure 1 were obtained in several different solutions, including artificial seawater (3, ■ in Figure 1), 0.7 M NaCl (4, Δ in Figure 1), and 0.9% NaCl + 0.1% NaHCO₃ (2, 0 in Figure 1). The similarity among these data sets shows that seawater does not have a different solubility than the simpler salt solutions.

3. Inhibition of silica dissolution by sepiolite formation in seawater.

Wollast, et al. (28) suggested that silica concentrations in seawater may be limited by the precipitation of sepiolite ($\text{Mg}_2\text{Si}_3\text{O}_8 \cdot 2 \text{H}_2\text{O}(\text{s})$) which can be written as follows:



Wollast, et al. (28) report that the equilibrium constant for this reaction is in the range of 10^{-18} to 10^{-19} at 25°C in seawater. Ion activity products calculated for the data in Willey (1) all indicate solutions undersaturated by several orders of magnitude with respect to sepiolite, and slightly

undersaturated for data in Jones and Pytkowicz (3) assuming a small temperature and pressure effect on this equilibrium constant. In order to calculate these ion activity products, 0.22 was used as the activity coefficient for Mg^{2+} , 1.0 was used as the activity coefficient for dissolved silica, the pH of the solutions used by Jones and Pytkowicz (3) was assumed to be between 7.5 and 8.0. The data produced by Willey (2) and Griffin, et al. (4) could not have been affected by sepiolite formation because no magnesium was present in the experimental solutions.

The solubility of sepiolite should increase with increasing pressure based on a simple calculation of $\Delta\bar{V}_1$ for the dissolution of sepiolite. Using partial molal volume data for Mg^{2+} and H^+ compiled by Berner (29), along with the value for $V_{Si(OH)_4(aq)}$ calculated in this study and a molal volume for sepiolite calculated from density data (2.08 to 2.45 gcm^{-3}) compiled in Donnay and Ondik (30), $\Delta\bar{V}_1$ should be between - 37 and - 59 cm^3 per mole of sepiolite dissolved. The sign of this number indicates that the solubility of sepiolite should increase with increasing pressure. Based on this calculation, sepiolite should not limit silica solubility any more at higher pressure than it does at lower pressure; this cannot be said with certainty, however, until more information on the solubility of sepiolite as a function of pressure is available. A similar calculation has been done by Sayles (31).

The pH decrease (Table II) observed in the early experiment when seawater came into contact with the amorphous silica surface suggested possible sepiolite formation. However, in subsequent experiments, a similar pH change was observed for unwashed silica surfaces in contact with 0.9% NaCl + 0.1% $NaHCO_3$ solution. The amount of base required to titrate each solution back to pH 8 after the solid phase was removed was greater in the salt solution than in seawater. This experiment shows that the pH decrease occurs in solutions with no $Mg^{2+}(aq)$, so sepiolite formation is not necessarily involved with the pH change.

The concentration of dissolved silica in salt water solutions in contact with solid amorphous silica may decrease for a time period of several weeks to several months after the initial dissolution, and then after this initial aging process is completed the concentration remains stable for months or years (2). Several studies have reported this equilibrium solubility. Jorgensen (16) found that three to five months were required to achieve equilibrium in his experiments, and after that time the same solubility was determined from undersaturated or oversaturated solutions in contact with silica for time periods up to two years. Jones and Pytkowicz (3) found the same solubility for aged silica after 66 or 123 days of equilibration time. Willey (2) found no change in the solubility of silica aged for two months in salt water solution after time periods of up to five years. Griffin, et al. (4) determined solubilities using the crossover method of Siever and Woodford (32) which does not require attainment of equilibrium. With this method (32), solutions which have different dissolved silica concentrations are placed in contact with solid amorphous silica. The change in concentration which results when either dissolution or precipitation occurs in the several solutions is used to calculate the solubility. In the study by Griffin, et al. (4), concentration change measurements were made after three weeks. Kato and Kitano (20) used an equilibration time of 500 days in their solubility experiments. All of these long term studies obtained similar values for the solubility of aged amorphous silica in salt water solutions. Siever (22) obtained a slightly higher solubility value after an equilibration time of two years. These studies show that the solubility of aged amorphous silica in salt water solutions is stable for many months or years after an initial aging time of several months. The trends observed for the aging of biogenic silica (11, 12) and thermodynamic calculations (7) suggest that this is not the ultimate equilibrium; eventually the amorphous silica should change to quartz which has a much lower solubility than amorphous silica (4, 7, 13, 15, 21).

Conclusions

1. The solubility of amorphous silica in salt water solutions (at 0-3°C or 19-26°C, and over the pressure range from 1 to 1000 atmospheres) decreases by approximately 20% with time due to aging of the solid silica.
2. This solubility change makes amorphous silica solubility difficult to determine, and contributes to the scatter in published solubility values.
3. Other trends associated with this aging of silica include a decrease in specific surface area and pore volume, and an increase in density. Similar trends have been identified for biogenic silica.

4. The rate of silica aging depends on experimental conditions, including the ratio of solid surface area to solution volume.

5. The solubility of amorphous silica in seawater or in salt water solutions similar to seawater is not affected by the extent of hydration of the solid phase, and is not limited by sepiolite formation.

Acknowledgments

Discussions of importance regarding this work were held with R. Dayal and R. K. Iler, and an earlier version of the manuscript was reviewed by L. M. Mayer. E. Malik typed the manuscript. All of this assistance is appreciated.

Literature Cited

1. Willey, J. D. Mar. Chem. 1974, 2, 239-250.
2. Willey, J. D. Geochim. Cosmochim. Acta 1980, 44, 573-578.
3. Jones, M. M.; Pytkowicz, R. M. Bull. Soc. R. Sci. Liege 1973, 42, 118-120.
4. Griffin, J. W.; Hurd, D. C.; Commeau, J.; Poppe, L. Am. J. Sci. (in preparation).
5. Duedall, I. W.; Dayal, R.; Willey, J. D. Geochim. Cosmochim. Acta 1976, 40, 1185-1189.
6. Owen, B. B.; Brinkley, S. R. Chem. Rev. 1941, 29, 461-473.
7. Walther, J. V.; Helgeson, H. C. Am. J. Sci. 1977, 277, 1315-1351.
8. Sheinfain, R. Y.; Neimark, I. E. Chapter 8, in "Adsorption and Adsorbents" (ed. D. N. Strazhesko), Wiley, 1973, pp. 87-95.
9. Okkerse, C.; de Boer, J. H. Chapter 25 in "Reactivity of Solids" (ed. J. H. de Boer), Elsevier, 1961, pp. 240-248.
10. Okkerse, C.; de Boer, J. H. Silic. Ind. 1962, 27, 195-202.
11. Hurd, D. C.; Theyer, F. Adv. Chem. Ser. 1975, 147, 211-230.
12. Hurd, D. C.; Wenkam, C.; Pankratz, H. S.; Fugate, J. Science 1979, 203, 1340-1343.
13. Stöber, W. Adv. Chem. Ser. 1967, 67, 161-182.
14. Hurd, D. C. Earth Planet. Sci. Lett. 1972, 15, 411-417.
15. Iler, R. K. "The Chemistry of Silica". Wiley, 1979.
16. Jorgensen, S. S. Acta Chem. Scand. 1968, 22, 335-341.
17. Vysotskii, Z. Z.; Galinskaya, V. I.; Kolychev, V. I.; Strelko, V. V.; Strazhesko, D. N. Chapter 7 in "Adsorption and Adsorbents" (ed. D. N. Strazhesko). Wiley 1973, 72-86.
18. Krauskopf, K. B. Geochim. Cosmochim. Acta 1956, 10, 1-26.
19. Kato, K.; Kitano, Y. J. Oceanogr. Soc. Jpn. 1968, 24, 147-152.
20. Lewin, J. C. Geochim. Cosmochim. Acta 1961, 21, 182-198.

21. Siever, R. J. Geol. 1962, 70, 127-150.
22. Iler, R. J. Colloid Interface Sci. 1973, 43, 399-408.
23. Kitahara, S. Rev. Phys. Chem. Jpn. 1960, 30, 131-137.
24. Marshall, W. L. Geochim. Cosmochim. Acta 1980, 44, 907-914.
25. Hurd, D. C. Geochim. Cosmochim. Acta 1973, 37, 2257-2282.
26. Willey, J. D. Geochim. Cosmochim. Acta (in press).
27. Willey, J. D. "The Physical Chemistry of Silica in Sea Water and Marine Sediments"; Ph.D. Thesis, Dalhousie University, 1975, 195 pp.
28. Wollast, R.; MacKenzie, F. T.; Bricker, O. P. Am. Mineral. 1968, 53, 1645-1662.
29. Berner, R. A. "Principles of Chemical Sedimentology"; McGraw-Hill Book Company, 1971, p. 212.
30. Donnay, J. D. H.; Ondik, H. M. "Crystal Data Determinative Tables"; Volume 12, U. S. Department of Commerce, National Bureau of Standards, and Joint Committee on Powder Diffraction, 1973, p. 0-51.
31. Sayles, F. T. Geochim. Cosmochim. Acta 1981, 45, 1061-1086.
32. Siever, R.; Woodford, N. Geochim. Cosmochim. Acta 1973, 37, 1851-1880.

RECEIVED March 2, 1982.

Silanol Groups and Properties of Silica Surfaces

J. J. FRIPIAT

C.N.R.S. C.R.S.O.C.I., 45045 Orléans, France

This paper begins by reviewing briefly different techniques, namely precipitation of organic and inorganic compounds, oxidation of volatile silicic compounds and acid attack of magnesium silicates, for preparing porous and non porous silicagels with various surface coverages and distributions of silanol groups, and the effect of heating on these materials. Infrared spectroscopic investigations coupled with chemical specific reactions as well as with magnetic nuclear resonance (NMR) permit a characterization of these surfaces.

The chemical properties of silanol groups and of silica surfaces are then studied from the point of view of adsorption processes, involving mainly water, methanol ammonia and amines. Proton interaction and exchange between silanol group and those reagents are studied using physical techniques and particularly pulse NMR. The proton exchange process is related to the acid properties of the silanol groups.

Estherification reactions of silanol groups with chloro-alkyl silane, methanol and other reagents and the properties of the reaction products are examined.

The reduction of silica surface at high temperature by the so-called spillover process leading to the formation of exposed silicon atoms and Si-H groups, is finally studied.

The hydrolysis of soluble silicates or of silicon organic derivatives such as silicic ether in aqueous solution yields silicagels with variable but generally high, specific surface areas.

For instance, as shown in Table I, when 0.6 ml of $\text{Si}(\text{OC}_2\text{H}_5)_4$ is mixed with 10 ml of water and treated at 150°C under the corresponding water pressure the precipitated solids outgassed at 100°C have specific surface areas between 52 and 578 m^2/g according to the initial pH conditions.

Table I - Nitrogen B.E.T. specific surface areas obtained by hydrolyzing $\text{Si}(\text{OC}_2\text{H}_5)_4$ at 150° under 6 atm water pressure (1)

Hydrothermal treatment, aging (days)	Precipitation pH	2	3.5	5.5	8
	Final pH	2.5	3.6	4.5	5.2
2		578	345	58	112
8		520	309	78	70
16		365	155	52	115

This is an illustration among many others of the importance of the aging time, and of the pH of hydrolysis on the final polymerization degree.

Silicagels are X-rays amorphous but the radial distribution function obtained according to the technique initially proposed by Warren and collaborators (2) reveals that in the tetrahedral unit SiO_4 the Si-O distances are between 1.66 and 1.61 Å, e.g. in the domain observed for crystallized silicates and that there is some order in the structural arrangement of the second coordination shell (1). The Si-O distance within a tetrahedron is slightly shorter in gels prepared from $\text{Si}(\text{OC}_2\text{H}_5)_4$ at pH between 3 and 6 and somewhat larger at lower or higher pH. The $\text{Si}_1\text{-O-Si}_2$ angle varies between 145 and 180° according to the preparation procedure (1).

In β cristobalite this angle is 180° whereas in α and β quartz and α cristobalite it ranges between 143° and 150° . Thus a silicagel may be considered as formed of small units, involving the second coordination shell, which are characterized by structural arrangements such as those found for these crystalline solids.

Silicagels prepared from distilled $\text{Si}(\text{OC}_2\text{H}_5)_4$ are of course quite pure, the main impurity being Na^+ ions from the NaOH solution used to adjust the pH. With respect to a crystalline silicate containing a dense network of silicon tetrahedra sharing corners, the main structure breaking element is the proton forming inner or external silanol groups. In addition, hydration water may be retained by these groups because of the formation of $\text{Si-OH}\cdots\text{O}\begin{matrix} \text{H} \\ \diagup \\ \text{H} \end{matrix}$ hydrogen bonds. The silanol group may be thus considered as a structural defect.

Numerous workers have tried to measure the relative contributions of the inner and external silanol group as well as that of hydration water. It is not a simple problem because the amorphous nature of the gel precludes the use of thermal methods such as

DTA or TGA. The hydration and constitutional water are lost in an almost monotonous manner.

Figure 1 shows an early attempt to make that type of distinction (3) using a combination of infrared technique and chemical determinations. All results are expressed as OH irrespective of the simultaneous presence of hydration water and of silanol groups. The gel is the Aerosil Degussa obtained by flame pyrolysis of SiCl_4 . Its N_2 B.E.T. surface area amounts to $180 \text{ m}^2/\text{g}$. Curve 1 is obtained from the weight loss. Curve 2 is obtained using the reaction of OH's (silanol or water) with LiCH_3 or CH_3MgI , producing methane, whereas curve 3 is the hydration water content deduced from the IR absorption bands in the OH stretching and the H_2O deformation regions. The gel was outgassed during 45 hrs at 25°C under a dynamic vacuum between 10^{-5} and 10^{-6} torr before these determinations were carried out. The total OH content was about $2.9 \cdot 10^{-3}$ mole/g at 25°C and the evolution of the ratio of the surface to the total hydroxyl content is shown in Figure 2. To obtain these results it was assumed that the surface silanols only react with the organometallic reagents.

This example illustrates the fact that the quantitative determination of surface silanol groups requires a combination of different techniques, and yet it requires hypothesis open to criticisms. According to Figure 1, the surface density in silanols is about 4.3 OH per nm^2 . It seems stable up to 300°C and it starts decreasing above that temperature. After heating between $600\text{--}700^\circ\text{C}$, the surface density reaches a value of about $1.5(\text{OH})/\text{nm}^2$. It is at this dehydroxylation state that an isolated OH stretching vibration appears as a narrow band at 3740 cm^{-1} . At lower dehydration temperature but above 250°C , when most of the hydration water is removed (see Figure 1, curve 3), the silanol stretching band is more complex because of contributions of inter hydrogen bonds. The value which is now generally accepted (4) for surface density in silanols is about $4.5 \text{ OH}/\text{nm}^2$.

It is to the properties of the surface silanols that this contribution is devoted.

Distribution of silanol groups on silica surfaces

On the surface of amorphous silicagels, the distribution of the silanol groups is most probably random. This means that there is some probability that any silanol group may have a near neighbour silanol which might be bound to the same silicon or most probably, which is linked to an adjacent silicon in a $=\text{Si}(\text{OH})\text{--O--Si}(\text{OH})=$ arrangement. For instance on a deuterated Aerosil surface outgassed at 27°C , the stretching OD region shows bands at 2760 cm^{-1} , 2665 cm^{-1} and a shoulder at 2573 cm^{-1} . These bands correspond to OH vibrational bands at 3740 , 3607 and 3480 cm^{-1} respectively. The 2573 cm^{-1} band reinforces when D_2O is physically adsorbed whereas the 2760 cm^{-1} individualized as a single band upon outgassing at increasing temperature. This band is, as said before, due to isolated deuterated silanol whereas the 2665 cm^{-1}

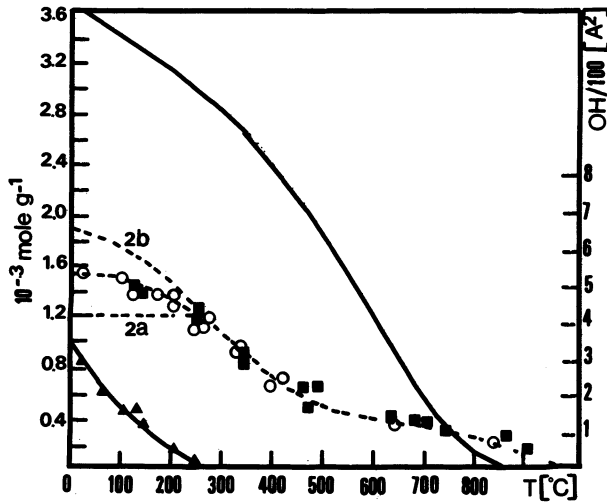


Figure 1. In abscissa: sample outgassing temperature under vacuum. Key: upper curve (—), OH (gravimetric) content (including H_2O); curve 2 (---), evolved CH_4 for the reactions with either CH_3Li (\circ) or CH_3MgI (\blacksquare); curve 2b, curve 2 corrected for physically adsorbed water; curve 2a; surface silanols content; lower curve (\blacktriangle) H_2O content (in OH) determined by IR spectroscopy.

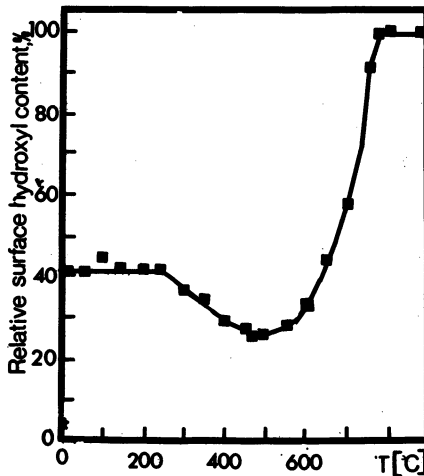


Figure 2. Relative surface hydroxyl content as a function of outgassing temperature.

band (e.g. the 3607 cm^{-1} OH band) may be tentatively assigned to hydrogen bonded silanols. Of course these vibrational bands are not necessarily those of surface silanols since deuteration may affect internal silanols as well. It has been shown (5) that the rates of isotopic exchange are different for isolated and bridged silanols but these kinetics data could not be used to calculate their respective contributions to the silanol surface density. The second moment of the proton NMR resonance line of silicagels from different origin has also been proposed to obtain more significant data (6). The classical equation for the second moment M_2 is

$$M_2 = 3.56 \frac{1}{N} 10^{-46} \sum_i \sum_j r_{ij}^{-6} \text{ (gauss}^2\text{)} \quad (1)$$

where r_{ij} is the distance between protons i and j in a volume that contains N protons. Any motion occurring in the domain of the proton nuclear resonance frequency ($\sim 10^8$ Hz) would reduce the second moment even if the average distance remains constant. If the protons were homogeneously spread on the surface in rigid positions M_2 should be 0.12 gauss^2 for a surface density of 4.4 proton/nm^2 (7).

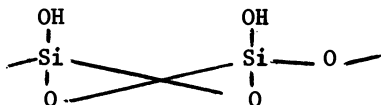
In Table II, the experimental second moments observed for various silicagels are given as well as the references to the paper where a particular gel has been characterized. The outgassing conditions and the temperature dependence of M_2 are also indicated.

Table II - Second moment of the proton NMR resonance line observed for various gels (6)

Gel	Outgassing temperature (°C)	M_2 (gauss ²)	Temperature dependence observed for M_2
Fibrous gel (6)	100	10.7	Variable see Table III
Aerogel (8)	100	2.33	Constant from 20°C to -160°C.
Xerogel (9)	100	3.00	Constant from 140°C to -160°C.
Davison (10)	500	0.51	Constant from 280°C to -210°C.
K_4 (11)	unknown	0.55	unknown.

The fibrous gel, with the highest M_2 was obtained by hydrolyzing completely asbestos chrysotile in a 6 N (50% water, 50% isopropanol) HCl solution at 50°C. In all cases, the experimental M_2 are considerably larger than that calculated for an homogeneous distribution. Because of the $1/r_{ij}^6$ dependence of M_2 , this means

that there are patches with higher concentrations in silanols. For the fibrous gel this can be qualitatively explained by sketching the structure of the hydrolysis product of the chrysotile by the following arrangement, each Si-O-Mg bond being replaced by one silanol group.



The approximate average distance between protons in such an arrangement is of the order of 2.3 Å whereas for the Xerogel it is of the order of 3.2 Å.

It may thus be expected that upon heating the fibrous gel above 500°C, the number of isolated OH will be rather small since water molecules nucleate readily from coupled OH's. Actually no band above 3700 cm⁻¹ appears in the fibrous gel in opposite to what is observed for the Xerogel under the same conditions.

Also the second moment is appreciably temperature dependent in the fibrous gel (Table III) whereas it is practically constant for the other gels (Table II). The proton mobility is thus enhanced by a more regular and close packed distribution of silanols. However the NMR technique of measuring second moment or the observation of the OH infrared bands as such do not allow to distinguish between internal and external OH.

Table III - Variation of M₂ with the measurement temperature for the fibrous silicagel (6)

T (°K)	S ₂ (Gauss ²)
293	10.7
198	16.5
118	17.5
80	18.6

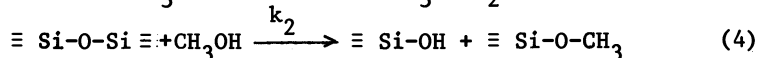
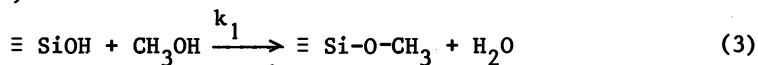
Measurements of the surface density in silanols groups are founded on two types of technique i) reacting the weakly acid hydroxyl group with an adequate reagent like chlorosilane, aminosilane, etc ; or ii) interacting the surface OH with physically adsorbed molecule. In both cases using I.R. the modification in the hydroxyl stretching region can be followed. The first type of method has been broadly used (12). The second type has been less popular specially for non-polar molecules condensed at low temperature. The adsorption of rare gases O₂, N₂, CH₄ on the stretching band of isolated silanols produces frequency shifts

between 8 and 43 cm^{-1} depending upon the polarizability of the adsorbate (13).

More recently, the spectroscopic properties of these isolated OH upon adsorption of weak hydrogen bond acceptor molecules, like benzene, acetonitrile, etc. were observed (14). The shifts were of course larger than those observed for non-polar adsorbates, ranging from 87 to 216 cm^{-1} . From hydrogen bonding studies in solution, the frequency shifts for two H bond donors R - HX and R' - X'H interacting with various acceptors are often compared by plotting the relative shift frequency ($\Delta\nu/\nu$) of one donor with respect to ($\Delta\nu/\nu_0$) for the other. Such BHW plots (Bellamy, Hallam and Williams) (15), are linear and quite different H-bond acceptors fit onto the same straight line when the proton bearing atoms in both bonds are the same. Therefore the frequency shifts observed for a reference proton donor provide a useful scale for predicting the shifts of donors containing the same functional group. The slope is an estimate of the relative H bonding strength. With p-fluorophenol, for example, linear relationships have been observed (14) and by comparing the BHW slope and the pK_a of various proton donors, the pK_a of isolated silanol groups is determined to be about 7. This is well in the range of the values reviewed by Iler (4) (p.660). The studies performed on isolated silanols offer the advantage of being rather simple to interpret since most of these groups are on the external surface available to the reagent (see Figure 2 for instance) and the problem is less complicated than for surface bridged OH's.

It is a matter fact that the problem of distributing the surface hydroxyls into two populations (bridged and isolated surface silanols) has not yet been satisfactorily solved. The techniques of reacting the surface with reagents forming real chemical bonds may be expected to change the original surface structure. Hence, even for a gel heated at 800°C, thus bearing isolated silanols, over 40% SiCl_4 molecules react with two OH groups (16). The use of diborane, first proposed by Shapiro and Weiss (17) in 1953, failed to lead to unambiguous results since none of the workers (18,20) who had followed by infrared this reaction agree with each other.

A good example of surface reconstruction by reacting the surface of silica with a mild reagent (CH_3OH) has been studied in detail (21). The methoxylation of an Aerogel surface pretreated at 110°C in vacuum was studied between 150 and 190°C. It was found that the reaction proceeds not only by esterification of the silanol group but also through the opening of the siloxane bridges, as follows



The competition of the two reactions is evidenced by a maximum

in the number of surface silanols (titrated by LiCH_3) during the course of the reaction. The analysis of the experimental results showed that $k_1/k_2 = 3.0$ at 150°C and 1.5 at 190°C . Thus, at high temperature the opening of siloxane bridges contributes more efficiently to the methoxylation process. It was also shown in this work that the probable intermediate in the reaction process is CH_3OH_2^+ . This aspect will be examined later.

Dynamics of adsorption processes on silicagel surfaces

There have been many studies concerned with the adsorption of water on silicagels but in order to study the dynamic aspects of these processes, H_2O is not the best suited molecule. Indeed proton exchange between the adsorbate and the surface silanols and surface diffusion occur simultaneously and these mechanisms cannot be separated easily. It is for this reason that methanol was chosen, for the methyl group doesn't exchange with surface OH whereas the alcoholic OH does. By using CD_3OH or CH_3OD and hydroxylated or deuterated surfaces, it is possible by measuring the ^1H or ^2H nuclear resonance relaxation rates, to distinguish between both kinds of processes. The spin-lattice relaxation rate T_1^{-1} obtained by pulse nuclear magnetic resonance is the Fourier transform of the auto-correlation function $G(\tau)$ which describes the evolution of the system.

$$T_1^{-1} = \int_0^{\infty} G(\tau) \cos \omega \tau \, d\tau \quad (4)$$

where

$$G(\tau) = \langle f(t) \, f^*(t + \tau) \rangle \quad (5)$$

f contains the information about the motions. Random reorientation or translational jumps obey generally the correlation function :

$$G = \langle f(0) \, f^*(0) \rangle \exp -\frac{\tau}{\tau_c} \quad (6)$$

where τ_c , the correlation time, defines the time scale of the microscopic events which causes relaxation. ω is the resonance frequency. The data obtained in references (8), (9) and (22) have been reviewed by Fripiat (23) and they will be summarized here after. In order to understand the experimental results, the surface heterogeneity must be accounted for. This is usually done by considering a log normal distribution of correlation time

$$P(\tau_c) \, d\tau_c = \beta^{-1} \pi^{-1/2} \exp(-Z/\beta)^2 \, dZ \quad (7)$$

where $Z = \ln \tau_c / \tau_m$, β being the spreading coefficient of the distribution function f_m and τ_m the average correlation time

$$\tau_m = \tau_0 \exp(\bar{H}/RT) \quad (8)$$

where \bar{H} is the average activation enthalpy of some kind of motion.

Since the adsorbent is made of a collection of surfaces randomly oriented and confined within an intricate network of pores, the approximation for isotropic motions (relationship 6) is acceptable.

The adsorption of methanol has been studied for two gels. The first, called Xerogel, is characterized by pores with an average diameter of 17.5 Å and the second called Aerogel, contains pores smaller than 10 Å. In order to assign the correlation times to some defined motion, information must be obtained about the magnitude of the local magnetic field acting on the proton and arising either from other protons in the same, or from other molecules. In this case the measurement of the proton second moment (the average quadratic local magnetic field) allows one to assign the measured correlation time (s) to some defined motion(s), these motion(s) modulating the local field and provoking relaxation.

In the Xerogel (X), independently of the degree of coverage (θ), the second moment at a temperature of the order of -140°C corresponds to a molecule in which the CH_3 group is already reorienting rapidly around the C_3 symmetry axis. By contrast, at that temperature, there is no free rotation of the CH_3 group in the Aerogel.

When the linear relationships shown in Figure 3 are compared it appears clearly that the average activation enthalpy (Equation 8) is of a comparable magnitude in the situations described by the Arrhenius plots 2, 3 and 5 whereas for plot 4, (Aerogel), it is much less. In solid methanol the activation enthalpy for the rotation is 1.6 kcal mole $^{-1}$ (29) whereas in the liquid state the activation enthalpy for diffusion is 3.2 kcal mole $^{-1}$. This remark and also what has been said about the low-temperature values of the second moment suggest that correlation times 2, 3 and 5 in Figure 3 are those of translational jumps, whereas correlation time 4 is that of the methyl group rotation. In the larger pores of Xerogel and in the temperature range -140° to $+50^{\circ}\text{C}$, the methanol would thus diffuse while the methyl group is rotating freely.

In the narrower pores of Aerogel (A), and in the same temperature range diffusion would not occur. The thermal activation results in a progressively freer rotation of the methyl group. In Aerogel at decreasing θ , the methyl group rotation becomes progressively hindered while in Xerogel, as shown in Figure 4, the translational correlation time decreases with θ .

The activation enthalpy for diffusion obtained at different degrees of coverage is shown in the enclosure. It increases from about 4 to about 6 kcal mole $^{-1}$ in passing from half to the complete monolayer content and then it decreases progressively toward the value obtained for the free liquid at $\theta > 2$. This indicates that the diffusional motions are still influenced by the surface for molecules in the third layer.

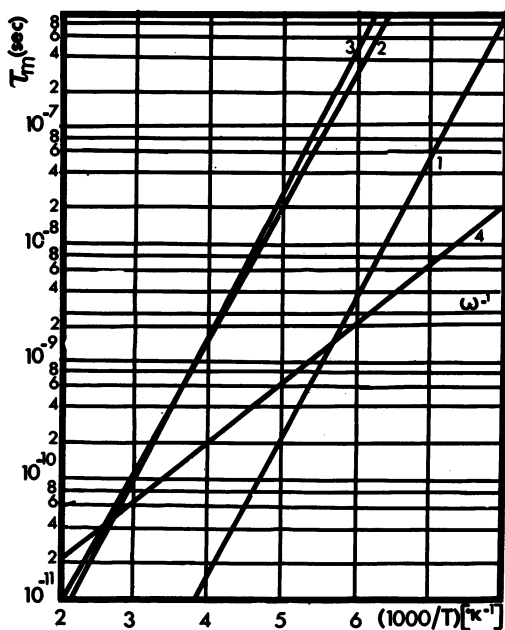


Figure 3. Correlation times observed at the coverage $\theta = 1.3$ for various systems. Key: 1, ^2H resonance in the $\text{CD}_3\text{OH-XOH}$ system, $\beta = 3$ and $\bar{H} = 5.4$ kcal/mol; 2, ^1H resonance in the $\text{CH}_3\text{OD-XOD}$ system, $\beta = 3.25$ and $\bar{H} = 5.5$ kcal/mol; 3, ^1H resonance in the same system, $\beta = 4$ and $\bar{H} = 5.2$ kcal/mol; 4, ^1H resonance in the $\text{CH}_3\text{OH-AOH}$ system, $\beta = 0.8$ and $\bar{H} = 2.32$ kcal/mol. X, Xerogel (average pore diameter: 17.5 Å); A, Aerogel (average pore diameter < 10 Å); ω , proton resonance frequency in the 14-kgauss field of the NMR instrument.

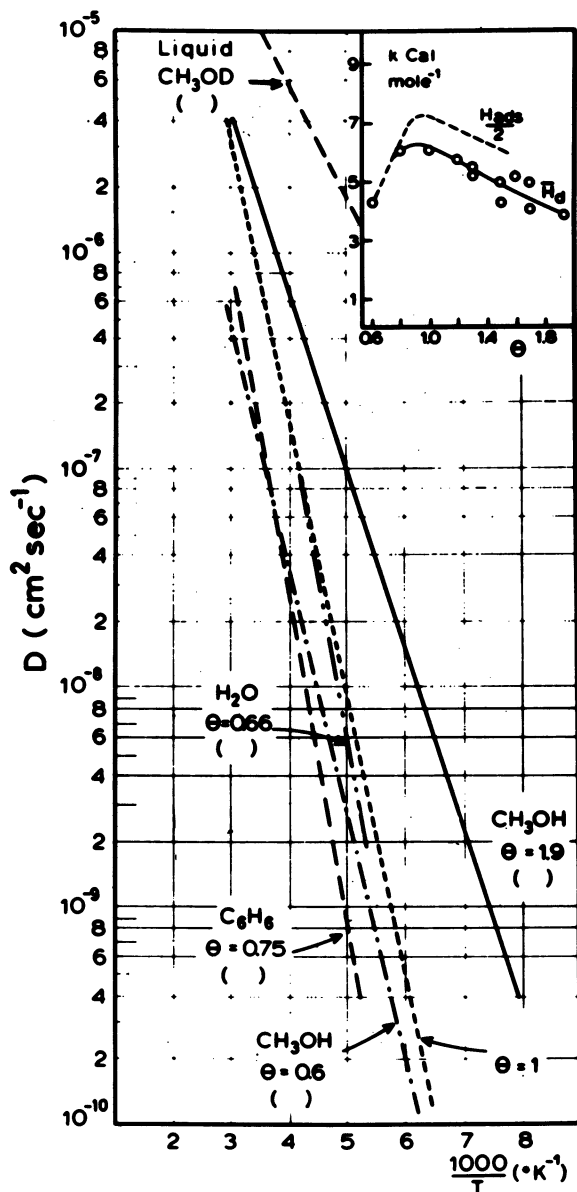


Figure 4. Variation of the surface diffusion coefficient measured at three different degrees of coverage for the $\text{CH}_3\text{OD-XOD}$ system. In enclosure: variation of \bar{H} with respect to the degree of coverage.

It is also interesting to point out that in agreement with de Boer (24), the activation enthalpy is approximately half the isosteric heat of adsorption obtained from

$$q_{st} = - R T^2 [(\partial \ln p) / \partial T]_{\theta} \quad (9)$$

Indeed (8), between $\theta = 0.7$ and $\theta = 1$, q_{st} increases from 10 to 14 kcal mole⁻¹ and then it decreases for 14 to 12 kcal mole⁻¹ in going from $\theta = 1$ to $\theta = 1.3$. The molecular area of methanol on the Xerogel and Aerogel surfaces is about 25.5 Å² at $\theta = 1$. If this value is considered as the quadratic diffusional jump distance $\langle \ell^2 \rangle$ and if the surface diffusion coefficient is approximated by

$$D = \langle \ell^2 \rangle / 6 \cdot \tau_m \quad (10)$$

then the surface diffusion coefficients shown by the solid line in Figure 5 are obtained for the Xerogel at 25°C. Between the half-monolayer and the monolayer content a rapid increase is observed. For Aerogel, the diffusion coefficient is probably smaller than 10⁻¹⁰ cm² sec⁻¹ since the translational motion is outside the range of observation e.g., $\tau_m > 10^{-6}$ sec.

By comparing the equations of state for mobile and immobile films with the information about the motions obtained by NMR, it was shown (8) using the procedure proposed by Ross and Olivier (25) that the equation for an immobile film was fitted by the adsorption data for Aerogel whereas the data obtained for Xerogel obeyed the equation for a mobile film.

Consider now the correlation time corresponding to line 1 in Figure 3. It represents the correlation time obtained from the deuteron spin-lattice correlation time for the CD₃OH - X OH systems at three degrees of coverage: $\theta = 0.8, 1.3,$ and $1.7,$ respectively. In that case there is no influence by the degree of coverage. This is not surprising because the quadrupole-inner electrical field gradient interaction (the so-called quadrupole coupling constant, (QCC), represents the main contribution to the deuterium nuclear relaxation. In that case the correlation time has been assigned to molecules tumbling within a surface potential well. Indeed, this motion should imply an average activation enthalpy similar to that of diffusion e.g., that of breaking hydrogen bonds, but it should be coverage independent since opposite to diffusion, it does not include any cooperative effect.

Finally it is interesting to point out the good agreement between correlation times 2 and 3 in Figure 3. Correlation time 3 has been computed from the diffusional contribution to the proton spin-lattice relaxation time measured for the CD₃OH - X OH system, after the proton exchange contribution has been removed, whereas correlation time 2 has been obtained, in a straight forward manner, for the CH₃OD-X-OD system.

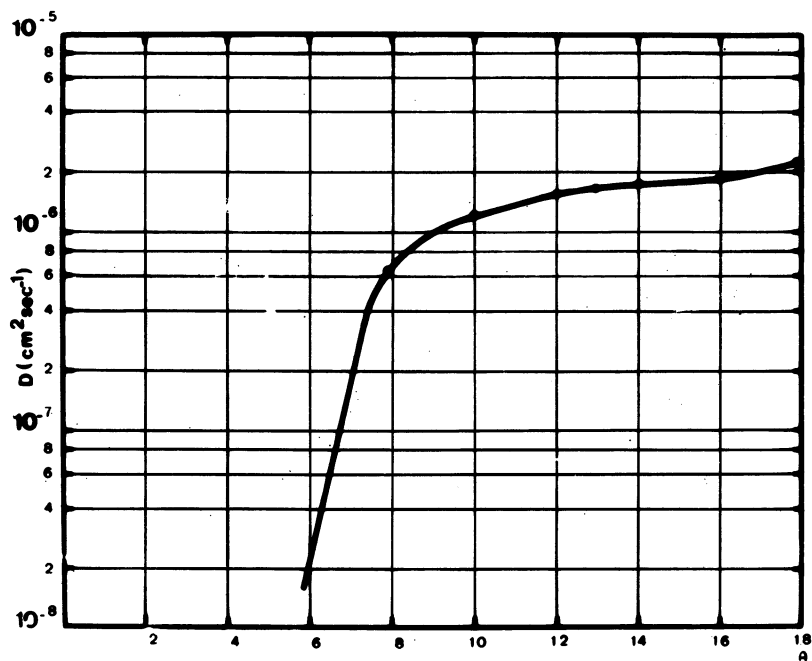
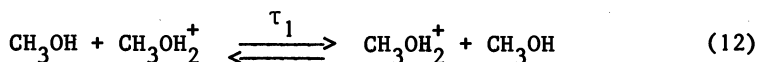
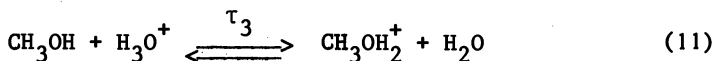


Figure 5. Variation of the diffusion coefficient of methanol on Xerogel with respect to the degree of coverage at 25°C. In the liquid phase the diffusion coefficient is about $2.6 \times 10^5 \text{ cm}^2/\text{s}$.

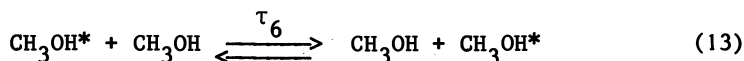
Proton exchange between silanols and adsorbate molecules

Although the silanol groups are weak acid, proton exchange may be observed by adsorbing NH_3 for instance. This process was studied simultaneously by IR spectroscopy and proton spin-lattice nuclear magnetic relaxation time measurements performed on Aerogel outgassed between 20°C and 200°C (26). Three deformation bands attributable to the adsorbed species were detected at 1450 cm^{-1} (NH_4^+), 1600 cm^{-1} (NH_3) and at 1500 cm^{-1} . The latter which becomes observable at degrees of coverage of the order or larger than the monolayer content for Aerogel outgassed at 120° or 200°C was tentatively assigned to a $\text{NH}_4^+\text{---NH}_3$ dimer. This suggests that proton may be transferred easily by tunneling along the N-H---N bond. At the monolayer coverage, the ratio ($\text{NH}_4^+/\text{NH}_3$) was of the order of 30%. At this degree of coverage the jump frequency was about $0.5 \cdot 10^9\text{ sec}^{-1}$ at 25°C . This value compares well with that deduced from the rate constant determined by Clutter and Swift (27) for proton transfer in liquid acidified ammonia and extrapolated to 25°C : their results was $2 \cdot 10^9\text{ sec}^{-1}$ for the same ratio $\text{NH}_4^+/\text{NH}_3$. On the Aerogel surface the rate of transfer is of course somewhat reduced but still of the same order of magnitude.

As compared to NH_3 , CH_3OH is a weaker base and it was therefore interesting to investigate proton transfer between methanol and silica surface. This was performed (9) by combining the values obtained for the spin-lattice (T_1) and spin-spin (T_2) proton relaxation times for CD_3OH adsorbed on Xerogel. In this system, two T_2 were observed. The short one and the short T_1 contribution to the experimental T_1 averaging the diffusion and the proton exchange processes permitted the correlation time (τ_e) of the proton exchange to be measured. It was found that τ_e is always higher than τ_d , but the activation energies for the two mechanisms are approximately the same. This again may be anticipated since both diffusion and proton exchange processes imply breaking hydrogen bonds. At 22° and for $0.8 < \theta < 1.7$, $\tau_e = (2.1 \pm 1) \cdot 10^{-8}\text{ sec}$. This value is one or two orders of magnitude longer than the pseudo first-order constants $\tau_2 = 4.5 \cdot 10^{-9}\text{ sec}$ and $\tau_3 \approx 4.2 \cdot 10^{-10}\text{ sec}$ determined (28) for proton exchange in acidified methanol according to the following processes



and much higher than $\tau_6 = 8 \cdot 10^{-2}\text{ sec}$ recorded for



This comparison suggests that a proton is transferred from the silica gel surface into a cluster of adsorbed CH_3OH molecules and that it jumps very rapidly from one molecule to another before recombining with a $\equiv \text{SiO}^-$ species.

The ratio $v_e/v_d = \tau_d/\tau_e$ represents the number of times a methanol molecule is protonated during its stay on an adsorption site. As shown in Figure 6, (v_e/v_d) increases as θ decreases and it tends towards the value it should take in the liquid protonated methanol. This ratio for the liquid system was obtained using $\tau_3 \approx \tau_4$, the diffusion coefficient obtained by O'Reilly et al., (29) and a molecular diffusion jump distance of 4 Å. The variation of (v_e/v_d) shown in Figure 6 supports the assumption that the surface proton initiates the exchange process since (v_e/v_d) decreases in "diluting" the surface acidity into more adsorbed molecules.

Reduction of a silica surface by hydrogen spillover

Isolated silanols with a surface density of the order of 1.5 OH/nm^2 are left by outgassing a silicagel above 500°C . If such a silica is treated at about 800°C in presence of molecular hydrogen and if the surface is covered with traces of metals able to dissociate H_2 , a surface reduction occurs with the formation of Si-H groups (30). A Si-H stretching vibration band is observed accordingly at 2300 cm^{-1} after quenching at room temperature.

In Figure 7 the variation of the optical density of this band is plotted with respect to the square root of the time for a silicagel wafer weighing 40 mg/cm^2 exposed to 60 torr H_2 at 880° in a quartz cell that contains metal chips of about $10\text{mm}/4\text{mm}$ located a few millimeters below the wafer holder, made of fused silica. If at the end of the reaction, wafers are transferred quickly into the specimen chamber of an ESCA spectrometer and are recorded in the energy regions where XPS peaks of the metal are expected, positive evidences of traces of metal are indeed observed. The transfer mechanism probably occurs through the intermediate formation of the corresponding oxide resulting from the reaction with traces of water present in the cell. The metal oxide is further reduced on the surface by H_2 .

About 0.2 Si-H groups are formed per nm^2 whereas the amount of Ta, (the only metal for which an approximate analysis by activation) was possible, is of the order of 38 ppm.

The surface reduction proceeds probably by hydrogen spillover. H_2 is dissociated onto the very small metal particules on the silicagel surface and atomic hydrogen reacts with oxygen of siloxane bridges producing traces of water and Si-H groups.

The infrared spectrum of surface Si-H is rather interesting: as shown in Figure 8, beside the 3750 cm^{-1} band of isolated silanols still present on the surface, a main Si-H band is observed at 2300 cm^{-1} . It decreases in intensity after long outgassing at 830°C . The weak band at 2225cm^{-1} is reinforced when the sample

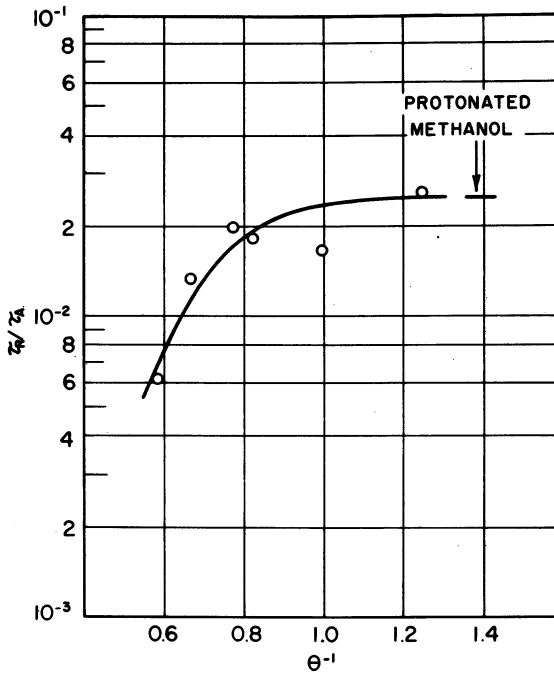


Figure 6. The $v_{poch}:v_{diff}$ ratio with respect to θ^{-1} (see text).

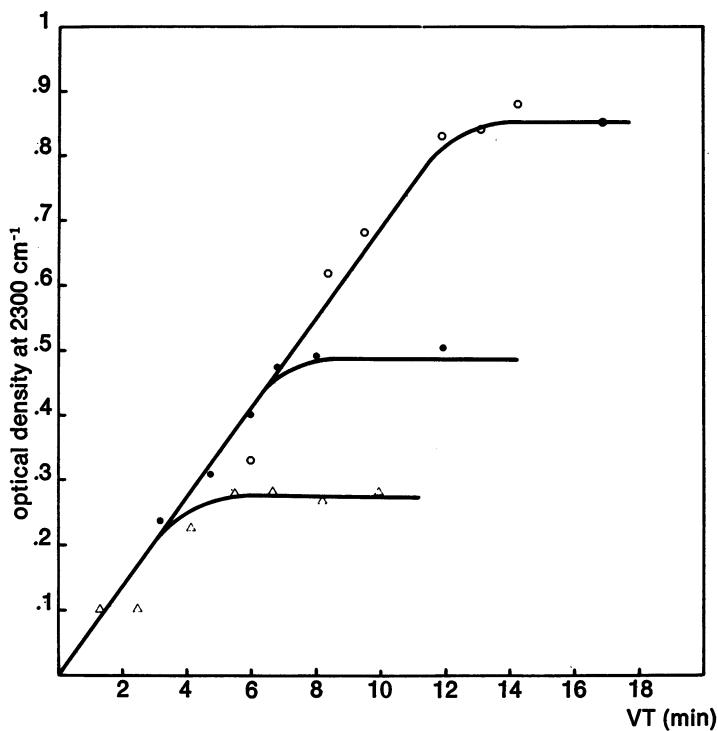


Figure 7. Variation of the optical density of the 2300 cm^{-1} Si-H stretching band with respect to the square root of the reaction time (min) at 880°C , 60 Torr H_2 , and in the presence of Ni, Pt, or Ta chips. The weight of the Aerosil wafer was 40 mg/cm^2 in all cases. Key: Δ , Pt; \bullet , Ni; and \circ , Ta.

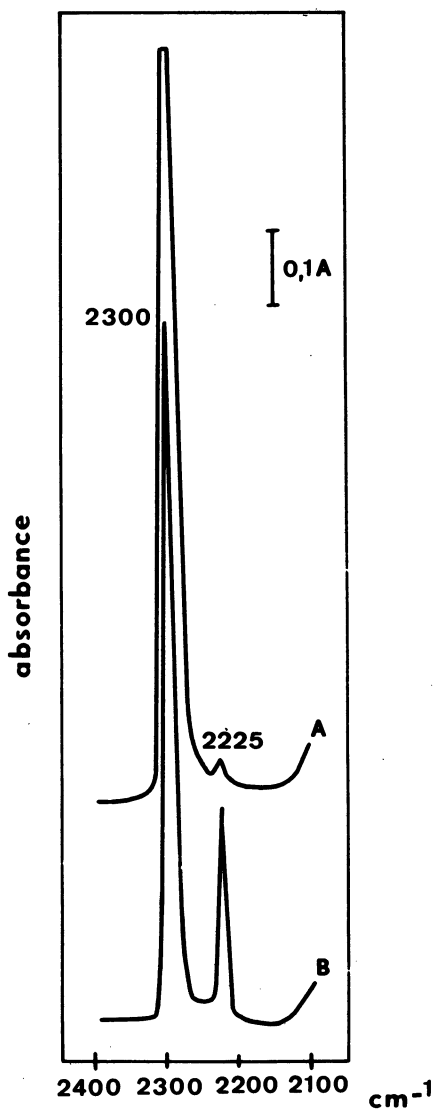


Figure 8. IR spectra observed for the Aerosil covered with Ta. Key: A, treated at 900°C in 60 Torr H₂ for 3 h; B, after outgassing at 830°C for 40 h and brought into contact at 350°C with 80 Torr H₂ for 13 h.

outgassed at 830°C is reexposed to H₂ at 350°C. The same bands were observed by Morterra and Low (31) after pyrolyzing and outgassing a methoxylated silica. The band at 2225 cm⁻¹ may be assigned to chemisorbed H₂.

The Si-H group is stable in air, at room temperature for several days but it disappears quickly when the sample is heated in air at 400°C. Morterra and Low have already emphasized the reactivity of partially reduced silica surface. It was shown (30) that it reacts with benzene vapor forming Si-C₆H₅ bonding whereas the intensity of the 2300 cm⁻¹ band decreases accordingly.

In its exhaustive review of the mechanisms of surface reaction of silica, Iler (4) (p.677 and followings) quoted the possibility for preparing Si(OH)H surface by high frequency discharge. Since atomic hydrogen is present in a plasma the reduction mechanism may be analogous to that operating by spillover from metal particles deposited on the surface.

Literature cited

1. Fripiat, J.J.; Leonard, A.; Barake N. Bull. Soc. Chim. France, 1963, 122.
2. Warren, B.E.; Gingrich, N.S. Phys. Rev. 1934, 46, 368.
3. Fripiat, J.J.; Uytterhoeven, J. J. Phys. Chem. 1962, 66, 800.
4. Iler, R.K. "The Chemistry of Silica," John Wiley, N.Y. 1979, 633.
5. Fripiat, J.J.; Gastuche, M.C.; Brichard, R. J. Phys. Chem. 1962, 66, 805.
6. Pacco, F.; Van Cangh, L.; Fripiat, J.J. Bull. Soc. Chim. France, 1976, 1021.
7. Fraissard, J.; Caillet, R.; Elston, J.; Imelik, B. J. Chim. Phys. 1963, 60, 1017.
8. Cruz, M.I.; Van Cangh, L.; Fripiat, J.J. Bull. Classe des Sciences, Acad. Roy. Belg. 1972, LVIII, 439.
9. Cruz, M.I.; Stone, W.E.E.; Fripiat, J.J. J. Phys. Chem. 1972, 76, 3078.
10. O'Reilly, D.E. J. Chem. Phys. 1958, 29, 970.
11. Kulvidze, V.I. D.A.N. SSSR, 1964, 157, 158.
12. Hair, M.L. "Infrared Spectroscopy in Surface Chemistry," Marcel Dekker, Inc. N.Y., 1967, p.121 and following.
13. McDonald, R.S. J. Am. Chem. Soc. 1957, 79, 850.
14. Rouxhet, P.G.; Sempels, R. J. Chem. Soc. Faraday, Trans. I 1974, 70, 2021.
15. Bellamy, L.J.; Hallam, H.E.; Williams, R.L. Trans. Farad. Soc. 1958, 54, 1120.
16. Peri; J.R. J. Phys. Chem. 1966, 70, 2937.
17. Shapiro, I.; Weiss, H.G. J. Phys. Chem. 1953, 57, 219.
18. Bavarez, M.; Bastick, J. Bull. Soc. Chim. France, 1964, 3226.
19. Mathieu, M.V.; Imelik, B. J. Chim. Phys. 1962, 59, 1189.
20. Fripiat, J.J.; Van Tongelen, M. J. Catalysis, 1966, 5, 158.

21. Mertens, G.; Fripiat, J.J. J. Colloid and Interface Sc. 1973, 42, 169.
22. Seymour, S.J.; Cruz, M.I.; Fripiat, J.J. J. Phys. Chem. 1973, 77, 2847.
23. Fripiat, J.J. "Colloid and Interface Sc." Academic Press, 1977, Vol.1, p.541, Edited by M.Kerker, A.C.Zettlemoyer and R.L.Rowell.
24. De Boer, J.M. "The Dynamical Character of Adsorption," Oxford Univ. Press, 1953.
25. Ross, S.; Olivier, J.P. "On Physical Adsorption," Interscience N.Y. 1964.
26. Fripiat, J.J.; Van der Meersche, C.; Touillaud, R.; Jelli, A. J. Phys. Chem. 1970, 74, 382.
27. Clutter, D.R.; Swift, T.J. J. Amer. Chem. Soc. 1968, 90, 601.
28. Lutz, Z.; Gill, D.; Meiboom, S. J. Chem. Phys. 1959, 30, 1540.
29. O'Reilly, D.E.; Peterson, E.M. J. Chem. Phys. 1971, 52, 2155.
30. Van Meerbeck, A.; Jelli, A.; Fripiat, J.J. J. Catalysis, 1977, 46, 320.
31. Morterra, C.; Low, M.J.D. Annals New-York Acad. Sc. 1973, 220, 133.

RECEIVED March 2, 1982.

Sodium Silicate in Chemical Flooding Processes for Recovery of Crude Oils

PAUL H. KRUMRINE

The PQ Corporation, Research and Development Center, Lafayette Hill, PA 19444

Sodium silicates have found numerous applications in the oil industry, particularly in EOR chemical processes. The objective of this paper is to review these applications and relate them to the basic properties and reactions of sodium silicate, in order to develop a better understanding of how silicates are used to solve a number of interesting problems in oil recovery. The silicate anion, in all its many forms, has specific properties which make it a valuable component in the various enhanced recovery processes. Among these properties are its ability: to sequester multi-valent metal cations; to act as a sacrificial agent in the adsorption process by clays; to maintain water-wettability; to reduce permeability in high permeability areas to improve sweep; and to aid in reducing IFT at the oil/water interface. Each of these properties depends on the size, charge, and basicity of the silicate molecule, which can be varied by changing ratio and concentration.

Alkaline chemicals have been suggested as an agent to improve oil recovery as early as 1917 by Squires (1). Several others such as Atkinson (2), Nutting (3), Beckstrom and Van Tuyl (4), Subkow (5), Reisburg and Doshier (6,7), and Wagner and Leach (8) have described the various mechanisms of displacement and benefits from injecting these chemicals. Nutting in 1925 was the first to suggest that sodium silicate might be used to improve waterfloods.

Over the years, several field trials have been reported using caustic with limited success (3, 9-13). More recently four alkaline field trials have been started, employing specifically sodium orthosilicates. These include projects by THUMS at the Wilmington field, by Aminoil USA at the Huntington Beach Field and by Union in their Van and Orcutt Fields.

Work by Holm (14, 15) has established the benefit of using alkaline chemicals as a preflush agent for micellar/polymer floods. A field trial of this process using an orthosilicate preflush has been carried out at Gary Energy's Bell Creek Field (16). Additional oil has been recovered, however, it is difficult to assess how much of this was due to the preflush.

Recently we have carried out laboratory tests (17, 18, 19) in which the sodium silicate was added directly to a dilute surfactant solution to recover oil. Such a process would be akin to alkaline flooding processes where a dilute surfactant is formed in-situ. In this case however the crude is lighter and does not contain the natural acids necessary to form surfactants in-situ. Therefore surfactant is injected and protected or enhanced by the sodium silicate such that a low tension waterflood is assured. Such a system is less complex and therefore more widely applicable than micellar/polymer techniques thus filling the void between the alkaline and micellar/polymer EOR processes.

Other techniques such as the mobility controlled caustic flooding process by Saram (20, 21, 22) and combinations of polymer and alkali have been investigated, but these have not been widely used as yet and are currently perceived as extensions of the three processes discussed above.

SILICATES IN ALKALINE FLOODING

Sodium orthosilicate alkaline flooding is one of the most promising EOR technologies now under development. The THUMS and Aminoil USA orthosilicate alkaline floods have received a good deal of publicity due to DOE participation in these projects, and therefore the parameters of these floods are well known, and shown in Table I. Reservoir conditions for these two floods are quite different as are the flood designs, however their characteristics are illustrative of the type of reservoir which is conducive to alkaline flooding. Both reservoirs have high concentrations of divalent metal cations contained in the connate water, and the oil in each reservoir is a heavier, more viscous crude containing some natural acids; therefore, both elected to use sodium orthosilicate instead of sodium hydroxide alone. The predicted benefit in increased oil production in the two reservoirs is shown in the core flood results of Tables II (23) and III (24). In each comparison the sodium orthosilicate was found to give an additional 20 to 50% more oil than the sodium hydroxide. Since the pH and alkali values of the two chemicals are nearly identical, the difference in performance is attributed to the silica moiety of the orthosilicate, and predominantly its interaction with the hardness ions. Also, other more subtle affects will be discussed.

TABLE IRESERVOIR PARAMETERS

Type of Reservoir Rock	<u>AMINOIL</u>	<u>THUMS</u>
	Unconsolidated Sand	Unconsolidated Sand
Average Porosity	0.24	0.26
Average Oil Gravity	23°	19.6°
Average Permeability (brine)	200 md	400 md
Average Depth	3750 ^o	3000 ^o
Average Net Sand Thickness	260 ^o	305 ^o
Bottom Hole Temperature	170°	125°
Average Oil Viscosity at Reservoir Temperature	11 cp	23cp
Acid Number	0.65	2.5
Pilot Area	64.7 ac	93 ac
Volume - acre feet	17,300	26,900
Tank Oil in Place - M bbl	12,300	33,900
Average Water/Oil Ratio	40/1	10/1
Initial Water Saturation (average)	18%	29%
Residual Oil Saturation after Waterflooding	35%	38%

Reproduced, with permission, from Ref. 24.

Copyright 1979, Society of Petroleum Engineers of AIME.

TABLE II
INCREASED RECOVERY OF WILMINGTON FIELD
RANGER ZONE CRUDE C-331 FROM PRESERVED
CORES BY ALKALINE FLOODING

<u>TEST NO.</u>	<u>ALKALINE MATERIAL</u>	<u>CONC. PREFLUSH WT.%</u>	<u>% PV (1% NaCl)</u>	<u>INCREASED RECOVERY % PV OVER WATERFLOOD AT PV INJECTED</u>			
				<u>1</u>	<u>5</u>	<u>10</u>	
39	NaOH	0.2	0.2	---	---	---	
40	NaOH	0.2	0.2	---	---	2.5	
41	NaOH	0.2	0.05	---	---	3.0	
42	NaOH	0.2	0.05	---	---	1.5	
43	Na ₄ SiO ₄		0.2	0.05	3.0	5.8	7.8
44	Na ₄ SiO ₄		0.2	0.05	2.7	4.8	7.9

Reproduced, with permission, from Ref. 24.
 Copyright 1979, Society of Petroleum Engineers of AIME.

TABLE III

ALKALINE FLOODS - HUNTINGTON BEACH FIELD CRUDE IN BEREASANDSTONE CORES USING 0.5 PV OF ALKALI INJECTION

<u>RUN</u>	<u>1</u>	<u>2</u>	<u>3</u>	<u>4</u>	<u>5</u>	<u>6</u>
Alkali	Na ₄ SiO ₄	NaOH	Na ₄ SiO ₄	NaOH	Na ₄ SiO ₄	NaOH
Conc., WT %	0.15	0.15	0.25	0.25	0.5	0.5
PV Alkaline Inj.	0.5	0.5	0.5	0.5	0.5	0.5
Total PV Inj.	3.3	3.1	3.5	3.3	3.1	3.4
PV, ml	237.8	239.3	251.2	247.5	247.0	245.3

(continued on next page)

TABLE III - continued
ALKALINE FLOODS - HUNTINGTON BEACH FIELD CRUDE IN BEREA
SANDSTONE CORES USING 0.5 PV OF ALKALI INJECTION

RUN	<u>1</u>	<u>2</u>	<u>3</u>	<u>4</u>	<u>5</u>	<u>6</u>
Soi	0.716	0.711	0.632	0.651	0.669	0.656
Sorwf	0.474	0.465	0.410	0.435	0.428	0.433
% WF Recovery	33.7	34.6	35.1	33.2	36.0	34.0
Soraf	0.415	0.421	0.319	0.359	0.355	0.401
% Residual Oil Recovered	12.4	9.4	22.2	17.4	17.1	7.5
% PV Recovered by AF	5.9	4.4	9.1	7.6	7.3	3.2
% of Maximum Recovery after 3.5 PV	63.4	81.5	79.1	50.9	73.7	41.0

Reproduced, with permission, from Ref. 24.
 Copyright 1979, Society of Petroleum Engineers of AIME.

SILICATES IN MICELLAR/POLYMER FLOODING

Micellar/polymer systems are generally applicable to the lighter crudes with low viscosity which have little natural acidity. In micellar/polymer systems hardness is also detrimental in that it causes instability in the micellar phase and decreased viscosity in the polymer phase. Therefore, in many instances a preflush is required to protect the micellar/polymer slugs from the connate brine of the reservoir. To effectively displace these hardness ions and reduce their effect, sodium orthosilicate is used as the preflush chemical. This was done in the Bell Creek Field by Gary Energy Corp. who used a 0.16 PV preflush of 0.45% sodium orthosilicate (16).

Data presented by Holm (14) which is extracted in Table IV shows how the different salt and alkali preflushes are effective in protecting the micellar/polymer flood. The upper portion of the table shows the effect of salt and orthosilicate in clean sandpacs containing no clays. A 1.0% Na_4SiO_4 preflush was found to be roughly equivalent to a 5.0% NaCl preflush. In the presence of clays, shown in the lower portion, the 1.0% Na_4SiO_4 is seen to be superior to the 5.0% NaCl for each clay tested. This indicates that the silicate may be inhibiting the ion exchange from the clays that would otherwise release hardness back into solution and subsequently destabilize the micellar solutions. Further evidence of the effect of silicates on hardness elution from Berea sandstone core was presented by Campbell⁽²⁵⁾ and is shown in Figure 1. The addition of a 0.25 PV of alkali (either NaOH or Na_4SiO_4) resulted in a significant drop off in the elution of hardness over the 3% NaCl alone. This effect was slightly more pronounced for the sodium orthosilicate.

SILICATES IN LOW TENSION WATERFLOODING

Low tension waterflooding is a method intermediate between alkaline and micellar/polymer technology. The LTWF employs a dilute surfactant to reduce IFT and mobilize residual oil. A few field trials (26-29) of this process have been tried with mixed success. None of these trials however employed sodium silicates in any part of the flood design. Instead, other alkalis such as sodium carbonate and sodium triphosphate were used. Some of the reasons proposed for the limited success in these trials were 1) high consumption of the sacrificial agents, leaving the surfactant unprotected, 2) poor sweep of the pay zone, 3) limited mobility control and lower than expected displacement efficiency. Recent work published and obtained in our laboratories has shown that sodium silicates may help to overcome some of these problems better than other alkalis.

On Table V are some of the Berea core flood data obtained

TABLE IV

EFFECT OF PREFLUSH ON MICELLAR FLOODS IN CLEAN SANDPACKS (3500 md)
CONTAINING HIGH SALINITY, BRINE AND RESIDUAL OIL*

<u>Preflush Used</u>		<u>Slug (PV%)</u>	<u>Oil Recovered (% OIP)</u>
<u>Type</u>	<u>Conc. (Wt.%)</u>		
None	--	10	69.9
NaCl	0.25	10	54.4
NaCl	2.0	10	82.6
NaCl	5.0	10	95.9
Na ₄ SiO ₄	1.0	10	96.2

EFFECT OF PREFLUSH ON MICELLAR FLOODS IN SANDPACKS CONTAINING VARIOUS CLAYS, HIGH SALINITY (9.4% by Wt) BRINE, AND RESIDUAL OIL

		<u>Preflush Used</u>			
<u>Clay Amount In Sandpack (Wt %)</u>	<u>Type</u>	<u>Conc. (Wt %)</u>	<u>pH</u>	<u>Oil Recovered (% OIP)</u>	
<u>Halloysite</u>					
0.5	None	---	---	63.4	
0.5	NaCl	5.0	7.8	69.1	
0.5	Na ₄ SiO ₄	1.0	12.2	85.8	
0.5	Na ₂ O(SiO ₂) 3.3	1.0	10.5	67.7	
<u>Montmorillonite</u>					
1.0	None	---	---	51.1	
1.0	NaCl	5.0	7.8	76.3	
1.0	Na ₄ SiO ₄	1.0	12.8	92.4	
1.0	Na ₂ O(SiO ₂) 3.3	1.0	10.3	71.2	
<u>Kaolinite</u>					
0.5	None	---	---	65.9	
0.5	NaCl	5.0	7.8	70.7	
0.5	Na ₄ SiO ₄	1.0	12.7	83.0	

*Fluids in place: 30% PV, 30° API crude oil and 70% PV Brine

Reproduced, with permission, from Ref. 14.
Copyright 1981, Society of Petroleum Engineers of AIME.

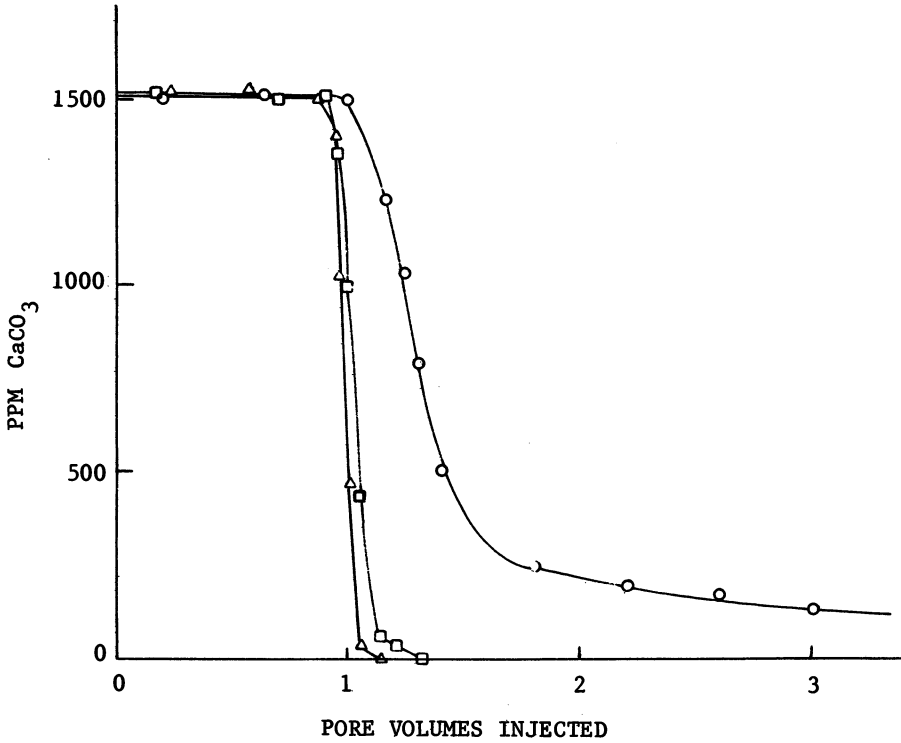


Figure 1. Elution of hardness ions by 0.25 pore volume of Na_4SiO_4 or NaOH followed by 3% NaCl . Key: \circ , 3% NaCl only; \triangle , 0.25 PV of 0.5% Na_4SiO_4 in 3% NaCl ; \square , 0.25 PV of 0.5% NaOH in 3% NaCl . (Reproduced, with permission, from Ref. 25. Copyright 1979, Society of Petroleum Engineers of AIME).

with a low acid number, mid-continent light crude oil. The results show the kinds of recoveries obtained with the rather long 2-3 PV continuous slugs of the dilute surfactant, and they also show the improvement in recovery from addition of the high ratio sodium silicate. The recoveries from shorter slugs of 0.5 to 1.0 PV are also given. Generally, recovery improvement of an additional 7 to 13% is noted when sodium silicate is added. Recoveries with the system are as good as or better than those normally found in alkaline flood systems, but not as good as with micellar/polymer systems. A polymer postflush with a LTWF could significantly increase the recovery also.

The benefits derived from the soluble silicates in these processes will be reviewed and are analogous to the benefits derived in the detergency and mining industries where silicates have been successfully utilized for many years.

SILICATE PROPERTIES IN EOR

The sodium silicates as a family are quite complex and exhibit a range of properties depending on the concentration and ratio of SiO_2 to Na_2O . It is this range of properties which allows them to be tailored to specific applications in the field, thereby optimizing the desired affect whether it be reduction of hardness, lower surfactant retention, or mobility control or other affects.

The alkalinity of sodium silicates allows them to react with the natural acids in the crudes thereby saponifying them into water soluble surfactants. These surfactants are then able to lower interfacial tension and emulsify the crude so that it can be mobilized through the pore space network. Even for crudes which do not contain sufficient acids to react - where surfactants must be injected - the silicates are important in helping the surfactants to partition between phases so that minimum IFT values can be attained. This effect is illustrated in Figure 2, where an order of magnitude decrease in IFT resulted from the addition of 0.37% of a 3.2 ratio silicate. The crude oil was relatively light and had an acid number of less than 0.1 mg KOH/gm of crude oil. This effect is largely one of pH however, since similar results can be attained with the proper concentration of most alkalis such as sodium hydroxide, sodium carbonate or any of the other sodium silicates as shown in Figure 3.

Another factor which affects IFT is hardness or the presence of divalent metal cations, because they can couple with the surfactants forming less active species in solution. Sodium silicates help maintain the lowest IFT possible, since they are very effective in sequestering and removing these ions. In most cases these divalent ions can never be completely removed from the reservoir systems because clays are present which continually reintroduce hardness into solution

TABLE V
EFFECT OF 3.2 RATIO SILICATE ON SURFACTANT FLOODING

<u>SLUG SIZE</u>	<u>SURFACTANT CONCENTRATION</u>	<u>NO SILICATE</u>	<u>1.0% 3.22 RATIO SODIUM SILICATE ADDED</u>	<u>% RECOVERY OF OIP (PV INJ) *</u>
Continuous	0.10 WT %	31.4 (4.0 PV)	43.2 (4.0PV)	
Continuous	0.25 WT %	45.6 (4.0 PV)	52.3 (4.0 PV)	
1.0 PV	0.10 WT %	-----	31.9 (2.5 PV)	
1.0 PV	0.25 WT %	33.1 (2.7 PV)	-----	
0.5 PV	0.10 WT %	8.8 (2.0 PV)	22.0 (2.5 PV)	

* Total PV Injected to Obtain Recovery Indicated, Including Preflush

SILICATE - 3.22 Ratio $\text{SiO}_2/\text{Na}_2\text{O}$, ACOR E32 Sodium Silicate
SURFACTANT - PETROSTEP 420 Petroleum Sulfonate
OIL - Kansas Crude, 34.5° API Gravity
CORE - Berea Sandstone, 150-250 md Permeability, 5 cm OD by 60 cm
TEMPERATURE - 22° - 23°C
FRONTAL VELOCITY - 30cm/day
PREFLUSH - 0.25 PV of 0.1% NaCl
SALT CONCENTRATION - 1.0% NaCl
BRINE COMPOSITION - 3% NaCl
1000 ppm Ca^{++}
500 ppm Mg^{++}

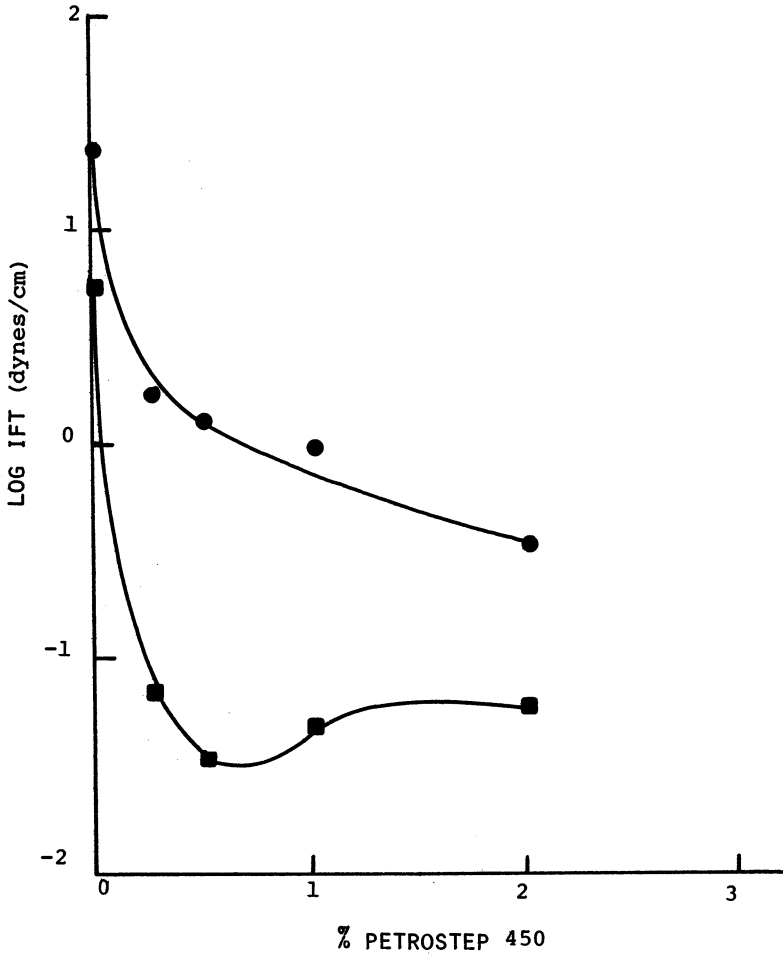


Figure 2. Interfacial tension reduction vs. surfactant concentration and silicate addition of Illinois crude, 1.5% NaCl. Key: ●, $\text{Na}_2\text{O}(\text{SiO}_2)_{3.5}$; and ■, 1.0% $\text{Na}_2\text{O}(\text{SiO}_2)_{3.5}$. (Reproduced, with permission, from Ref. 17. Copyright 1980, Society of Petroleum Engineers of AIME.)

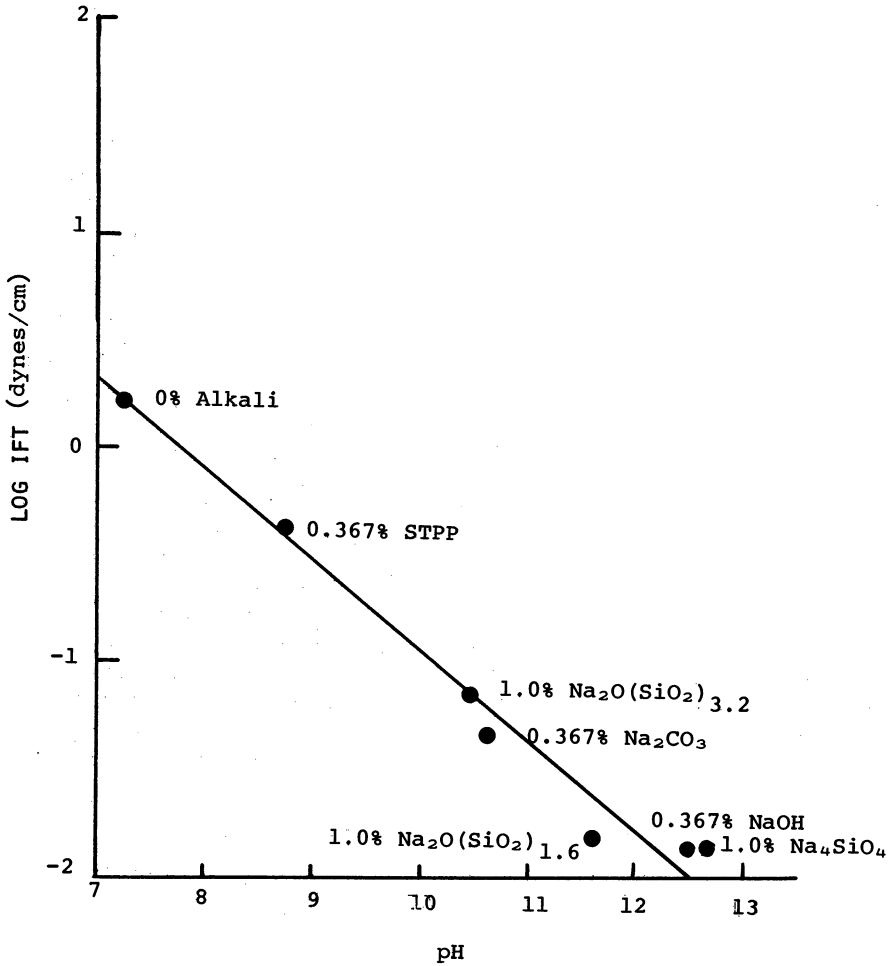


Figure 3. Comparison of alkaline interfacial tension reduction vs. pH of Illinois crude, 0.25% Petrostep 450, 1.5% NaCl. (Reproduced, with permission, from Ref. 17. Copyright 1980, Society of Petroleum Engineers of AIME.)

through ion exchange. Also, all portions of the reservoir cannot be completely swept clean by preflushing. However, when silicates are present in the surfactant solution, the surfactant is protected so that it can do its job of mobilizing the oil most effectively.

The effect of hardness ions on surfactant activity is further illustrated in Figure 4. Surfactant activity was monitored by means of a surfactant sensitive electrode as a function of hardness. The increase in potential in each curve between 900 and 1000ppm Ca indicates a reduction in activity. Only the sodium silicate maintained the surfactant activity at a constant level up to nearly 900ppm of Ca. The other alkalis resulted in a decrease in surfactant activity at about 400ppm.

A similar effect is shown in Figure 5 where surfactant was titrated into dispersions of a montmorillonite clay. In each case the surfactant activity in solution was reduced, but the amount of reduction was least when sodium silicate was present in the clay dispersion. The mechanism at work is probably the displacement of surfactant or preferential adsorption of silicate anions at the edges and discontinuities in the sand, as well as on clay minerals where cations are exposed.

This phenomena was also observed in some Berea core flood results in which the dilute surfactant systems were injected into the sandstone which contained no oil, so that only sandstone/surfactant chemical reactions could be noted. A summary of those results is presented in Table VI. All of the alkalis effectively reduced the hardness levels to less than 10-20ppm, however some did it much more rapidly. There was a big difference however in the amount of surfactant recovered in the effluent or the amount retained per volume of sandstone. Both the high ratio silicates and the sodium triphosphate were quite effective at protecting the surfactant. Sodium carbonate, trisodium phosphate and orthosilicate were somewhat less effective, and sodium hydroxide was only slightly better than no alkali at all. Of the alkalis tested, only the sodium silicates were significantly retained by the core, with the higher ratio silicates being retained in greater quantity. This shows the sacrificial nature of the silicates. Also some work by Somasundaran (30) has shown that the sodium silicates are more effective than the other alkaline chemicals in reducing surfactant adsorption on rock surfaces.

Another factor which can affect surfactant retention by these high surface area porous structures is the charge relationships between the surfaces and the various chemical species. Since the surfactant is negatively charged, the more positive (or less negative) the surface becomes, the easier it is for adsorption to occur. Work by Tsai and Falcone (31) has shown that multivalent metal cations at relatively low levels can cause a surface to become more positive in certain pH ranges. The addition of silicates and certain other alkalis

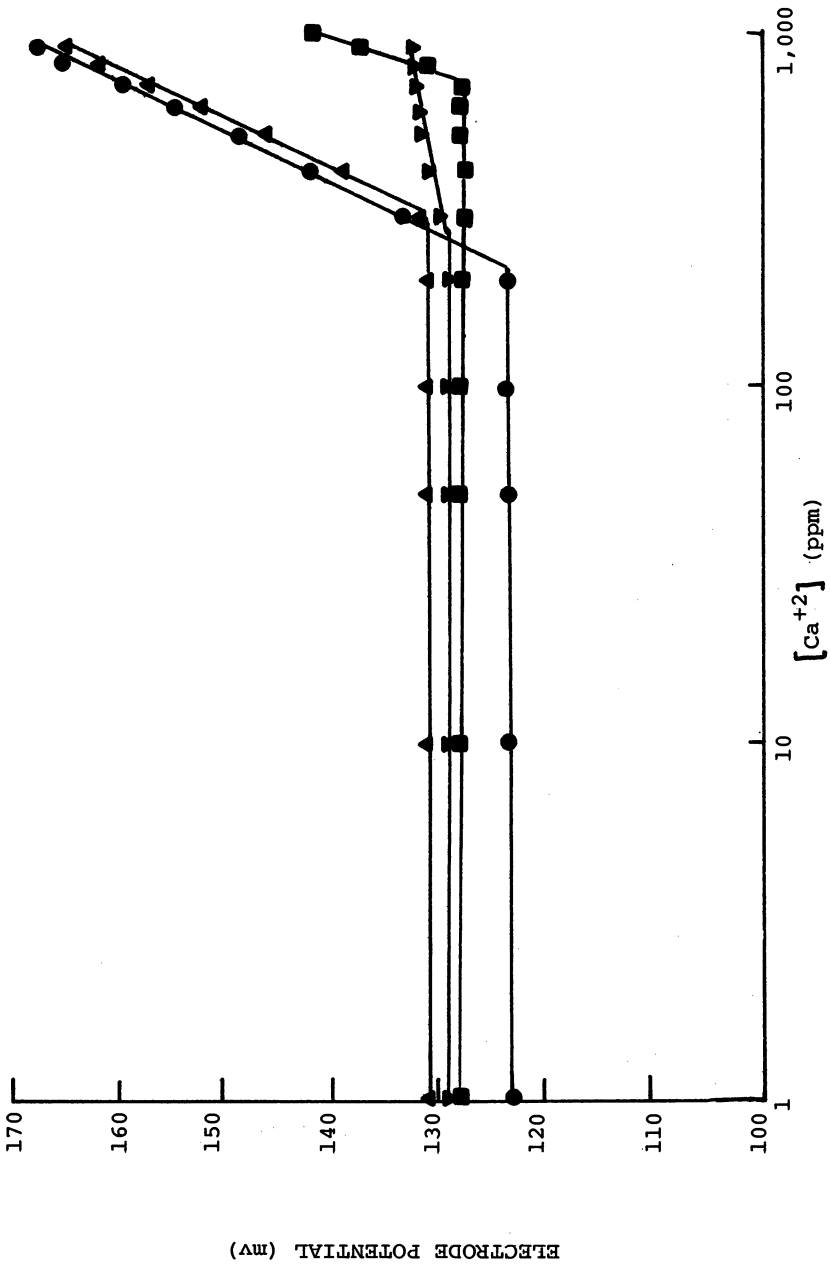


Figure 4. Electrode potential vs. Ca^{+2} concentration for several surfactant/alkali systems. Key:
 ●, Na-SDS + 1% NaOH; ▼, Na-SDS + 1% NaCl + 0.367% Na_2CO_3 ; ▲, Na-SDS + 1%
 NaCl + 1% NaOH; and ■, Na-SDS + 1% NaCl + 0.367% $Na_2O(SiO_2)_2.nH_2O$.

Publication Date: June 1, 1982 | doi: 10.1021/bk-1982-0194.ch012

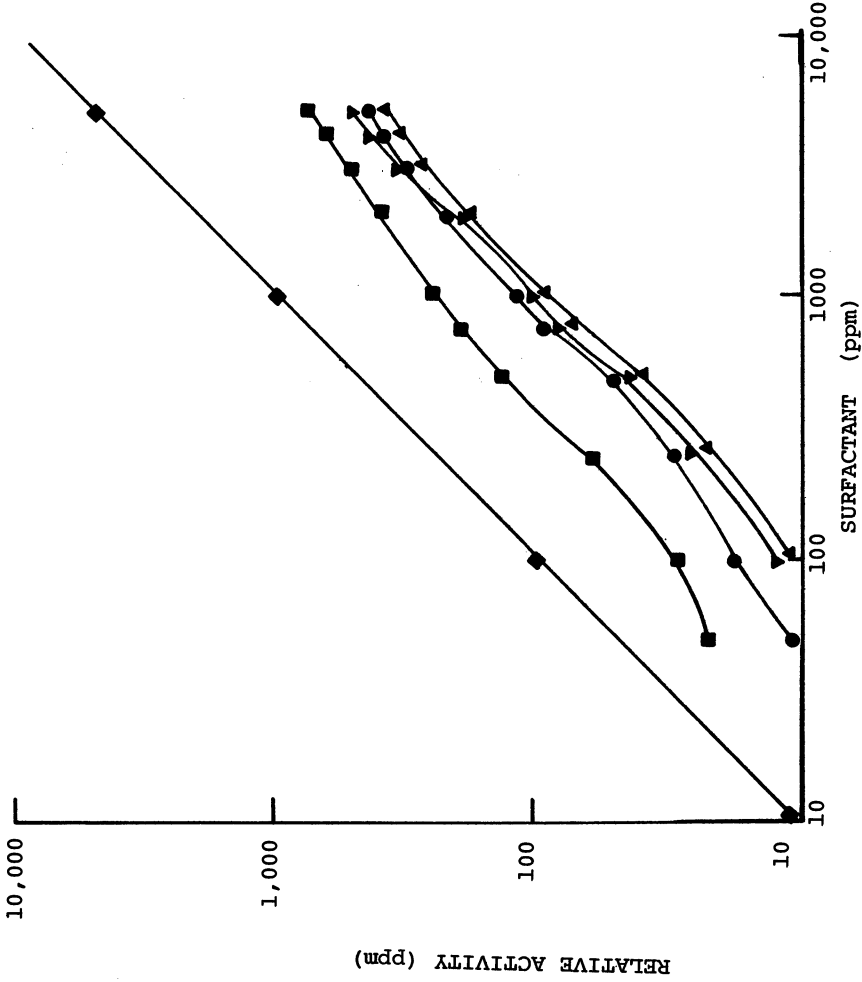


Figure 5. Relative surfactant activity as affected by alkalis and Na-montmorillonite clay. Key: \blacklozenge , 1% NaCl; \bullet , 1% NaCl + 2% Na-montmorillonite; \blacktriangledown , 1% NaCl, 2% Na-montmorillonite + 0.367% Na_2CO_3 ; \blacktriangle , 1% NaCl, 2% Na-montmorillonite + 0.01% NaOH; and \blacksquare , 1% NaCl, 2% Na-montmorillonite + 0.367% sodium silicate.

TABLE VI
ALKALI EFFECTS ON SURFACTANT RETENTION IN BEREA SANDSTONE

<u>Alkaline Additive</u>	<u>Hardness</u>	<u>Surfactant Recovery</u>	<u>Surfactant Retention/ kg Berea</u>	<u>Alkali Recovery</u>
None	100-300ppm	15%	0.68g	---
0.376% NaOH	20ppm	15.5%	0.65g	90%
0.376% Na ₂ CO ₃	10-20ppm	65%	0.26g	98%
0.376% Na ₃ PO ₄	10ppm	64%	0.28g	95%
0.376% STPP	10ppm	75%	0.18g	100%
0.376% Na ₂ O(SiO ₂) 3.2	10ppm	80%	0.15g	20%
0.426% Na ₂ O(SiO ₂) 1.6	10ppm	72.5%	0.20g	68%
1.0% Na ₄ SiO ₄	10ppm	65.8%	0.25g	74%

can help to maintain the negative charge on these surfaces as shown in Table VII. Charges on minusil (very fine quartz) and montmorillonite clay particles were measured in a variety of alkaline and surfactant solutions. The surface charge in these solutions as measured by electrophoretic mobility was found to become more negative in the presence of the silicate ions.

If surfactant, inorganic precipitates, or other chemical species are being retained in the cores, then the pores may begin to become blocked or decrease in average diameter. This can affect flow patterns and the mobility of the various phases within that network. Severe plugging or reduction in permeability is harmful due to lost injectivity, while selective permeability reduction may be quite useful in diverting fluids into previously unswept areas. Several tests on large Berea slabs which can simulate an areal pattern rather than a linear drive have shown that the areas swept by silicate enhanced surfactant floods are larger than simple surfactant LTWF processes. A visual comparison of the swept areas in two examples is shown in Figures 6 & 7. In Figure 6 no silicate was used. A large slug of the dilute surfactant solution was injected into the lower left-hand corner of the slab and produced from the upper right-hand corner. After about 3 PV of injection only about 26% of the residual oil had been recovered whereas a linear flood using the same solution recovered about 37%. Upon later visual inspection of the cross-sectioned core it appeared that only about 65% of the core area had been swept by the flood solutions. A similar test where a high ratio sodium silicate was added showed that recovery of residual oil was about 46% as compared to 49% in a linear flood test. This was verified by the cross-sectioned core diagrammed in Figure 7 which showed that nearly 91% of it had been swept. Overall permeability reduction was only about 20%.

Another set of core flooding experiments showed how the addition of sodium silicate can help to improve the sweep and recovery in multipermeable zones. Two cores of different permeability were individually prepared and then connected in parallel through a "T" type connection with the effluents collected separately. The composite recovery curves for these tests are shown in Figure 8. Initial production occurred from the higher permeability section. At the point where each curve diverges into two curves is the beginning of production contribution from the lower permeability section. These tests showed that the use of a high ratio sodium silicate results in earlier production as well as more production from the lower permeability section. When the effluent flow ratios between the two permeability zones were compared, it was found that initially the major portion of the fluid is diverted into the high permeability zone. Then, gradually, this zone is selectively reduced in permeability so that more fluid is

TABLE VII. ELECTROPHORETIC MOBILITY OF TYPICAL RESERVOIR MINERALS VS. VARIOUS ALDALINE SOLUTIONS

SOLUTION COMPOSITION (%)				pH	CONDUCTIVITY (m mho/cm)	ELECTROPHORETIC MOBILITY ($\mu\text{m cm/volt sec}$)	
NaCl	PETROLEUM SULFONATE	ALKALI				MINUSIL	MONTMORILLONITE
1.0	--	---		5.95	1.53	-1.90	-2.40
1.0*	--	---		5.85	1.53	-1.70	-2.40
1.0	--	0.37 NaOH		12.97	3.09	---	-2.40
1.0	--	0.37 Na ₂ CO ₃		11.06	2.24	---	-2.90
1.0	--	0.37 Na ₂ O(SiO ₂)	3.22	10.86	2.03	-2.75	-2.80
-	--	0.37 Na ₂ O(SiO ₂)	3.22	10.99	0.21	-4.40	-2.50
1.0	0.25	---		7.34	1.57	-2.10	-3.00
1.0	0.25	0.37 NaOH		13.0	3.11	-2.60	-2.50
1.0	0.25	0.37 Na ₂ CO ₃		11.0	2.18	-2.25	-3.75
1.0	0.25	0.37 Na ₂ O(SiO ₂)	3.22	10.80	2.05	-2.75	-3.75

* plus 10 ppm Ca + Mg ions

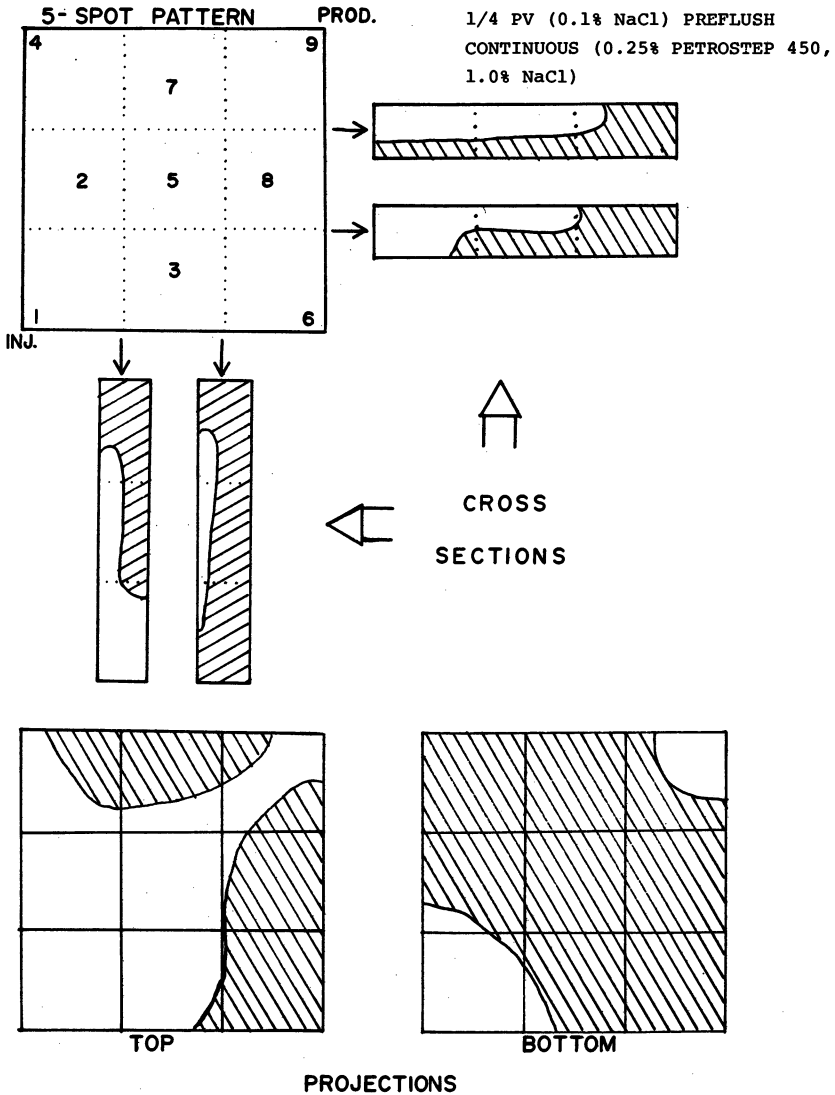


Figure 6. Radial flood using low tension water-flood system without silicate. (Reproduced, with permission, from Ref. 18. Copyright 1981, Society of Petroleum Engineers of AIME.)

Publication Date: June 1, 1982 | doi: 10.1021/bk-1982-0194.ch012

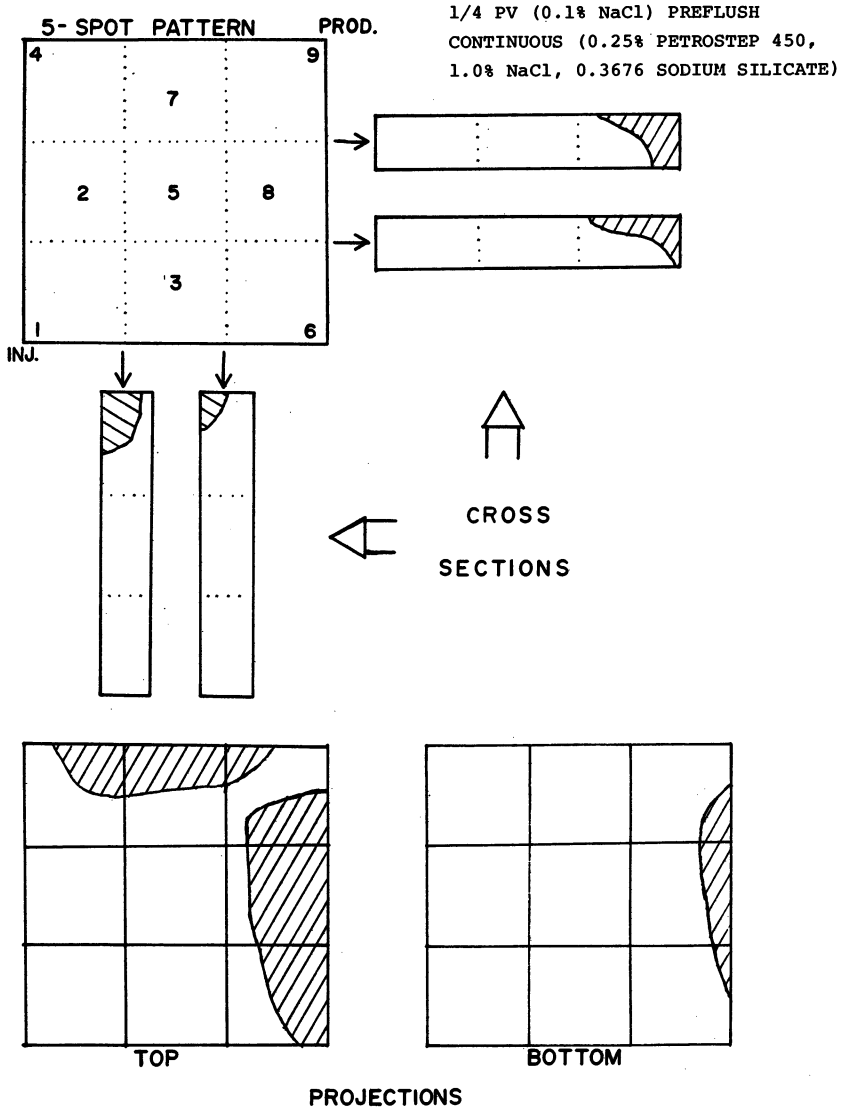


Figure 7. Radial flood using low tension water-flood system plus sodium silicate. (Reproduced, with permission, from Ref. 18. Copyright 1981, Society of Petroleum Engineers of AIME.)

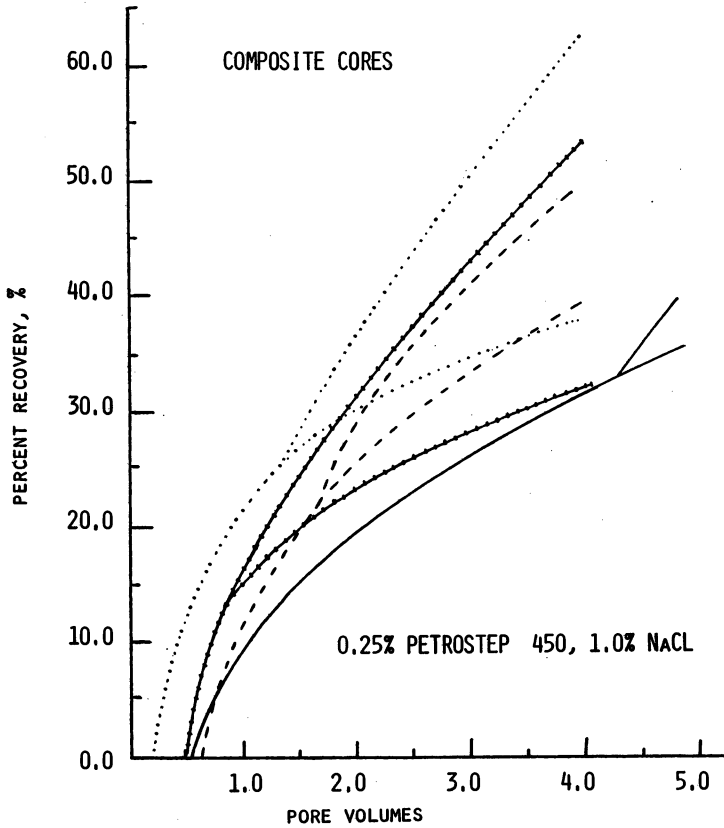


Figure 8. Recovery profiles from multipermeable zone floods. Key: —, no alkali; —→, 0.01% NaOH; ---, 0.367% Na₂CO₃; and ···, 0.367% sodium silicate. (Reproduced, with permission, from Ref. 18. Copyright 1981, Society of Petroleum Engineers of AIME.)

diverted into the low permeability zone, but only after the oil has been recovered from the higher permeability zone.

Some of this mobility control and improvement in sweep could be due to the emulsions formed which exhibit a higher bulk viscosity. Some work by Wasan et al (32) has shown that the sodium silicates will result in emulsions with lower shear or interfacial viscosities than sodium hydroxide. These lower interfacial viscosities at the micro-level help promote oil coalescence so that oil banking can occur and oil droplets are not retrapped and left behind. The oil banking and rapid emulsification on the macro-level or in the bulk help to give good mobility control. Also some recent work by Wasan (33) has indicated that the silicates tend to keep the surfaces more water-wet, thereby improving recovery. It has been noted that the thickness of the water film on quartz surfaces is thicker when silicates are present. Further work in these areas is currently being done to determine the limits and effects on the oil recovery mechanisms.

CONCLUSIONS

Sodium silicates can impart a number of significant benefits in chemical flooding techniques. Among these benefits are the following:

- sequestration or reduction of hardness
- maintenance of negative surface charges on clays and emulsion droplets.
- improved coalescence of oil droplets
- increased water-wetness
- reduced surfactant retention
- reduced IFT and improved emulsification
- reduced alkali consumption or reaction
- improved sweep efficiency and mobility control
- overall improved recovery of residual crude oil.

The properties and benefits all depend on the nature of the silicate molecules and their reactivity or adsorptivity which can be controlled by adjustments in the $\text{SiO}_2/\text{Na}_2\text{O}$ ratio and concentration. As these silicate molecules are present in a reservoir environment over long periods of time, the distribution and concentration of species will change due to the many reactions which can occur. However, it is such sacrificial reactions of the silicates which allow more of the surfactants, which are either formed in-situ or deliberately injected, to accomplish their intended role of mobilizing and producing residual crude oil.

Acknowledgments

The author would like to thank the PQ Corporation for granting me the permission to publish this paper. I would also like to thank the many people who have contributed to the knowledge and role of silicates in EOR processes and have shared this knowledge with me.

Literature Cited

1. Squires F. U.S. Patent No. 1,238,355,(Aug. 28, 1917).
2. Atkinson, A. U.S. Patent No. 1,651,311, (Nov. 29, 1927).
3. Nutting, P.G. Ind. Engr. Chem. 1925, 17, 1035.
4. Beckstrom, R.C.; Van Tuyl, F.M. Bull. AAPG 1927, 223.
5. Subkow, P., U.S. Patent No. 2,288,857, (July 7, 1942).
6. Reisburg, J. and Doscher, T.M. Prod. Monthly 1956, 43.
7. Doscher, T.M.; Reisburg, J. Canadian Patent No. 639,050 (March 27, 1962).
8. Wagner, O.R.; Leach, R.O. Trans. AIME 1959, 216, 65.
9. Leach, R.O.; Wagner, O.R.; Wood, H.W.; Harpke, C.F. J. Pet. Tech. 1967, 206.
10. Emery, L.W.; Mungan, N.; Nicholson, R.W. J. Pet. Tech. 1970, 1569.
11. McAuliffe, C.D. J. Pet. Tech. 1973, 721.
12. Graue, D.J.; Johnson, C.E. J. Pet. Tech. 1974, 1353.
13. Raimondi, P.; Gallagher, B.J.; Bennett, G.S.; Ehrlich, R.; Messmer, J.H. J. Pet. Tech. 1977, 1359.
14. Holm, L.W.; Robertson, S.D. J. Pet. Tech. 1981, 161.
15. Holm, L.W. U.S. Patent No. 4,011,908, (March 15, 1977).
16. Goldberg, A.; Stevens, P. "Proceedings of the 5th Annual DOE Symposium on EOR";The Petroleum Publishing Co.:Tulsa, OK,1979 p A-4/1.
17. Krumrine, P.H.; Campbell, T.C.; Falcone, J.S. SPE Preprint #8998, 1980.
18. Krumrine, P.H.; Falcone, J.S.; Campbell, T.C. SPE Preprint #9811,1981.
19. Krumrine, P.H.; Ailin-Pyzik, I.B.; Falcone, J.S.; Campbell, T.C."The Effect of Alkaline Chemicals on the Adsorption of Anionic Surfactants by Clays", ACS Symposium on the Chemistry of EOR, March 1981.
20. Sarem, A.M. U.S.Patent No. 3,805,893, April 23, 1974.
21. Sarem, A.M. U.S. Patent No.3,876,002, April 8, 1975.
22. Sarem, A.M. SPE Preprint #4901, 1974.
23. Carmichael, J.D. "Improved Oil Recovery by Controlled Waterflooding, Caustic", DOE Progress Review No. 20, BETC-79/4, Quarter Ending Sept. 30, 1978, p. 28.
24. Campbell, T.C.,; Krumrine, P.H. SPE Preprint #8328, 1979.
25. Campbell, T.C. SPE Preprint #7873, 1979.
26. Whiteley, R.C.; Ware, J.W. J. Pet. Tech. 1977, 925.

27. Widmyer, R.H.; Satter, A.; Frazier, G.D.; Graves, R.H. J.Pet. Tech. 1977, 933.
28. Talash, A.W.; Strange, L.K. SPE Preprint #10162, 1981.
29. Murphy, C.L.; Thiede, D.M.; Eskow, J.O. SPE Preprint #6005, 1976.
30. Somasundaran, P.; Hanna, H.S. SPE Preprint #7059, 1978.
31. Tsai, F.S.; and Falcone, J.S. "Influence of Sodium Silicates and Other Reagents on Zeta Potential of Oxide-Water Interfaces", ACS/CSJ Chem. Cong., Honolulu, HI, April 1979.
32. Wasan, D.T.; Sampath, K.; McNamara, J.; Perl, J.; Aderange, N.; Shah, S. M.; Shah, R.; Chan, M.; Nevrekar, P.; Pasquarelli, C.; Srivatsa, S.; Venkataraman, K. "The Mechanism of Oil Bank Formation, Coalescence in Porous Media and Emulsion Stability", 4th Annual DOE Symposium, Tulsa, OK, Aug. 1978.
33. Chang, M.M.; Wasan, D.T. SPE Preprint #9001, 1980.

RECEIVED March 8, 1982.

The Role of Emulsification Phenomena in Alkaline Waterflooding of Heavy Crude Oils

P. R. BRAUER¹ and D. T. WASAN

Illinois Institute of Technology, Department of Chemical Engineering,
Chicago, IL 60616

Greater improvements in Enhanced Oil Recovery by alkaline flooding occurred in linear core floods where more in-situ emulsification was observed. These in-situ generated emulsions aided in tertiary recovery by improving the areal sweep efficiency of the alkaline slug and by improving the dynamic mobility ratio within the core.

Previous work in our laboratory (1) implied that higher recovery efficiency may be achieved through the injection of an extracted resinous component, deasphalted crude oil slug, prior to the injection of the alkaline phase. Results indicated that improvements in tertiary recovery efficiency did occur. The injection of this extracted resinous crude component aided in recovery by preventing asphaltene deposition, thereby increasing permeability of oil to rock, by forming an oil bank, and again, in-situ emulsification was observed to aid in enhanced recovery.

A microwave attenuation technique was used to monitor in-situ oil/water saturations during enhanced recovery for each alkaline core flood.

Alkaline flooding is based on the reaction that occurs between the alkaline water and the organic acids, naturally occurring in some crudes, to produce in-situ surfactants or emulsifying soaps at the oil/water interface. Recent literature (2-5) summarizes several proposed mechanisms by which alkaline waterflooding will enhance oil recovery. These mechanisms include: emulsification and entrapment, emulsification and entrainment, and wettability reversal (oil-wet to water-wet or water-wet to oil-wet). Depending on the initial reservoir and experimental conditions with respect to oil, rock and injection water properties, one or more of these proposed mechanisms may be controlling.

¹ Current address: Cities Service Company, Energy Resources Group, Exploration and Production Research, Tulsa, OK 74102.

Many studies to date, have related emulsification to oil recovery. McAuliffe's results (6,7) showed that the injection of dilute oil-in-water emulsions, prepared external to the porous medium, enhanced oil recovery. D'Ella's (8) also showed that the injection of prepared water-in-oil emulsions can be used effectively in secondary and tertiary recovery of viscous crude oils. Rather than the external preparation of emulsions for enhanced recovery, Cash (9) proposes that residual oil can be mobilized by spontaneous emulsification within the core. Each of these investigators has shown the capabilities of either externally prepared emulsions or in-situ generated emulsions for improving oil recovery. These emulsions can enhance recovery by improving the areal sweep efficiency (3). In the case of the oil external emulsion, miscibility with residual oil can occur, leading to additional oil recovery through miscible displacement.

Results of our experimentation (1) suggests that the occurrence of permeability reductions during enhanced oil recovery may be avoided and the formation of a continuous oil bank may be initiated and maintained by using a slug of an extracted resinous fraction. These results support the work of Lichaa and Herrera (10,11), where they found that severe permeability reductions due to asphaltene deposition, could be avoided by the injection of a mixture of highly resinous Boscon Crude (29% wt. resin) with a Boscon refined oil. Cooke (2) recommended a similar process where a bank of highly acidic crude oil would be injected prior to the injection of the alkaline water for cases where the crude oil acid concentration is low.

The present study utilizes a microwave attenuation technique to study oil bank formation and propagation during linear core tests. This technique, first developed by Parsons (12), was employed to monitor the dynamic in-situ water concentration during the alkaline core flooding experiments.

Experimental

Two crude oils were used for this study. Huntington Beach Crude from Well S-47, which has an API of 23.0°, an acid number of 0.65 mg KOH/gram of crude, and a bulk shear viscosity of 10 cp at the reservoir temperature of 165°F. The other Californian crude oil used was Wilmington Field Crude from Well C-331. This crude has an API of 21.3°, an acid number of 0.86, and a bulk shear viscosity of 35 cps at the reservoir temperature of 125°F.

The tertiary oil recovery experiments were performed in one inch by four inch by twelve inch Berea sandstone cores. The average porosity was 0.20 and average brine permeability was 600 md. Each experiment was conducted in the following sequence:

- (1) Purge core with nitrogen
- (2) Evacuate and brine flood at 45mm Hg Abs. to achieve full initial saturation.

- (3) Heat core to reservoir temperature while flowing two additional pore volumes of brine for clay conditioning. Determine brine saturated pore volume and brine permeability at reservoir temperature.
- (4) Oil saturation until produced oil/aqueous ratio exceeds 100/1.
- (5) Brine flood (secondary recovery) until produced aqueous/oil ratio exceeds 100/1.
- (6) 1.0% Brine preflush (0.05 pv. for Wilmington test only)
- (7) Continuous injection of alkaline solution until final produced water/oil ratio exceeds 100/1.

Frontal advance rates were 1 ft/day after initial brine saturation and 3 ft/day during brine saturation. The brine used for the Huntington Beach core test contains 0.75% NaCl, whereas the brine used for the Wilmington Field core tests contained 1.0% NaCl and 1100 ppm Calcium Ion. Sufficient back pressure was maintained on the system throughout the experiment to prevent the oil from de-gasing while within the core.

Microwave scans were performed every two hours during tertiary recovery and more frequently where required. The data for each core flood is presented in the form of microwave profiles showing the variation in average oil saturation with distance along the core.

During tertiary recovery, the produced fluids were analyzed microscopically for the presence of oil-in-water and water-in-oil emulsions. Karl Fischer analysis was performed on the produced fluid samples in order to determine the amount of oil present in the aqueous phase and the amount of water present in the oil phase. Also pH readings were recorded for the produced aqueous phase throughout tertiary recovery.

Results and Discussion

Several alkaline chemicals have been employed for various aspects of enhanced oil recovery. Two of the most favorable alkaline chemicals tested and used in tertiary oil recovery are sodium orthosilicate and sodium hydroxide. Comparing their characteristics, both chemicals react with acids in crude oil to form surfactants, precipitate hardness ions and change rock surface wettability. One difference between the two chemicals is that the interfacial properties for sodium orthosilicate systems are less affected by hardness ions (13), hence slightly lower interfacial tensions would occur. Lower interfacial tensions can aid in in-situ emulsion formation.

This study is the start of a systematic study of various concentrations of sodium orthosilicate and sodium hydroxide against Wilmington Field Crude. Initial alkaline core tests were performed using 0.6% sodium orthosilicate or sodium hydroxide with 1.0% NaCl. Prior to the continuous injection of the alkaline phase, a 0.05 pv slug of 1.0% NaCl was injected as a pre-

flush solution to separate the alkaline phase from the hardness ions in the connate brine. Core tests results are presented in Tables I and II. Results show that slightly better oil recovery efficiency (27-28% vs. 21-22%) can occur when using the sodium orthosilicate system.

A typical microwave profile for secondary recovery of Wilmington Field crude is presented in Figure 1. Examination of the microwave oil saturation profile during tertiary oil recovery for each of the floods, shows similar oil banking characteristics for each alkaline chemical. In core tests 1 and 2, using sodium orthosilicate, early formation of an oil bank was observed (Figure 2). This oil bank flows down the length of the core and oil is produced at hour 18 into tertiary oil recovery. Comparing the microwave saturation profiles for core tests 3 and 4 using sodium hydroxide, early formation of an oil bank was again observed (Figure 3). This oil bank also is continuous and is produced at hour 18 into tertiary recovery. Comparison of the oil banking during tertiary oil recovery for similar concentrations of sodium orthosilicate and sodium hydroxide within a hardness ion environment, did not indicate why one chemical may be preferred.

Comparison of the produced fluid analysis for these floods will give us an indication of why one process may be preferred. Produced fluid analysis for these floods show pH breakthrough occurring at similar times for each process (Figure 4,5). So, the two processes cannot be separated by comparing caustic breakthrough times.

Each of these floods produced oil-in-water and water-in-oil emulsions coincident with pH breakthrough. These in-situ generated emulsions did not cause significant increases in the total pressure drop across the length of the core. Karl Fischer analysis of produced oil and aqueous phase showed that more emulsification occurred in the sodium orthosilicate floods. Results indicate over 2.3% incorporation of water into the oil phase and over 4.0% incorporation of oil into the water phase for the sodium orthosilicate floods. For the sodium hydroxide floods, only 1.4% water-in-oil emulsion and 0.6% oil-in-water emulsion was produced. These preliminary results suggest that this sodium orthosilicate system emulsifies oil better than the sodium hydroxide system. These in-situ generated emulsions may have increased the displacement capabilities of the alkaline phase by improving the mobility ratio and/or the areal sweep efficiency within the core, thus causing the slight increase in tertiary oil recovery for the sodium orthosilicate floods.

Previous work (1) in core floods with the system, Huntington Beach Crude vs. $0.5\% \text{Na}_4\text{SiO}_4$ plus $0.75\% \text{NaCl}$, showed channeling of the crude oil during the injection of the caustic slug (Figure 6). The channeling phenomena along with the fact that emulsions were not observed until after 95% of the recovered oil was produced, could have lead to lower oil recovery efficiencies. To

TABLE I. CORE TEST DATA

CORE TEST	POROSITY	CRUDE OIL	ALKALINE SLUG
1	0.205	Wilmington Field	0.6% Na ₄ SiO ₄ + 1.0% NaCl
2	0.225	Wilmington Field	0.6% Na ₄ SiO ₄ + 1.0% NaCl
3	0.229	Wilmington Field	0.6% NaOH + 1.0% NaCl
4	0.228	Wilmington Field	0.6% NaOH + 1.0% NaCl
5	0.215	Huntington Beach	0.5% Na ₄ SiO ₄ + 0.75% NaCl
6	0.210	Huntington Beach	0.5% Na ₄ SiO ₄ + 0.75% NaCl

TABLE II. CORE TEST DATA

CORE TEST	SO _I	SO _R	% SECONDARY RECOVERY	SO _F	% TERTIARY RECOVERY
1	0.72 pv	0.45 pv	38	0.33 pv	27
2	0.71 pv	0.41 pv	41.6	0.29 pv	28
3	0.73 pv	0.44 pv	39	0.35 pv	22
4	0.715 pv	0.42 pv	41.4	0.33 pv	21
5	0.64 pv	0.41 pv	37	0.31 pv	25
6	0.61 pv	0.37 pv	39	0.24 pv	31

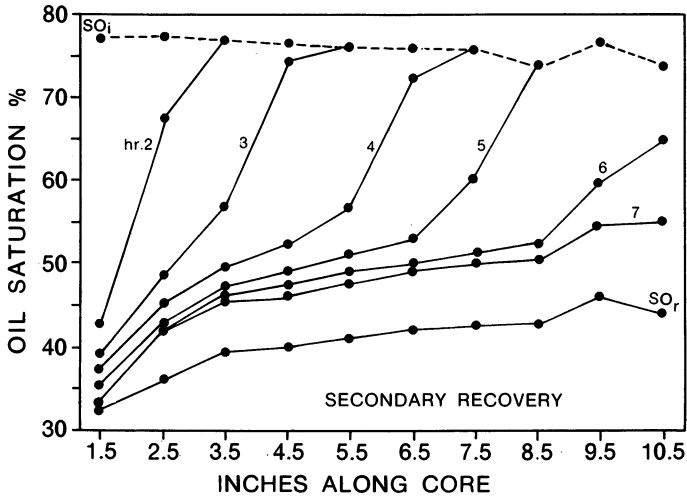


Figure 1. Secondary recovery profiles for core test 1.

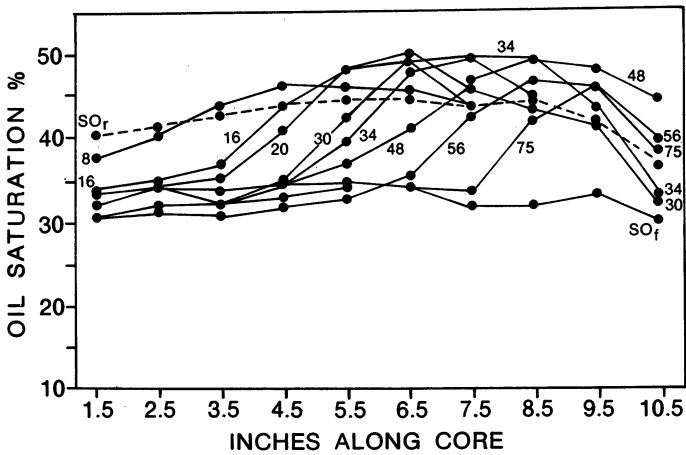


Figure 2. Microwave profiles for tertiary recovery, core test 2; 0.6% sodium orthosilicate and 1.0% NaCl.

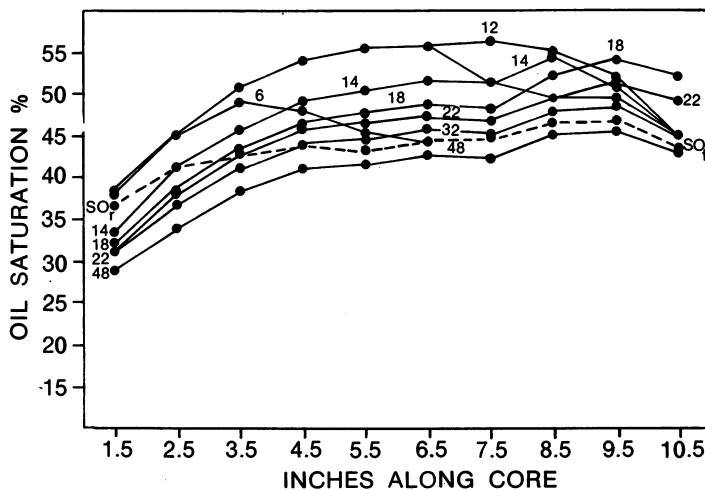


Figure 3. Microwave profiles for tertiary oil recovery, core test 3; 0.6% NaOH + 1.0% NaCl vs. C-331 crude.

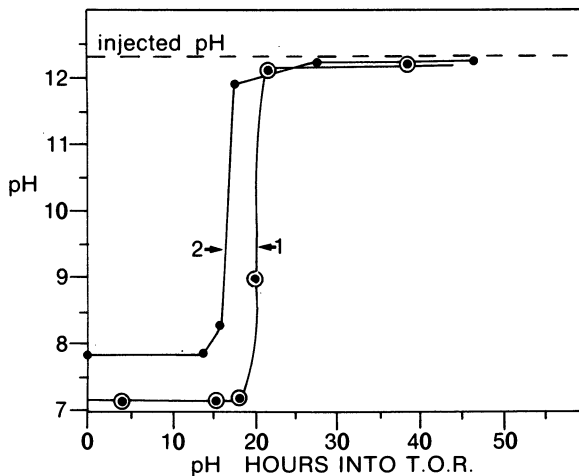


Figure 4. The pH analysis of produced fluids, core tests 1 and 2; 0.6% Na_4SiO_4 + 1.0% NaCl vs. C-331 crude.

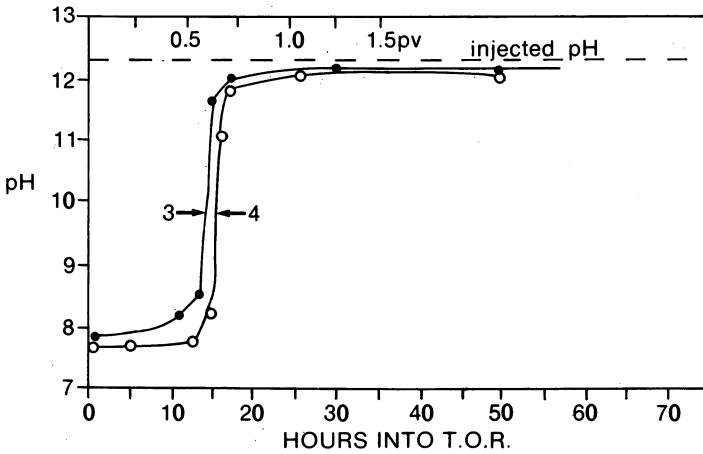


Figure 5. The pH analysis of produced fluids, core tests 3 and 4; 0.6% NaOH + 1% NaCl vs. C-331 crude.

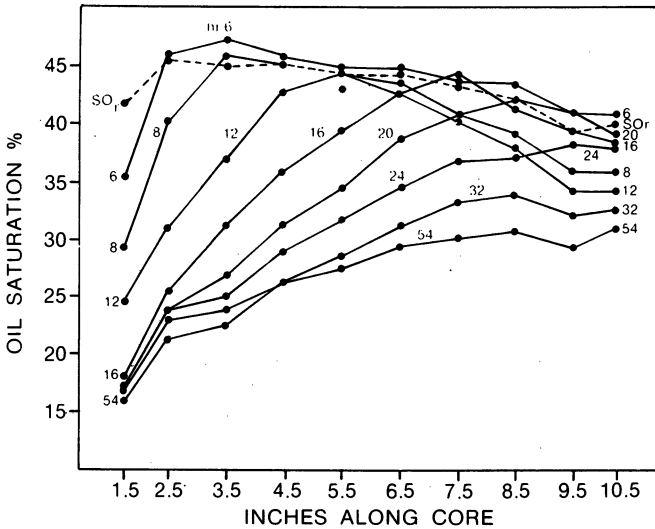


Figure 6. Microwave profiles during tertiary recovery for core test 5; Huntington Beach crude vs. 5000 ppm orthosilicate + 7500 ppm NaCl.

examine the idea of using an extracted resinous component to improve recovery efficiency, a deasphalted slug of Huntington Beach Crude was prepared following standard ASTM procedures (13). Following completion of secondary recovery and prior to the continuous injection of the alkaline phase, a 0.05 pv slug of this deasphalted Huntington Beach Crude was injected. Results for this core test are also summarized in Tables I and II. Tertiary oil recovery increased to 31% from the 25% recorded in the core test where a deasphalted slug was not employed. Comparing the tertiary oil saturation profiles for the two core tests, the early formation of an oil bank at hour 2 for core test 6 is observed (Figure 7). This oil bank is formed because of the injection of the 0.05 pv slug of deasphalted crude. The volume of oil above residual saturation (SO_R) at hour 2 represents the volume of oil injected in the deasphalted crude slug. This oil bank flows down the length of the core and is produced at hour 9 (Figure 8). Produced fluid analysis showed pH breakthrough occurring at hour 21 (Figure 8). The initial oil that is produced within the bank does not contain any emulsions, but the remainder of the produced oil did contain water-in-oil emulsions. Oil-in-water emulsions were produced coincident with the oil bank. These in-situ generated emulsions may have aided in improving the recovery efficiency for the deasphalted crude core test according to the reasons stated previously.

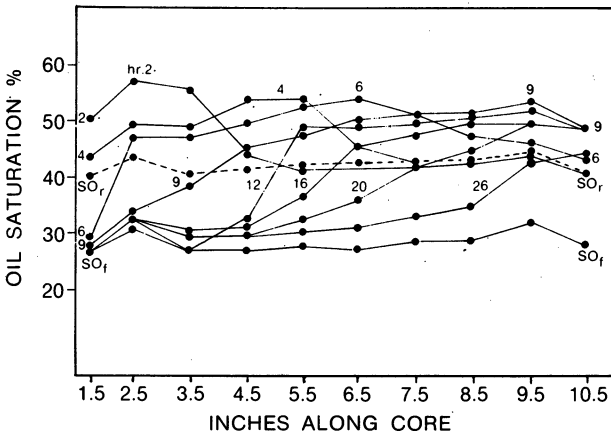


Figure 7. Microwave profiles during tertiary recovery for core test 6.

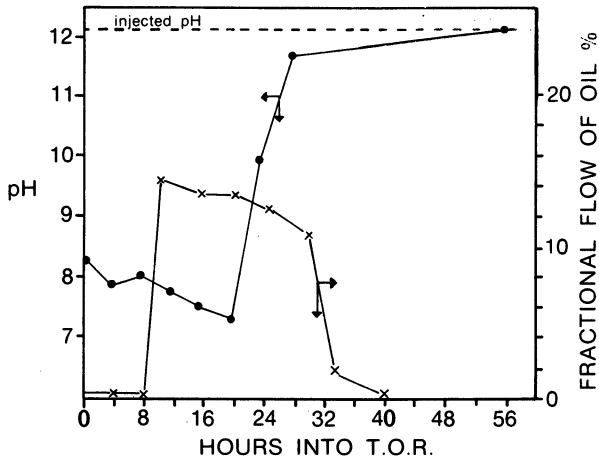


Figure 8. The pH and fractional flow of produced fluids, core test 6.

Summary and Conclusion

1. In-situ generated emulsions were produced coincident with pH breakthrough.

2. More in-situ emulsification was observed with the sodium orthosilicate system rather than the sodium hydroxide system.

3. In-situ generated emulsions could enhance recovery techniques by improving the areal sweep efficiency of the alkaline slug and by improving the dynamic mobility ratio within the core.

4. Improvements in enhanced recovery occurred when a de-asphalted crude oil slug was injected prior to the continuous alkaline phase.

5. The deasphalted crude oil slug, extracted resinous component, may have improved tertiary recovery by preventing asphaltene deposition, thereby increasing permeability of oil to rock, by forming an oil bank, or again, in-situ emulsification may have enhanced oil recovery.

Literature Cited

1. Pasquarelli, C. H.; Brauer, P. R.; Wasan, D. T.; Ciempil, M.; Perl, J. P., "The Role of Acidic, High Molecular Weight Crude Components in Enhanced Oil Recovery", SPE 8895. Paper presented at the 50th Annual California Regional Meeting of the Society of Petroleum Engineers of AIME. Los Angeles, California, April 9-11, 1980.
2. Cooke, C. E., Jr.; Williams, R. E.; Kolodize, P. A., "Oil Recovery by Alkaline Waterflooding", JPT. December 1974, pp. 1365-1374.
3. Jennings, H. Y.; Johnson, C. B.; McAuliffe, C. D., "A Caustic Waterflooding Process for Heavy Oils", JPT. December 1974, pp. 1344-1352.
4. Johnson, C. B., "Status of Caustic and Emulsion Method", JPT. January 1976, pp. 85-92.
5. Mayer, E. H.; Berg, R. L.; Carmichael, J. D.; Weinbrandt, R. M., "Alkaline Injection for Enhanced Oil Recovery--A Status Report", SPE 8848. Paper presented at the 50th Annual California Regional Meeting of the Society of Petroleum Engineers of AIME. Pasadena, California, April 9-11, 1980.
6. McAuliffe, C. D., "Crude Oil-in-Water Emulsions to Improve Fluid Flow in an Oil Reservoir", JPT. June 1973, pp. 721-726.
7. McAuliffe, C. D., "Oil-in-Water Emulsions and Their Flow Properties in Porous Media", JPT. June 1973, pp. 727-733.
8. D'Elia-So, R.; Ferrer-G, J., "Emulsion Flooding of Viscous Oil Reservoirs", SPE 4674. 48th Annual Fall Meeting. Las Vegas, Nevada, September 30 - October 3, 1973.
9. Cash, R. L., Jr.; Cayisas, J. L.; Haynes, M.; MacAllister, D. J.; Schares, T.; Schechter, R. S.; and Wade, W. H., "Spontaneous Emulsification--A Possible Mechanism for Enhanced Oil Recovery", SPE 5562. Paper presented at 50th Annual Fall Meeting of the Society of Petroleum Engineers of AIME. Dallas, Texas, September 28 - October 1, 1975.
10. Lichaa, P. M., "Asphaltene Deposition Problem in Venezuelan Crudes--Usage of Asphaltenes in Emulsion Stability". Paper presented at the Canada--Venezuela Oil Sands Symposium 77. Edmonton, Alberta, Canada, May 27 - June 4, 1977.
11. Lichaa, P. M.; Herrera, L., "Electrical and Other Effects Related to the Formation and Prevention of Asphaltene Deposition Problem in Venezuelan Crudes", SPE/AIME No. 5304. 1975.
12. Parsons, R. W., "Microwave Attenuation--A New Tool for Monitoring Saturations in Laboratory Flooding Experiments", SPE J. August 1975, pp. 302-310.

13. Campbell, T. C., "The Role of Alkaline Chemicals in the Recovery of Low Gravity Crude Oils". SPE 8894. Paper presented at the 50th Annual California Regional Meeting of the Society of Petroleum Engineers of AIME. Pasadena, California, April 9-11, 1980.
14. Pasquarelli, C. H., M.S. Thesis, Illinois Institute of Technology, Chicago, 1980.

RECEIVED March 2, 1982.

Long-Term Consumption of Caustic and Silicate Solutions by Petroleum Reservoir Sands

VAN T. LIEU—California State University, Chemistry Department,
Long Beach, CA 90840

SAMUEL G. MILLER—Department of Oil Properties, City of Long Beach,
Long Beach, CA 90802

STEPHEN J. STAPHANOS—California State University, Chemistry Department,
Long Beach, CA 90840

A number of laboratory investigations were made into different aspects of consumption of sodium hydroxide and sodium orthosilicate in alkaline flooding of petroleum reservoirs for enhanced oil recovery. One investigation studied the role of reversible adsorption and of chemical reaction when petroleum reservoir sands are contacted with alkaline solutions. Another investigation studied the effect of flow rate on caustic consumption by means of a series of flow experiments through reservoir sand packs. A third series of high rate flow experiments studied changing alkaline consumption with time.

The long term pulse study was devised to determine the time required for the alkalinity of a solution in the pores of a sand pack to reduce to zero. This method provides a means for estimating the longevity of a given volume and concentration of alkaline chemical solution injected into an actual petroleum reservoir.

In the past several years, renewed interest in enhanced oil recovery by alkaline flooding has been evidenced. Although the addition of alkaline chemicals to injection water has been proposed by many workers over the past 50 years, in recent years, the subject has recently been seriously studied by several workers as prelude to actual field injection trials (1-4). At the present time, several field trials of alkaline flooding have been completed, are in progress or are being planned (5-10). One of the critical alkaline flood design parameters is the proper concentration of alkaline chemical to use. This concentration is dependent on the alkaline consumption by the reservoir sand during the time that it takes for the solution to traverse the reservoir.

The consumption of alkaline chemical in the reservoir is a function of the amount and type of rock minerals, surface area and of the sands compactness, alkaline chemical concentration used, reservoir temperature and the time the alkaline chemical is exposed to the reservoir sand (1, 4, 11). These factors are interdependent and together determine the overall consumption.

Over the past several years ideas have changed about what constitutes the proper alkali concentration for alkaline flooding. Much higher concentrations are now being considered because it is now known that with sufficient time, the alkaline consumption can become very large.

Initially, it was thought that the "interfacial tension window" should determine the proper concentration. This window is a range of concentrations of alkali in formation brine which gives extremely low interfacial tension values with oil, thus producing the desired enhanced recovery effect. Concentrations below and above the window do not have the extremely low interfacial tension. Typically, this concentration range is in the region of 0.2% sodium hydroxide. In the sands we have studied, concentrations of this level will not survive where there is a considerable duration of time in the reservoir (measured in several years, rather than in several months). Basically, a higher initial alkaline chemical concentration is required to provide for the continued depletion of the alkaline chemical, which must survive the lapse of time between injection and producing well.

This paper describes our studies of various aspects of alkaline consumption in reservoir sands and our efforts to develop a test for determining the optimum concentration to use in an alkaline flood.

Apparatus and Chemicals

All sand packs were prepared in lucite columns approximately 6" or 12" in length and 1-1/2" in diameter. The two ends of a column were equipped with solid lucite plugs. Each column was also equipped with a stainless steel cage to hold the assembly in place. In sand pack preparation, wire gauze and a layer of reagent grade sand were packed at each end of the column to hold the reservoir sand sample in place. The sand pack pore volumes for the 6" column were approximately 50 mls, and for the 12" column were approximately 110 mls. The pore volume was determined gravimetrically by evacuation of the sand pack under vacuum and saturation with 1% NaCl.

A stock 10% sodium hydroxide and 1% sodium chloride solution was prepared from reagent grade solid sodium hydroxide and sodium chloride. A stock 10% sodium orthosilicate (i.e. a molar ratio of $\text{Na}_2\text{O}/\text{SiO}_2$ of 2/1) and 1% sodium hydroxide solution was prepared by mixing 112.5 parts by weight of "N sodium silicate" (PQ Corporation), 147.9 parts by weight of 50% sodium hydroxide and 739.6 parts by weight of 1% sodium chloride. All sodium hydroxide and sodium orthosilicate solutions used were prepared by dilution of the stock solutions with 1% sodium chloride.

Sands from two different Pliocene-Miocene reservoirs in Southern California were used in our studies, from the THUMS Ranger Zone of East Wilmington and from the Lower Main Zone (LMZ) of Aminoil at Huntington Beach. All experimental work with THUMS Ranger sand was conducted at 125F and with Aminoil LMZ sand at 165F.

Static Equilibrium Study

In order to gain some initial understanding of the extent and rate of alkaline consumption of reservoir sands, static equilibrium tests commonly known as "Jar" tests were performed individually by mixing Aminoil, THUMS and crushed Berea sandstone sands with a large excess of 0.2% or 0.4% sodium hydroxide in tightly capped plastic bottles. The sand samples were disaggregated and, in the case of THUMS Ranger sand, the sample was extracted with toluene. Aliquots of the caustic solutions were collected at different times and analyzed for their alkalinities. The samples were agitated occasionally during soaking.

As can be seen from Figure 1, where sodium hydroxide consumption is plotted as a function of time, the consumption of caustic by all three sands was rapid; as much as 35 to 60 meq/100g sand were consumed after 62 days. The consumption reactions were still in progress when the experiments were terminated. From this study, it became obvious that caustic consumption by reservoir sand can be a long term phenomenon.

One notes that the alkaline consumption values obtained after 62 days are much larger than the consumptions which corresponded to the range near the interfacial tension window concentration of 0.2% NaOH or 0.625 meq/100g sand. They are also far larger than those which were determined by the earlier short tests of some few hours or days duration and much larger than those which we determined for longer term flow study using sand packs. The reason for such high consumption is the large

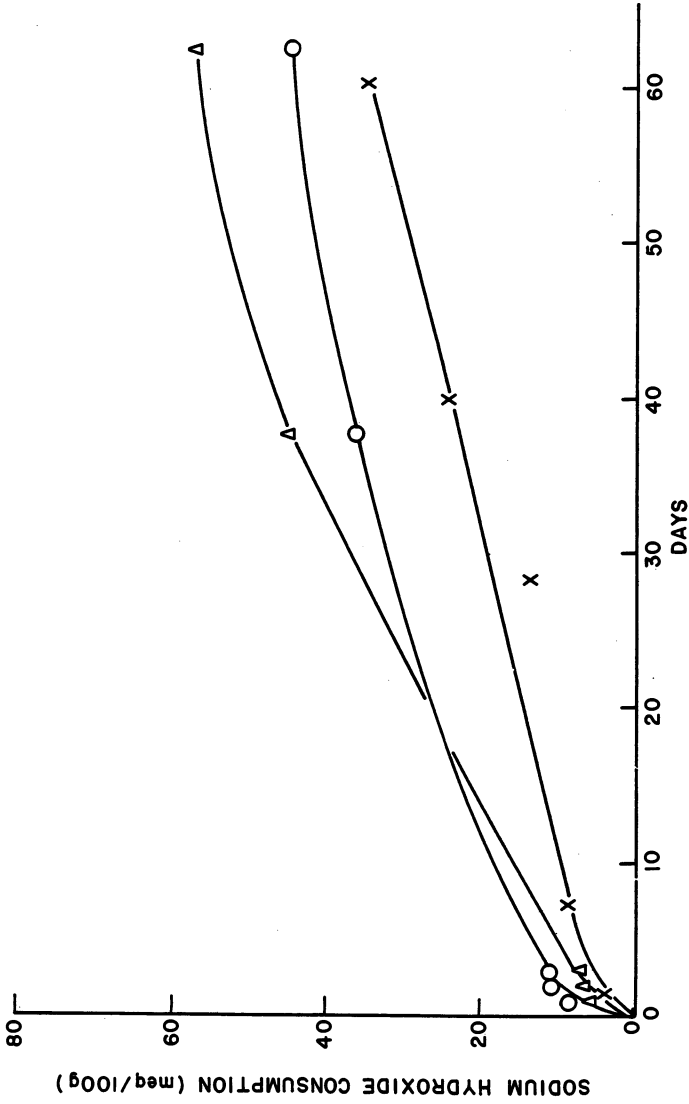


Figure 1. Static equilibrium experiments to study caustic consumption of reservoir sands in the presence of large excess of NaOH solution. Key: Δ , Aminoil LMZ sand at 165°F in 0.2% NaOH; \circ , THUMS Ranger sand at 125°F in 0.2% NaOH; \times , Berea sandstone sand at 125°F in 0.4% NaOH.

surface area of the disaggregated sands and the large volume of chemical solution available for reaction.

Table I gives the results of short term (5-7 days) static equilibrium experiments by Holm (12) and Ehrlich (4) in studying the alkaline consumption of some minerals and sands. It is our opinion that the consumption values given are conservative because the minerals were soaked in alkaline chemical only 5 days to 1 week. With longer time, further alkaline consumption can be expected. It is of interest to note that the alkaline consumption for Berea sandstone obtained by Ehrlich after 7 days of exposure to alkaline chemicals is 4.7 meq/100 grams. This is in general agreement with our finding from the Berea sandstone sand alkaline consumption plot in Figure 1 which gives 6 meq/100 grams at the point after 7 days exposure to 0.4% sodium hydroxide.

TABLE I

ALKALINE CONSUMPTION BY MINERALS AND SAND

<u>Minerals and Sands</u>	<u>Alkaline Consumption (meq/100g)</u>	
	<u>Short Term</u>	<u>Long Term</u>
Kaolinite	9.2 (a), 13 (b)	
Illite	19 (a), 136 (b)	145 (c)
Montmorillonite	118 (a), 228 (b)	
Calcite	5 (d)	21 (c)
Dolomite	35 (d)	245 (c)
Chlorite	11 (d)	58 (c)
Gypsum	164 (d)	900 (c)
		1,469 (e)
Berea sandstone sand	4.7 (b)	21 (c)

(a) L. W. Holm: 0.7% sodium orthosilicate at 25C for 5 days.

(b) R. Ehrlich: 1.25 N sodium hydroxide at room temperature for 7 days.

(c) Authors of this paper: 1.5% sodium orthosilicate at 125F for 62 days.

(d) Authors of this paper: 1.5% sodium orthosilicate at 125F for 5 days.

(e) By stoichiometric calculation.

Table I also gives the alkaline consumption of some minerals and sands obtained by treating 10 grams of sample with excess 1.5% sodium orthosilicate after 5 and 62 days. Although the experimental conditions, such as concentration, type of alkaline chemicals, temperature, particle size, used by different investigators varied, the results clearly show that with longer time of contact, alkaline consumption will increase.

In another set of static equilibrium tests, one pore volume (PV) of alkaline solution was mixed individually with Aminoil LMZ, THUMS Ranger and Berea sandstone sands. The volume of one PV used was calculated from the porosity of the same sand when it was packed for sand pack flow study. After standing for a number of days, the mixtures were filtered and the filtrates were analyzed for their alkaline consumption by titration with standard acid. As depicted in Table II, the consumptions were rapid in all cases and the alkaline chemicals were totally or almost totally consumed after 6 to 9 days for the THUMS Ranger and Aminoil LMZ sands. The consumption with Berea sandstone sand was slower by comparison but still quite significant.

TABLE II

STATIC EQUILIBRIUM STUDY TO DETERMINE THE RELATIVE REACTIVITY OF RESERVOIR SANDS AND BEREA SANDSTONE SAND WITH THE USE OF ONE PORE VOLUME ALKALINE CHEMICALS AT 125 F

	<u>% NaOH Consumed</u>	
	<u>1 PV 0.2% NaOH</u>	<u>1 PV 1.0% NaOH</u>
Aminoil LMZ Sand	100% (after 6 days)	94% (after 9 days)
THUMS Ranger Sand	100% (after 6 days)	97% (after 9 days)
Berea Sandstone Sand		49% (after 12 days)
	<u>% Orthosilicate Alkalinity Consumed</u>	
	<u>1 PV 0.2% Orthosilicate</u>	<u>1 PV 1.0% Orthosilicate</u>
THUMS Ranger Sand	100% (after 9 days)	95% (after 9 days)
Berea Sandstone Sand		31% (after 12 days)

Reversible Adsorption and Non-Reversible Chemical Consumption

Interaction of alkali with rock minerals in reservoir sand is complicated. Somerton and Radke (11) classified these interactions into surface exchange and hydrolysis, congruent and incongruent dissolution reactions, and insoluble salt formation by reaction with hardness ions in the pore fluids and exchanged from sand surfaces. These interactions may also be classified into reversible adsorption or non-reversible chemical consumption, and kinetic controlled or instantaneous reactions.

This section describes our study of the extent of reversible adsorption (and/or ion exchange) as compared with non-reversible chemical consumption between alkaline chemicals and reservoir sands. This is significant because in the case of reversible adsorption, the loss of alkaline chemical is temporary and thus the alkalinity may be recovered; on the other hand, chemical consumption is permanent and cannot be recovered.

The effect of time on the reversible and nonreversible consumption should be considered in evaluating the extents of instantaneous and kinetic controlled reactions.

The study was carried out by mixing thoroughly four 10g THUMS Ranger sand samples with 100 ml of 0.1 weight %, 0.2%, 0.5% and 1.0% sodium hydroxide. The sand samples were cleaned by extraction with toluene and were disaggregated. All the solutions contained 1% (weight percent) sodium chloride. After standing for 30 minutes, the samples were filtered, then washed with 1% NaCl solutions. The extent of reversible adsorption and of chemical consumption are expressed in terms of alkalinity and are determined by titration with standard 0.1N hydrochloric acid to its phenolphthalein end point. The losses in alkalinity due to the sum of reversible adsorption and chemical consumption (a) were determined by analysis of the filtrates. The losses in alkalinity due to reversible adsorption (b) were determined by analysis of the wash liquids. The difference between (a) and (b) gives the loss in alkalinity due to chemical consumption. Identical experiments were performed on three additional sets of samples except the filtration-washing step was carried out after 2, 9, and 36 days respectively.

The results obtained are depicted in Figure 2. The curve obtained for reversible adsorption is typical of adsorption isotherms and the results obtained are in general agreement with the hydroxide exchange isotherms by Somerton and Radke (11) using the same sand. They are of the order of 1 meq/100g sand.

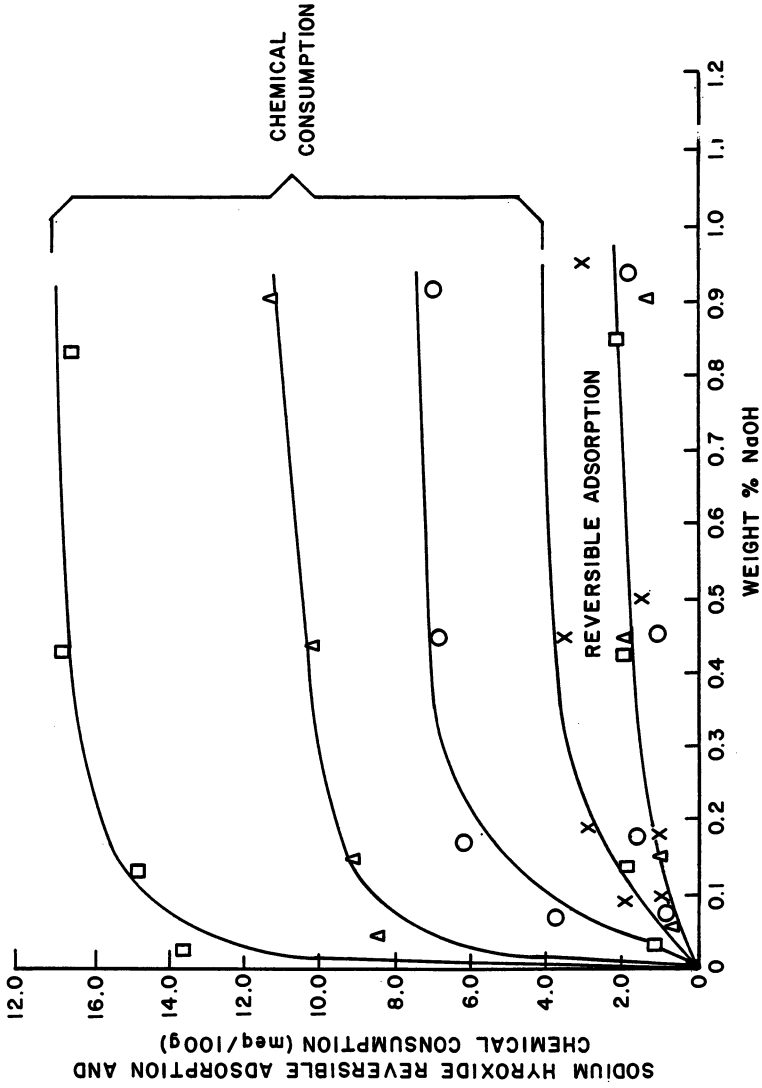


Figure 2. Reversible adsorption and chemical consumption of NaOH in 1% NaCl by THUMS Ranger sand at 125°F. Key: X, 0; O, 2; Δ, 9; and □, 36 d.

Similar experiments were carried out to study the reversible adsorption and chemical consumption of sodium orthosilicate by THUMS Ranger sand. Results obtained are depicted in Figure 3.

As can be seen from Figures 2 and 3, for both sodium hydroxide and sodium orthosilicate the reversible adsorption increases with the concentration of the alkaline solution, but is independent of the time the sand sample is exposed to the alkaline solution. On the other hand, chemical consumption increases with concentration of the alkaline solution as well as with the time the sand sample is exposed to alkaline solution. Given sufficient time and in the presence of large excess of the alkaline chemicals, the loss in alkalinity due to chemical consumption is much greater than that due to reversible adsorption.

Flow Rate Effect On Caustic Consumption

Four 6" sand packs were prepared with Aminoil LMZ sand. A 0.18 weight % sodium hydroxide and 1% sodium chloride solution was injected into the four sand packs at 0.25, 0.33, 0.50 and 1.0 pore volume per day respectively. The sand packs were first saturated with a 1% sodium chloride solution, then saturated with the Aminoil LMZ oil. They were then waterflooded with a 1% NaCl solution in distilled water until oil had essentially stopped being produced. At this point the alkaline injection was begun. Aliquots of the alkaline solution were collected after passing through the sand packs and analyzed for their alkalinities.

Figure 4 plots % NaOH of the effluent as a function of pore volume for the different flow rates. For purposes of comparison, points were taken at 5 pore volumes, which is in the plateau region of all the plots, and the % NaOH consumed was calculated for each of the points.

Figure 5 is a plot of % NaOH consumed versus the flow rate. It can be seen that the % NaOH consumed increases with reduction in flow rate. This is to be expected since with the slower flow rate, longer time is available for the caustic solution to react with the reservoir sand. That is, slower flow rates increase the reaction residence time. For example, 1/3 PV/day corresponds to a residence time of 3 days, allowing longer exposure between the caustic and reservoir sand, and hence, more consumption.

From the same data of Figure 4, Figure 6 plots of space-time-consumption of caustic as a function of space velocity.

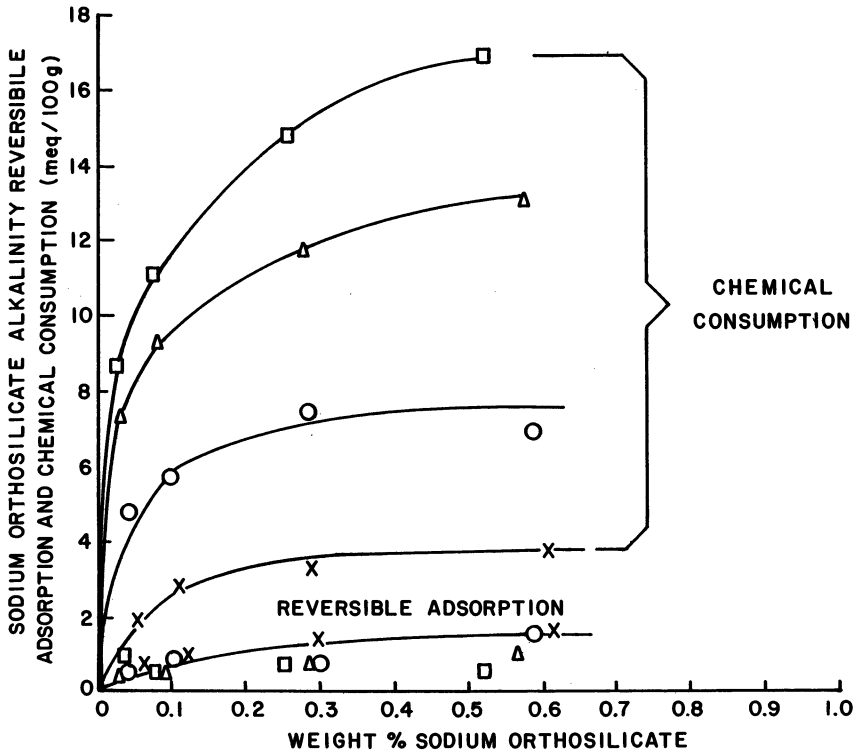


Figure 3. Reversible adsorption and chemical consumption of orthosilicate alkalinity in 1% NaCl by THUMS Ranger sand at 125%. Key: X, 0; O, 2; Δ, 9; and □, 36 d.

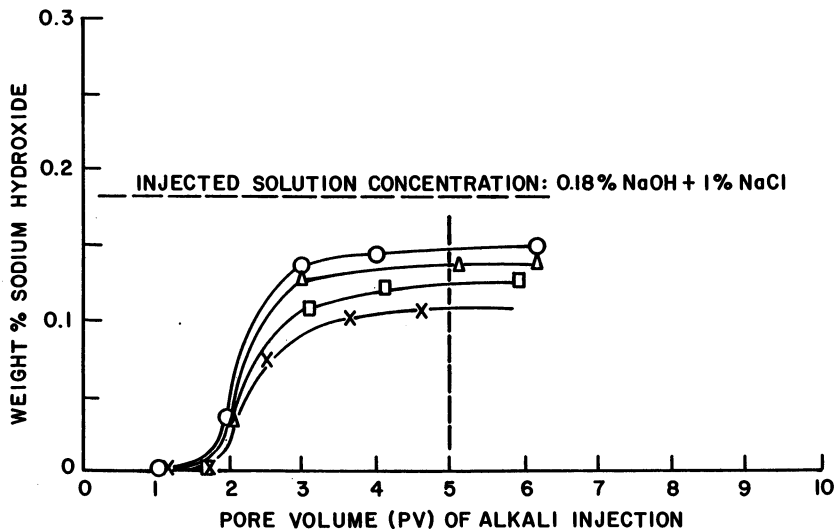


Figure 4. Effect of flow rate on caustic consumption. Plots of % NaOH of effluent vs. flow rate of NaOH through Aminoil LMZ sand packs at 165°F. Key for pore vol/d and % consumption: \times , 0.25, 32%; \square , 0.33, 25%; \triangle , 0.50, 20%; and \circ , 1.0, 16%.

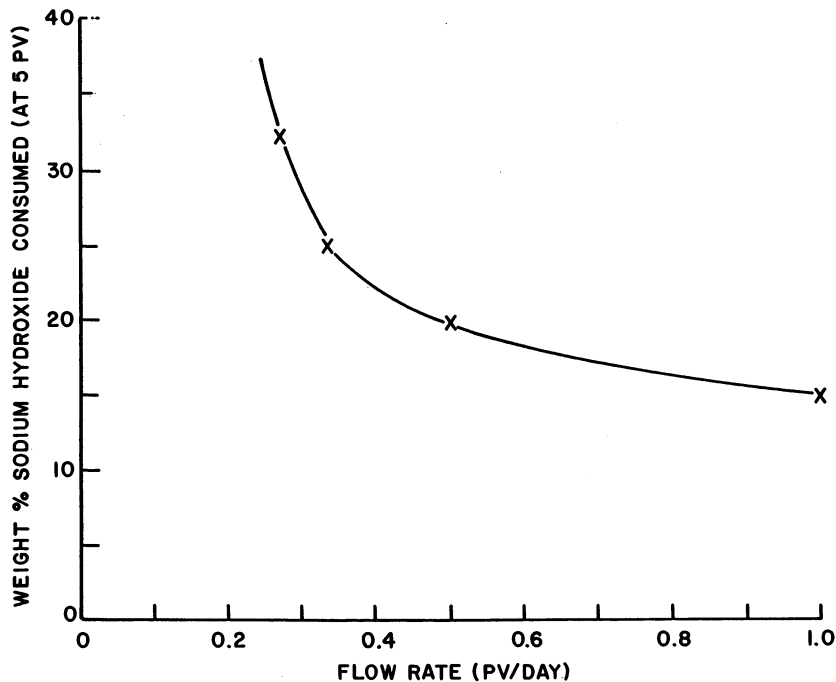


Figure 5. Effect of flow rate on caustic consumption. Plot of % NaOH consumed as a function of flow rate at 5 pore vol. Conditions: 0.18% NaOH + 1% NaCl solution through Aminoil LMZ sand packs at 165°F.

The space velocity is the volume (PV) of caustic solution passing through in unit time (day) per unit pore volume. Space-time-consumption is the caustic consumption in unit time (day) per unit pore volume and is equal to the product of fractional caustic consumed and space velocity.

It is seen from Figure 6 that space-time-consumption (or amount of caustic consumed per day) changes slowly with lower space velocities. Accordingly, a flow rate (or space velocity) of 1/3 PV/day was selected for all the subsequent flow tests. This rate is an average oil reservoir velocity and has the advantage determined here that the amount of caustic consumption per day would not be greatly affected by slight variation in flow rates.

Again, from the same data from Figure 4, Figure 7 plots % NaOH in the effluent at 5 pore volume versus time (days). It is significant to note that with higher flow rates the time required for alkalinity "breakthrough" to occur is reduced.

Long Term Flow Study

Seven flow study experiments were conducted to determine the long term effects of the consumption of alkaline chemicals on reservoir sands using 12" long sand packs. The treatment of Aminoil LMZ sand packs before alkaline injection was the same as that described in the study of Flow Rate Effect On Caustic Consumption. The treatment of THUMS Ranger sand was also the same except that after saturation with THUMS crude oil, the sand packs were waterflooded with 1% NaCl to water "breakthrough". Water "breakthrough" is defined as the point where water begins to appear in the effluent in significant quantity. Sodium hydroxide or sodium orthosilicate solutions in 1.0% sodium chloride were then injected at the rate of 1/3 pore volume per day. The effluents collected were analyzed by titration with standard hydrochloric acid to their phenolphthalein end points.

Weight % alkaline chemical alkalinity effluent vs. pore volume are plotted in Figure 8(a) and 8(b). The following observations and interpretation can be made on the results obtained:

The consumption of sodium hydroxide and sodium orthosilicate in reservoir sand is a long term phenomenon. The number of pore volumes required for the concentration of effluent alkaline solution to reach the concentration of the injected solution ranges from 10 to 33 pore volume (or 30 to 99 days). On reducing the flow rate from 1/3 pore volumes per day to 1/10 pore volume per day after the effluent appeared to have reached the concentration level of the injected solution, the concentration level of the effluent dropped to a lower value, indicating the

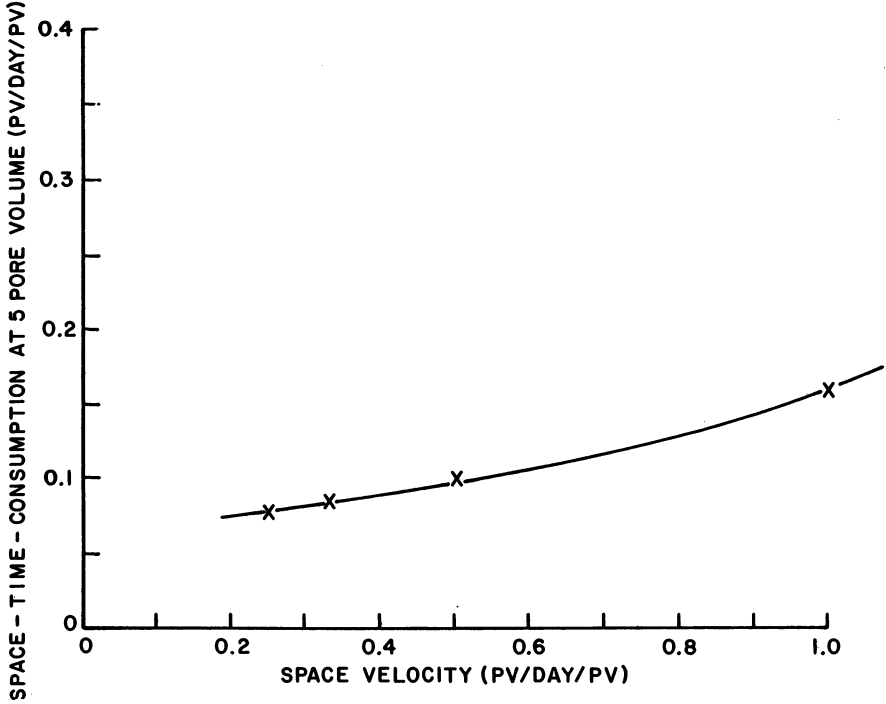


Figure 6. Effect of flow rate on caustic consumption. Plot of space-time-consumption vs. space velocity. Conditions: 0.18% NaOH + 1% NaCl solution through Aminoil LMZ sand packs at 165°F.

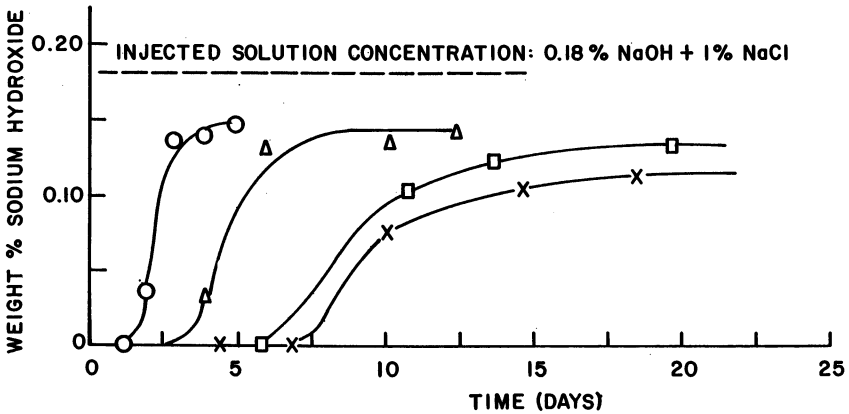


Figure 7. Effect of flow rate on caustic consumption. Plot of % NaOH of effluent vs. time. Conditions: 0.18% NaCl solution through Aminoil LMZ sand packs at 165°F. Key: X, 0.25; □, 0.33; △, 0.50; and ○, 1.0 pore vol/d.

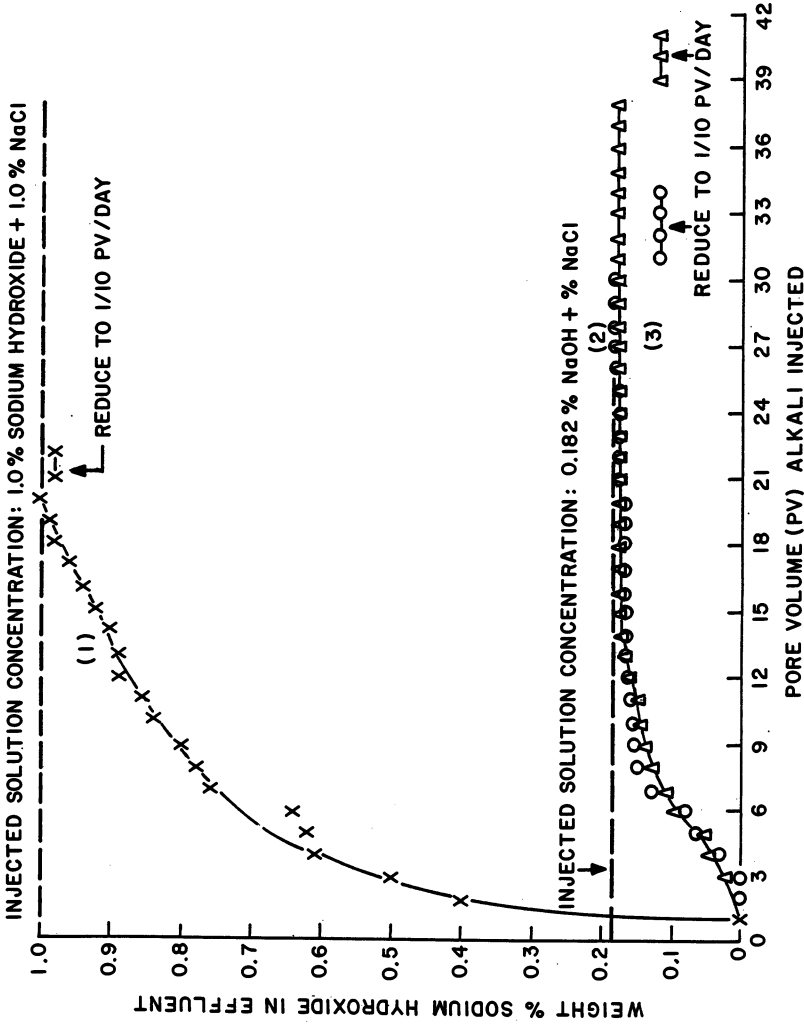


Figure 8(a). Long-term flow test with use of: X, 1.0% NaOH and 1.0% NaCl through THUMS Ranger sand pack; O, 0.182% NaOH and 1.0% NaCl through THUMS Ranger sand pack; and Δ, 0.182% NaOH and 1% NaCl through Aminoil LMZ sand pack.

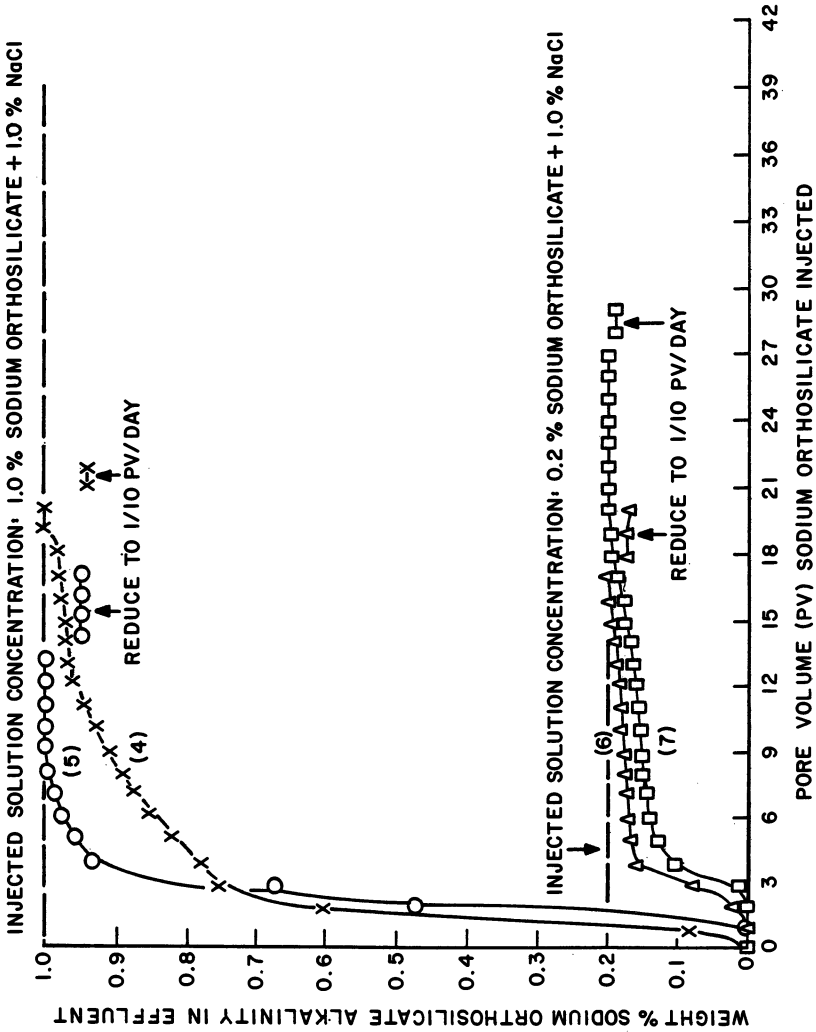


Figure 8(b). Long-term flow test with the use of: x, 1.0% sodium orthosilicate and 1% NaCl through THUMS Ranger sand pack; ○, 1.0% sodium orthosilicate and 1% NaCl through Amin-oil LMZ sand pack; △, 0.2% sodium orthosilicate and 1% NaCl through THUMS Ranger sand pack; and □, 0.2% sodium orthosilicate and 1% NaCl through Aminoil LMZ sand pack.

consumption of the alkaline chemical was still in progress but at a lower rate.

The alkaline consumption for each of the flow experiments can be determined by measurement of the area between the "Injected solution concentration" line and the "% alkaline chemical alkalinity in effluent" curve less the area of the first pore volume. The first pore volume is not included in the calculation to take into account that the sand pack was filled with 1% sodium chloride before alkaline injection.

As shown in Table III, which gives the alkaline consumptions for the seven flow experiments, the alkaline consumption, as expected, increased with increase in concentration of the alkaline chemical solution used. For example, the alkaline consumption for THUMS Ranger sand increased from 2.8 meq/100g sand using 0.2% sodium orthosilicate to 9.2 meq/100g sand using 1.0% sodium orthosilicate.

In comparing sodium hydroxide and sodium orthosilicate solutions of the same concentration, the alkaline consumption for sodium orthosilicate was significantly lower than that for sodium hydroxide. For example, the alkaline consumption of THUMS Ranger sand was 9.2 meq/100g sand for 1.0% sodium orthosilicate while the consumption was 25.1 meq/100g for 1.0% sodium hydroxide. Thus sodium orthosilicate seems to be superior to sodium hydroxide for alkaline flooding.

The same conclusion can be made by comparing the numbers of pore volumes of the two chemicals (of the same or approximately the same concentration) required for the effluent alkalinity concentration to reach the concentration of the injected solution. For example, in THUMS Ranger sand packs, about 30 pore volumes of 0.182% sodium hydroxide were required for the effluent alkalinity to reach the injected concentration, (Figure 8(a) 2), while only 15 pore volumes were required in the case of 0.2% sodium orthosilicate (Figure 8(b) 6).

Campbell (13) measured rock consumption by stirring unconsolidated reservoir sand with 0.5% sodium hydroxide or 0.5% sodium orthosilicate and the alkaline consumptions were found to be about the same for the two solutions. The difference in the conclusions between our study and that of Campbell is not understood and is presently being studied. It seems to be related to the difference in methods used ("Jar" test vs. Flow test), the chemical compositions of the sands, and the chemical compositions of the alkaline solutions in equilibrium with the sands.

TABLE IIIALKALINE CONSUMPTIONS IN LONG TERM FLOW STUDY

<u>Alkaline Chemical</u>	<u>Sand</u>	<u>Alkaline Consumption (meq/100 g)</u>
1.0% NaOH + 1% NaCl	THUMS Ranger	25.1
0.182% NaOH + 1% NaCl	THUMS Ranger	6.8
0.182% NaOH + 1% NaCl	Aminoil LMZ	6.0
1.0% Na ₄ SiO ₄ + 1% NaCl	THUMS Ranger	9.2
1.0% Na ₄ SiO ₄ + 1% NaCl	Aminoil LMZ	6.9
0.2% Na ₄ SiO ₄ + 1% NaCl	THUMS Ranger	2.8
0.2% Na ₄ SiO ₄ + 1% NaCl	Aminoil LMZ	3.8

As can be seen from table III the loss of alkalinity (due to reversible adsorption and chemical consumption) in a sand pack, by comparison, is lower than that shown in Figures 2 and 3 which involves reaction of sand in plastic bottles. This is because the sand in a sand pack is more tightly packed, and thus lower surface area is available for chemical consumption, reversible adsorption or ion exchange. However, this loss of alkalinity can be expected to retard the advance rate of alkaline chemical. As shown in the elution plots in Figures 8(a) and 8(b), in almost all cases, more than one pore volume of alkaline chemical solution was required for alkaline "breakthrough". Similar retardation results were also observed by other workers (4,11,14). Furthermore, as the injection solution concentration is lower, the alkaline chemical takes progressively longer to elute from the sand pack. For both sodium hydroxide and sodium orthosilicate, the alkaline "breakthrough" or 0.2% solution occurred after about 2 to 3 pore volumes of injection. However, the alkaline "breakthrough" or 1.0% solution occurred after only about 1 to 2 pore volumes of injection.

The delay in alkaline "breakthrough" can be explained by the theory of chromatography. According to the theory, the reversible adsorption isotherm slope controls the advance rate

of alkaline chemical through the sand pack. The slope, under ideal conditions, is a constant. Deviation from a straight line to a lower slope indicates the saturation of the active adsorption or ion exchange sites of the reservoir sand and thus there is a reduction of the retardation effect on the advance of alkaline chemical. As can be seen from the reversible adsorption curves for both sodium hydroxide and sodium orthosilicate, the slopes decrease with increase in concentration of the alkaline chemicals in the solutions. Higher concentrations have smaller slopes and hence yield shorter delays in alkaline "breakthrough". Similar interpretation has been made by Bunge and Radke (14).

As shown in Figures 2 and 3, the loss of alkalinity due to reversible adsorption or ion exchange is of the order of 1 meq/100g sand for both sodium hydroxide and sodium orthosilicate. It may be noted in Figures 2 and 3 that in addition to loss of alkalinity due to reversible adsorption, loss of alkalinity due to non-reversible chemical consumption also occurs. In flow studies, the alkalinity of effluents in the initial two or three pore volumes is very low (as shown in Figures 8(a) and 8(b)). For the initial two or three pore volumes, the portion of the sand near the inlet where the pH of the chemical solution is still sufficiently high, chemical consumption is expected to occur and contribute to the delay in alkaline "breakthrough". As the solution advances through the sand pack, the pH of the solution becomes lower. In the portion of the sand pack near the outlet where the pH is low, little or no chemical consumption is expected to occur.

As the pH of the effluent from a sand pack increases, chemical consumption is expected to become more important and becomes the main source of loss of alkalinity.

The long term flow study seems to reveal that at the initial one to three pore volumes there is a chemical consumption which is limited to the front portion of the sand pack where the pH is sufficiently high and a rapid reversible adsorption or ion exchange reaction which retard the advance rate of alkaline chemicals. After the initial one to three pore volumes, this is coupled with a slow non-reversible chemical consumption reaction which will continue for a very long time.

Long Term Pulse Study

It was felt that none of the experiments that had been devised thus far truly approached representing what is happening in the reservoir. The static equilibrium study experiments were

simply not long enough and the sands not appropriately compacted. The long term flow study experiments likewise were of too short a duration, measured in weeks, or months rather than in years; they involved many pore volumes of solution and thus vastly overpowered the sand pack with fresh alkaline chemical. In an actual petroleum reservoir, the time may be a total of several years, the volume used is usually even less than one pore volume, and the alkaline chemical concentration declines with time. To address this, the long term pulse study was undertaken.

Five sand packs were prepared with THUMS Ranger sand. The samples were made from the same disaggregated and extracted sand described above in the Long Term Flow Study. Without any pre-treatment, the sand packs were each saturated with a complete pore volume of an alkaline solution containing either sodium hydroxide or sodium orthosilicate and 1% NaCl. The alkaline solutions were then displaced in opposite direction to that of the initial alkaline injection input with a 1% NaCl solution in twelve small periodic increments over a long period of time. Each displaced increment was analyzed for its alkalinity. The time period between increments was governed by the rate of alkaline consumption.

Although this is not exactly what happens in a reservoir, it may be imagined that the overall results approach being similar to what would be expected if a "slug" of one complete pore volume of such a solution were placed in the pores of a reservoir. Figure 9 is a schematic depicting the long term pulse experiment compared with what is occurring in a reservoir. In the experiment, only one pore volume of alkaline solution is used. It is expected to last at least two months and possibly much longer. The initial increments of effluent collected will have been in contact with the sand pack for relatively short periods of time and should resemble the alkaline solution near the injection well in field conditions. The increments following the initial increments will have been in the sand pack for longer periods of time and would contain much of the chemical reaction products. They might be expected to resemble the solution behind the alkaline slug front under field conditions. In general terms, the pulse study statically measures the time decay of the alkaline concentration in a sand pack in a way that resembles the dynamic time decay in a similar 100% pore volume slug exposed to an actual petroleum reservoir.

The last few increments were not used as some dilution due to mixing of the alkaline solution and the 1% NaCl displacing fluid could have occurred. The extent of dilution is presently

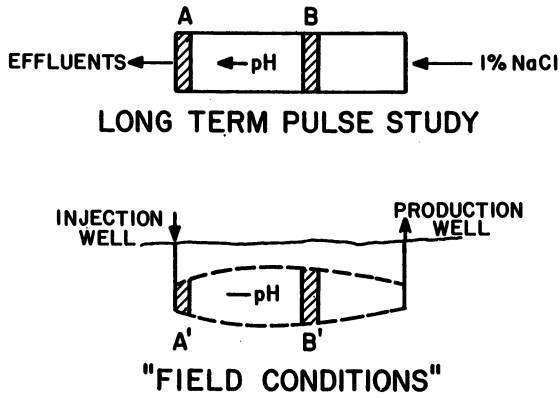


Figure 9. Schematic comparison long-term pulse study and the "field conditions" in a reservoir.

being studied with the use of lithium chloride and sodium thiocyanate. In the study, after the collection of 5 increments out of a total of 12 increments and after 240 days, little or no mixing has been found by analysis of lithium and thiocyanate in each increment of the effluents.

Comparing results obtained from Figure 10, using 1.0% sodium hydroxide and Figure 11, using 1.0% sodium orthosilicate, the elapsed times required for the % NaOH and % sodium orthosilicate alkalinity in the backflow to drop to zero are 115 days and 145 days respectively. Since the last increment of the effluent in the backflow may resemble the solution at the alkaline slug front under field conditions, the 115 days and 145 days could represent the elapsed times required for the alkalinity of the slug fronts to drop to zero. However, as the alkaline slug is being carried forward, the solution behind the slug front retains alkalinity which would be expected to persist beyond these elapsed times, since the later part of the slug will contact sands which have already been partially reacted.

Figure 11 depicts plots of long term pulse study experiments involving the use of different concentrations of sodium orthosilicate. It can be seen that 0.4% sodium orthosilicate survived only about 50 days. However, as the concentration of orthosilicate increased, the elapsed time required for the alkalinity in the backflow to reduce to zero also increased. The experiment with 2.0% sodium orthosilicate is still in progress, and after 240 days it seems the curve has leveled out, which would imply the alkalinity will survive for a much longer time. Although it is still quite uncertain, it is hoped that such a concentration would survive in this kind of reservoir for several years. As a result, for field situations which do take an average of several years between injection well and producing well, enough alkalinity should be present for the desired oil enhancement effect to take place.

For purpose of comparison, 2.0% sodium orthosilicate is equivalent to 5.25 meq/100g sand in a 25% porosity sand pack. Thus, for those operations which take several years to traverse from injector to producer, in this type of reservoir, the 1.5% - 2.0% sodium orthosilicate might be the lower limit for the proper concentration for slug design.

Field results from alkaline waterflooding have thus far been very limited. However, a survey (9) of field trials that reports positive enhanced oil recovery results including Harrisburg Field, Nebraska, North Ward-Estes Field, Texas, and Singleton Field, Nebraska, all involved the use of caustic or sodium orthosilicate at concentrations of 2.0% or higher. The

**American Chemical
Society Library
1155 16th St. N. W.
Washington, D. C. 20036**

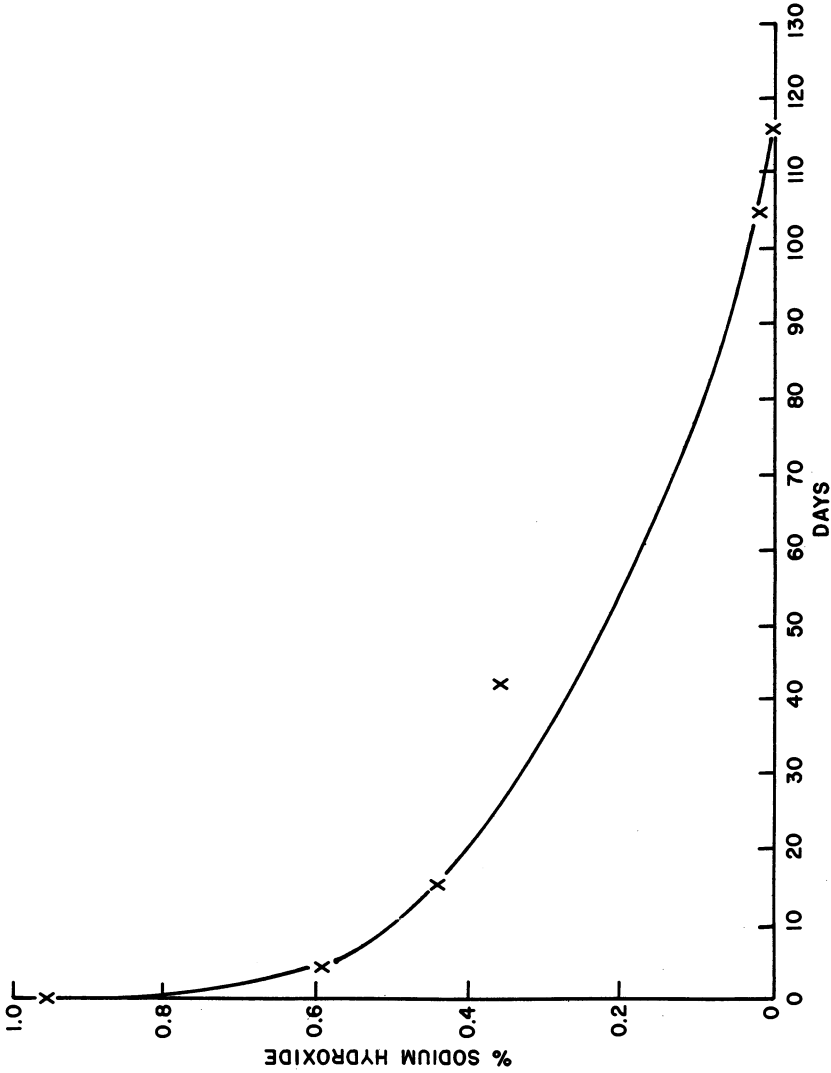


Figure 10. Long-term pulse study. Conditions: 1 pore vol of 1% NaOH and 1% NaCl in THUMS Ranger sand pack being displaced in small increments with 1% NaCl solution at 125°F.

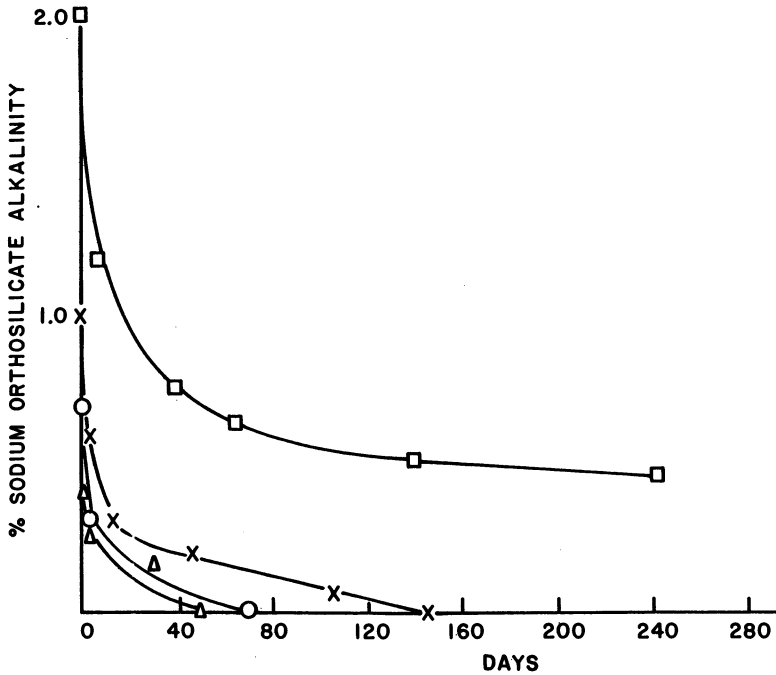


Figure 11. Long-term pulse study. Conditions for pore vol each: Δ , 0.4% sodium orthosilicate + 1% NaCl; \circ , 0.7% sodium orthosilicate + 1% NaCl; \times , 1.0% sodium orthosilicate + 1% NaCl; and \square , 2.0% sodium orthosilicate + 1% NaCl in THUMS Ranger sand packs being displaced in small increments with 1% NaCl solution at 125°F.

notable exception is the Whittier trial in California (7) where, because of the short distance between injector and producer, caustic reached the producing wells within a few months or less, a situation compatible with survival of the 0.2% concentration which was used. The extent to which the long term pulse study is applicable to an actual petroleum reservoir is dependent on more field results, which will be forthcoming in the next several years.

Acknowledgments: Thanks are extended to the Department of Oil Properties of the City of Long Beach and THUMS Long Beach Company for the support of this study, to PQ Corporation for its support to participate in the Soluble Silicates Symposium and to Drs. R.M. Weinbrandt and T.C. Campbell of Aminoil, USA, Inc. for their help in providing material and technical assistance.

Literature Cited

1. Cooke, C.E. Jr.; Williams, R.E.; Kolodzie, P.A. J. Pet. Tech. 1974, 26, 1365-1374.
2. Jennings, H.Y. Jr.; Johnson, C.E. Jr.; MacAnliffe, C.D. J. Pet. Tech. 1974, 26, 1344-1352.
3. Johnson, C.E. Jr. J. Pet. Tech. 1976, 28, 85-92.
4. Ehrlich, R.D.; Wygal, R.J., SPE J. 1977, 17, 263-270.
5. Leach, R.O.; Wagner, O.R.; Wood, H.W.; Harpke, C.F. J. Pet. Tech. 1962, 15, 206-212.
6. Emery, L.W.; Mungan, N.; Nicholson, R.W.; J. Pet. Tech. 1960, 12, 1569-1576.
7. Graue, D.J.; Johnson, C.E. Jr. J. Pet. Tech. 1974, 26, 1353-1358.
8. Carmichael, J.D.; Mayer, E.H.; Alpay, O.A.; Boyle, P.R. 5th DOE Symposium on Enhanced Oil and Gas Recovery and Improved Drilling Methods 1979.
9. Mayer, E.H.; Berg, R.L.; Carmichael, J.D.; Weinbrandt, R.M. SPE 8848, First Joint SPE/DOE Symposium on Enhanced Oil Recovery, 1980, 407-415.
10. Weinbrandt, R.M.; Buck, R.A.; Anderson, G.H. 31st Annual Technical Meeting of the Petroleum Society of CIM, 1980.
11. Somerton, W.H.; Radke, C.J. SPE 8845, First Joint SPE/DOE Symposium on Enhanced Oil Recovery, 1980, 363-378.
12. Holm, L.W.; Robertson, S.D. J. Pet. Tech. 1981, 33, 161-172.
13. Campbell, T.C. SPE 6514, 47th Annual California Regional Meeting of SPE of AIME, 1977.
14. Bunge, A.L.; Radke, C.J. SPE 10288, The 56th Annual Fall Technical Conference of SPE of AIME, 1981.

RECEIVED March 2, 1982.

Dehydrated Sodium Silicate Bound Core Sand for Aluminum Casting

R. F. KIESEL and H. VAN OENE

Ford Motor Company, Engineering and Research Staff, Dearborn, MI 48121

Presented are properties of sodium silicate and dehydrated silicate bound sand which delineate the utility of sodium silicate as a binder for foundry cores. These properties are: worklife of coated sand, variables affecting bound sand strength, storage stability of sand cores, and their high temperature properties. A new method of determining worklife of coated sand is presented. Data is given relating sand strength to processing variables. Moisture absorption rates, which affect storage life of bound sand, are found to depend on relative humidity of the atmosphere and sodium content of the silicate. The strength, storage life and shake-out properties of cores produced by this process differ substantially from those of cores produced by the "CO₂-Silicate" process.

A process has been developed at Ford Motor Company that uses dehydrated sodium silicate as a core binder for aluminum casting. Silicate sand binders are attractive for their environmental qualities, such as the lack of organic emissions and odor, and for other properties beneficial to the casting process (1).

A foundry core is a sacrificial aggregate that produces the interior configuration, or cavity, of a cast metal part. The main component of this core is usually silica sand but other particulate inert materials have been used. Sand is bonded by a core binder, which may be an organic resin composition such as a phenolic, furan, alkyd or isocyanate. Inorganic compositions of phosphates and silicates have also been used as core binders.

A core process encompasses the operations of a casting plant. In this paper some of the specific and unique material and process variables of the dehydrated silicate process are reported. These are:

Sand Coating and Coated Sand Worklife.

Core Production from Coated Sand.

Bound Sand Strength.

Bound Sand Storage Stability.

High Temperature Properties and Collapsibility of Sand from Aluminum Castings.

Other process variables have been considered but will not be reported in this paper.

Sand Coating and Coated Sand Worklife

Sand is coated with aqueous sodium silicate by conventional mulling. In practice, sand has been mixed in batches from 1Kg, laboratory scale, to 600Kg, production scale. There is no restriction as to type of sand muller used. However, if solvent water evaporation is significant the amount of water in the formulation must be increased. This is particularly the case when using "speed" mullers.

Two factors define the worklife of coated sand and determine the usefulness of a coated sand mixture: the ability to flow and be formed into a shape and the ability to be cured into a rigid sand body. For the purposes of this paper, coated sand was judged unsuitable if a cured sand body had a tensile strength lower than 0.7MPa, 100psi. Flow properties of coated sand are less readily defined. Since a suitable test has not been accepted by the foundry industry, the following test was devised to determine the flowability of a sand formulation:

Coated sand, in a glove box, is riddled through a #4 Standard Screen sieve, 4.76mm mesh opening, into a 3cm deep pan. The relative humidity, carbon dioxide content and temperature of the box is measured and controlled. The sand mass is struck off but not tamped down. The bulk density of the resulting sand mass is approximately 0.7 to 0.9 g/cc. At given time intervals steel ball bearings, 1/2 inch O.D. weighing 8.33g, are dropped on the sand from a height of 48 cm. The steel balls penetrate the sand and are not removed until the test is terminated. As the sand gets stiffer, due to environmental conditions or to the binder curing, the depth of penetration decreases. At the conclusion of the test the sand assembly is transferred to a laboratory oven to set the remaining viable sand. The impact depths are determined and normalized to the initial impact depth. This ratio is called the Flow Index and is an indication of the

flow property of the coated sand when an imposed stress is applied. The higher the Flow Index the easier it is to form a sand body by impact ramming, squeezing or blowing.

Flow Indices for the same sand formulation, exposed to four test environments, are shown in Fig. 1. These test environments are characterized only by different relative humidity since the Flow Index for silicate coated sand is not significantly influenced by changes in temperature and anticipated CO₂ levels in ambient air. When the Flow Index of this formulation drops to 0.55, cores blown with 85psi air pressure have the minimum acceptable strength. Sand with a higher Flow Index would produce more dense sand bodies and have higher strength.

The work life of sand coated with aqueous sodium silicate is dependent on the relative humidity of the environment. At 20% RH and 60% RH, the work life is found to be 30 minutes and 90 minutes respectively, Fig. 1. Coated sand that is sealed to prevent water loss or CO₂ absorption, has a work life in excess of three weeks. Even a simple cover retards moisture loss and extends the work life; for example, at 20% RH a cover increases the work life from 30 minutes to over 3 hours.

Core Production from Coated Sand

A common method of producing foundry cores is to fluidize the coated sand and blow it into a core box using air pressure. The strength of bound sand is determined in part by the bulk density of the sand body which in turn is determined by the air pressure used to blow the coated sand. Core blowing tends to dry coated sand prior to forming into a sand body. Consequently, water based silicate coated sand formulations must contain more moisture to allow for this production condition. The amount of added water would depend on the relative humidity of the environment as well as production variables.

In the laboratory bound sand bodies are also prepared by ramming, squeezing and hand tucking. Ramming results in extremely consistent but high bulk densities and consequently high strengths. Although core blowing more closely represents production conditions, most of the strength comparisons made will be with samples prepared by ramming because of the reproducibility of the properties of the test samples prepared by this technique.

Sand properties are determined using standard compression and tensile samples prepared according to the "Foundry Sand Handbook, 7th.Ed."; American Foundrymen's Society Pub., pp8-4

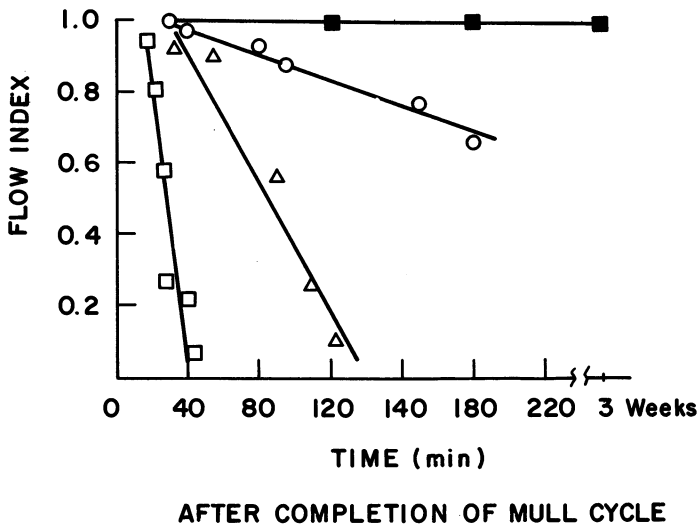


Figure 1. Work life of silicate-coated sand. Key (% relative humidity and 340 ppm CO_2): □, 20%; △, 60%; ○, 90%, loose cover over sand in 20% relative humidity environment; and ■, 97% sealed container.

and 13-1. Blown tensile samples were prepared using a No.372 Hot Box Tensile Curing Machine from Harry W. Dietert Co.

Silicates are already used as sand binders in casting operations. The "CO₂-Silicate Process" makes use of the acid base chemistry of soluble silicates (2). However, sand bodies produced using this gassing technique are weak. It is not the purpose of this paper to discuss the "CO₂-Silicate Process" as this has been presented in the literature (3). The process described here is the physical dehydration of soluble silicate coated sand. Fig. 2 shows the compressive strength of bound sand produced by the CO₂ process and the strengths produced by this dehydration process. Dehydration produces strengths an order of magnitude higher than those reported for the "CO₂-Silicate Process" at the same binder level.

Hot-Box, Core Oven, and Microwave Radiation equipment have been used to dehydrate sand. The differences in these processes are in their rate of core production, the efficiency of energy utilization and the availability of process equipment in the plant. No matter what process is used to dehydrate the sand formulation so long as the entire sand body is heated above 105°C, the bound sand properties, ie. strength, storage life and post-casting sand shake-out remain the same.

With Hot-Box dehydration, one inch thick test samples are dehydrated completely in 50 seconds by contact with hot, >230°C, metal plattens. In this process the sand is heated by conduction so the rate of dehydration varies with the thickness of the sand body. The Hot-Box process is inefficient since there are significant energy losses by radiation from the hot metal patterns; however, Hot-Box equipment is readily available in the casting industry (4).

The advantage of using microwave power is its efficiency. Only the sand and silicate binder are heated (5). The dehydration rate depends on the microwave power used. The power requirement is between 0.044 and 0.15 Kw hr/Kg sand (6). While microwave ovens are available commercially, only few casting plants have microwave facilities (7).

Bound Sand Strength

The strength of a bound sand system is perhaps its most important property. The effect of process variables on strength is shown in Figures 2-5. The term "silicate solid" describes the silicate content of the dehydrated sand specimen. This term applies to that portion of the silicate binder that will not evaporate when heated above 105°C. Thus, the solvent water and

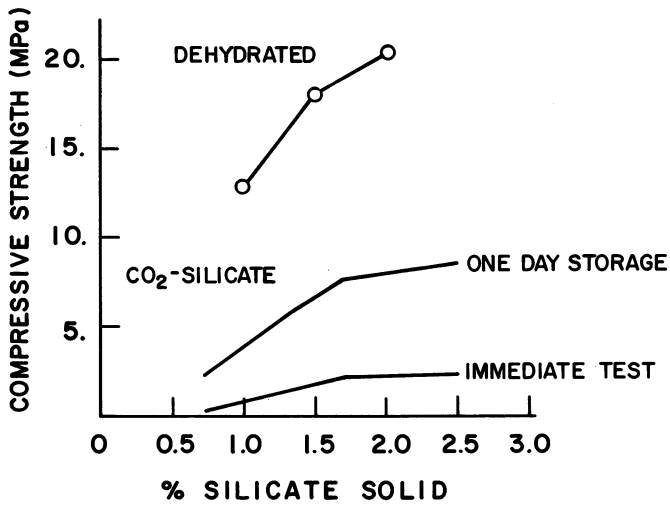


Figure 2. Compression strength of silicate-bound sand. Silicate mol ratio 2.0:1. (CO₂-silicate data from Ref. 3.)

loosely bound water are excluded from the silicate concentration figures.

The term "silicate ratio" is used to describe the mole ratio of silica, SiO_2 , to soda, Na_2O , used to manufacture the silicates. The "bound water ratio," $\text{Na}_2\text{O}:\text{H}_2\text{O}$, depends on the silicate ratio and the dehydration temperature (8). The network structure, hence, the cohesive bond strength, of the cured polysilicate binder, is defined by both the silicate ratio and bound water ratio.

Mold Density and Sand Grain Shape. Each wetted grain to grain junction contributes to the strength of the dehydrated sand body. The greater the number of these junctions and the more binder solid at these junctions, the higher the strength of the bound sand part. As the bulk density of a sand body increases, the number of grain to grain contact points increase.

For any sand used, the higher the air pressure, or ramming pressure, used to form the sand shape the greater will be the bulk density of the resultant sand body. Fig. 3 shows the relationship between tensile strength and blown sand bulk density for two different sand systems. The lowest strength on each curve was obtained using 0.35 MPa, 50 psi, blow pressure. The highest strength was obtained using 0.65 MPa, 95 psi, blow pressure.

High bulk density sand bodies are produced from base sands that have a rounded grain shape and have broad grain size distribution, such as Wedron 5010 sand. The surface tension of the silicate solution will draw the silicate solids into the region of the grain to grain contacts. When dehydrated, the silicate solid efficiently contributes to the strength of the sand body.

Lake sand is typical of that used by large casting plants. The sand grains have a more uniform size and are more angular in shape. Lake sands are not pure silica but also contain other minerals in minor amounts. The silica cleavage planes are sharp. When blown the bulk density of the resulting sand body is not as high as with round grain sand. However, this by itself is not sufficient to account for the lower strengths, since even at equivalent mold densities round grain sand yields stronger sand bodies than does angular sand.

Silicate Solid Content and Viscosity. As the silicate solids content of a bound sand body increases, the strength of the sand body also increases as shown in Fig. 4. The mold densities of all samples were held constant at 1.55-1.58 gm/cc

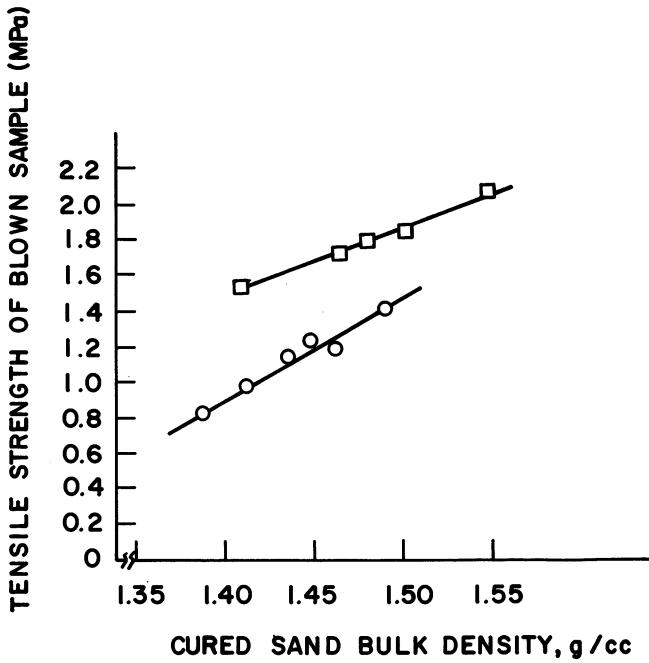


Figure 3. Tensile strength vs. sand type and bulk density. Key: \square , Wedron 5010 silica sand, round grain, AFS 65, four screen, 1.5% 3.0:1 silicate; and \circ , Lake Michigan silica sand, angular to subangular grain, AFS 45, two screen, 1.5% 3.32:1 silicate.

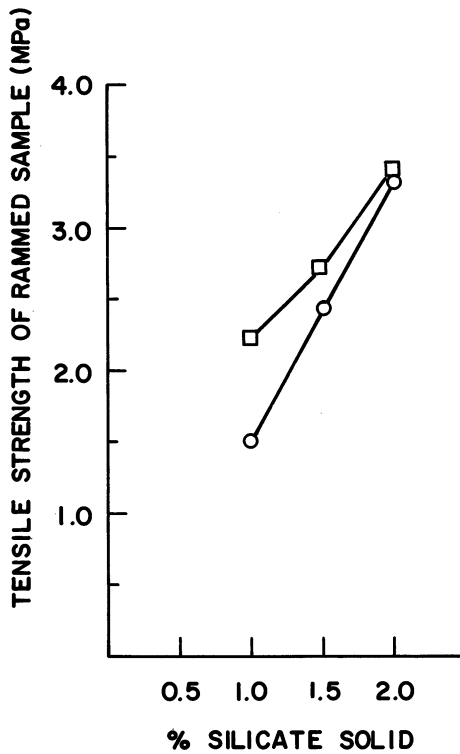


Figure 4. Tensile strength vs. silicate solid content; silicate ratio 3.0:1. Key: □, 39% solid, 61% solvent water; and ○, 43% solid, 57% solvent water.

and the same base sand type was used for both series. However, as is also shown on Fig.4, for a given silicate solid content the strength also depends on the water content of the silicate solution.

This effect may be due to differences in wetting of the sand by the two solutions described on Fig. 4. The greater volume of dilute silicate solution allows for more efficient wetting of the sand as well as buildup of solid silicate at grain to grain junctions and a more efficient bond is formed. The viscosity of the silicate solution provides an alternate explanation for this phenomenon. The viscosity of soluble silicates increases sharply in the concentration range used in this investigation (9). Solution viscosity would determine how much silicate would be drawn into the grain to grain junction points.

As the silicate solid content is increased in the coated sand, the strength of each junction point attains its maximum value. In these higher silicate solids cases, the viscosity of the silicate solution is not a determining factor and additional water has no effect on the strength of the bound sand samples. For each sand studied, and each silicate ratio investigated, there is a specific water content of the silicate solution that gives optimum strength properties.

Silicate Ratio. Tensile strength varies with the silicate mole ratio as shown in Fig. 5. The silicate solid concentration, the bulk density and the base sand are kept constant in these samples. The tensile strength is shown at the optimum water level for each silicate ratio. However, the 3.86:1 material was not investigated fully. The strongest sand bodies were found with silicate mole ratios approximately 3.0:1.

Bound Sand Storage Stability

Existing casting plant practice is to prepare sand cores ahead of demand and then store them for later use. The question arises, how long will dehydrated silicate bound sand remain strong in a casting plant environment?

Test samples from different sand formulations were exposed to sets of environmental conditions and the resultant reduction in strength was determined as a function of exposure (10)(11). Tensile strengths were determined using an Instron Mechanical Tester with a model "F" load cell. Because of the many variables involved in strength properties, the strengths of the various bound sand systems are normalized to the pre-exposure strengths. The fraction of initial strength that remains after exposure is plotted as a function of the duration of exposure.

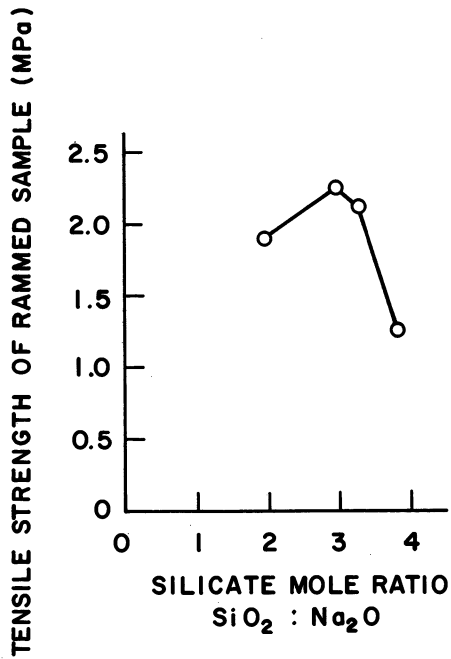


Figure 5. Tensile strength vs. silicate mol ratio; 1% silicate solids, Wedron 5010 sand, 1.56–1.58 g/cm³ bulk density.

A family of curves is shown in Fig. 6 that have the same shape. These curves are characterized by an induction period with little or no change in properties, followed by an abrupt and catastrophic loss in strength. The loss of strength did not depend on the initial strength of the test samples but only on the relative humidity and the sodium content of the silicate solid.

This water absorption is caused by hydration of the sodium cation (12). Fig. 7 shows the moisture absorbed by a silicate formulation when exposed to different relative humidities. In this case the silicate ratio is 3.32:1. The slopes of the curves on Fig.7 correspond to the rate of moisture absorption from humid atmospheres. It is important to notice that the absorption is linear with time, at least until the H_2O/Na ratio equals one.

The initial moisture absorption rates from Fig. 7 and the corresponding water vapor pressures are plotted on Fig. 8. An exponential relationship is found between the initial rate and the vapor pressure of water in the storage atmosphere. Two curves are shown for silicates that differ in their relative sodium content: 2.0:1 ratio silicate has a high sodium concentration and 3.32:1 ratio silicate is low sodium material. The slopes of these rate curves are approximately the same indicating the same physical process is occurring. This sodium dependent process is interpreted as the chemisorption of water by sodium in the sodium silicate.

Water absorption by different silicate formulations is shown in Fig. 9. In these cases the relative humidity was kept constant at 97%. The difference in these formulations is the relative concentration of sodium in the silicate solid. As in Fig. 7, the initial absorption rates are linear with time. As shown in Figure 10, this initial rate is linear with the atom fraction of sodium in the dehydrated silicate formulation. The atom fraction is calculated from the silica to soda ratio.

Water absorption rates were investigated because of a relationship expected in the storage life of bound sand. Instead of plotting the exposure conditions, ie times and humidity levels, as shown in Figure 6, the normalized strength of a sand sample is plotted according to its H_2O/Na ratio, Figure 11. All the retained strength data for exposure conditions are presented on this single curve.

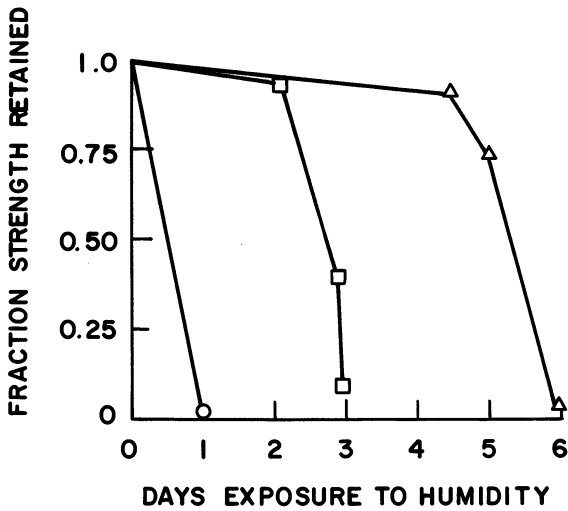


Figure 6. Strength retained after humid exposure. Key: ○, 97%; □, 75%; and △, 53% relative humidity.

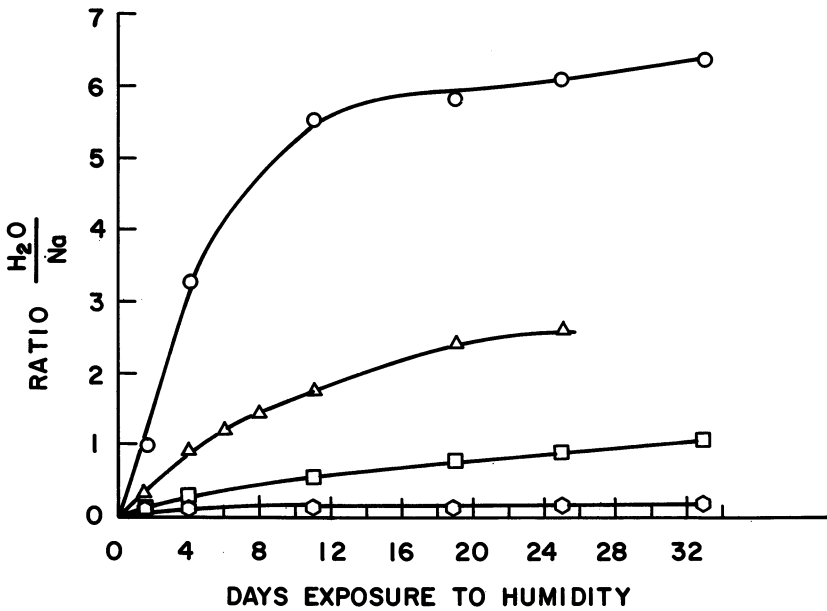


Figure 7. Moisture absorbed by silicates at various humidities. Key: ○, 97%; △, 75%; □, 53%; and ⊙, 33% relative humidity.

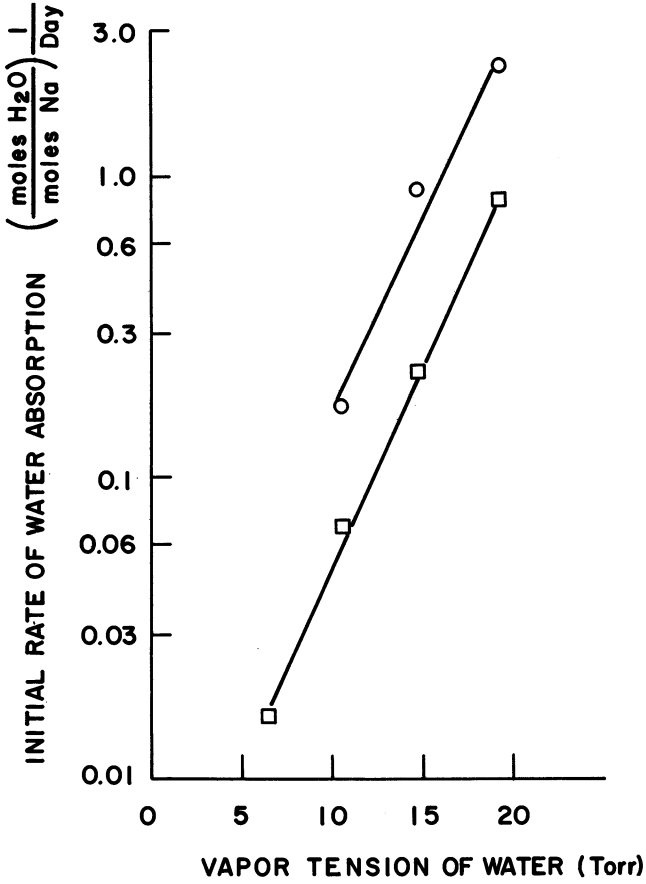


Figure 8. Dependence of the initial rate of water absorption on the vapor pressure of water. Key: \circ , 2.0:1; and \square , 3.32:1 silicate ratio.

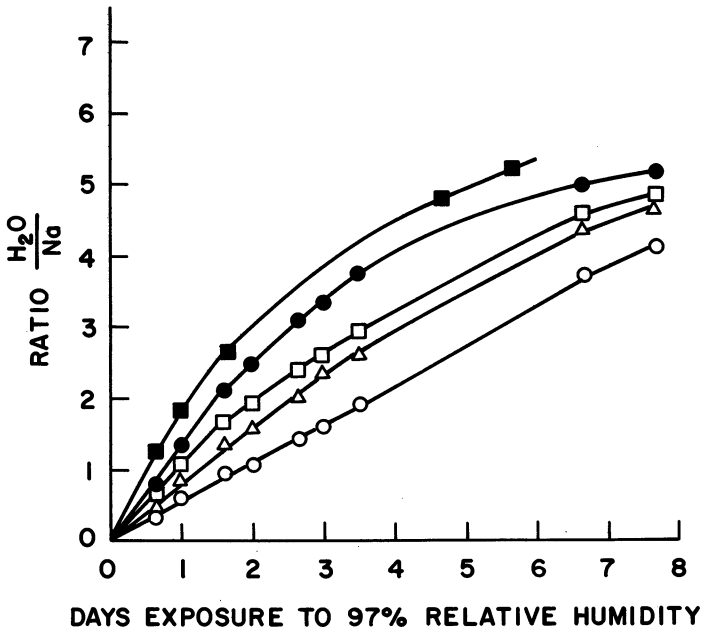


Figure 9. Moisture absorbed by various silicates at constant 97% relative humidity. Key for silicate ratios: ■, 2.0:1; ●, 2.38:1; □, 3.00:1; △, 3.32:1; and ○, 3.86:1.

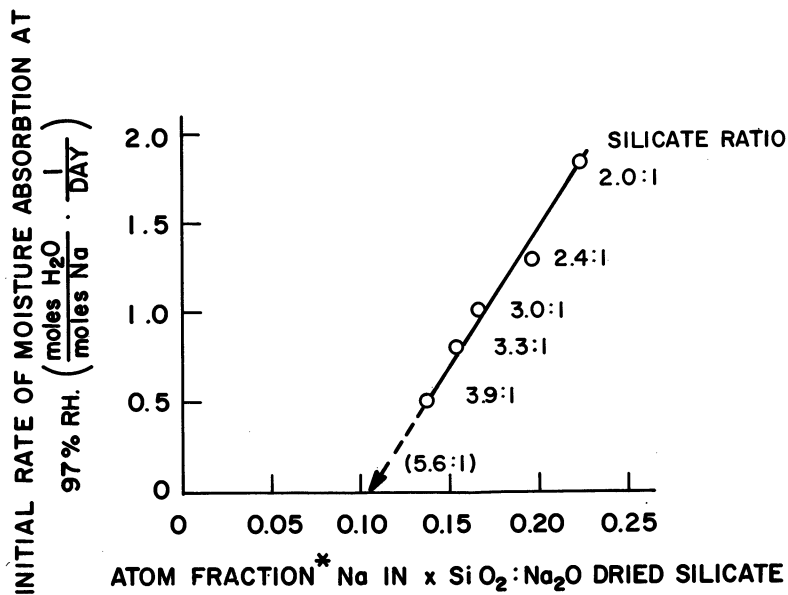


Figure 10. Dependence of the rate of water absorption on the sodium content of the silicate. Atom fraction $\text{Na} = 2 \cdot (3x + 3)$.

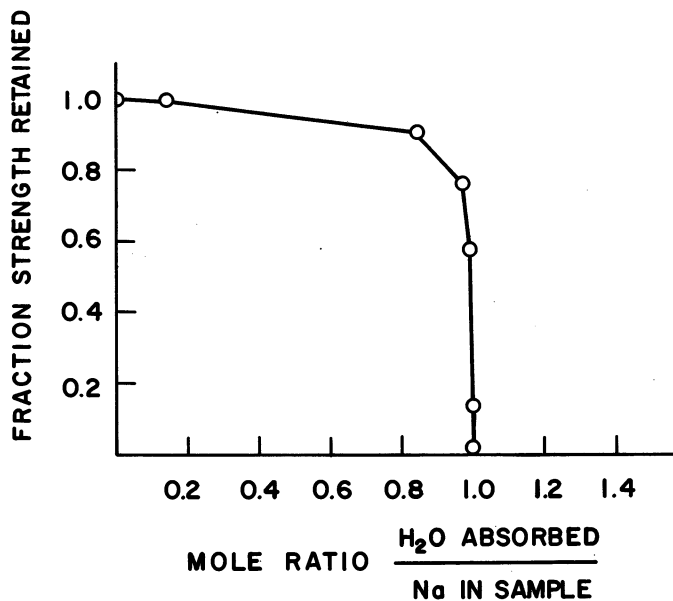


Figure 11. Retained strength vs. water absorbed per sodium.

The induction period observed in Fig. 6 applies to the time necessary to absorb moisture to give H_2O/Na levels of approximately 0.8. Very little strength is lost by this initial water uptake. Low or even moderate amounts of moisture can be absorbed without extreme effects on the retained strength. When the H_2O/Na ratio approaches unity, there is catastrophic strength failure.

Moisture absorption is reversible. If a sand body has absorbed water so that its strength is beginning to be lost, the system may be dehydrated again and regain its entire strength. The rate of moisture absorption is not the same as the rate of strength loss, implying that the two processes are different.

The first step in the strength loss process is the hydration of sodium. Little strength is lost in this step since the polysilicic acid network is not destroyed. Absorption of another water molecule by sodium causes strength failures through cleavage of the silicate network, probably catalyzed by hydroxide ion. When even small numbers of silicate bonds are broken, the polysilicate network is destroyed and the strength of the bound sand system is lost.

High Temperature Properties and Collapsibility of Sand from Aluminum Castings

The next step in the casting process is the pouring of molten aluminum at $700^{\circ}C$ in a mold containing dehydrated silicate cores. A "4-On" mold was designed to hold four standard briquet tensile samples. The wall thickness of metal in the completed castings from this mold are 1/8, 1/4, 3/8, and 1/2 inch respectively. When aluminum is cast into this mold containing dehydrated silicate bound cores no volatile hydrocarbon products are formed. Consequently, there are no gassing defects in the casting, and no smoke or fumes in the workplace. The need for environmental control equipment is reduced.

The strength of dehydrated silicate test samples decreases slightly as the temperature is raised from ambient to $450^{\circ}C$. A silicate formulation which has 4.68 MPa, 680psi, compressive strength at ambient temperature, was found to have 3.7 MPa after 19 minutes at $450^{\circ}C$. However, exposure to higher temperatures causes drastic strength reduction; for example, after 19 minutes at $500^{\circ}C$ the compressive strength is 1.75 MPa and only 7 minutes at $600^{\circ}C$ reduces the strength to 0.44 MPa, 60psi. At molten aluminum temperature the bound sand samples have 0.1 MPa compressive strength. The strength retained by bound sand after heating and cooling to ambient temperature shows the same

phenomenon. Both of these high temperature properties depend on the length of time the sand mass is exposed to the temperature in question.

The final step in a core process is the destruction of the core within a solidified casting and the removal of used core sand. The time necessary to remove used core sand is called the shake-out time. The technique used for de-coring aluminum castings is to hit them with an impact hammer (13).

To investigate formulation and process variables, the amount of core sand shaken out of a casting is monitored as a function of impact hammer exposure. Fig. 12 shows shake-out data for one silicate solid concentration and one cast metal to core sand weight ratio. The most obvious effect is that the more angular "lake" sand shakes out of castings faster than round grain sand. This was found true for all silicate ratios and silicate binder contents investigated. Low ratio silicates, i.e. those with higher sodium concentration, are removed from aluminum castings faster than high ratio silicates. This was found true for all binder levels tested.

Summary

The properties of sodium silicate, silicate coated sand, and of dehydrated silicate bound sand bodies have been examined in terms relevant to a foundry core process. The material and process variables of particular significance to manufacturing conditions are as follows:

. Silicate coated sand has been prepared using existing equipment in the casting plant.

. Silicate coated sand has a work life that depends directly on the relative humidity of the atmosphere. A cover over the coated sand storage container can be used to extend the worklife by retarding moisture evaporation.

. Cores can be manufactured in existing core blowing equipment. Water can be added to the coated sand/silicate formulation to avoid premature solvent water evaporation and consequent loss of properties.

. Optimum strength, 1.4 MPa, was found with 3.0:1 ratio silicate at 1.5% binder solids level, using lake sand.

. The storage life of cores depends inversely on the logarithm of the water vapor pressure in the atmosphere and inversely on the sodium atom fraction in the silicate.

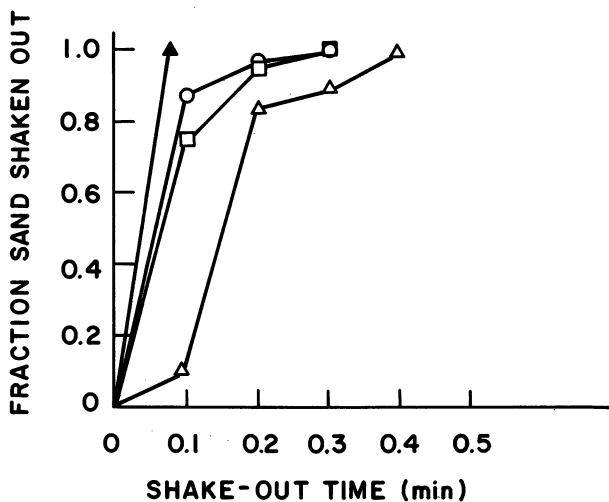


Figure 12. Shake-out time vs. fraction sand removed. Key for 1.5% silicate solids: (using Wedron 5010 sand) Δ , 3.32:1; \square , 3.00:1; \circ , 2.00:1; and (using Lake Michigan sharp sand) \blacktriangle , 3.32:1 silicate ratio.

. Aluminum is cast onto dehydrated silicate cores with no hydrocarbon emissions.

. Core sand can be removed from cooled castings in 0.1 to 0.2 minutes using impact hammer techniques.

Acknowledgments

The authors are grateful to G.S. Cole for comments concerning the post casting shake-out tests and to D. Gohl for performing the casting trials.

Literature Cited

- 1) Kiesel, R.F., and H. van Oene, Org. Coat. and Plas. Chem. **39** (1978) 276.
- 2) Nicholas, K.E.L., "The CO₂-Silicate Process in Foundries"; British Cast Iron Research Association, Alvechurch, Birmingham, England, 1972.
- 3) For example see Rusin, K. and J. Cihlar, AFS International Cast Metals Journal, June 1981, p56. and references cited.
- 4) Wallace, R.B., in "Proceedings of AFS-CMI Energy Management Conference"; Rosemont, Ill. Sept. 20, 1978.
- 5) Cole, G.S., R.M. Nowicki, and Y.A. Owusu, Am. Foundrymens Soc. Trans., **83** 605 (1979).
- 6) Schroeder, R.F., and W.S. Hackett, Am. Foundrymens Soc. Tran. **77** 141 (1969).
- 7) Crowley, T., and J. Apelbaum, Electronic Progress **18** #1, Raytheon Company, (1976) p13.
- 8) Dent Glasser, L.S., and C.K. Lee, J. Appl. Chem. Biotechnol. **21** 127 (1971).
- 9) Vail, J.G., "Soluble Silicates-Vol.1" Reinhold 1952, 81-90.
- 10) ASTM E 104-51 (1971).
- 11) Young, J.F., J. Appl. Chem. **17** (1967) 241.
- 12) Horikawa, N.R., K.R. Lange, and W.L. Schleyer, Adhesives Age July 1967 p30.
- 13) Cole, G.S., and R.M. Nowicki, Am. Foundrymens Soc. Trans. **87** (1979) paper 79-84.

RECEIVED March 2, 1982.

Silicates in Detergents

RONALD S. SCHREIBER

Colgate-Palmolive Company, Piscataway, NJ 08854

The role of silicates in detergents in recent years has been altered by both the commercial introduction of "new" raw materials - some with deficiencies that silicates can overcome - and the increased cost of energy which is changing cost-benefit decisions and the ways in which detergents are used and made. A great deal of the recent work is devoted to overcoming specific problems with combinations of these new materials.

Soluble silicates have been widely used in laundry detergents for many years. A comprehensive review of their properties and their utility as detergent ingredients up to 1952 can be found in the last ACS Monograph on soluble silicates (1).

A recent paper by Schweiker (2) lists nine functions for sodium silicates in detergents:

1. Alkalinity and Buffering ...
2. Emulsification ...
3. Neutralization or Saponification ...
4. Deflocculation ...
5. Soil Suspension ...
6. Corrosion Inhibition ...
7. Hard Water Control Aid ...
8. Surface Active Agent ...
9. Processing Aid ...

The first eight functions are important during the cleaning process, while the last pinpoints the importance of silicates in manufacturing the final product - something which is often ignored, except in the patent literature.

Although these functions were recognized in the earlier literature, their relative importance has been affected by several recent developments. These include legislative restrictions on the amount or presence of phosphates in detergents and the use of alternate organic and inorganic builders as a consequence.

The increased use of surfactants with unique properties and the higher cost of energy, which affect household washing temperatures as well as the cost of manufacturing detergents by spray drying, have also had their impact. Other fairly recent developments - widespread introduction of new dispensing forms such as liquid detergents (often with low pH) and very concentrated detergents - have also affected the use of silicates.

It must be stressed that modern detergents are complex mixtures of ingredients optimized to give beneficial cleaning activity at low cost, while minimizing objectionable features of the individual components. As an example of these interactions, a review paper by Lange (3) discusses the synergistic benefits to detergency and surface tension when silicates and phosphates are used together. They lower an anionic surfactant's critical micelle concentration and the silicates slow the reversion of sodium tripolyphosphate. He also describes the use of silicates in an illustrative detergent manufacturing process without spray drying and comments on the effect of soluble sodium silicates with different $\text{Na}_2\text{O}/\text{SiO}_2$ ratios in helping prevent separation of a nonionic surfactant from solid detergent particles. The final portion of his paper discusses some aspects of corrosion prevention, the use of silicates in dishwashing products, and the formation of silica insolubles, an undesirable side reaction.

In a similar vein, Warren (4) illustrates the often complex interactions between detergent ingredients, temperature, soil, etc., which must be considered for satisfactory cleaning. He specifically examines the effect of various detergent formulations (and silicates) on soil removal and the prevention of soil redepositon in the presence of carboxymethylcellulose (5), a widely used anti-redeposition agent.

Recently zeolites have found commercial application as builders. The effect of sodium silicate in conjunction with zeolites on water hardness and laboratory detergency performance is discussed by Campbell, et al. (6). They investigated both Ca and Mg ion concentrations (water hardness) as well as laboratory detergency using sodium silicate, Zeolite NaA and Zeolite NaX and combinations of these materials as builders. From their experiments, they concluded that the use of Zeolite NaA together with sodium silicate was more effective than either material by itself. Perhaps even more interesting was the effectiveness of the sodium silicate in lowering Mg ion concentration in the wash water which they found to be even better than Zeolite NaX or NaY.

Several other recent papers on the effect of soluble silicates and other salts with specific surfactants have been published. One by Ashimov and Mursalova (7) discusses dialkylbenzenesulfonates in Launder-Ometer tests and another by Degterev (8) used nonionic surfactants to remove mineral oil from steel surfaces. Both report that soluble silicates improved detergency.

Liquid detergents face the problem of high demands on storage stability (avoidance of precipitate formation, liquid phase separation and stability to extremes of temperature). In some initial formulations attempts, there were problems with silicate-phosphate interactions which were overcome, to some extent, by a better understanding of their solubility relationships. The partial substitution of potassium for sodium, the use of different phosphates (pyro- versus tripoly-) and a higher $\text{SiO}_2/\text{M}_2\text{O}$ ratio were beneficial in these formulations. (9) The partial use of glassy sodium hexametaphosphate (10) changed the stability areas of the system. Under these conditions, it was found that the most economic stable concentrate was a 50-50 mixture of sodium tripolyphosphate and sodium hexametaphosphate with sodium silicate.

Other problems in the use of silicates in liquid detergents are the separation of formulations with high levels of surfactant into two phases and the difficulty of including polymeric anti-redeposition agents. These problems can often be solved, as in the previous examples, by the application of classical chemical techniques and principles, or by the use of hydrotropes. The demand for no-phosphate detergents led to an investigation of alternate approaches to heavy duty liquid detergents by Campbell (11). Under his test conditions, he showed good cost-effectiveness for a liquid detergent with silicates, but without citrate as a builder.

The effect of a sodium silicate on both the cloud point of a solution of a nonionic surfactant (stability of the liquid) and on its ability to solubilize heptane (cleaning property) is discussed in an article by Saito and Shinoda (12). This again illustrates that silicates in a final detergent formula have complex interactions which must be considered in view of the desired properties of the overall formulation.

Corrosion control is one of the demonstrated uses of silicates in detergents since builders may be imagined as breaking the structural integrity (and increasing the rate of corrosion) of the hydrous oxide films that protect metals such as aluminum in contact with water. Other metals (e.g. zinc) and combinations of materials are sometimes attacked by alkaline detergents.

For aluminum it is usually thought that an inhibitor film is formed with silica (13, 14, 15). The problem is complicated when variables such as pH, temperature, concentration, the presence of other salts and oxidizing agents (16) are considered.

The data on corrosion is voluminous. A few other particularly pertinent references are: Lindqvist and Magnusson (17) indicate that there is an optimum NaOH to SiO_2 ratio for minimizing scale formation while still retaining good corrosion protection for dairy cans and pipelines; Wildbrett et al. (18) discuss corrosion of aluminum by alkaline sprays; Savchenko

et al. (19) measured the weight loss for various metals and alloys in aqueous test solutions of Na_2CO_3 or Na_2SiO_3 ; and several papers discuss attack on glass and pigments (20, 21, 22). The overall conclusion to be drawn is that in alkaline detergents, even during processing in the plant (3), silicates help control corrosion.

Silicates are often used to protect bleaches such as isocyanuric acid (3) from unwanted reactions. Bleaches are widely used in European detergents and domestic laundry aids. One patent (23) claims that sodium percarbonate particles sprayed with a silicic acid sol have a longer shelf life than untreated particles in detergents. It appears likely that some protective action is due to silicate - heavy metal interactions.

Particularly with other components, silicates have been reported to minimize surface deposits on cloth. For example, Nigrin and Tenglerova (24) report that sodium metasilicate added to a detergent not only increased its washing ability for cotton, but also decreased formation of deposits on the fabric, although by itself the metasilicate caused deposits.

The patent literature discloses techniques designed to overcome problems with silicates such as the formation of insolubles, particularly with the absorption of water and CO_2 with time. One recent patent (25) claims that specific silicates can be modified by reaction with a water soluble salt of Al, Ti, Zn, Zr, Sn, V, Mo, W, Se, or Ge and an organic carboxylate; the resulting silicate when used in a detergent is less liable to cake or form insolubles and has processing advantages. Two other recent patents claim that undesired gellation reactions in crutcher slurries of sodium carbonate, sodium bicarbonate and sodium silicate can be prevented by small amounts of citric acid or water soluble citrates (26); or citrates and magnesium sulfate (or alternatively, magnesium citrate) (27).

The literature has many other examples of techniques that are designed to help overcome the problems inherent in silicates, or to enhance their unique properties in manufacturing detergents. For example, Weldes and Vessey (28) describe a process for overspraying a powder of sodium silicate and a builder (as a core) with a detergent slurry (low silicate) to give a final product in which insolubles don't materially increase with time. A patent (29) claims a non-spray dry process (heated screw conveyer) for making a free flowing, non-agglomerating, soluble silicate. In another process (30), detergent granules are sprayed with a combination of sodium silicate, sulfate, or hydroxide and Al or Mg sulfate to reduce caking in storage.

Weldes, et al. (31) describe a process for "blending composites of hydrated alkali metal silicate glass and sequestering agents" with the other components which have been spray dried. This gives a product with decreased insolubles and increased

production rates. Another patent claims that a storage stable, non-phosphate detergent can be made by mixing porous sodium silicate granules holding a nonionic surfactant with spray dried beads containing an anionic surfactant (32).

Many other patents on the production of detergents by agglomeration, granulation or two step processes have issued. Several advantages are often claimed for such processes such as control of particle size, better properties for the finished material, economy, etc. In most of these processes, the silicates play an important role due to their ability to act as a structure former-binder as well as for their effect on detergency.

New demands are being placed on silicates since the use of phosphates is often restricted. Their shortcomings are being examined with a desire to overcome them; and their utility in new detergent manufacturing processes is being investigated even more assiduously both because of problems with the "new" raw materials that are being introduced and because of increased energy costs.

Literature Cited

1. Vail, J. "Soluble Silicates" Vol. I and II; ACS Monograph 116, Reinhold: New York, NY, 1952.
2. Schweiker, G. C. J. Am. Oil Chemists' Soc., 1978, 55, 36.
3. Lange, K. R. J. Am. Oil Chemists' Soc., 1968, 45, 487.
4. Warren, A. Soap Chem. Specialties, 1963, 39, 50.
5. Davidsohn, A.; Milwidsky, B. M. "Synthetic Detergents"; 5th ed.; CRC Press: Cleveland, OH, 1972.
6. Campbell, T. C.; Falcone, J. S.; Schweiker, G. C. Soap/Cosmetics/Chemical Specialties, 1978, 54(3), 33.
7. Ashimov, M. A.; Mursalova, M. A. Dokl. Akad. Nauk Azerb. SSR, 1967, 23, 23.
8. Degtarev, G. P. Maslo-Zhir. Prom., 1973, 28.
9. Getty, R.; Stericker, W. Soap Chem. Specialties, 1960, 36, 45.
10. Getty, R.; Stericker, W. Soap Chem. Specialties, 1961, 37, 45.
11. Campbell, T. C. Soap/Cosmetics/Chemical Specialties, 1976, 52(1), 31.
12. Saito, H.; Shinoda, K. J. Colloid Int. Sci., 1967, 24, 10.
13. McCune, H. W. J. Electrochem. Soc., 1959, 106, 63.
14. Getty, R.; McCready, N. W.; Stericker, W. ASTM Bulletin, 1955, 205, 3.
15. Stüpel, H.; Koch, F. Seifen-Ole-Fette-Wachse, 1959, 85, 311.
16. Daufin, G.; Kerherve, L.; Labbe, J. P.; Pagetti, J., Mater. Tech. (Paris), 1978, 66, 379.
17. Lindqvist, B.; Magnusson, F. Proc. 6th Int. Dairy Congr. 1966, 5, 493.

18. Wildbrett, G.; von Grundherr, K.; Kiermeier, F. Werkst. Korros., 1967, 18, 217.
19. Savchenko, V. I.; Ochkovskii, N. A. Mekhaniz. i Elektrifik. Sots. S.-kh., 1978, 48.
20. Hellsten, M. Tenside Deterg. 1972, 9, 1978.
21. Joubert, D.; Van Daele, H. Seifen-Oele-Fette-Wachse, 1971, 97, 273.
22. Joubert, D.; Van Daele, H. Rev. Fr. Corps Gras 1971, 18, 211.
23. Jayawant, M. D.; Yates, P. C. Ger. Offen, 2,448,453 (1975).
24. Nigrin, M.; Tenglerova, E. Prumysl Potravin 1965, 16, 456.
25. Llenado, R. A.; U.S. Patent 4,157,978 (1979).
26. Schreiber, R. S. U.S. Patent 4,298,493 (1981).
27. Kaeser, J. A. U.S. Patent 4,294,718 (1981).
28. Weldes, H. H.; Vessey, E. W. U.S. Patent 3,783,008 (1974).
29. Henkel & Cie. G. m.b.H. Belgian Patent 612,494 (1962).
30. Toyada, S.; Takenouchi, K.; Ohno, N.; Hara, N. Ger. Offen. 2,443,073 (1975).
31. Weldes, H. H.; Schleyer, W. L.; Vessey, E. W. U.S. Patent 3,753,930 (1973).
32. Bonaparte, L. R.; Golliday, J. B.; Zeller, H. J. U.S. Patent 3,920,586 (1975).

RECEIVED March 22, 1982.

Durable Glass by Reconstitution of Hydratable Sodium Silicate Glasses

R. BARTHOLOMEW, W. HAYNES, and R. SHOUP

Corning Glass Works, Sullivan Science Center, Corning, NY 14831

Sodium silicate glasses containing from 15 to 21 wt. % Na_2O were hydrated in an autoclave at about 140°C to contain up to 40 wt. % water. These hydrosilicates were then dealkalinized in salt solutions ($< 100^\circ\text{C}$) to as little as 100 ppm residual alkali. Kinetics of dealkalinization depended on alkali content and extent of hydration of the glass. The pore structure of the dealkalinized body was dependent on salt concentration, temperature and pH of the leach bath. It, also, depended on alkali and water content of the hydrosilicate regardless of its origin, hydrated glass or dehydrated sodium silicate solution. Consolidation of 1 to 4mm thick porous bodies to coherent transparent glass was accomplished above about 1200°C . Uniformity of pore structure affected transparency.

The role of water in glass has been studied extensively in recent years. It has been concluded from both infrared^(1,2,3,4) and NMR⁽⁵⁾ data that in addition to hydroxyl groups, molecular water exists in glasses of high water content (> 1 wt. % H_2O). Conventionally melted commercial glasses contain usually less than 0.1 wt. % water, present as hydroxyl groups. Certain borate and phosphate compositions have reported water contents approaching one weight percent. To synthesize glasses with water contents greater than a few tenths of a percent high pressures and temperatures, attainable in an autoclave, are required^(6,7,8). Such glasses, containing mostly molecular water, are called hydrosilicates. Work on hydrosilicates has led to the finding that glasses based on silica either, (1) take up a fixed water content, giving stable transparent glasses, (2) pick up water continuously and finally form gels, or (3) take up water to a certain concentration where they crystallize to form hydroceramics.⁽⁹⁾

Anhydrous sodium silicate glasses which are composed of between 12 and 21 wt. % Na_2O are difficult to form into useful, durable glass objects because of their rapid phase separation or crystallization. However, they hydrate easily in an autoclave to contain up to 40 weight percent water. These sodium hydrosilicates are thermoplastic in behavior, but more importantly the molecular water provides a means for dealkalinizing the silicate structure.

The objective of this paper is to describe a process which was found to be capable of reconstituting a poorly durable anhydrous alkali glass into a durable high silica glass with the aid of molecular water. Except for dimensional shrinkage, the structure retained its integrity and shape during the various stages. These include hydration (or dehydration of silicate solution), dealkalinization in salt solutions, drying and firing to consolidate at temperatures greater than about 1200°C (Figure 1).

Experimental

Sample Preparation. Two methods were used to produce sodium silicate glass samples for this study. The primary method used conventional glass melting techniques to produce compositions ranging from 12 to 21 wt. % Na_2O . Batch ingredients, African sand, sodium carbonate, and sodium nitrate, were melted at 1600°C for six hours in platinum crucibles, poured into patties and fine ground into 1 1/2" diameter discs with thickness of one to four millimeters. These anhydrous discs were fully hydrated in a one cubic foot autoclave under saturated steam conditions and stored in controlled relative humidity desiccators at room temperature.

The second method for sample production consisted of pouring S-35, a Philadelphia Quartz sodium silicate solution, into polyethylene molds (1 1/2" diameter) to a depth approximating one millimeter and storing in controlled relative humidity desiccators at room temperature. Dehydration of the S-35 solution produced solid glass samples. Thicker S-35 hydrosilicate was produced by dehydration in an autoclave to avoid wrinkled surfaces.

Various sample water contents were achieved by specific humidity environments produced by using saturated salt solutions. Relative humidities from 30 to 75% produced water content ranges from 22 to 35 wt. %. A time period approximating a week was needed to reach equilibrium sample weights. Water contents were measured by loss-on-ignition techniques. Lack of an anhydrous core confirmed complete sample hydration.

Dealkalinization. The rate of dealkalinization and calculated diffusion coefficients were determined by monitoring the release of Na^+ ions from the hydrated samples into the ammonium nitrate leach solution. All dealkalinization was accomplished in a closed system measured by calibrated pH, reference, and Na^+ ion electrodes.

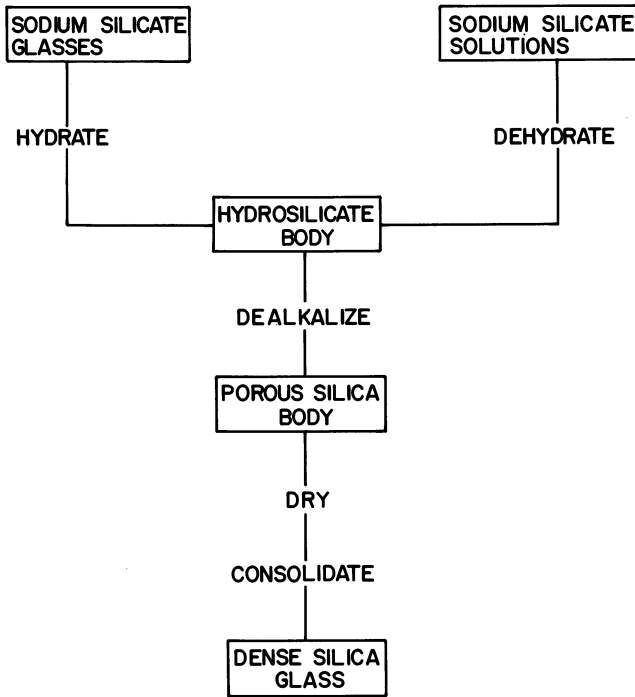


Figure 1. Reconstitution process.

The millivolt output from the Na^+ ion electrode was monitored by a pH meter and recorder. The temperature of the leach solution was kept constant through the use of a circulating water bath.

This investigation was mainly concerned with the influence of water content on the rate of dealkalization at 50°C and a pH of 8. Further experimentation centered around dealkalization variables such as temperature, pH, leach solution concentration and time. This was accomplished by using a Metrohm End Point/pH Stat Titrator. The predetermined pH was controlled by automatic addition of titrant to the leach solution.

Consolidation. Once dealkalization was complete, the resulting porous samples were removed from the leach solution, rinsed with warm distilled water, and allowed to air dry at room temperature. Other drying techniques that were used included exchange of methanol for water for the purpose of drying with solutions of lower surface tension. This helped to overcome some cracking problems in the small pore porous bodies by capillary forces.

Consolidation was done in tube furnace in flowing helium at temperatures from 1200°C to 1450°C . Hold times at 800 to 1000°C were used to help dispel water vapor which evolved as silanol groups on the high surface area silica were combined. Very rapid heating schedules could produce foamed bodies as water was trapped in the porous body.

Results and Discussion

Hydrosilicate Compositions: Hydration/Dehydration. For the purpose of demonstrating the feasibility of the reconstitution process the work reported here used only cut discs or plates of sodium silicate glass. In this way the dimensions of the sample could be easily controlled and dealkalization data was more meaningful. In those cases where thermally molded items, such as lens shapes, were processed the results were identical.

Table I shows several sodium silicate glass discs (2mm x 38mm dia.) that were hydrated at 140°C in 100% relative humidity in an autoclave. The water contents range from about 21% to 41% for glass containing 12.4% and 21.4% Na_2O , respectively. Hydration was directly proportional to alkali content and exposure time at 140°C . It is also directly proportional to autoclave temperature.

Hydration of Sodium Silicate Glass*

TABLE I.

Wt/o Na ₂ O**	Temp. (°C)	Time (hrs)	Wt.% H ₂ O
21.2	140°C	4	31.9
21.4	140°C	10	41.2
18.0	140°C	5	32.7
15.5	140°C	6	32.5
12.4	140°C	10	20.9

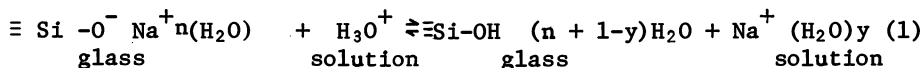
* Sample size - 2mm x 38mm dia.

**Remaining composition was SiO₂.

Dealkalization. Various salt solutions were tested for dealkalization of hydrosilicate bodies. The salts somewhat buffered the solutions and also retarded dissolution of the hydrosilicate. Sodium nitrate solutions despite the common sodium ion were capable of reducing the alkali level in the sample by about 50% in several hours. The most effective and least contaminating salt was NH₄NO₃. Exposure of 2mm x 38mm disc containing 21 wt/o Na₂O to two baths of 0.6M NH₄NO₃ solution over a 24 hour period at pH 7 reduced the residual alkali to about 100 ppm. Several bath changes over a short period were preferable to exposure of the sample to a single bath for long times.

The effects of water content and pH of the dealkalization solution (0.6M NH₄NO₃) on sodium ion release are shown in Figure 2. At constant water content, lower pH (7 vs 8) always results in faster removal of sodium ion from the hydrosilicate. Likewise, at constant pH, hydrosilicates with highest water contents release sodium ion at a faster rate.

In a discussion of diffusion kinetics for dealkalization of Na₂O-SiO₂-H₂O glasses it appears best to describe it as an ion-exchange reaction.



The equilibrium constant K is given by:

$$K = \frac{a_{\text{Si-OH}}^{\text{glass}} \cdot a_{\text{Na}^+}^{\text{solution}}}{a_{\text{Na}^+}^{\text{glass}} \cdot a_{\text{H}_3\text{O}^+}^{\text{solution}}} \quad (2)$$

For the solution the reference state is chosen such that $\lim_{\delta_{\text{Na}^+} \rightarrow 1}$ and similarly for H₃O⁺, where δ is the activity coefficient. The reference state for the solid exchange is that in

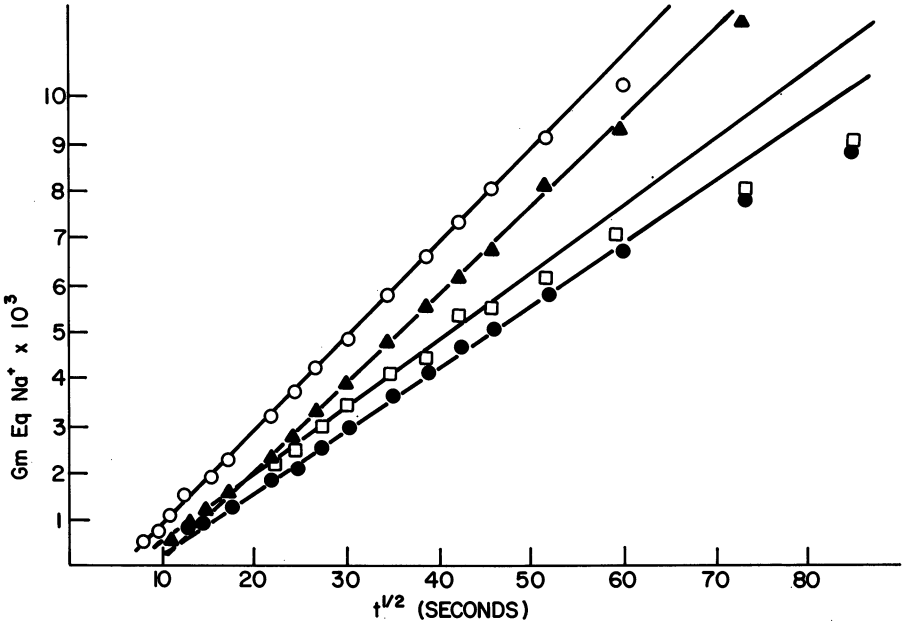


Figure 2. Effect of water content and solution pH on dealcalization rate. Key for % H_2O and pH: \circ , 32.4%, 7; \blacktriangle , 34.2%, 8; \square , 24.4%, 7; and \bullet , 24.4%, 8.

which all of the exchangeable cations are of the ion in question. The fact that the glass prefers to exist in the dealkalized state when placed in NH_4NO_3 solution (pH = 8), i.e. the equilibrium described in (1) lies far to the right, indicates a very large value for K . Thermodynamic analysis was not pursued because of this high selectivity of the matrix for protons compared to sodium.

Diffusion limits for the exchange process described in equation (1) can be arrived at using the following assumptions. There is no dissolution of the SiO_2 network (experimentally verified). The fluxes of the two interdiffusing species are equal in magnitude because of the electroneutrality requirement. The more mobile ion is slowed down by electric field potentials, while the slow ion is accelerated. Diffusion is unidirectional and the sample is semi-infinite in the direction parallel to the direction of diffusion.

The following boundary conditions hold for the diffusion of sodium ions out of the glass:

$$C = C_0, \quad x > 0, \quad t = 0 \quad (3)$$

$$C = 0, \quad x = 0, \quad t > 0. \quad (4)$$

Solution of Fick's Law

$$\frac{dc}{dt} = \frac{d^2c}{dx^2} D \quad (5)$$

yields the result that M_t (g. equiv. Na^+), the total amount of diffusing substance which has left the glass at time t is given by,

$$M_t = 2C_0 \cdot A \left(\frac{Dt}{\pi}\right)^{1/2} \quad (6)$$

where D is the mean interdiffusion coefficient ($\text{cm}^2 \text{sec}^{-1}$), t is time (sec), C_0 concentration of Na^+ ions per unit volume initially in the glass at $t = 0$ (expressed in equivalent $\text{Na}^+ \text{cm}^{-3}$) and A is the area. The mean interdiffusion coefficient is independent of concentration of the exchanging ions. If concentration dependence of the interdiffusion coefficient exists, then the value for D obtained from equation (6) is in reality the mean integral interdiffusion coefficient (10). A plot of M_t versus $t^{1/2}$ (Figures 2 and 3) should be linear with a slope of $2C_0 \cdot A \left(\frac{D}{\pi}\right)^{1/2}$ from which D can readily be calculated. The quantity C_0 is obtained from,

$$C_0 = \frac{2(100-x)y\rho}{10^4 M_{\text{Na}_2\text{O}}} \quad (7)$$

where x is wt % H_2O in the glass, y is the wt % Na_2O in the glass (dry basis), ρ is the density of the hydrated glass and $M_{\text{Na}_2\text{O}}$ is the molecular weight of Na_2O .

The mean integral interdiffusion coefficient obtained for three different Na_2O levels in the starting compositions are plotted as a function of initial water content in the glass

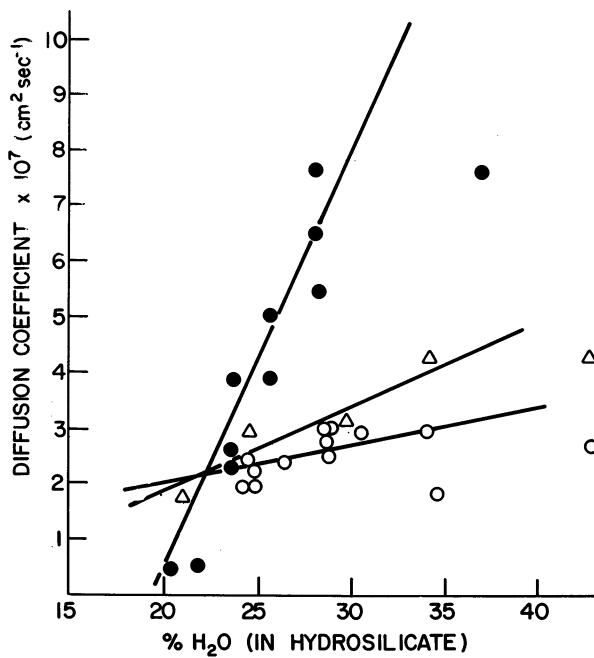


Figure 3. Effect of water and soda content on diffusion coefficient. Key for % Na₂O: ×, 15.5%; △, 18.0%; and ○, 21.2%.

(Figure 3). It is obvious from these data that the mean integral interdiffusion coefficient, D , increases with increasing water content and with decreasing Na_2O content of the glass. The explanation for the water content case can be explained on the basis of a more expanded structure allowing increased diffusion rate. However, it is not clear why the diffusion should be slower as alkali content increases unless it is related to some minimum water requirement for Na^+ transport, or phase separation.¹¹

Porous Structures and Consolidation. The silica body obtained after dealcalization was found to vary dramatically in pore structure. The soda content of the original hydrosilicate body as well as dealcalization conditions affected the final porous structure. Figure 4 shows SEM's of the central cores of structures obtained by dealcalizing hydrosilicates containing from 16 to 21% Na_2O . After dealcalizing them at 80°C for 24 hours, the pore size was directly proportional to the original Na_2O content. More importantly, the pore distribution was very broad in the higher alkali containing bodies.

High dealcalization temperatures were found to contribute to poor pore size distributions and large internal pore sizes. Figure 5 shows SEM scans of the porosity of dealcalized bodies from their surface to their central core. The original hydrosilicate had 18% Na_2O and was dealcalized in 0.6M, NH_4NO_3 . These pictures (5a) show that 24 hours at 80°C creates a broad gradient in pore size across the structure's cross section. On the other hand, one hour at 80°C followed by 23 hours at 50°C produces a more uniform pore structure (5b) in the same hydrosilicate composition.

When bodies with pore structures similar to Figures 5a were consolidated at 1200°C or higher a dense glass with a porous central core was obtained (Figure 6a,b). However, when a sample similar to Figures 5b was consolidated a transparent dense high silica glass was obtained. (Figure 6c).

Conclusions

A process was developed that is capable of transforming poorly durable sodium silicate glasses (12 to 21% Na_2O) into durable high silica glasses. Sodium hydrosilicates with up to 40% H_2O were prepared by either dehydrating commercial sodium silicate solutions or by autoclaving anhydrous glasses of comparable compositions. Regardless of their origin, dealcalization kinetics of these hydrosilicates favored high water content and lower alkali content.

Uniform pore distribution in dealcalized structures was required for attaining dense transparent glass on consolidation at $> 1200^\circ\text{C}$. Hydrosilicates with Na_2O between 15 and 18 wt/o and dealcalized at 50° to 60°C in 0.6 NH_4NO_3 solutions were most likely to have the desired pore structures. High silica, low expansion glass up to 4mm thick was obtained by this approach. Shape and size limitations may exist.

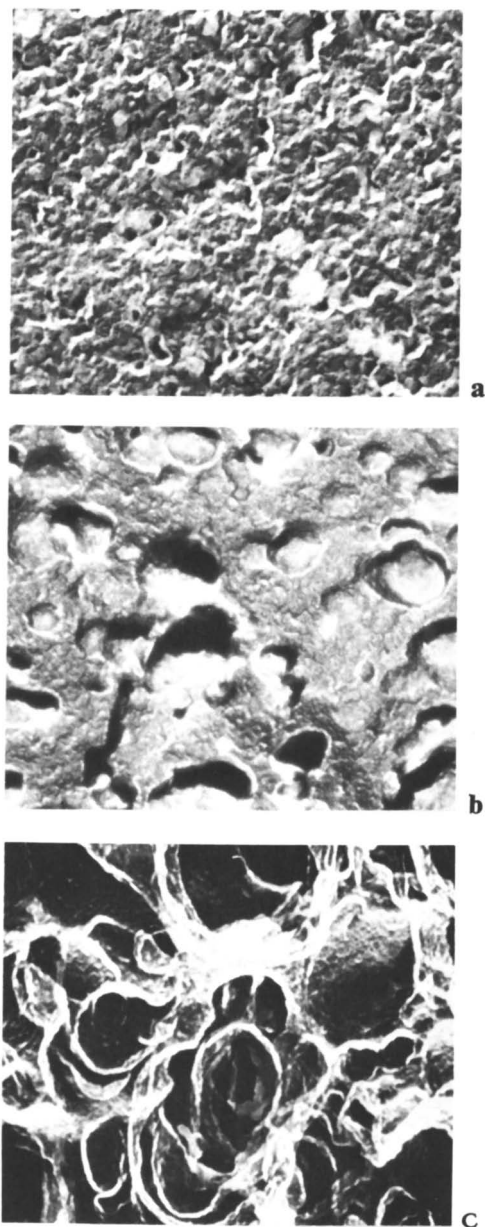


Figure 4. Porosity as a function of alkali content in hydrosilicate. Key for % Na_2O : a, 16%; b, 18%; and c, 21%.

Publication Date: June 1, 1982 | doi: 10.1021/bk-1982-0194.ch017

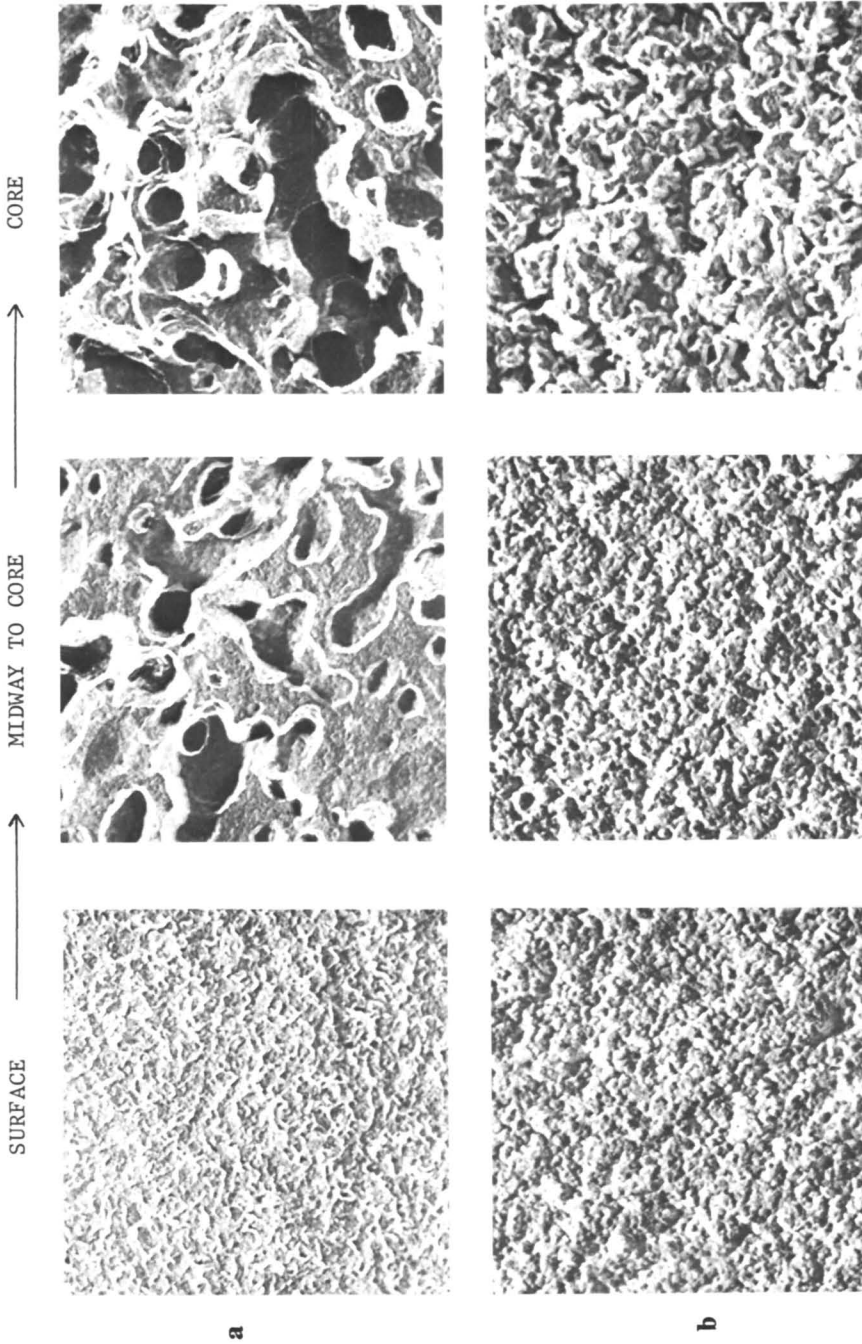


Figure 5. Porosity as a function of dealcalization temperature. Conditions: a (top series), 80°C, 24 h, pH 8; and b (bottom series), 80°C, 1 h, 50°C, 23 h, pH 8.

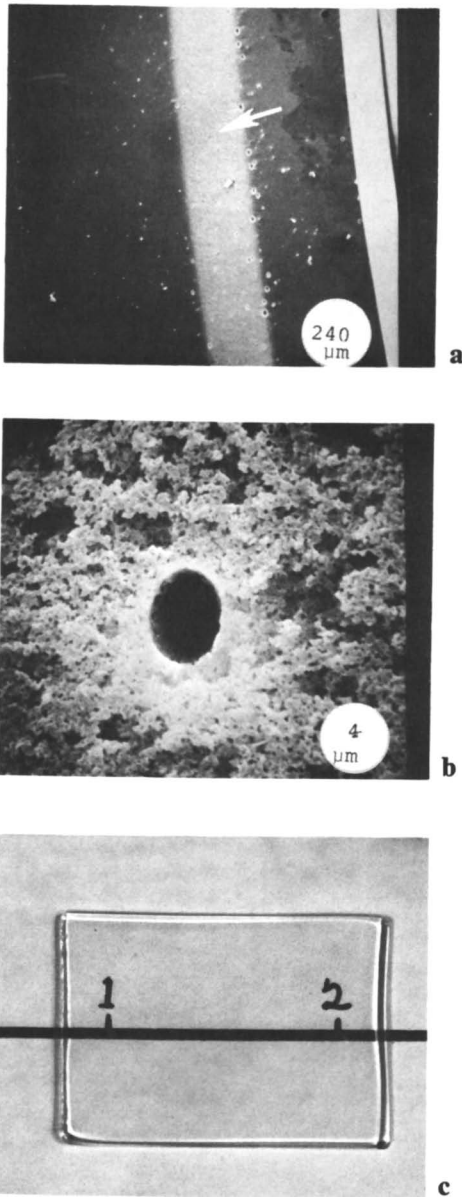


Figure 6. Consolidated silica glass. Key: a, cross section with opaque core; b, magnified porous layer; and c, transparent glass body.

Literature Cited

1. Schloze, H.; Glass Ind. 1966, 47, 546, 622, 670.
2. Boulos, E. N.; Kreidl, N. J., J. Can. Ceram. Soc. 1972, 41, 83.
3. Ernsberger, F. M.; J. Am. Ceram. Soc. 1977, 60, 91.
4. Bartholomew, R. F.; Butler, B. L.; Hoover, H. L.; Wu, C. K., J. Am. Ceram. Soc. 1980, 63, 481.
5. Bartholomew, R. F.; Schreurs, J.W.H., J. Non-Crystall. Solids, 1980, 38/39, 679.
6. Bartholomew, R. F.; Tick, P. A.; Stookey, S. D., J. Non-Crystall. Solids, 1980, 38/39, 637.
7. Moriya, Y.; Nogami, M., J. Non-Crystall. Solids, 1980, 38/39, 667
8. Takata, M.; Tomozawa, M., J. Am. Ceram. Soc. 1980, 63, 710.
9. Wu, C. K., J. Non-Crystall. Solids, 1980, 41, 381.
10. Garfinkel, H. M. "Membranes, A Series of Advances:", Eisenman, G., Ed., Marcel Dekker, N. Y., 1972, Vol. 1, p. 199.
11. Doremus, R. H., "Glass Science," John Wiley and Sons, N.Y., N. Y. 1973.

RECEIVED March 2, 1982.

Silicon Alkoxides in Glass Technology

L. C. KLEIN and G. J. GARVEY

Rutgers University—The State University of New Jersey, Ceramics Department,
Piscataway, NJ 08854

The sol-gel process for forming glasses from silicon alkoxides is described. The processing steps are forming the solution, gelling, drying and firing. The chemical reactions hydrolyzation and polymerization occur in solution depending on combinations of the variables pH, electrolyte, percent water, solvent and temperature. The advantages of the process are high purity, homogeneity and low temperature. Commercial applications of sol-gel glasses include coatings, microballoons, fibers, substrates and porous monolithic shapes.

Though ethyl silicates and other silicon alkoxides have been commercially available for some time (1), their use in glass technology has only recently been well publicized (2). Perhaps the reason for so few investigations in the past into their use in glass technology is that the traditional ideas about glass formation have always involved high temperature. That is to form a glass, a material is heated above its liquidus temperature to disrupt its crystalline structure and, because of its viscous nature, the random liquid structure is trapped by a rapid quench. Once at room temperature, the glass is an unstable solid which is isotropic and in some cases transparent. Accepting this the formation of an isotropic, transparent amorphous material at low temperature is in conflict with this definition. Nevertheless, such a material can be made at room temperature through a sequence of chemical reactions including hydrolyzation and polymerization with silicon alkoxides. In the broader sense of glass formation, this paper will cover the raw materials for what is called the sol-gel process, the processing steps and variables, the applications of the technology and its advantages over traditional methods.

Raw Materials

Most silicate glasses are made with sand grains that range from a few to hundreds of microns in size. The process of melting and homogenizing these glasses requires high temperatures and long times for solid state reactions to occur. Suppose the source of the silica in the silicate glass was a fluid or a liquid. This would eliminate the long times needed for reactions. Colloidal silicas (3) and soluble silicates (4) can be used as fluid sources of silica. Silicon alkoxides can be used as well, and in particular the clear liquid tetraethyl orthosilicate (TEOS from Dynamit-Nobel) was selected for this study.

Of the available silicon alkoxides, tetraethyl orthosilicate (TEOS) appears to be the most popular. This is because it reacts more slowly with water than tetramethyl orthosilicate, comes to equilibrium as a complex silanol and in a partially hydrolyzed state is stable over longer periods of time (5). The clear TEOS liquid is the product of the reaction of SiCl_4 with ethanol. The reaction produces HCl along with the ester $\text{Si}(\text{OC}_2\text{H}_5)_4$ (1). This colorless liquid of a density of about 0.9 g/cm^3 is easy to handle and through multiple distillation extremely pure.

Tetraethyl silicate is insoluble in water (6). In order to initiate the hydrolysis reaction, the TEOS and water must be introduced into a mutual solvent. In this study the mutual solvent is ethanol. A typical mixture is 43 volume % TEOS, 43 volume % ethanol and 14 volume % water.

For multicomponent glasses, the desired additions may be in the form of alkoxides (7) or soluble salts such as acetates and nitrates (8). In this way glasses containing B, Al, Ti, Na, K, transition metals, rare earths and others are relatively straightforward in practice to prepare. A longer chain alcohol such as propanol may be used to slow the rates of the chemical reactions and allow adequate time for complete mixing.

In some cases where the high purity of TEOS is not needed, a partially condensed material may be used. Such liquids have up to 40% by weight SiO_2 and densities of about 1.05 g/cm^3 . When it is possible to start with this partially condensed TEOS, the advantage is reduced weight loss in the conversion to an inorganic glass.

These raw materials are practical in small scale operations as well as large scale. For specialty applications such as coatings for solar cells, the materials offer high purity and ease of application (9). For coating window glass either to improve chemical durability or to reduce reflection losses, the stability of the solution makes the coating of many square meters of glass a continuous process (10). In either case, it is practical to recycle ethanol generated by the chemical reactions in the solution back into the production of the raw material, thus producing more TEOS.

Processing Steps and Nomenclature

The apparatus needed for laboratory scale processing is relatively simple. As shown in Figure 1, it consists of a three-necked flask, a mechanical stirrer, a reflux condenser and a temperature probe controlling a constant temperature bath. The ingredients are TEOS, ethanol and water. An electrolyte such as HCl or NH₄OH may be used. The neck of the flask filled by the temperature probe may also be used for electrolyte additions or sampling.

The processing steps are, in short, forming the sol, gelling, drying, and firing. During the first step, all components must be mixed to form a clear sol. Cloudiness or precipitation indicates a segregation of components which needs to be cleared up by an electrolyte addition or different solvent. Once all of the components are mixed, the water and alkoxides react to begin the gelling, the second step. While being continuously stirred the fluid sol will become increasingly more viscous. At a definite point the viscous sol becomes an elastic gel, and at this point bubbles cease rising. One way to picture the gel is as an elastic sponge now filling the volume once filled by the sol. During the third step, the porous gel will exude liquid and shrink. While drying organics and water trapped in pores will escape. Eventually, the dried gel comes to an equilibrium with ambient conditions, and this amorphous rigid solid is from then on fairly insensitive to moisture. If the goal of this process is to make a material with the same physical properties as glass, the final step is to heat the inorganic sponge, drive off absorbed water, react hydroxyls to form bridging oxygens linking the SiO₂ network, collapse pores and sinter to dense glass. All of this can be accomplished at 1/3 to 1/2 lower temperatures in °K than used in the conventional method, with (11) and without pressure (8), in vacuum and in air (12).

At the sol-gel transition, the molecular structure of the gel determines the probability that a gel will dry in one piece or will break into fragments. It is convenient to think of this transition as the formation of the last bond needed to create an infinite molecule. However, this transition has not been defined in terms of thermodynamics, so it may be misleading to call it the sol-gel transition at all. Yet, in practice the transition is determined by qualitative inspection when an abrupt increase in viscosity occurs. The goal of this work with TEOS is to find the optimum combination of variables which gives a structure at the sol-gel transition which can be processed to form variously fibers, beads, frits, microballoons, shapes, seals, coatings or inorganic sponges.

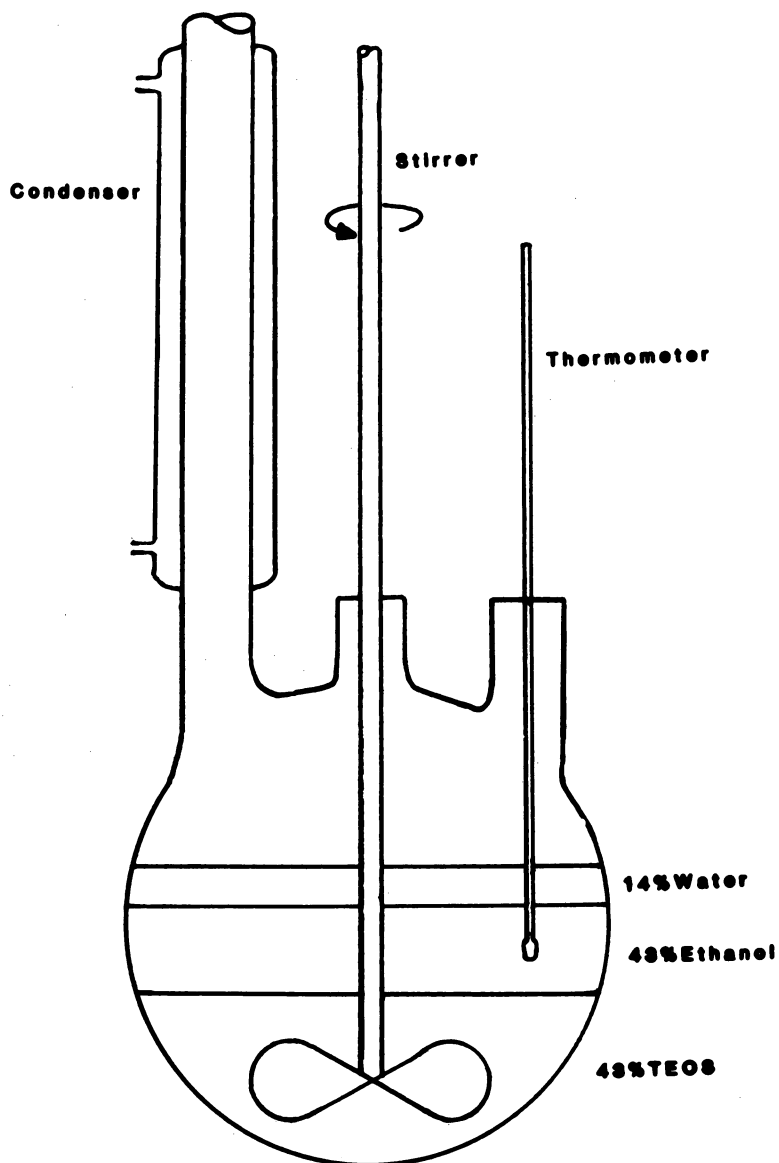


Figure 1. Schematic of apparatus for preparing gels from silicon alkoxides.

Chemical Reactions and Reaction Rates

The chemical reactions that occur when water and TEOS are dissolved in ethanol are hydrolyzation and condensation polymerization. The solution is activated once the water reacts with alkoxy groups on the silicon to form hydroxyl groups and alcohol. This hydrolyzation produces complex silanols and ethanol with TEOS, but this never goes to completion. That is the water is not used up to form silicic acid. Instead condensation polymerization takes partially hydrolyzed units and makes larger units with bridging oxygens. This condensation polymerization regenerates water.

While hydrolyzation uses water as a reactant, polymerization regenerates water as a product. The kinetics of this process are very complex. In fact, the mechanism for reactions catalyzed by acid is different from that catalyzed by base (5, 12). To monitor the extent of these reactions, an experiment was devised to simultaneously measure ethanol and water content in the reaction flask (7). An increase in ethanol content would indicate progress in hydrolyzation. A minimum in water with a subsequent rise would indicate progress in polymerization.

The experiment involves periodic sampling of the solution in the reaction flask. With a syringe, a sample is extracted for ethanol analysis in a calibrated gas chromatograph (Bendix 2600 with 6 foot Porapak S column). At the same time, the solution is titrated with Karl Fisher reagent to give semiquantitative water analysis. The data collected are plotted in Figure 2. The open symbols are the volume percent ethanol. Notice that the ethanol level reaches a plateau. The time at which the ethanol level reaches this plateau corresponds to the minimum in the water level. The filled symbols are the volume per cent water. The data were collected at 20°C, 60°C and 80°C, the refluxing temperature for the solution.

An interesting feature is that the plateau in the ethanol level is the same for all three temperatures. When the plateau is reached, the polymerization process appears to dominate the hydrolyzation process. Another interesting feature is that the water level does not go to zero. There is a minimum indicating polymerization has begun before complete hydrolysis of all alkoxy groups. Beyond the minimum, the water level increases logarithmically with time. The rate of increase of the water level increases with increased temperature indicating that polymerization speeds up with temperature. The data for water level extends to the gel point, so increases in temperature shorten the time to gel.

The behavior for volume percent ethanol and volume percent water in Figure 2 is typical for solutions of TEOS in ethanol with enough water for complete hydrolysis. The time to reach the ethanol plateau and the slope of the volume percent water

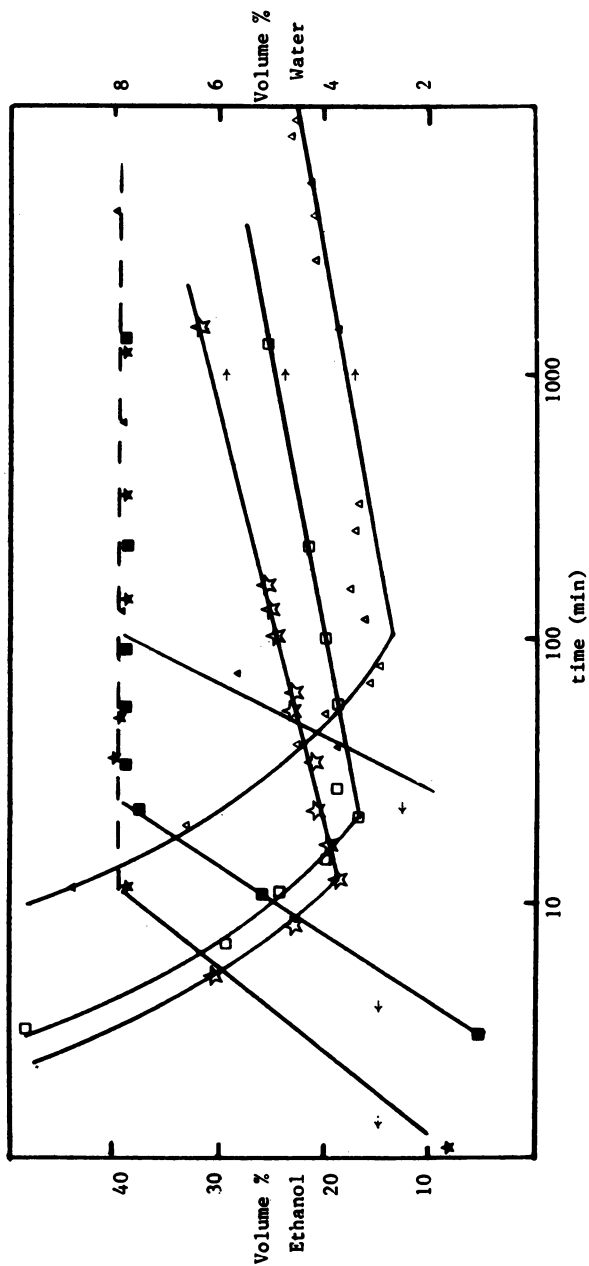


Figure 2. Volume % of products of chemical reactions as a function of time. Key: filled symbols are vol % ethanol, and open symbols are vol % water: Δ and \blacktriangle , 20°C; \square and \blacksquare , 60°C; and \star and \blackstar refluxing 80°C.

vs time curve can be changed by changing the following variables: pH, electrolyte, percent water, nature of solvent and temperature.

First, the pH can be changed by adding more of an electrolyte, for example 1N HCl. In Figure 3, the effect of additions of 1N HCl on the viscosity is shown on a plot of viscosity vs time. These measurements were made with a Brookfield Viscometer at 50 RPM. The interesting feature is that the shape of the curve remains the same whereas the position of the so-called knee shifts to longer times with larger acid additions. The knee starts at about 30 centipoise. For practical purposes the sol-gel transition is at 2000 cp. The effect of these small acid additions would appear to be a retardation of the bond formation needed to set to a gel, though the eventual structure is pretty much the same.

Second, it has already been mentioned that base catalyzed reactions are different from acid catalyzed reactions. Some preliminary observations in this study were that an acid such as HCl drove the hydrolysis reaction while impeding gelling. Then a base such as NH_4OH limited hydrolysis which made gelling impossible. However a salt such as NH_4Cl postponed hydrolysis, but this was quickly followed by gelling. In a crude way, it can be suggested that to speed up the overall sol-gel process, initial treatment should be with acid followed by a final treatment with base.

Third, the effect of water additions to a solution with 20 weight % Na_2O is listed in Table I. With small additions, the gelling time was several weeks and the product was particulate. With additions greater than 1 mole water per mole of ethoxy groups, or 4 moles of water per mole of TEOS, the gelling time was less than 40 seconds and the product was a friable shape. Intermediate additions gave a shape which stayed in one piece, but the interference of pores with light transmission made the piece opaque. In general an increase in water increases the rate of gelling.

Table I - Effect of Water Addition on Gellation Time
For 20 Weight % Na_2O -80 Weight % SiO_2 Solution

Water Addition moles H_2O /moles Ethoxy Group	Time to Gel	Comment
0.18	3 weeks	Particulate
0.36	3 weeks	Particulate
0.53	36 sec	Monolithic, opaque
0.71	48 sec	Monolithic, opaque
0.89	43 sec	Monolithic, opaque
1.07	40 sec	Monolithic, opaque
1.25	<40 sec	Friable
>1.25	<40 sec	Friable

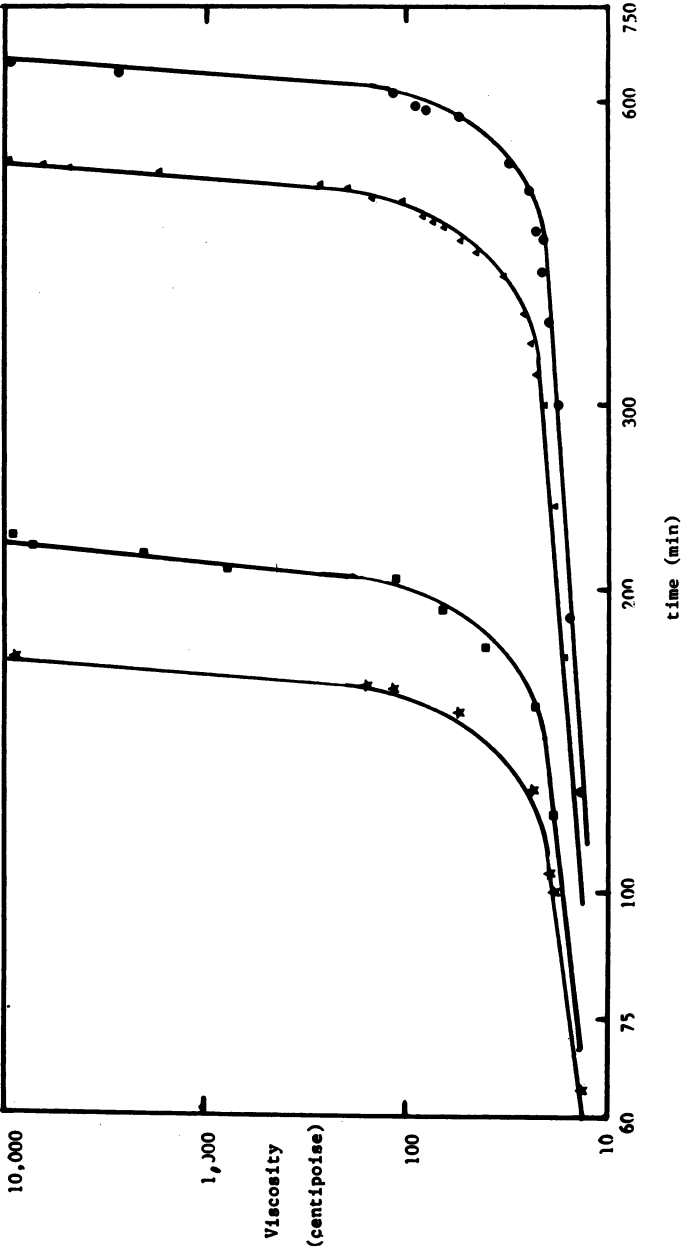


Figure 3. Viscosity in centipoise measured with Brookfield viscometer at 50 RPM plotted against time. Key for acid concentrations: ★, 10; ■, 15; ▲, 30; and ●, 100 drops.

Fourth, the effect of solvent is that the longer chain alcohols slow down the hydrolysis and gelling. For example, substitution of propanol for ethanol gives a longer time for mixing several alkoxides before reactions occur (7). This is desirable when mixing TEOS with A1 or B alkoxides which tend to hydrolyze rapidly. The choice of solvent in general is made to insure a homogeneous solution.

Finally, the effect of temperature seen in Figure 2 is apparently to shorten the time at which polymerization dominates hydrolyzation. In general it can be said that the number of variables in this sol-gel process make it possible to engineer structures in the final product by controlling the sol-gel transition.

Applications

Already the sol-gel process has many commercial applications. The first applications are in the field of coating a variety of substrates. These coatings may be used to improve chemical durability of glasses (10), increase oxidation resistance of Si_3N_4 (13), produce antireflection coatings on solar cells (8) and on silicon (14).

Another area of interest is microballoons for inertial confinement fusion (15). In this application dried gel fragments filled with a blowing agent can be dropped through a furnace to produce hollow glass spheres with high uniformity in wall thickness and sizes from 20 to 1500 microns in diameter.

The porous gels can be dried to form high surface area adsorbents (16) or substrates for heterogeneous catalysts (17). For example, the dried silica gel can be treated with a precious metal organometallic solution which upon reduction leaves highly dispersed metal particles of controlled size for optimum catalytic activity.

Fibers of refractory compositions can be drawn directly from solution (18). These fibers can be compacted for use in corrosive environments such as reinforced cement.

One other application which is being developed in this laboratory is the casting and drying of monolithic shapes (19). Because of the shrinkage during drying, the gels tend to break. When the solvent and adsorbed water are drawn off by vacuum distillation prior to casting, the monolithic shapes survive the 25 percent shrinkage in one piece. An example of such a sample is shown in Figure 4. This shape, initially 90 mm in diameter, after 3 months is seen to be about 65 mm. The sample is optically transparent, undistorted, rigid and only 60 percent dense. This material is completely amorphous and was processed entirely at room temperature.

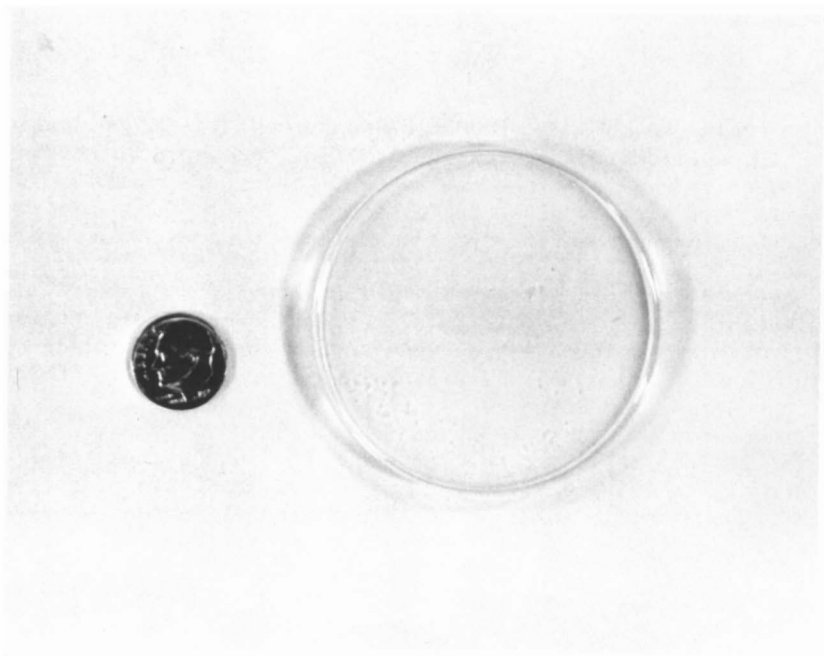


Figure 4. Monolithic dried gel of amorphous silica.

Advantages and Disadvantages

The advantages of this process over conventional methods for forming glass which are frequently cited include high purity, homogeneity and low temperature. Because the raw materials such as TEOS can be multiply distilled, the products can be relatively free of impurities. Because the mixing is accomplished in solution, components such as Ti and Si mix on the atomic scale in relatively short times. If the intention is to use this process to make a duplicate for glass, the porous dried gel can be compacted to a dense glass at temperatures 1/3 to 1/2 lower than the melt temperature in °K.

In addition to an energy saving for this low temperature process, there is a reduction in volatilization of components such as Pb and Cd. In fact, some compositions which cannot be made by conventional means because of phase separation or devitrification can be made by this process. For glasses which cannot practically be made because the melt temperature exceeds that of available furnaces or the quench rate cannot be obtained without shattering the piece, the sol-gel process is the only means to obtain these compositions as a glass. In a sense the sol-gel process extends the range of glassforming compositions in many systems.

The only disadvantages at this time are the cost of raw materials and the inherent volume reduction during the process. These are prohibitive when the process is considered for replacing the bulk of glass manufacture, but are not so serious for specialty applications or those cases where conventional glass technology fails. As more research is pursued in the area of sol-gel processing, there will undoubtedly be many new applications. One way to look at this technology is a way to duplicate the physical properties of glass made by conventional melting, but without the high temperature. A broader view of this technology is that there is an amorphous material available in which a high surface can be maintained without losing transparency while its structure can be engineered to suit particular applications.

Acknowledgments

The authors thank D. Gallagher, T. Gallo, W. Hasz, G. Mucci and J. Reed for their technical assistance and the National Science Foundation (Grant No. DMR 8012902) for their financial assistance. Also, we appreciate the invitation to participate in this symposium extended by Dr. James S. Falcone, Jr., PQ Corporation.

Literature Cited

1. Bradley, D. C.; Mehrotra, R. C.; Gaur, D. P. Metal Alkoxides, Academic, New York, 1978.
2. Sakka, S.; Kamiya, K.; J. Non-Cryst. Solids 1980, 42, 403-422.
3. Roy, R. Am. Ceram. Soc. 1956, 39, 145-146.
4. Shoup, R. D.; Haynes, W. L.; Bartholomew, R. F.; this volume.
5. Aelion, R.; Loebel, A; Eirich, F. Am. Chem. Soc. 1950, 72, 5705-5712.
6. Cogan, H. D.; Setterstrom, C. A. Ind. Eng. Chem. 1947, 39, 1364-1368.
7. Klein, L. C.; Garvey, G. J. J. Non-Cryst. Solids 1980, 38/39, 45-50.
8. Brinker, C. J.; Mukherjee, S. P. Thin Solid Films 1981, 77, 141-148.
9. Brinker, C. J.; Mukherjee, S. P. J. Mat. Sci. 1981, 16, 1980-88.
10. Dislich, H. Angew. Chemie, Int. Edition 1971, 10, 363-370.
11. Mukherjee, S. P.; Zarzycki, J. J. Am. Ceram. Soc. 1979, 62, 1-4.
12. Nogami, M.; Moriya, Y. J. Non-Cryst. Solids 1980, 37, 191-201.
13. Schlichting, J.; Neumann, S. J. Non-Cryst. Solids, in press.
14. Yoldas, B. E. Applied Optics 1980, 19, 1425-1429.
15. Downs, R. L.; Miller, W. J. International Congress on Glass, July 6-11, 1980, Abstract.
16. Yoldas, B. E. J. Mat. Sci. 1978, 13, 865-870.
17. Gottardi, V. Hungarian Academy of Sciences Conference, Vezsprem, October 29, 1979.
18. Kamiya, K.; Sakka, S.; Tatemichi, Y. J. Mat. Sci. 1980, 15, 1980, 1765-1771.
19. Klein, L. C.; Garvey, G. J. J. Non-Cryst. Solids, in press.

RECEIVED March 2, 1982.

Tetrabutylammonium Hydrogen Silicate: Synthesis, Chemical, Thermal, and Crystallographic Properties

H. GERKE, H. GIES, and F. LIEBAU

Mineralogisches Institut der Universität, D-2300 Kiel, Federal Republic of Germany

A new crystalline highly acid tetrabutylammonium silicate (1) and several of its derivatives have been synthesized from aqueous solutions. (1) is face-centered cubic with $a_0 = 28.605(6)\text{\AA}$, $\rho(\text{exp}) = 1.448(5)\text{ g cm}^{-3}$; the approximate unit cell content is $[\text{N}(\text{C}_4\text{H}_9)_4]_{24}\text{H}_{144}[\text{Si}_{168}\text{O}_{420}] \cdot 144\text{H}_2\text{O}$. In the presence of polydentate amines $\text{H}_2\text{N}(\text{CH}_2\text{CH}_2\text{NH})_n\text{H}$, $n = 1, 2, 3$ (*en*, *dien*, *trien*) the hydrate water is partly (with *en*) or completely (with *dien* and *trien*) replaced by these amines. The *en*-containing phase is cubic with $a_0 = 28.715(3)\text{\AA}$, $\rho(\text{exp}) = 1.446(5)\text{ g cm}^{-3}$; the approximate cell content is $[\text{N}(\text{C}_4\text{H}_9)_4]_{24}\text{H}_{144}[\text{Si}_{168}\text{O}_{420}] \cdot 84\text{H}_2\text{O} \cdot 36\text{en}$. Syntheses using $[\text{P}(\text{C}_4\text{H}_9)_4]\text{OH}$ instead of $[\text{N}(\text{C}_4\text{H}_9)_4]\text{OH}$ in the presence of *en* produced the corresponding cubic tetrabutylphosphonium hydrogen silicate.

Within recent years a fair knowledge of the influence of temperature and in particular of cation properties such as valence, electronegativity and size on the constitution as well as on the conformation of silicate anions has been obtained (1, 2). For instance, cations of low electronegativity favour topologically linear and highly stretched silicate anions. A decrease of cation valence has a very similar effect. In comparison, the influence of cation size, temperature and pressure on the structure of silicate anions is much weaker. Therefore, in order to study the influence of cation size, it is essential to vary the cation radius as much as possible while keeping the other parameters as constant as possible.

Unfortunately, for monovalent monoatomic cations the radius varies only between 0.59\AA for tetrahedrally coordinated Li^+ and 1.88\AA for 12-coordinated Cs^+ , for divalent monoatomic cations be-

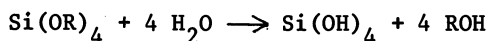
tween 0.27Å for 4-coordinated Be^{2+} and 1.61Å for 12-coordinated Ba^{2+} (Shannon - Prewitt radii).

In order to increase the range of cation size it is possible to replace the monoatomic cations by polyatomic inorganic complexes or by organic cations. For instance, silicates containing the rare double ring anions $[\text{Si}_6\text{O}_{15}]^{6-}$, $[\text{Si}_8\text{O}_{20}]^{8-}$ and $[\text{Si}_{10}\text{O}_{25}]^{10-}$ have been obtained by using ethylenediamine (*en*) complexes such as $[\text{Co}(\text{en})_3]^{2+}$, $[\text{Ni}(\text{en})_3]^{2+}$ and $[\text{Cu}(\text{en})_2]^{2+}$ (3, 4, 5) or $[\text{N}(\text{CH}_3)_4]^+$ and $[\text{N}(\text{CH}_2\cdot\text{CH}_2\text{OH})_4]^+$ (6, 7, 8) as cations.

To study the influence of cation size in more detail we started a program to synthesize silicates of organic cations. Here we report the first results of these studies.

Syntheses

Tetrabutylammonium hydrogen silicate hydrate has been synthesized from aqueous solutions of tetraalkylorthosilicates and tetrabutylammonium hydroxide. In a typical experiment $\text{Si}(\text{OCH}_3)_4$ or $\text{Si}(\text{OC}_2\text{H}_5)_4$ is added at room temperature to a 10 percent aqueous solution of $n\text{-}[\text{N}(\text{C}_4\text{H}_9)_4]\text{OH}$ under continuous agitation. Hydrolysis of the tetraalkylorthosilicate according to the equation



leads to a homogeneous solution of silicic acid. Such solutions with a ratio $\text{SiO}_2 : [\text{NR}_4]\text{OH}$ of about 3 : 1 are subsequently concentrated in vacuum at room temperature by evaporating the alcohol and part of the water within a few minutes. From such concentrated solutions a new phase crystallized slowly after about one week at room temperature and normal pressure.

Crystallographic properties

Single crystals with 0.2 mm maximum diameter have been obtained. The optically isotropic crystals are terminated by the crystal forms $\{100\}$ (cube), $\{110\}$ (rhombdodecahedron), and $\{111\}$ (octahedron) (Figure 1). Quite often crystals are intergrown and their faces are convex (Figure 2).

The lattice constant determined from single crystal X-ray diagrams is $a_0 = 28.605(6)\text{Å}$. From the systematic extinctions of reflections a face-centered cubic cell is inferred. With a mixture of bromobenzene and tetradecan the density was found to be $1.448(5) \text{ g cm}^{-3}$. X-ray powder diffraction data are presented in Table 1.

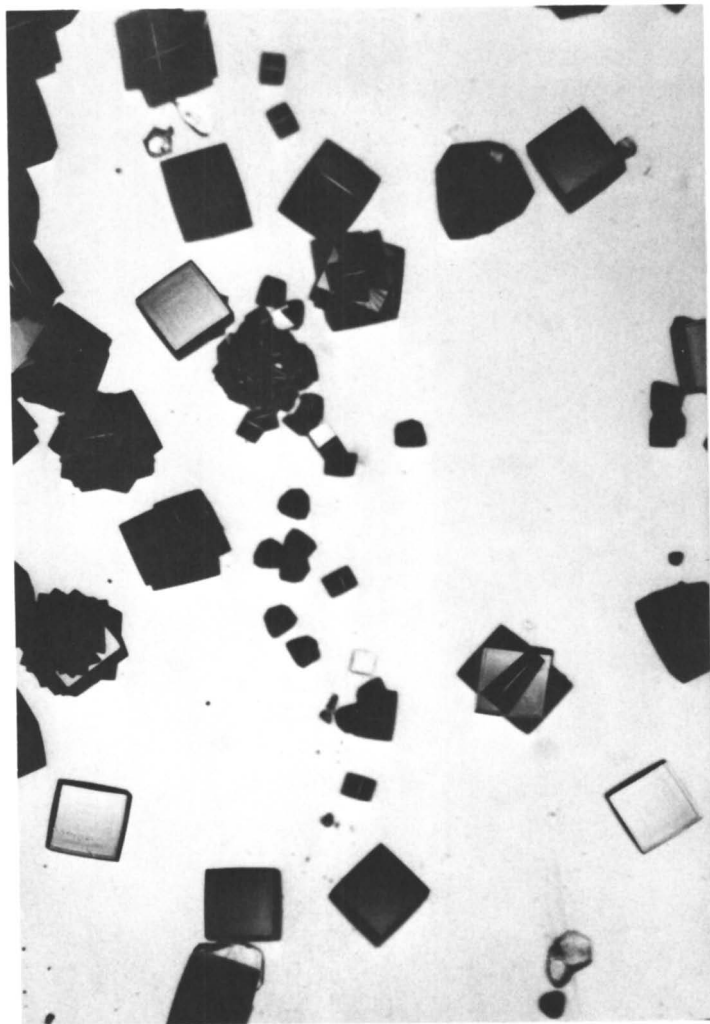


Figure 1. Single crystals of tetrabutylammonium hydrogen silicate hydrate.

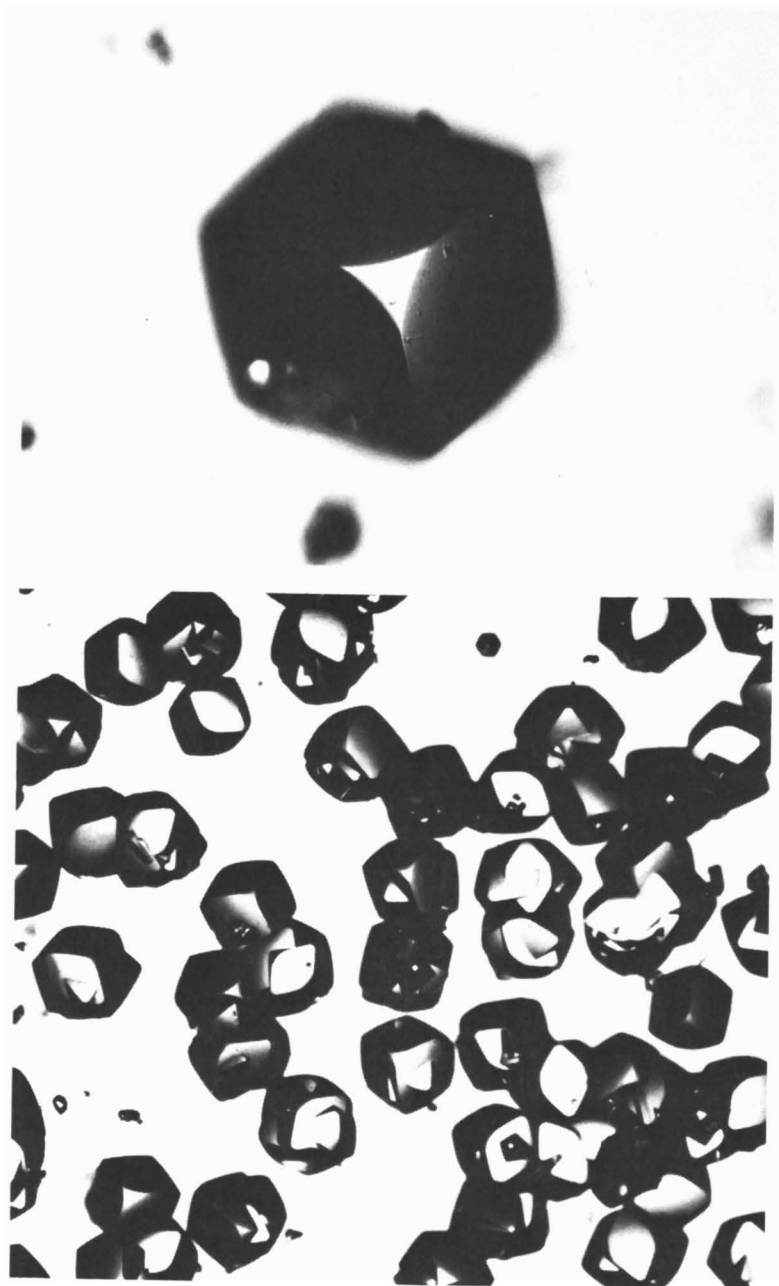


Figure 2. Intergrown crystals of tetrabutylammonium hydrogen silicate hydrate exhibiting convex faces.

Table I. X-ray powder diffraction data of tetrabutylammonium hydrogen silicate hydrate ($\text{CuK}\alpha$, $\lambda = 1.5418\text{\AA}$).

$d[\text{\AA}]$	I/I_1	hkl	$d[\text{\AA}]$	I/I_1	hkl
14.47	90	200	3.2079	50	840
10.22	85	220	3.0582	20	664
8.322	10	222	3.0079	15	931
7.190	35	400	2.8139	20	10.2.0, 862
5.859	8	422	2.5355	5	880
4.783	12	600, 442	2.5061	10	11.3.1, 971
4.328	50	622	2.4960	9	10.4.4, 882
4.137	10	444	2.4597	5	10.6.0, 866
3.985	7	640	2.4244	2	10.6.2
3.8355	25	642	2.3890	7	12.0.0, 884
3.7385	100	553, 731	2.3037	10	11.5.3, 975
3.5870	5	800	2.2389	2	12.4.2, 886
3.4810	95	820			10.8.0
3.3772	15	822, 660	2.1925	5	13.1.1, 11.7.1
3.3119	20	751, 555			11.5.5, 993
3.2903	15	662	2.0534	8	13.5.1, 11.7.5

The crystals are hydrophobic, insoluble in water, acetone, diethylether, toluene and trichloromethane, and soluble in methanol, diluted acids and bases.

Chemical composition

With chemical analyses the total amount of Si, C, N and H and the oxygen content in excess of SiO_2 have been determined. The atomic ratios observed are presented in Table II. They are in good agreement with atomic ratios calculated for the chemical composition

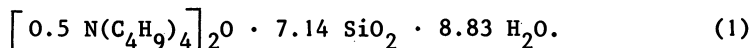


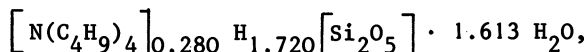
Table II. Comparison between observed atomic ratios and those calculated for $0.5 \left[\text{N}(\text{C}_4\text{H}_9)_4 \right]_2 \text{O} \cdot 7.14 \text{SiO}_2 \cdot 8.83 \text{H}_2\text{O}$ (calc. 1) and for $\left[\text{N}(\text{C}_4\text{H}_9)_4 \right]_{24} \text{H}_{144} \left[\text{Si}_{168}\text{O}_{420} \right] \cdot 144 \text{H}_2\text{O}$ (calc. 2)

	Si	excess O	C	N	H
observed	7.14	9.33	16	1.053	54.92
calc. 1	7.14	9.33	16	1.000	53.64
calc. 2	7.00	9.50	16	1.000	54.00

The slight excess observed for N and H over those calculated from chemical composition (1) is perhaps due to some replacement of $2 \left[\text{N}(\text{C}_4\text{H}_9)_4 \right]^+$ by $2 \text{N}(\text{C}_4\text{H}_9)_3 + 2 \text{H}^+ + \text{H}_2\text{O}$, the tributylamine being formed by decomposition of tetrabutylammonium ions.

Titration of an aqueous suspension of the material against 0.1n HCl and 0.1n NaOH indicates four different reactions A, B, C and D (Figure 3). The sharp step in the titration curve at $p_{\text{H}} = 6$ is due to the neutralization of the $\text{Si}-\text{O}^-$ groups that are equivalent to the number of $\left[\text{N}(\text{C}_4\text{H}_9)_4 \right]^+$ cations of the silicate. At lower p_{H} values (region A of Figure 3) the solid crystals are dissolved obviously by hydrolysis of Si-O-Si bonds. In the basic region C acid hydrogen atoms of the silanol groups Si-OH react with OH^- ions. At still higher p_{H} values (region D) Si-O-Si bonds are hydrolyzed by hydroxyl groups.

The amount of silanol groups determined from the amount of base used in region C is in agreement with the chemical formula



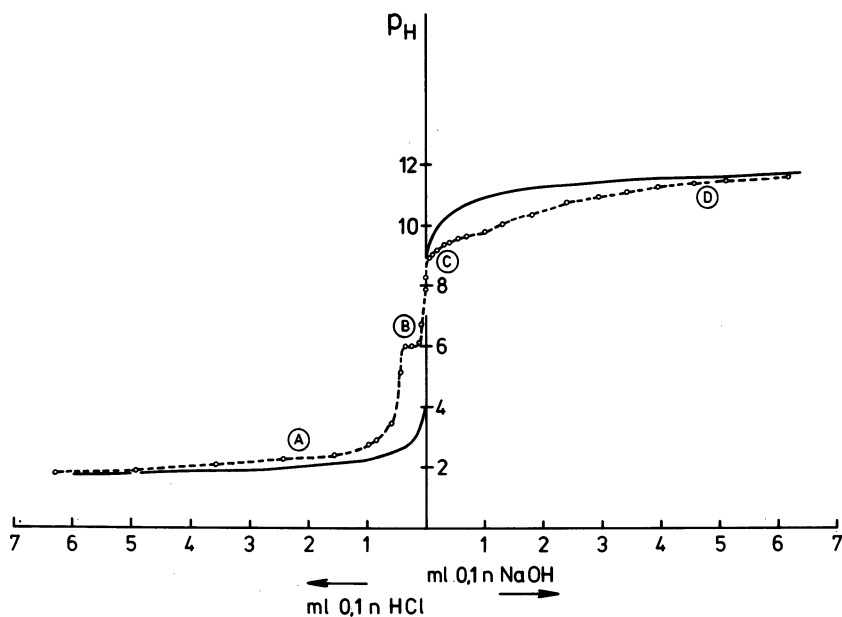
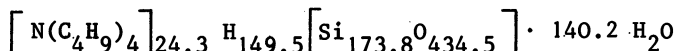
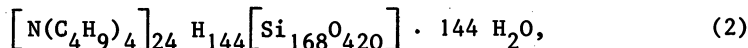


Figure 3. Titration curve for tetrabutylammonium hydrogen silicate hydrate in aqueous suspension. Key: (A), $\text{SiOSi} + \text{H}_2\text{O} \rightleftharpoons \text{SiOH} + \text{HOSi}$; (B) $\text{SiO}^- + \text{H}^+ \rightleftharpoons \text{SiOH}$; (C), $\text{SiOH} + \text{OH}^- \rightleftharpoons \text{SiO}^- + \text{H}_2\text{O}$; and (D), $\text{SiOSi} + \text{OH}^- \rightleftharpoons \text{SiO}^- + \text{HOSi}$.

which is recalculated from the chemical composition (1). Taking into account the lattice constants and the density of the crystals a cell content of



is calculated. This is near to



a cell content suggested by the face-centered lattice of the crystals. The atomic ratios calculated for this composition (calc. 2) are in fair agreement with the observed ratios (Table II).

Thermal properties

2.10 mg of the material have been used to measure the thermal weight-loss curve (TGA) and 3.1 mg for the Differential Scanning Calorimetry curves (DSC) both with 10°C per minute heating rate (Figure 4). These curves indicate five different regions of decomposition. The structural formula given in the preceding paragraph suggests that these steps are due to the following reactions:

- 45°C - 95°C: Loss of slightly more than half the hydrate water molecules. This dehydration is accompanied by decrepitation of the crystals.
- 95°C - 145°C: Loss of the remaining hydrate water molecules in a rather smooth reaction.
- 145°C - 185°C: Loss of the decomposition products of part of the $\left[\text{N}(\text{C}_4\text{H}_9)_4 \right]^+$ ions or, more likely, of the $\text{N}(\text{C}_4\text{H}_9)_3$ molecules that have replaced $\left[\text{N}(\text{C}_4\text{H}_9)_4 \right]^+$ ions. This loss takes place under decrepitation at the beginning and becomes less violent towards the end of the deamination.
- 185°C - ca. 300°C: Loss of the decomposition products of the remaining $\left[\text{N}(\text{C}_4\text{H}_9)_4 \right]^+$ ions (decationization).
- above ca. 300°C: Loss of water due to condensation of Si-OH groups.

The volatile decomposition products have been proved by mass spectroscopy. In Figure 4 the theoretical values of sample weight after dehydration, deamination, decationization and condensation calculated from structural formula (2) of the phase are indicated by horizontal lines.

Derivatives

When the synthesis was modified by adding ethylenediamine (*en*), diethylenetriamine (*dien*) or triethylenetetramine (*trien*) to the aqueous solution of tetrabutylammonium hydroxide and

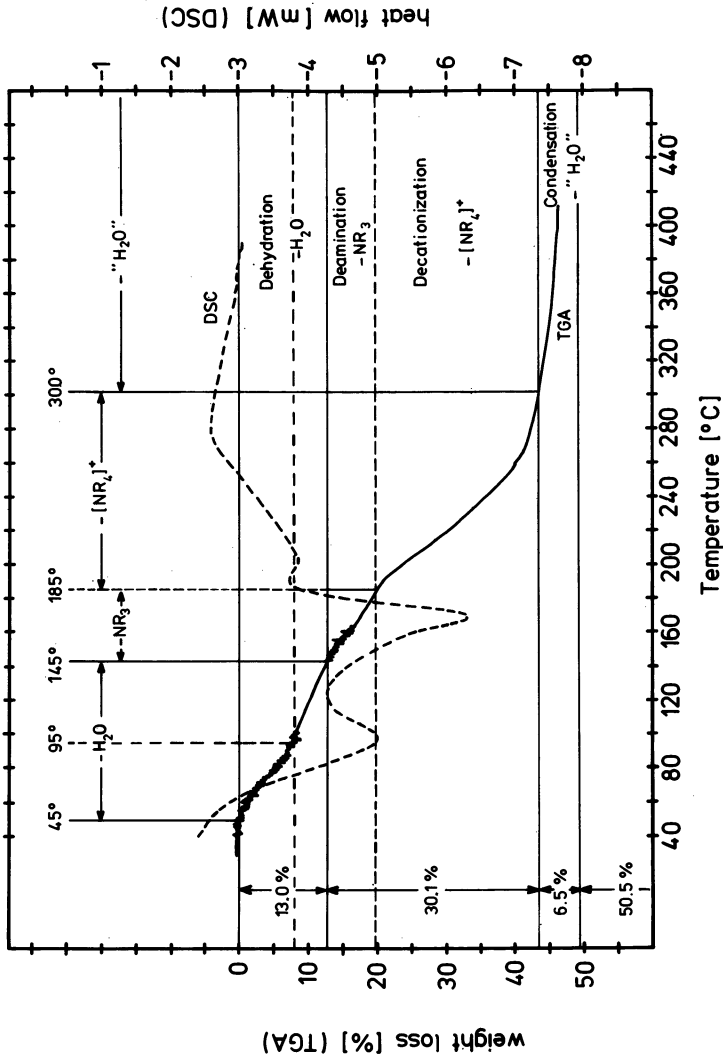
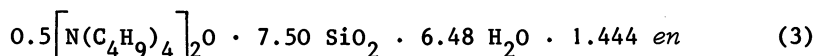


Figure 4. Thermal decomposition of tetrabutylammonium hydrogen silicate hydrate studied by TGA and DSC. Theoretical weight losses for the individual steps of decomposition calculated from the structural formula (2) of the sample are indicated at the left side of the diagram.

silicic acid then crystals formed yielding X-ray powder patterns indistinguishable from those of the phase described so far. For the phase formed in the presence of en $a = 28.715(3)\text{\AA}$ has been obtained from single crystal diagrams and a density of $1.446(5)\text{ g cm}^{-3}$ has been measured. These observations suggest that the two phases are chemically and structurally very similar and, in particular, that their silicate anions are at least very similar.

Unfortunately, the material available for chemical analysis of the en -containing phase was less pure than that of the en -free phase; it probably contained a small amount of a highly siliceous impurity, possibly amorphous silica.

The atomic ratios found by chemical analyses are in fair agreement with those calculated for the chemical composition

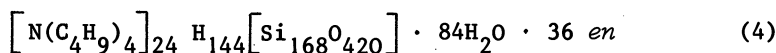


(Table III). Comparisons of the TGA curves (Figure 5), DSC curves (Figure 6) and titration curves (Figure 7) of the two phases indicate that their main difference is a partial replacement of water by en .

Table III Comparison between observed atomic ratios and those calculated for $0.5\left[\text{N}(\text{C}_4\text{H}_9)_4\right]_2\text{O} \cdot 7.50 \text{ SiO}_2 \cdot 6.48 \text{ H}_2\text{O} \cdot 1.444 \text{ en}$ (calc. 3) and for $\left[\text{N}(\text{C}_4\text{H}_9)_4\right]_{24} \text{ H}_{144} \left[\text{Si}_{168}\text{O}_{420}\right] \cdot 84\text{H}_2\text{O} \cdot 36 \text{ en}$ (calc. 4).

	Si	excess O	C	N	H
observed	7.50	6.98	18.89	3.89	61.31
calc. 3	7.50	6.98	18.89	3.89	60.51
calc. 4	7.00	7.00	19.00	4.00	61.00

Based on all these observations a unit cell content close to



is suggested for the en -containing phase. In Table III the atomic ratios calculated for this formula are compared with the observed ratios. The replacement of nearly half the water content of the en -free silicate by en is supported by the fact that the thermal dehydration of the former takes place in two steps (Figure 4).

TGA curves of the derivative synthesized in the presence of diethylenetriamine (Figure 7) seem to indicate that in this phase the hydrate water of the en -free phase is completely replaced by $dien$.

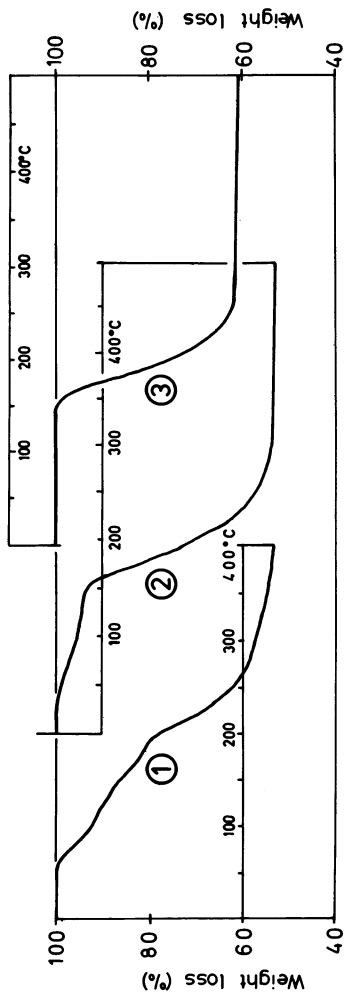


Figure 5. Thermal decomposition of three varieties of tetrabutylammonium hydrogen silicate studied by TGA. Key: ①, $H_2N(CH_3 \cdot CH_3 \cdot NH)_4H$, free phase (the same curve as shown in Fig. 4); ②, $H_2N \cdot CH_3 \cdot CH_3 \cdot NH_2$, containing derivative; and ③, $H_2N(CH_3 \cdot CH_3 \cdot NH)_2H$, containing derivative.

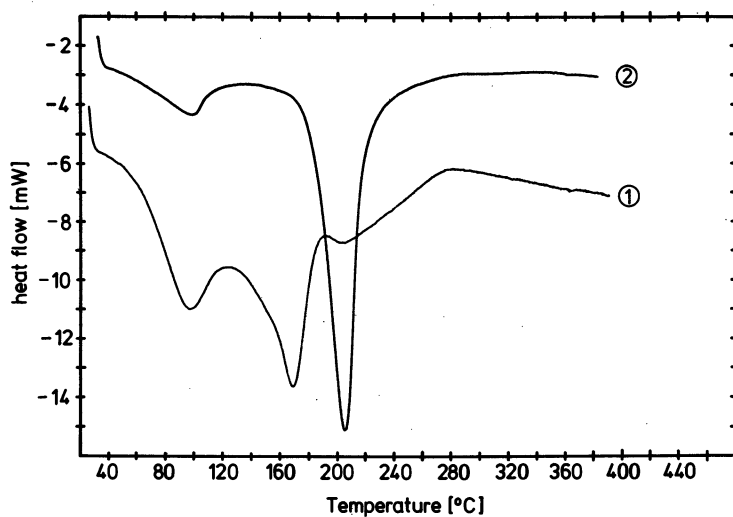


Figure 6. Thermal decomposition of two varieties of tetrabutylammonium hydrogen silicate studied by DSC. Key: ①, $H_2N(CH_2 \cdot CH_2 \cdot NH)_nH$, free phase (the same curve as shown in Fig. 4); and ②, $H_2N \cdot CH_2 \cdot CH_2 \cdot NH_2$, containing derivative.

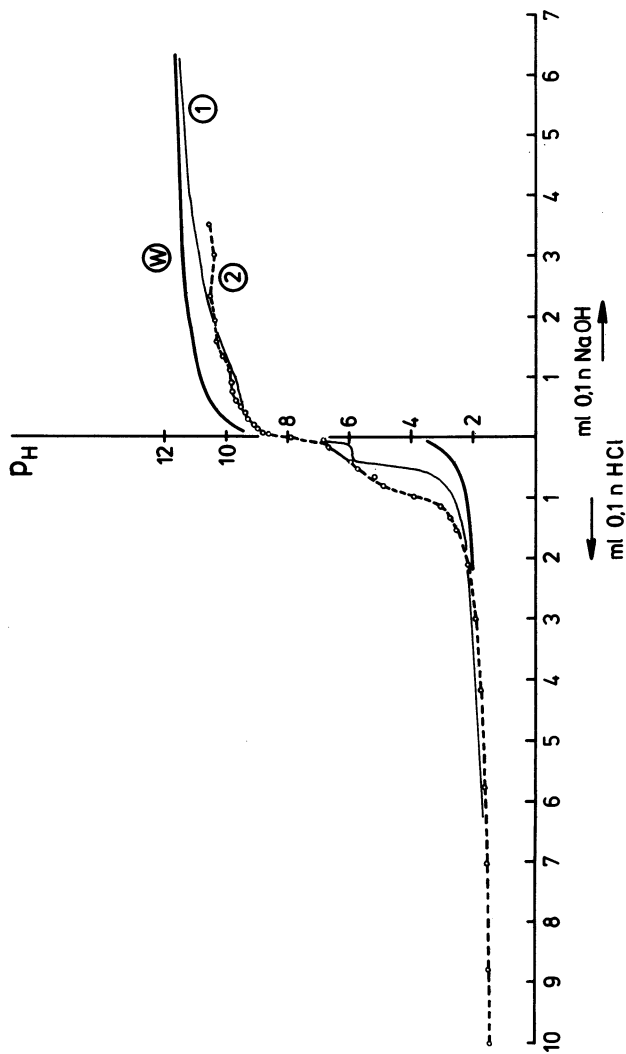


Figure 7. Comparison of the titration curves of two varieties of tetrabutylammonium hydrogen silicate. Key: \odot , $H_2N(CH_2 \cdot CH_2 \cdot NH)_2$, free phase (the same curve as shown in Fig. 3); \ominus , $H_2N \cdot CH_2 \cdot CH_2 \cdot NH_2$, containing derivative; and \textcircled{W} , titration curve for water.

Hydrolysis of tetramethylorthosilicate by an aqueous solution of tetrabutylphosphonium hydroxide $[\text{P}(\text{C}_4\text{H}_9)_4]\text{OH}$ instead of the corresponding ammonium compound produced, in the presence of ethylenediamine, cubic crystals that gave X-ray diffraction diagrams almost identical to those of the corresponding tetrabutylammonium silicate derivative.

Summary

A group of crystallographically homeotypic acid silicates of general formula

$0.5[\text{T}(\text{C}_4\text{H}_9)_4]_2\text{O} \cdot 7 \text{SiO}_2 \cdot (9 - x) \text{H}_2\text{O} \cdot y \text{A}$ with $\text{T} = \text{N}, \text{P}$ and $\text{A} = \text{en}, \text{dien}, \text{trien}$ has been synthesized. The phases are face-centered cubic with $a \approx 28.7\text{\AA}$ and approximate unit cell contents of $[\text{N}(\text{C}_4\text{H}_9)_4]_{24} \text{H}_{144} [\text{Si}_2\text{O}_5]_{84} \cdot (144 - 24x) \text{H}_2\text{O} \cdot 24y \text{A}$, where $x = 0, y = 0$ when polydentate amines are absent and $x = 2.5, y = 1.5$ in the presence of *en*.

Acknowledgment

We thank Prof. G. Lagaly and K. Beneke for performing the titration analyses, and Prof. R. N. Schindler for providing the mass spectrometer.

Literature Cited

1. Liebau, F.; Pallas, I. Z. Kristallogr. 1981, **155**, 139-153.
2. Liebau, F.; "Structure and Bonding in Crystals"; O'Keeffe, M.; Navrotsky, A., Ed.; Academic Press: New York, Vol. II, Chapter 23, in press.
3. Smolin, Yu. I.; Shepelev, Yu. F.; Pomes, R.; Hoebbel, D.; Wieker, W. Sov. Phys. Crystallogr. 1975, **20**, 567-570.
4. Smolin, Yu. I. Sov. Phys. Crystallogr. 1970, **15**, 23-27.
5. Smolin, Yu. I.; Shepelev, Yu. F.; Butikova, I. K. Sov. Phys. Crystallogr. 1972, **17**, 10-15.
6. Hoebbel, D.; Wieker, W. Z. anorg. allg. Chem. 1971, **384**, 43-52.
7. Hoebbel, D.; Wieker, W.; Franke, P.; Otto, A. Z. anorg. allg. Chem. 1975, **418**, 35-44.
8. Rademacher, O.; Scheler, H. Z. anorg. allg. Chem. 1979, **450**, 187-192.

RECEIVED March 2, 1982.

Fibrous Organosilicon Polymers Derived from Silicates

JESSE HEFTER¹ and MALCOLM E. KENNEY

Case Western Reserve University, Cleveland, OH 44106

A new, inherently fibrous organosilicon polymer having pendent trimethylsilyl groups is reported. It has been made from the rare ladder or tube silicate litidionite using a Lentz-type extraction-substitution process. The constituent fibers of this polymer have very small diameters, often 40-60 Å, and are flexible and inert. They are believed to have frameworks closely related to that of the parent silicate ion. A polymer which appears to be the same as this one has been made from the synthetic silicate $\text{Na}_2\text{CuSi}_4\text{O}_{10}$, a close structural analog of litidionite. In addition a related polymer carrying dimethylvinyl groups has been made from litidionite by a like Lentz-type procedure. Both silicates have been made by simple thermal procedures.

Recently we have been seeking new types of organosilicon polymers with the hope of finding polymers having unique structures and interesting combinations of properties. Out of this work has come a new siloxane that is, at least in part, inherently fibrous. The fibers characteristic of it have very small diameters and are flexible and inert.

The technique used to make this siloxane is based on a well-known procedure for derivatizing silicates originated by Lentz (1). In this procedure the metal ions are extracted from the silicate and trimethylsilyl or other silyl groups are grafted on the silicate framework thus exposed. (Initially the procedure was used in structural studies of silicates containing monomeric and oligomeric ions (1). Later it was used for the synthesis of silicones from silicates containing polymeric silicate ions (2). Among the silicones yielded by this latter work are sheet and

¹ Current address: Shell Development Company, Houston, TX 77001.

scroll silicones carrying pendent trimethylsilyl groups (2, 3, 4). The scroll silicone, like the silicone described in this paper, is inherently fibrous. However, the fibers in it are an order of magnitude larger than those in the new silicone.)

The silicate which has been used most frequently for the synthesis of this new polymer is litidionite, $\text{NaKCuSi}_4\text{O}_{10}$. This silicate, while occurring naturally, is very rare (so far it has been found only in the crater of Mt. Vesuvius) (5). The silicate ion in it (6), Figure 1, can be described as being a complex ladder ion or as being a tube ion (6, 7). Examination of its structure shows that it is constructed of fused 8- and 16-membered rings. The arrangements of the oxygens about the metal ions in it are those shown in Figure 2.

This silicate has been made by the hydrothermal technique (8, 9). However, relatively elaborate equipment is required for its preparation by this approach and, as a result, it is not well-suited to incorporation in a synthetic sequence requiring litidionite.

Results and Discussion

In the present work two syntheses for litidionite have been developed which are straightforward and require only simple apparatus. In one a sodium-potassium-copper silicate glass is made and then devitrified over a period of weeks at approximately 765 °C. In the other a mixture of sodium carbonate, potassium carbonate, cupric oxide, silicon dioxide, again with a Na:K:Cu:Si ratio of 1:1:1:4, is sintered at approximately 765 °C for a number of days.

The litidionite made by this latter procedure can be purified, after being powdered, by a process involving a combination of washing and decantation. Water buffered at pH 5 is used in this process. In practice the process is repeated a number of times.

As might be expected litidionite is a medium blue. A micrograph of a crystallite of this silicate obtained by crushing a sample of it made by the devitrification process is shown in Figure 3. From this micrograph it is clear that litidionite itself is not fibrous in nature. In accordance with expectations both the litidionite made by the sintering process and that made by the devitrification process are satisfactory for use in the synthesis of the polymer.

The polymer, as already indicated, is made by a Lentz-type procedure. In the version of this procedure used, the litidionite is treated with a mixture of chlorotrimethylsilane, water, and a solvent such as dioxane, tetrahydrofuran, or acetone. The reaction is run over a period of days at room temperature.

Purification of the polymer can be effected by repeatedly subjecting a suspension of it in a solvent such as tetrahydrofuran to sonication and settling, and then isolating the polymer in the

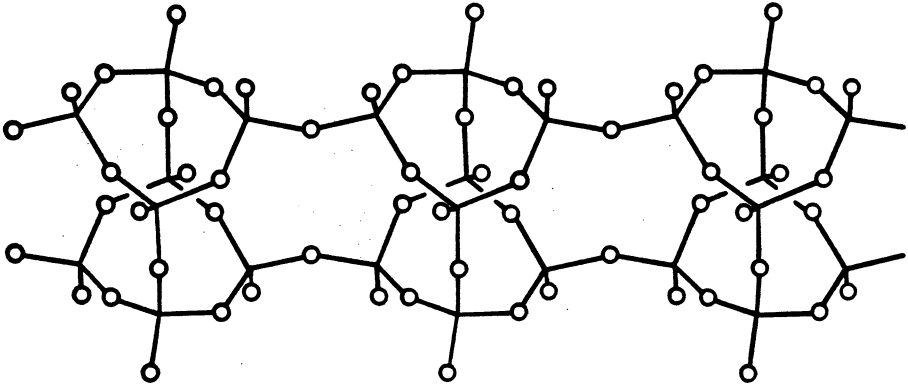


Figure 1. Silicate ion in litidionite. Junctions represent silicon atoms; circles represent oxygen atoms. (Reproduced from Ref. 7. Copyright 1981, American Chemical Society.)

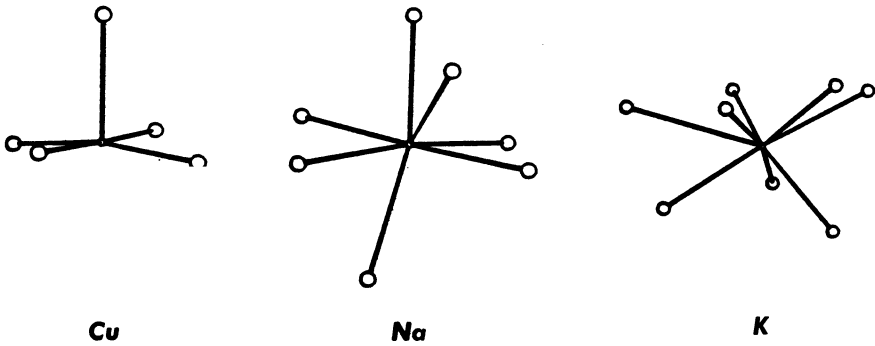


Figure 2. Coordination arrangements of the metal atoms in litidionite. Junctions represent metal ions; circles represent oxygen ions.

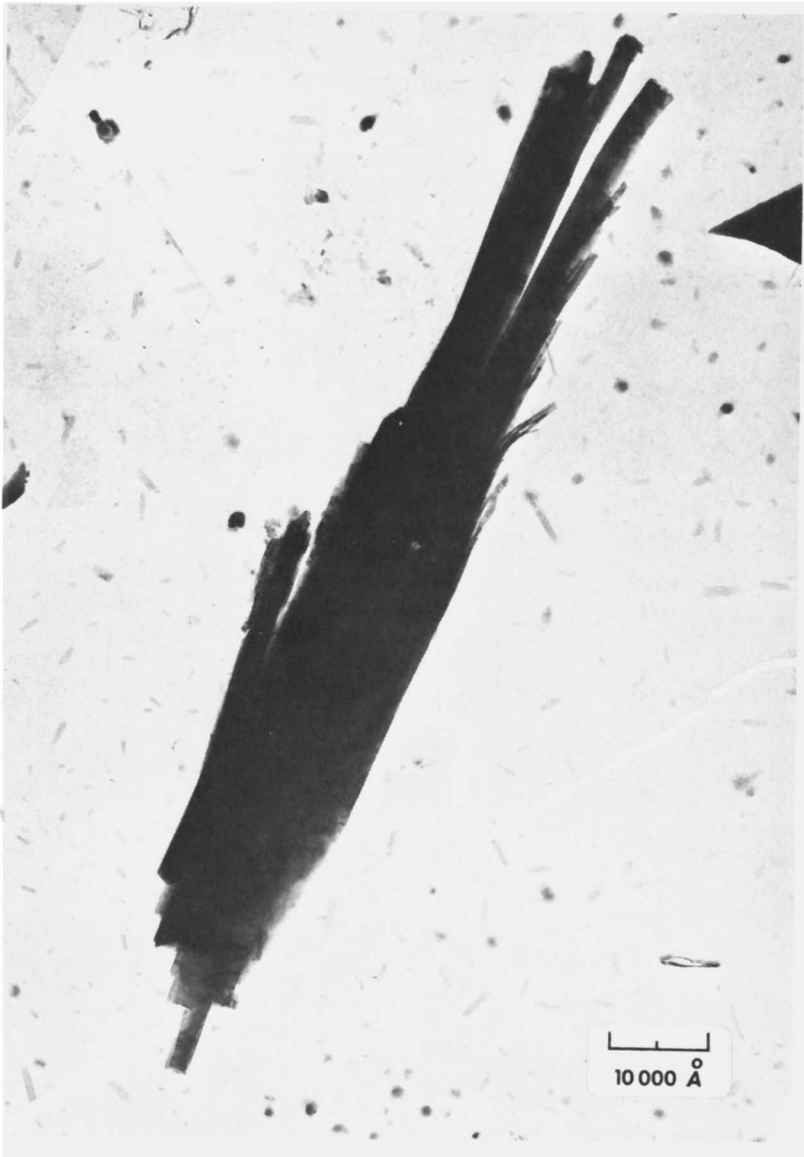


Figure 3. Transmission electron micrograph of a litidionite crystallite.

upper portion of the suspension. Generally multiple refractionations of the residue are necessary in order to get a sufficient amount of material.

The polymer has a waxy texture and is insoluble in a wide range of organic solvents. It does, however, form gel-like materials with solvents such as tetrahydrofuran, dioxane and chloroform. Not surprisingly in view of this, a mixture of a small amount of it and a large amount of a 1000 cs dimethylsilicone oil forms a stiff, stable grease. When purified the polymer is a very pale blue.

The infrared spectrum of the polymer shows SiMe_3 , SiOH , and SiOSi bands while its $\text{Si } 2p_{3/2}$ X-ray photoelectron spectrum shows overlapping SiO_4 and SiOC_3 peaks, Figure 4. Micrographs of the polymer show that it is composed at least in part of fibers, Figure 5, and that these fibers are flexible, Figure 6. Fibers that are 40-60 Å in diameter are commonly seen. A few with diameters somewhat above 20 Å are seen.

One sample was found to contain 14.08, 14.27 %C, 3.47 %H, and 38.93 %Si. The $\text{Si } 2p_{3/2}$ X-ray photoelectron spectrum of this sample indicated that the ratio of SiO_4 -type silicon to SiOC_3 -type silicon was 73:27, while the $\text{K } 1s_{1/2}$, $\text{Na } 1s_{1/2}$ and $\text{Cu } 2p_{3/2}$ spectra of it gave evidence for the presence of a small amount of potassium but no sodium or copper. The same sample gave the differential thermal analysis thermogram shown in Figure 7.

It is concluded on the basis of the available physical and synthetic evidence that some of the fibers in the polymer have frameworks that are like those of its parent silicate ion except for the presence of additional crosslinks, i.e., are at least semitubular in nature. It is further concluded that the rest of the fibers have composite frameworks built up of frameworks which are similar to those just described. These component frameworks, it is believed, are joined by well-spaced oxygen bridges. In the case of the sample of the polymer examined in detail, it seems probable that about 37% of the backbone silicon atoms carried silyl groups.

Further work along these same lines has shown that a polymer of the same general type carrying dimethylvinylsilyl groups can be made using an analogous synthesis. This polymer is of interest because the vinyl groups provide a potential site for the attachment of a wide variety of groups.

Other work has shown that a polymer that is apparently the same as the trimethylsilyl polymer can be made from another silicate. This silicate is the synthetic species $\text{Na}_2\text{CuSi}_4\text{O}_{10}$. It contains the same ladder or tube ion as does litidionite (9). As with litidionite it has been made by the hydrothermal technique (10, 11, 12).

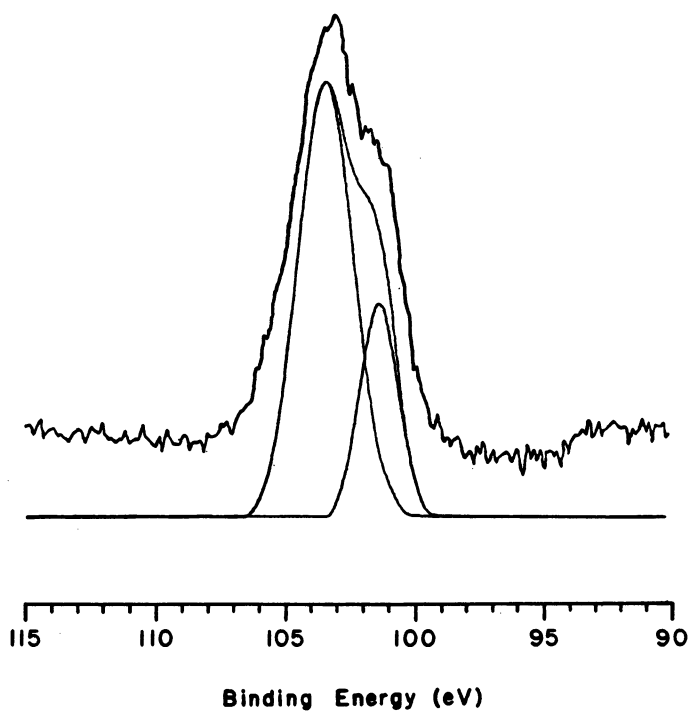


Figure 4. Si 2p_{3/2} X-ray photoelectron spectrum of the trimethylsilyl polymer, and the SiO₄ and SiOC₃ curves into which it can be resolved.

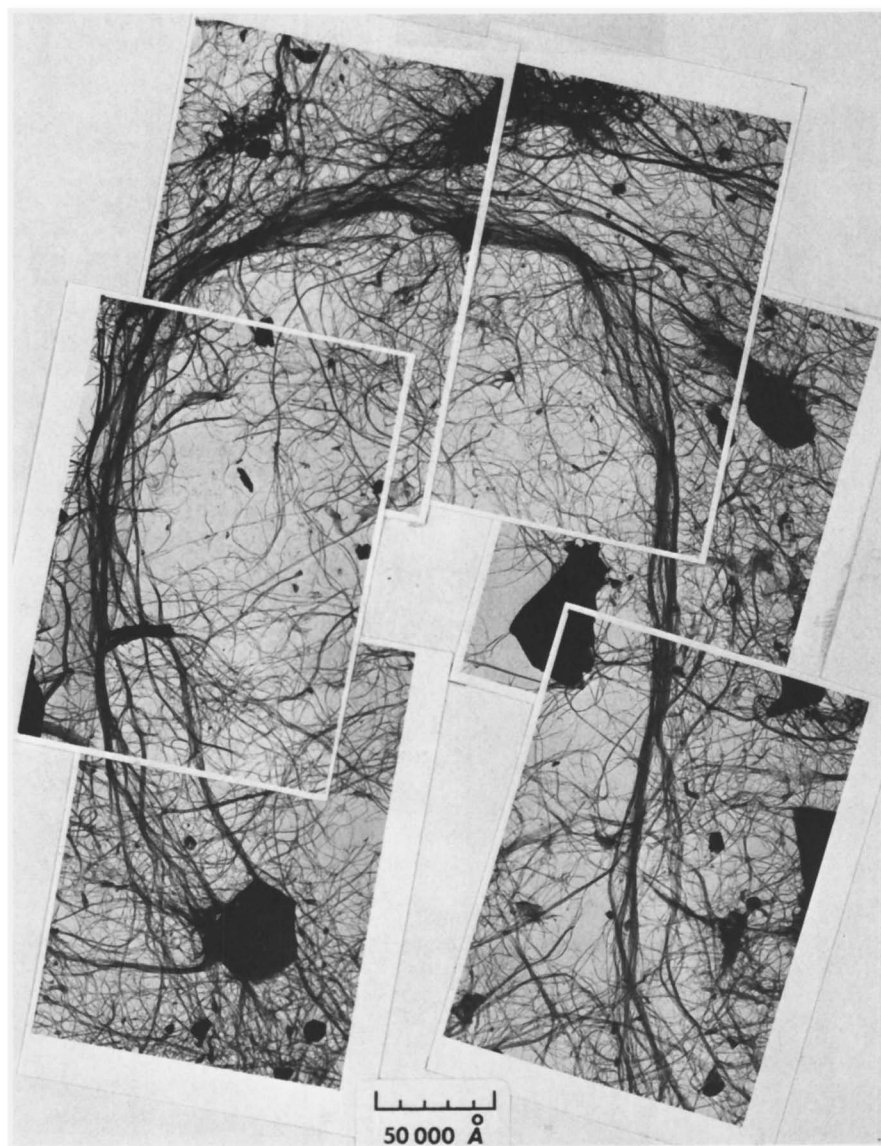


Figure 5. *Composite transmission electron micrograph of the trimethylsilyl polymer showing its fibrous nature.*



Figure 6. Transmission electron micrograph of the trimethylsilyl polymer showing the flexibility of its fibers.

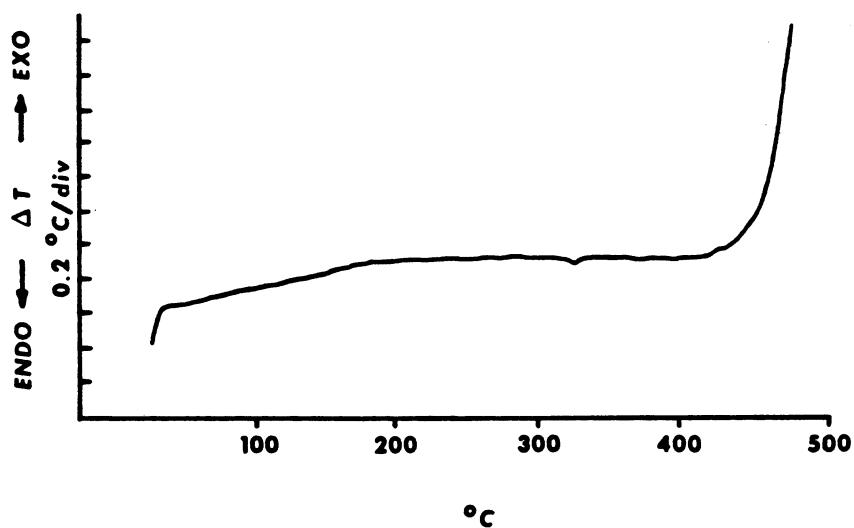


Figure 7. Differential thermal analysis thermogram of the trimethylsilyl polymer.

In the present work this silicate has been made by a procedure similar to the sintering procedure used to make litidionite. The polymer has been made from it by a route parallel to that used for making the trimethylsilyl polymer from litidionite.

Acknowledgment

We gratefully acknowledge the support of this work by Dow Corning Corporation and B.F. Goodrich Corporation Fellowships and by the Office of Naval Research.

Literature Cited

1. Lentz, C.W. Inorg. Chem. 1964, 3, 574-9.
2. Frazier, S.E.; Bedford, J.A.; Hower, J.; Kenney, M.E. Ibid. 1967, 6, 1693-6.
3. Fripiat, J.J.; Mendelovici, E. Bull. Soc. Chim. Fr. 1968, 483-92.
4. Linsky, J.P.; Paul, T.R.; Kenney, M.E. J. Polym. Sci., Polym. Phys. Ed. 1971, 9, 143-60.
5. Zambonini, F. "Mineralogia Vesuviana", 2nd ed.; S.I.E.M.: Naples, 1935, pp. 435-9.
6. Martin Pozas, J.M.; Rossi, G.; Tazzoli, V. Am. Mineral. 1975, 60, 471-4.
7. Hefter, J.; Kenney, M.E. J. Am. Chem. Soc. 1981, 103, 5929-30.
8. Guth, J.-L.; Kalt, A.; Perati, B.; Wey, R. C. R. Hebd. Seances Acad. Sci., Ser. D 1977, 285, 1221-4.
9. Kawamura, K.; Kawahara, A. Acta Crystallogr., Sect. B 1977, 33B, 1071-5.
10. Kornev, A.N.; Maksimov, B.A.; Lider, V.V.; Ilyukin, V.V.; Belov, N.V. Sov. Phys. Dokl. (Engl. Transl.) 1973, 17, 735-7; Dokl. Akad. Nauk. SSSR 1972, 205, 831-33.
11. Hubert, Y.; Guth, J.-L.; Perati, B.; Wey, R. C. R. Hebd. Seances Acad. Sci., Ser. D 1976, 283, 291-4.
12. Kawamura, K.; Kawahara, A.; Henmi, A. Kobutsugaku Zasshi 1976, 12, 403-14.

RECEIVED March 15, 1982.

Structure of Water Soluble Silicates with Complex Cations

YU. I. SMOLIN

Institute of Silicate Chemistry of the USSR Acad. Sci., Leningrad, USSR

The results of X-ray determinations of the crystal structures of silicates with complex cations are discussed. Watersoluble single crystals of silicates with Ni(en)_3 , Cu(en)_2 , Co(en)_3 , $\text{N(CH}_3)_4$ and $\text{N(C}_2\text{H}_5)_4$ cations have been studied. It is shown⁴ that in all structures determined the silicate anions have the form of double trigonal and tetragonal rings of the $[\text{Si}_6\text{O}_{15}]^{-6}$, $[\text{Si}_8\text{O}_{20}]^{-8}$ and $[\text{Si}_8\text{O}_{18}(\text{OH})_2]^{-6}$ compositions. The reasons of stability of these anions in aqueous solutions are discussed.

Among a small group of silicates that can be obtained from aqueous solutions at room temperature and normal pressure are silicates with complex cations. Silicates with chelate complexes of transition metals were first obtained by V. Molchanov and N. Prikhid'ko at the Institute of Silicate Chemistry (1). Silicates with alkylammonium cations were prepared in aqueous solutions by S. Glixelli and T. Krokowski (2) and D. Hoebbel and W. Wieker (3).

The characterization of the structure of these compounds is of considerable interest for the crystal chemistry of silicates. In most of the silicate structures the silicon-oxygen anion is joined to cations by sufficiently strong bonds. Because of this the size of cation plays the decisive role in the determination of the structure type due to the great capability of the configuration of the silicon-oxygen anion to adapt itself to cationic polyhedra. These

ideas were confirmed by many determinations of the silicate structures.

In their structure the silicates with complex cations represent a rare exception among a great number of silicate structures. The presence of large quantities of water in these compounds permits one to assume that anionic-cationic interactions occur with participation of water molecules via a system of hydrogen bonds. It is known that water molecules can adapt themselves well to either structural configuration therefore in the compounds studied the size and the form of the cation cannot influence considerably the geometry of the silicon-oxygen anion. Severe conditions determining this geometry in usual silicate structures may be significantly softened here. It could be expected therefore that the silicon-oxygen radicals in silicates with complex cations possess unusual configuration.

These considerations prompted a study of the structure of these compounds by methods of X-ray structural analysis. In recent years silicates with complex cations found also important practical application.

Cell parameters and intensity data for all crystals were obtained with a counter diffractometer using M α K monochromatic radiation. The structures were determined by three-dimensional Patterson and electron density syntheses and refined by least squares method with isotropic temperature factors for the silicate with chelate complexes and with anisotropic temperature factors for all others.

Table I shows the compositions and crystallographic data for the compounds studied. (It should be noted that the exact formulae of some of these compounds were unknown before since using chemical analysis only established that the Si/O ratio in these silicates was equal to 2:5). The formulae given are based on the X-ray structural analysis.

The crystal structure of the silicate Ni(en)₃ was determined using crystals obtained during the interaction of ethylenediamine solution of nickel hydroxide with a solution of silica in ethylenediamine. In air the crystals weather therefore they must be protected during the experiment.

The structure scheme is given in Figure 1 where the Z-coordinates of atoms are shown in hundred fractions of the period.

The silicate anion [Si₆O₁₅]⁻⁶ has the formal charge 6. It can be seen from Figure 2 that in the studied structure corresponding by analysis to the

Table I. Crystal data

Compound	Space Group	a (Å)		b (Å)		c (Å)		F(hkl) R %	
		α (°)	β (°)	γ (°)	δ (°)	ϵ (°)	ζ (°)		
$3 [\text{Ni}^{\text{II}}(\text{en})_3] \cdot \text{Si}_8\text{O}_{15} \cdot 26\text{H}_2\text{O}$	P6 ₃	16.375(5)	90	17.375(5)	90	15.185(5)	120	980	9.2
$4 [\text{Cu}^{\text{II}}(\text{en})_2] \cdot \text{Si}_8\text{O}_{20} \cdot 38\text{H}_2\text{O}$	PT	10.77(1)	106.03(5)	15.62(1)	110.30(5)	13.89(1)	72.08(5)	1990	8.9
$2 [\text{Co}^{\text{III}}(\text{en})_3] \cdot \text{Si}_8\text{O}_{18}(\text{OH})_2 \cdot 16.4\text{H}_2\text{O}$	P2 ₁ /n	20.48(1)	90	14.565(5)	94.73(5)	9.046(5)	90	1950	7.1
$8 [\text{N}(\text{CH}_3)_4] \cdot \text{Si}_8\text{O}_{20} \cdot 64 \cdot 8\text{H}_2\text{O}$	PT	15.62(1)	110.80(9)	15.56(1)	119.69(9)	15.98(1)	88.46(9)	4030	7.3
$8 [\text{N}(\text{C}_2\text{H}_5)_4] \cdot \text{Si}_6\text{O}_{15} \cdot 37\text{H}_2\text{O}$	P1	13.91(1)	96.12(8)	22.52(2)	99.89(8)	17.23(1)	94.66(8)	4300	8.6
$\text{Si}_8\text{O}_{20} \cdot [\text{Si}(\text{CH}_3)_3]_8$	P1	11.13(1)	97.97(8)	13.36(1)	84.03(8)	11.06(1)	102.30(8)	2100	7.7

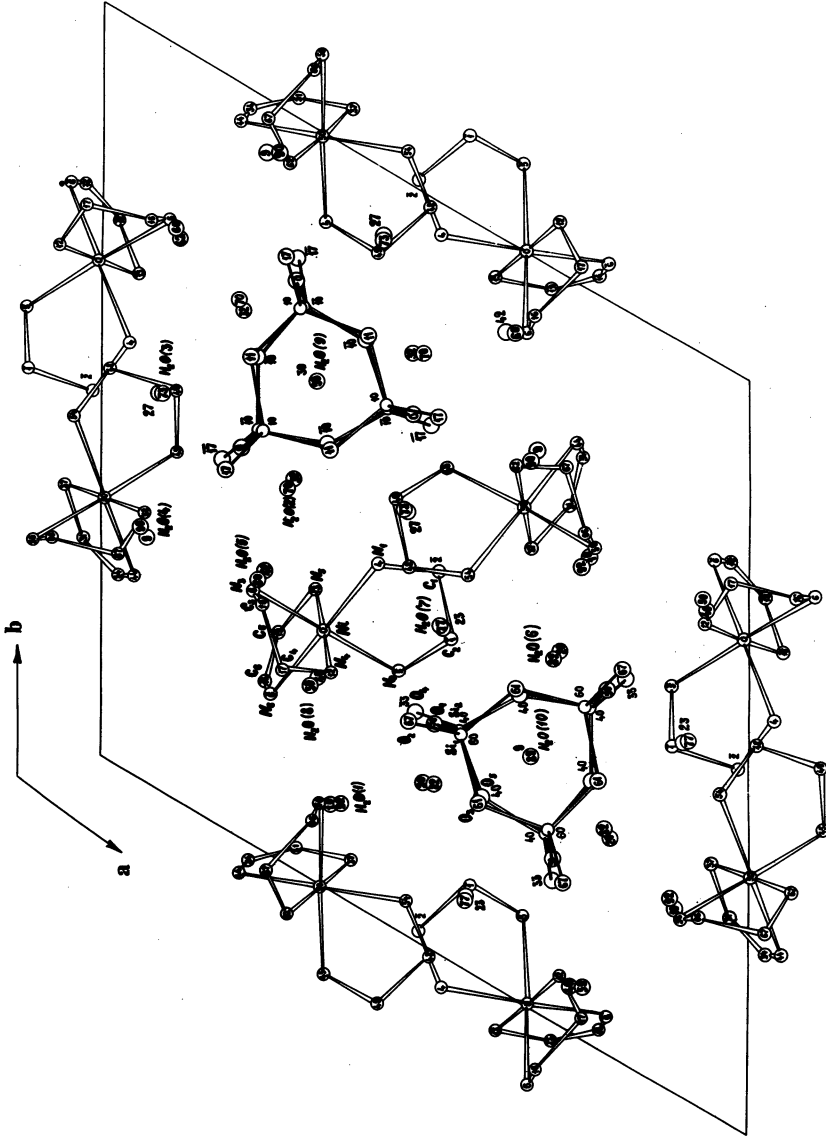


Figure 1. Projection of the $3[\text{Ni}(\text{en})_2] \cdot \text{Si}_6\text{O}_{18} \cdot 26\text{H}_2\text{O}$ structure along the c -axis. (Reproduced, with permission, from Ref. 4.)

formula of disilicate a new form of the silicon-oxygen radical not described earlier is realized, the double trigonal rings closed up around the threefold axis. The silicon atoms and the common oxygen atoms of the trigonal rings formed by three silicon-oxygen tetrahedra lie approximately in one plane. Two rings share common tops of the tetrahedra and form a double trigonal ring. As each tetrahedron has three common tops and one free top, the Si/O ratio will be equal to 2:5, with the gross formula of the ring Si_6O_{15} .

Figure 3 shows also the chelate complex of $\text{Ni}(\text{en})_3$ which has a gauche-gauche configuration and lll-conformation.

The cations and the silicate anions are attached to each other with a system of hydrogen bonds formed by the water molecules. Each terminal oxygen atom of the ring is bonded to three water molecules. The chelate complex is included in the system of hydrogen bonds through the NH_2 -groups (4).

Figure 4 is a schematic representation of the structure of the silicates with the copper ethylenediamine complex. It is seen that the nuclei of chelate complexes - copper atoms - occupy private positions at the centers of symmetry at the beginning of the coordinates and at the centers of all faces of the unit cell. The silicate anion is located in the center of the cell and can be better seen in Figure 5. This anion is composed of two rings, each built up of four silicon-oxygen tetrahedra. These two rings share four common tops yielding the double tetragonal ring. Thus, if the preceding structure was found to contain the double trigonal ring, in the given structure the silicon-oxygen radical is realized in the form of double tetragonal ring $[\text{Si}_8\text{O}_{20}]^{8-}$. A similar radical was earlier described only for the structure of ekanite.

The ethylenediamine complexes with atoms completing the coordination of the complex nucleus to the octahedron are shown in Figure 6. The coordination polyhedra of copper atoms have the form of elongated tetragonal dipyramids. The nitrogen atoms form an almost regular square at the bases of the pyramids. The copper-nitrogen distance is much shorter than that of the nucleus of the complex - the tops of the dipyramids. Such a form of the coordination polyhedra of copper atoms can be explained by the peculiarities of the electronic configuration of the divalent copper atom and is described in many structure determinations.

The water molecules are joined in a three-dimen-

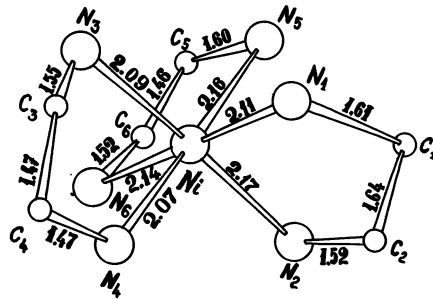


Figure 3. $Ni(NH_2CH_2CH_2NH_2)_3$ complex. (Reproduced, with permission, from Ref. 4.)

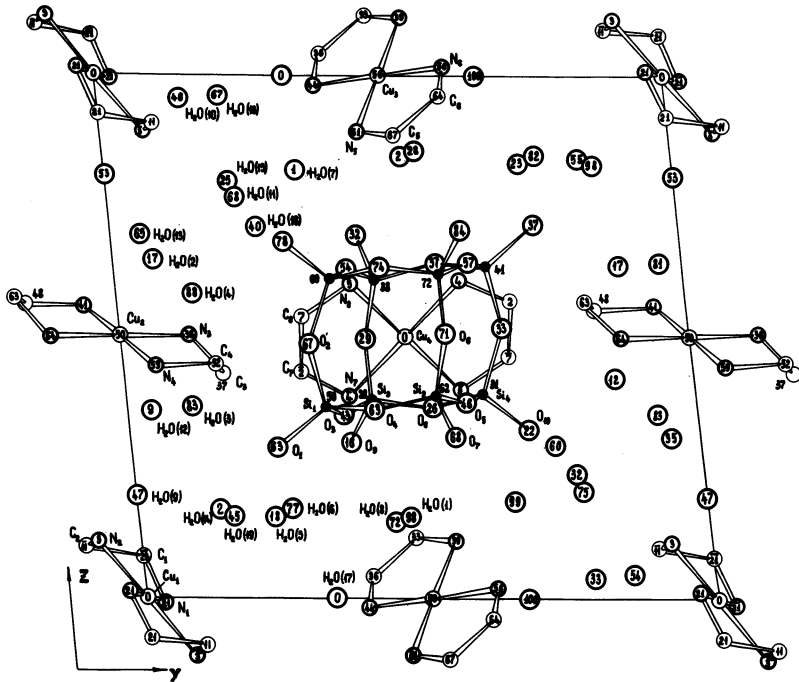


Figure 4. Projection of the $4[Cu(en)_2] \cdot Si_8O_{20} \cdot 38H_2O$ structure along the *a*-axis. (Reproduced, with permission, from Ref. 5.)

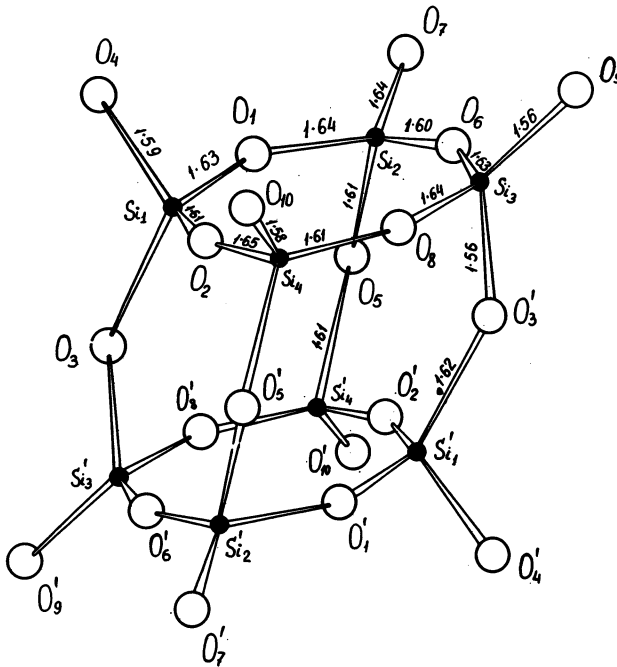


Figure 5. Silicate anion $[\text{Si}_8\text{O}_{20}]^{8-}$, the double tetragonal ring. (Reproduced, with permission, from Ref. 5.)

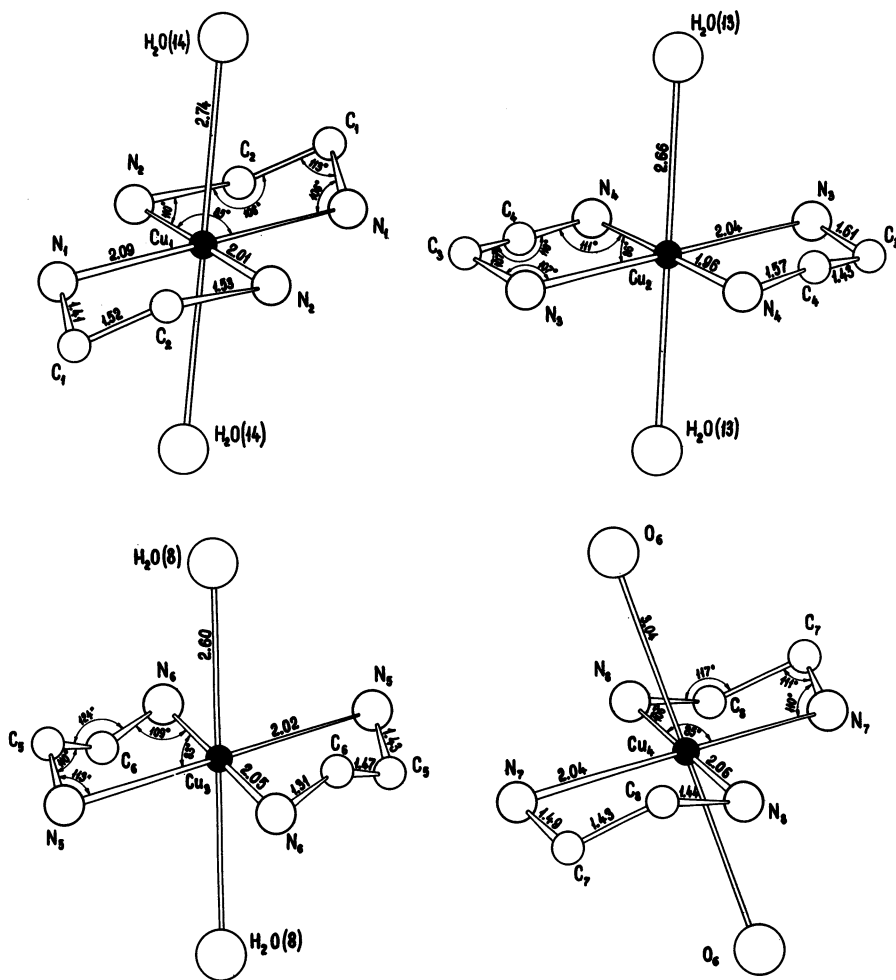


Figure 6. $\text{Cu}(\text{en})_2$ complex. (Reproduced, with permission, from Ref. 5.)

sional network by a system of hydrogen bonds which includes the ligand NH_2 groups and the terminal oxygen rings (5).

Figure 7 shows the structure of $\text{Co}(\text{en})_3$ silicate. Crystals of this compound utilized for X-ray analysis were obtained by D. Hoebbel and W. Wieker by the reaction of an aqueous solution of cobalt ethylenediamine hydroxide with a solution of tetramethylsilane in methanol (6).

The hydrogen atoms were also localized in this structure which is of great significance here as it followed from the results obtained that the silicon-oxygen anion, which was first represented in the form of double ring $[\text{Si}_8\text{O}_{20}]^{-8}$ and two additional $\text{Co}(\text{en})_3$ complexes with the +3 charge, are not compensated by charges.

Figure 8 shows the silicon-oxygen anion which in the given structure also consists of two rings, each being built out of four silicon-oxygen tetrahedra. These rings are joined by common tops in a double tetragonal ring and hydrogen atoms are bonded to two free oxygen atoms. Thus, the localization of hydrogen atoms established the existence of the acidic silicate anion $\text{Si}_8\text{O}_{18}(\text{OH})_2^{-6}$ in the crystal studied. Each such ring forms 2 hydrogen bonds with translational-equivalent rings along the c-axis thus building up infinite columns composed of acid radicals which are joined to each other by hydrogen bonds.

The chelate complexes and water molecules are located between these columns and connect them both electrostatically and through the system of hydrogen bonds.

The chelate complex is shown in Figure 9. As the crystal is centrosymmetric, d and l forms of optically active $\text{Co}(\text{en})_3$ are present in the structure in equal amounts. The atom of cobalt is in an almost regular octahedron composed of nitrogen atoms. Each atom of chelate cycle is located in the tetrahedron two tops of which are occupied by the neighbouring atoms of the ethylenediamine ring and the two others by the hydrogen atoms.

The crystal structure of tetramethylammonium silicate of the composition $8[\text{N}(\text{OH})_3] \cdot \text{Si}_8\text{O}_{20} \cdot 64\text{H}_2\text{O}$ was then determined. The crystals studied were obtained by D. Hoebbel and W. Wieker by a method in which colloidal silica was dissolved in an aqueous solution of tetramethylammonium hydroxide (7). The crystallization was carried out with a slow increase in solution concentration. The structure determination was made at a temperature of -100°C . The use of low-temperature

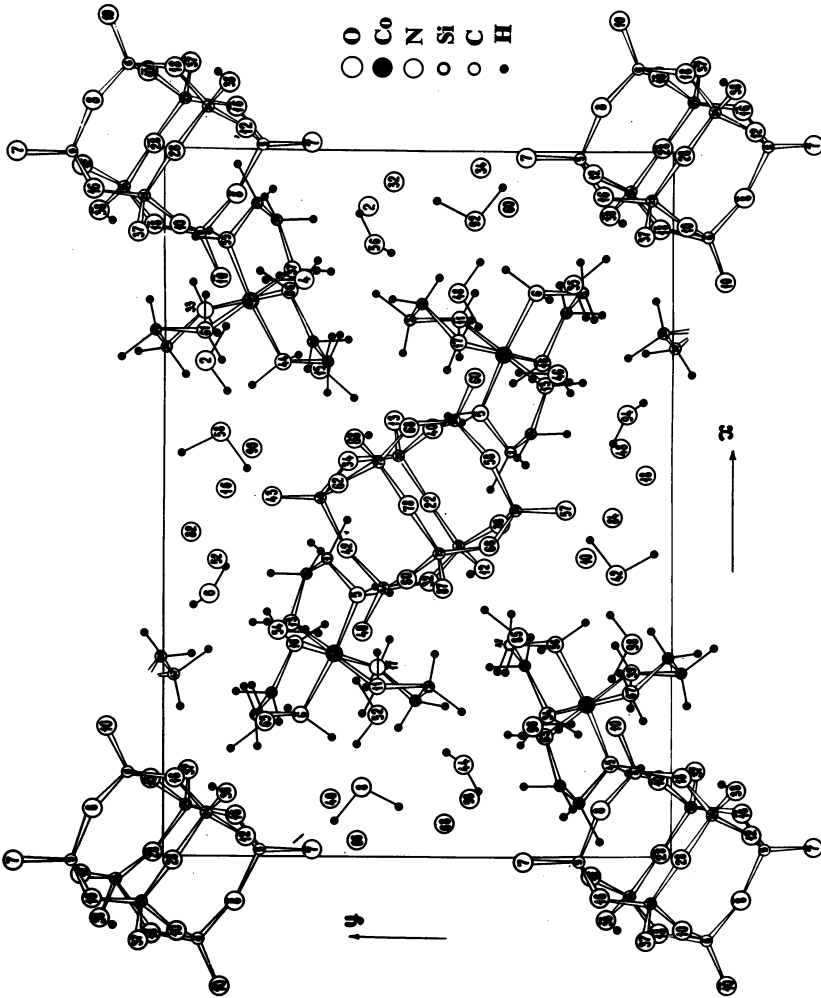


Figure 7. Projection of the $2[\text{Co}(\text{en})_3] \cdot \text{Si}_8\text{O}_{18}(\text{OH})_2 \cdot 16.4\text{H}_2\text{O}$ structure along the c -axis. (Reproduced, with permission, from Ref. 6.)

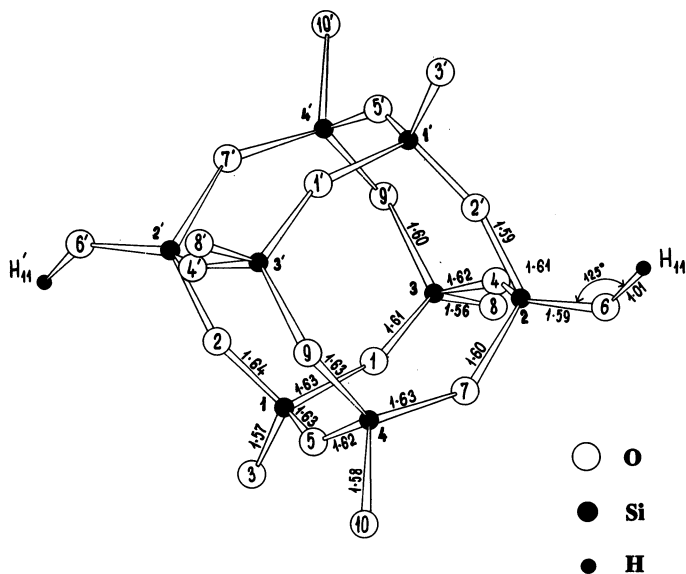


Figure 8. Silicate anion $[Si_8O_{18}(OH)_2]^{6-}$. (Reproduced, with permission, from Ref. 6.)

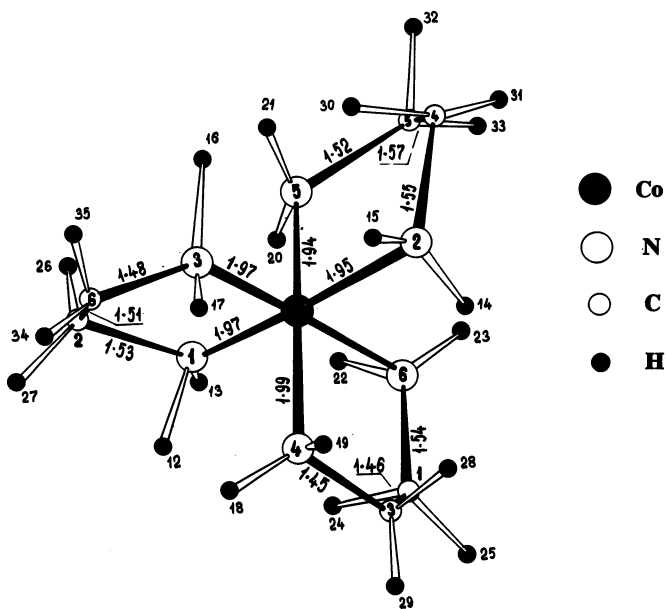


Figure 9. $Co(en)_3$ complex. (Reproduced, with permission, from Ref. 6.)

mechanics was necessary here, firstly, for preservation of the crystal which easily evaporates at room temperature and, secondly, for the greater accuracy of structure determination at the expense of a decrease of the amplitude of thermal vibrations of the crystal atoms. It should be pointed out here that the methyl groups possess a high amplitude of thermal vibrations at room temperature.

In Figure 10 the atoms are shown by ellipsoids of thermal vibrations. In this structure, like the two above-mentioned structures, the silicon-oxygen tetrahedra, each joined by three tops to other tetrahedra, form a double tetragonal ring Si_8O_{20} which is better seen in Figure 11.

The distribution of cations around the large anion $[\text{Si}_8\text{O}_{20}]^{-8}$ should be considered as an interesting and significant feature of this structure. In most inorganic structures the cations are approximately equally removed from anions. In a given case six of the eight tetramethylammonium groups surround the anion octahedrally, the nitrogen atom of each of these complexes being located on the straight line passing through the anion center and the center of each tetragonal ring of the Si_8O_{20} group. These six tetramethylammonium complexes are joined directly to the anion thus forming the $6[\text{N}(\text{CH}_3)_4]\text{Si}_8\text{O}_{20}$ group with the formal charge -2. The two other Si_8O_{20} cations are located between these groups and connect them with each other.

Figure 12 shows the structure of tetraethylammonium silicate. The crystals were obtained from solution prepared by dissolution of precipitated silica in an aqueous, approximately unimolar solution of tetraethylammonium hydroxide (8). As seen from Figure 12, the silicon-oxygen radical is represented here by the double trigonal ring. In Figure 13 this anion with the formal charge -6 is shown separately. Like the structure of tetramethylammonium silicate, five of the six cations surround the pentahedral anion and the remaining cation connects these groups with each other. The water molecules also form here a three-dimensional system of hydrogen bonds.

It seems reasonable to assume that similar groups can also exist in solutions of alkylammonium silicates and that such surrounding of the silicate anion by complex cations protects it from being destroyed by water molecules.

Studies of aqueous solutions of these silicates made by Hoebbel and Wieker (9) using paper chromatography show the existence of silicate groupings main-

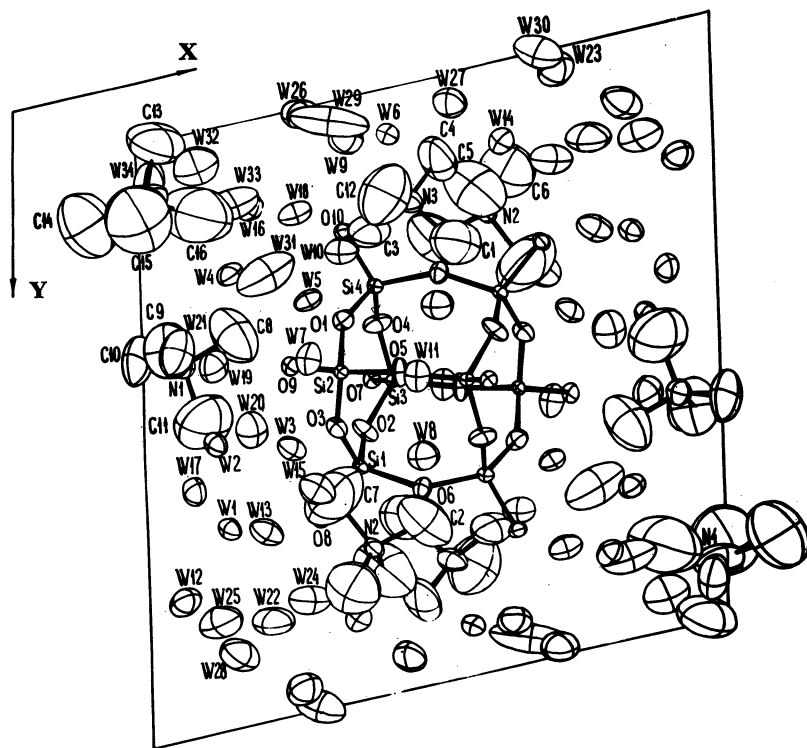


Figure 10. Projection of the $8[N(CH_3)_4] \cdot Si_8O_{20} \cdot 64.8H_2O$ structure along the *c*-axis. (Reproduced, with permission, from Ref. 7.)

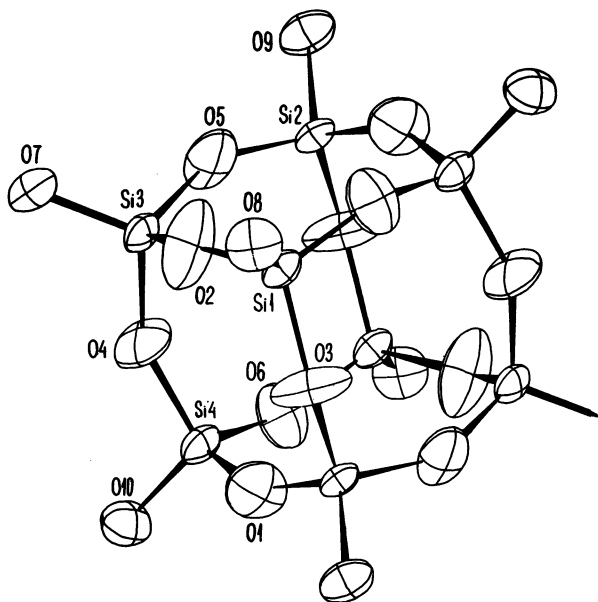


Figure 11. $[\text{Si}_8\text{O}_{20}]^{8-}$ radical in the tetramethylammonium silicate. (Reproduced, with permission, from Ref. 7.)

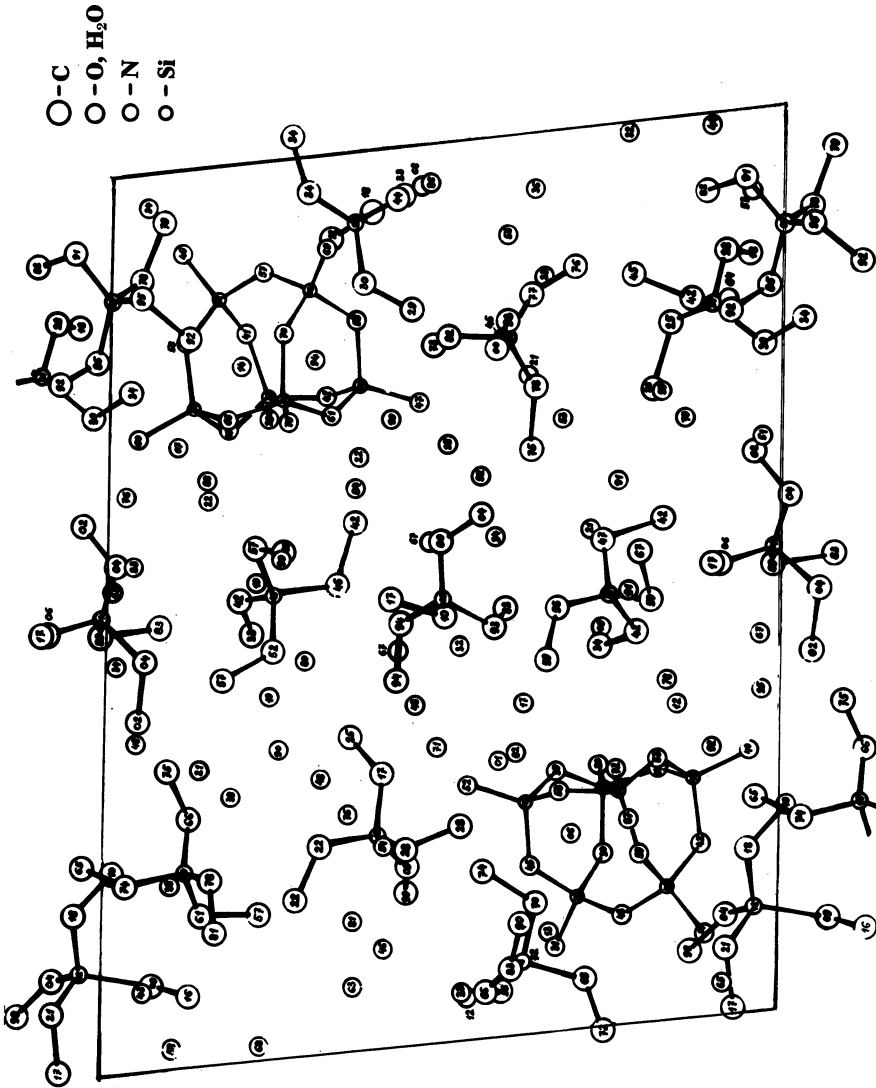


Figure 12. Projection of the $6[\text{N}(\text{C}_2\text{H}_5)_3] \cdot \text{Si}_6\text{O}_{15} \cdot 37\text{H}_2\text{O}$ structure along the a -axis.

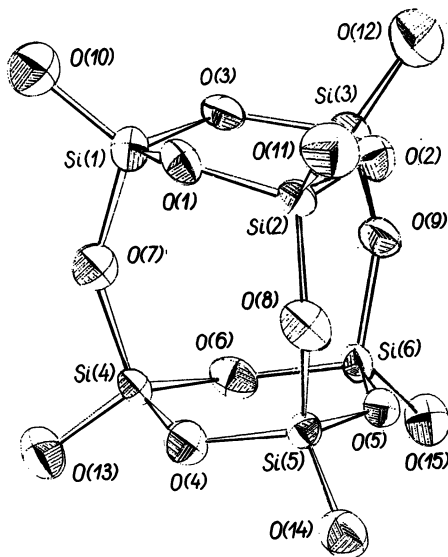


Figure 13. $[\text{Si}_6\text{O}_{16}]^{-6}$ radical in the tetraethylammonium silicate.

ly of the same structure as has been found in the corresponding crystals. This finding can be used for the synthesis of new compounds. The crystal structure of a molecular crystal obtained from solution of tetramethylammonium silicate by bonding of trimethylsilyl groups to the silicon-oxygen radicals was determined by us at a temperature of -110°C . The crystals of this compound are insoluble in water, transparent and stable in air.

Figure 14 shows the molecule of this compound. As can be seen, it has a nucleus representing the double tetragonal ring Si_8O_{20} close in structure to the silicon-oxygen radical of the primary product - the tetramethylammonium silicate. The trimethylammonium groups are bonded to the free tops of the ring tetrahedra.

It is obvious that the use of silicate radicals stable in solution may serve as a way to the synthesis of several new compounds. In this connection of special interest is the work of E. Flanigen et al(10) who managed to obtain a new zeolite-type form of silica under hydrothermal condition from solution of colloidal silica in aqueous solution of tetrapropylammonium hydroxide.

It can be expected that the use of silicates with complex cations and their solutions will permit one to obtain in the nearest future some compounds of great importance for chemical technology.

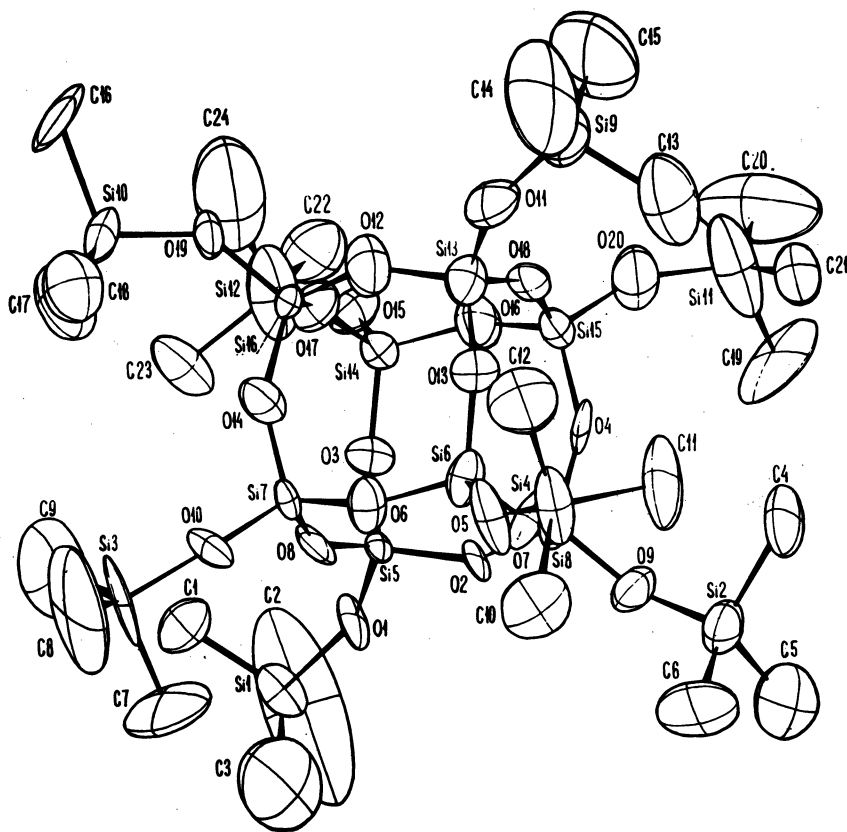


Figure 14. $\text{Si}_8\text{O}_{20} \cdot [\text{Si}(\text{CH}_3)_3]_8$ molecule.

Literature Cited

1. Prikhid'ko, N.E.; Molchanov, V.S. Dokl. Akad. Nauk SSSR 1952, 86, 83-6.
2. Glixelli, S.; Krokowski, T. Roczn. Chem. 1937, 17, 309-16.
3. Hoebbel, D.; Wieker, W. Z. anorg. allg. Chem. 1971, 384, 43-52.
4. Smolin, Yu.I. Kristallografiya 1970, 15, 31-7.
5. Smolin, Yu.I.; Shepelev, Yu.F.; Butikova, I.K. Kristallografiya 1972, 17, 15-21.
6. Smolin, Yu.I., Shepelev, Yu.F.; Pomes, R.; Hoebbel, D.; Wieker, W. Kristallografiya 1975, 20, 917-24.
7. Smolin, Yu.I.; Shepelev, Yu.F.; Pomes, R.; Hoebbel, D.; Wieker, W. Kristallografiya 1979, 24, 38-44.
8. Hoebbel, D.; Garzo, G.; Engelhardt, G.; Ebert, R.; Lippmaa, E.; Alla, M. Z. anorg. allg. Chem. 1980, 465, 15-33.
9. Wieker, W.; Hoebbel, D. Z. anorg. allg. Chem. 1969, 366, 139-51.
10. Flanigen, E.M.; Bennet, J.M.; Grose, R.W.; Cohen, J.P.; Patton, R.L.; Kirchner, R.M.; Smith, J.V. Nature 1978, 271, 512-16.

RECEIVED March 14, 1982.

INDEX

A

AA—*See* Atomic absorption
 Absorption onto dehydration
 core sand 262–267
 Absorption onto silica particles
 of alkali ions 95
 Acid and alkaline flooding 215–224
 Acid-base equilibria 115–116
 Acid
 molybdc, reaction with sodium
 silicate 97
 monosilicic 63, 104
 pH concentration, and reaction
 rate 120–124
 second-order rate constant for
 dimerization 90, 92*f*
 polysilicic, silicon-29 NMR spectra
 ethyl esters 77*f*
 silicic
 aqueous methanolic solution 84, 90, 91*f*
 dissociation 155
 polymerization 116, 120
 silicate conversion 97
 Acid complex, silicomolybdate,
 spectroscopic detection in
 visible spectrum 19–21
 Acidified methanol, proton
 exchange 178–179
 Acidity
 of solvated silicate
 species 135–136, 144–146
 and stability boundary 127
 Acidity constant 135–136, 144–146
 Acid solution 102–106
 aging and rate constant 99
 polymerization 120
 Activation enthalpy 172–173
 Activity
 hydrogen ion, measurement 137
 metal ion 138–146
 surfactant, hardness ion 202
 Activity coefficient, diffusion kinetics
 for dealkalinization 281–282
 Adhesive applications 8, 10
 Adsorption
 dynamics 172–177
 onto gel, and hydrogen bond
 acceptor molecules 171
 of methanol 173
 proton exchange 178–179

Adsorption—*Continued*

 of rare gases 170
 reversible, and nonreversible
 chemical consumption 233–235
 and valence of metal ions 135–146
 Aerosol surface, methoxylation 171
 African sand 278
 Agencies, Public Health 58–61
 Aging of amorphous silica in salt
 water solutions 149–163
 Aging of silicic acid sols 99
 Aging time, and polymerization
 degree 166
 Algae 65–67
 Alkali
 interaction of rock minerals in
 reservoir sand 233
 titration determination 18–19
 Alkali content and dealkalinization
 temperature, hydrosilicate
 porosity as function 286*f*–287*f*
 Alkali ion(s)
 absorption onto silica particles 95
 atomic spectrometry 19–21
 flame photometry 19–21
 Alkaline condition, colloid
 formation 124–129
 Alkaline consumption
 minerals and sand, static equi-
 librium studies 231*f*
 petroleum reservoir sands 227–250
 Alkaline flooding
 Enhanced Oil Recovery 187–224
 sodium hydroxide and sodium
 orthosilicate consumption 227–250
 Alkaline hydrous sodium polysilicate
 materials 38–41
 Alkaline interfacial tension
 reduction 201*f*
 Alkaline irritation 59
 Alkaline silicate solution,
 silicon-29 NMR 79–90
 Alkaline slug, porosity 219*f*
 Alkaline waterflooding of heavy crude
 oils, emulsification phe-
 nomena 215–224
 Alkalinity and health and safety 32, 49–67
 Alkali silicate
 detection 21–25
 and detergents 10–12

- Alkali silicate—*Continued*
 glasses, silicon-oxygen bond 26-27
 preparation, and historical
 perspective 3-11
 Alkoxide, in glass technology 293-303
 Alkyl esters of polysilicic acid,
 NMR studies 75
 Alumina impurities 21-25
 Aluminum
 corrosion 273-274
 spectral lines 23, 24*t*
 Aluminum casting
 dehydrated sodium silicate
 bound core sand 251-270
 high temperature properties and
 collapsibility of sand from 267-268
 Aminoil LMZ sand 232*t*, 235-244
 Ammonia adsorption onto gels 178-179
 Ammonium molybdate, reaction with
 sodium silicate 97-101
 Amorphous silica
 monolithic dried gel 302*f*
 solubility 116, 117*f*
 solubility and aging in salt water
 solution 149-163
 Anhydrous sodium silicate glasses 277-278
 Animal studies
 aquatic toxicity 65, 66*t*
 dogs, renal threshold 54
 hamsters, inhalation 62
 nitrogen and phosphorus retention .. 54*f*
 rabbits
 esophageal test 55*t*
 skin contact 58-59
 rats
 lethal dose 50-51
 reproductive system 57*t*
 Anionic detection, impurities in
 alkali silicates 21-25
 ANSI Standard 33
 Application
 commercial, zeolite 272
 silicon alkoxide gel 301-303
 Aquatic toxicity 65, 66*t*
 Aqueous solutions 63
 methanolic solution of silicic
 acids 84, 90, 91*f*
 silicate solution, kinetics 80-90
 Arson plasma emission
 spectroscopy (PES) 21-25
 Arrhenius plots 173
 Artificial seawater, solution
 studies 160
 Asbestos chrysotile 169-170
 Ash, soda 5
 Asphaltum 4
 Assays of soluble silicates 18-21
 Atomic absorption (AA) 19-25
 Atomic ratios, tetrabutylammonium
 hydrogen silicate 310, 314
 Atomic spectrometric determinations
 of alkali ion 19-21
 Atomized liquid silicate 10
 Automated determination in de-
 tergents using spectroscopy 19-21
- B**
- Base, ammonia adsorption 178
 Base exchange gel for softening water 12
 Berea Sandstone 228-232
 BET surface area determina-
 tions 156, 166-167
 Binder for foundry cores 251-270
 Binding energy (EV) 27*f*
 Biogenic silica 158-162
 Biological testing 49-62
 Bleach 274
 Blue-green algae 65-67
 Bond, Si-O-Mg 170
 Bond length in tetrahedron 166
 Bond strength, hydrogen 171
 Borax 10, 12
 Bound
 dehydrated sodium silicate,
 core sand for aluminum
 casting 251-270
 sand storage stability 260-267
 sand strength 255-260
 Branching units 73-78
 Bridging and nonbridging oxygens ... 26-27
 Brine 217
 Brucite form of magnesium
 hydroxide 140-141
 Buffering characteristics 41
 Building units of polymeric siloxane .. 73-74
 Burns 59
- C**
- Cadmium ion and adsorption 135
 Caking in storage, detergents 274-275
 Calcite, alkaline consumption min-
 erals and sand, static equilib-
 rium studies 231*t*
 Calcium ion
 and adsorption 135-139, 144
 concentration, and electrode
 potential, surfactant-
 alkali systems 203*f*
 impurities 21-25
 spectral lines 23, 24*t*
 and water hardness in detergents ... 272
 Capping, with trimethylsilyl
 (TMS) groups 118-119
 Carbon, discoloration by, prevention .. 6
 Carbon dioxide-silicate process 255
 Carbonate impurities 21-25
 Carcinogenicity 58

- Casting
 aluminum
 dehydrated sodium silicate
 bound core sand251-270
 high temperature properties and
 collapsibility of sand
 from267-268
 monolithic shapes 301
- Cation(s)
 degree of polymerization, effect of
 interactions133-147
 detection, impurities in alkali
 silicates21-25
 multivalent metal 202
 size influence 306
- Caustic consumption of reservoir
 sand, static equilibrium experi-
 ments 230f
- Caustic solutions by petroleum
 reservoir sand, long term
 consumption227-250
- Cell
 F load260-262
 quartz 179
- Chain, tetrahedron 124
- Change rock surface wettability 217
- Channeling phenomena, emulsions 218, 223
- Characterization of silicate species 119t
- Chemical composition and properties,
 tetrabutylammonium hydrogen
 silicate310-312
- Chemical flooding processes for
 recovery of crude oil187-211
- Chloride impurities21-25
- Chlorite, alkaline consumption min-
 erals and sand, static equilib-
 rium studies 231t
- Chromatography, ion21-25
- Chrysotile, asbestos169-170
- Clay, montmorillonite202, 204f, 206
- Cleaning of food contact surfaces40-41
- Cloud point of a solution and
 tergents of a nonionic surfactant 273
- Coated sand worklife252-254
- Cold trap, mercury vapor 23
- Collapsibility and high temperature
 properties of sand from alumi-
 num castings267-268
- Colloidal solution135-146
 components95-112
 formation116, 119, 124-129
 polymer, tetrahydrofuran
 extraction99-101, 108-110
 ultrafiltration 129t
- Color, of precipitates141, 144
- Commercial aspects and history of
 manufacture 3-13
- Commercial preparations
 impurity levels 45t
 NMR studies73-78
- Companies, manufacture of soluble
 silicates 3-13
- Comoposite transmission electron
 micrograph, trimethylsilyl
 polymer325f, 326f
- Concentrated silicates and dilute
 silicic acid102-104
- Concentration
 effluent, long term flow study238-242
 and solubility in salt water150-155
- Condensation polymerization,
 silicon alkoxides297-301
- Connectivity (Q)119, 121, 125f
- Consolidation, reconstitution of
 hydratable sodium silicate
 glasses280, 285
- Consumer products 38
- Consumer Product Safety Commission 58
- Consumer Product Safety Commission
 and ingestion 54
- Consumption
 alkaline, minerals and sand, static
 equilibrium studies 231t
 long term, of caustic solutions by
 petroleum reservoir sands227-250
 reversible adsorption and non-
 reversible chemical233-235
 of sodium hydroxide, and ortho-
 silicate alkalinity, THUMS
 Ranger sand234f, 236f
- Convex faces, tetrabutylammonium
 hydrogen silicate 308f
- Coordination shell 321f
 metal atoms in litidionite 81-90
 and symmetry81-90
- Copper ion
 and adsorption135, 137, 141-145
 in solution equilibria 141
- Core production from coated
 sand253-255
- Core sand for aluminum casting,
 dehydrated sodium silicate251-270
- Corrosion control and detergent273-274
- Corrosion inhibitor in drinking
 water39-41
- Corrosivity and safety regulation43-44
- CO₂-silicate process 255
- Coupling constant, quadrupole 176
- Cristabolite 166
- Cristabolite, silicon-29 NMR81, 83-90
- Crude oil
 in chemical flooding processes
 for recovery187-211
 heavy, emulsification phenomena
 in alkaline waterflooding215-224
 Huntington Beach216-219
 Wilmington Field190t, 216-219
- Crystallinity
 hydrated sodium metasilicates,
 phase relationship10-11

Crystallinity—*Continued*

- litidionite, transmission electron micrograph 320, 322f
 quartz 63
 Crystallographic properties, tetra-butylammonium hydrogen silicate 306–310
 Cubic octamer 110
 Cubic octamer, silicon-29 NMR 81, 83–90
 Cyclic, silica 64f
 Cyclic tetramer, silicon-29 NMR 81, 83–90
 Cyclic tetramer of monosilicic acid, concentration and reaction rate .. 120
 Cyclic trimer, silicon-29 NMR 84, 87–90

D

- Dealkalization
 kinetics 278–284
 temperature, hydrosilicate porosity as function of alkali content 286f–287f
 Degree of polymerization 124
 aging time and pH effects 166
 cation interactions 133–147
 Dehydrated sodium silicate bound core sand for aluminum casting 251–270
 Dehydration, sand 255
 Density
 high bulk, sand bodies 257
 of silica surface 156–163
 of silanol group surface 170
 Depth profiles of hydrogen and sodium in glass 29f
 Derivative, tetrabutylammonium hydrogen silicate 312–317
 Dermatitis 59
 Desiccant gel 12
 Detection limit for impurity analysis in silicates 21–22
 Detergent(s)
 and alkaline silicates 10–12
 liquid, and storage stability 273
 low-phosphate and phosphate-free 38
 review of silicates in 271–275
 safety regulations 31–46
 using spectroscopy, automated determination of silicate 19–21
 Diameter, pore 112–113, 156–163
 alkali/surfactant interactions 206
 ultrafiltration 110–112
 Diatoms 65–67
 Diet and silicate 54–58
 Differential Scanning Calorimetry curves (DSC) 312–315
 Differential thermal analysis thermogram, trimethylsilyl polymer 327f

- Diffusion coefficient
 dealkylation 278–280
 surface 175f
 Diffusion kinetics for dealkalization .. 281
 Digestion 58
 Dilute silicic acids from concentrated silicates 102–104
 Dilute solutions 95–96, 101–107
 Dimer, silicon-29 NMR 81, 83–90
 Dimerization of monosilicic acid, second-order rate constant 90, 92f
 Discoloration by carbon, prevention using oxidizing agent 6
 Dissociation constant, and stability boundary 127
 Dissolution of amorphous silica, equilibrium constant 155
 Dissolution rate in salt water 158f
 Distribution of silanol groups on silica surfaces 167, 169–172
 Divalent ion solution activity 144
 Dolomite, alkaline consumption minerals and sand, static equilibrium studies 231f
 Dose, lethal, sodium silicate
 in man 54
 in rats 50–51
 DOT—*See* US Department of Transportation
 Double resonance, homonuclear 84
 Draiz method 58–59
 Drying of monolithic shapes 301
 DSC—*See* Differential Scanning Calorimetry
 Dynamics of adsorption processes on silica gel surfaces 172–177

E

- EOR—*See* Enhanced Oil Recovery
 Effluent concentration, long term flow study 238–242
 Egg preservation 10, 39
 Electrical field gradient interaction, quadrupole-inner 176
 Electrode(s), ion selective 21–25
 sodium ion 280
 specifications 136–137
 surfactant sensitive 202
 Electrode potential and calcium concentration, surfactant/alkali systems 203f
 Electron micrograph
 composite transmission, trimethylsilyl polymer 325f–326f
 transmission, litidionite crystallite 320, 322f
 Electron spectroscopy for chemical analysis (ESCA) 26–27, 179

- EMF data for metal ion solutions 137
- Emulsification phenomena in alkaline waterflooding of heavy crude oils 215-224
- Enhanced oil recovery, sodium hydroxide and sodium orthosilicate consumption 227-250
- Enrichment in silicon-29 NMR 80-90
- Enthalpy, activation 172-173
- Environmental chemistry 63-65
- Environmental effects 31-32, 41-44, 49-62, 67
- Environmental Protection Agency (EPA) 41-46
- Equilibria
 acid-base 115-116
 copper ions in solution 141
 diffusion kinetics for dealkylation 281-285
 dissolution of amorphous silica 155
 oligomeric species, silicon-29 NMR 79-92
 silicate building units 77-78
 static, experiments, caustic consumption of reservoir sand 230f
- ESCA—*See* Electron spectroscopy for chemical analysis
- Esophageal test, rabbit 54-55
- Ester
 ethyl, of polysilic acid, silicon-29 NMR spectra 77
 silicate, NMR studies 73-78
- Esterification of silanol group 171, 172
- Ethylenediamine addition, tetrabutylammonium hydrogen silicate 312-314
- Ethyl esters of polysilicic acids, silicon-29 NMR spectra 77f
- Exchange gels 12
- Excretion, urinary, of sodium silicate in rats 56-58
- Exposure, human 59-61
- Extraction of colloidal polymer, tetrahydrofuran 99-101, 108-110
- Extraction-substitution process, Lentz-type 320
- Eye contact 33, 59-61
- F**
- Face-centered cubic 305
- FDA—*See* Food and Drug Administration
- Federal Food, Drug, and Cosmetic Act 39
- Federal Hazardous Materials Transportation Act and skin contact 58-59
- Federal Hazardous Substance Act 38, 58-59
- Federal regulatory status of soluble silicates 31-46
- Federal Water Pollution Control Act 43
- Fiber, of refractory compositions, silicon alkoxide gels 301
- Fibrous organosilicon polymer 319-328
- Fick's Law, diffusion kinetics for dealkalization 283
- First order rate constant, sodium silicate reaction with molybdc acid 97
- Flame atomic absorption 21-25
- Flame photometry, alkali metals 19-21
- F load cell 260-262
- Flooding—*See also* Waterflooding
- Flooding
 alkaline
 Enhanced Oil Recovery 187-224
 sodium hydroxide and sodium orthosilicate consumption 227-250
 micellar/polymer 193-195
- Flowability, sand formulation 252-258
- Flow Index and impact depth 252-253
- Flow rate effect on caustic consumption, petroleum reservoir sands 235-241
- Flow study, long term 238-244
- Fluorescence, x-ray 19
- Flurosilicate method for silica content 18
- Food additive regulation status, sodium metasilicate 40
- Food Chemicals Codex 39-40
- Food contact surfaces, cleaning 40-41
- Food and Drug Administration and safety regulations 31-32, 38-41
- Food uses 38-41
- Formation, colloid, alkaline conditions 124-129
- Formation, sepiolite 160-162
- Foundry cores, binder 251-270
- Fourier transform 172
- Furnace atomic adsorption 21-25
- Fusion, inertial confinement, microballoons 301
- G**
- Gases, rare, adsorption 170
- GC and silicon alkoxides 298
- Gel
 base exchange for softening water 12
 formation 116-121
 hydrogen bond acceptor molecules and adsorption 171
 interaction with cations 135-136, 145-146
- monolithic dried, of amorphous silica 302f

Gel—*Continued*

- porous and nonporous, preparation and behavior 165-183
 proton NMR 169-183
 silicon alkoxide 294-303
 solid silica 116
 Gelation and pH 120, 124-126
 Generally Recognized as Safe list—
See GRAS list

Glass

- depth profiles of hydrogen and sodium 29f
 hydratable sodium silicate, glass by reconstitution 277-288
 melting techniques 278
 reconstitution of hydratable sodium silicate glasses 277-288
 technology, silicon alkoxides 293-303
 Government agencies—*See also the specific agencies listed* ... 31-46, 58-61
 Granulated sodium metasilicates 11
 Gravimetric silica procedure 18
 GRAS list 38-41
 Guinea pig studies, sodium metasilicate pentahydrate 58
 Gypsum, alkaline consumption minerals and sand, static equilibrium studies 231f

H

- Hamsters, inhalation studies 62
 Hardness ion precipitate 217
 surfactant activity 202
 Health aspects and hazards 31-46, 49-62
 Heat, isotheric, of adsorption 173, 176
 Heptane and detergent 273
 Hexamer, prismatic, silicon-29 NMR 81, 83-90
 High bulk density sand bodies 257
 High-field silicon-29 NMR spectra 85f
 High-resolution, silicon-29 NMR, solid silicates 84f
 High temperature properties and collapsibility of sand from aluminum casting 267-268
 High vapor pressure compounds and impurity analysis 23
 History of manufacture in US 3-13
 Homonuclear decoupling, silicon-29 NMR 80-89
 H₂O as solvent, NMR studies 73-78
 Human exposure 59-61
 Humidity and coated sand work-life 252-253, 262-263
 and water content range 278
 Huntington Beach Crude 216-219

- Hydratable sodium silicate glass by reconstitution 277-288
 Hydrated orthosilicate ratio 11
 Hydrated silicate, hydronium ions 28
 Hydrated sodium metasilicates, phase relationship for crystallization 10-11
 Hydration, effect of solid phase 160
 Hydroceramics 277
 Hydrogen, in glass, profile 28-29
 Hydrogen bond acceptor molecules and adsorption onto gel 171
 Hydrogen ion activity measurement 137
 Hydrogen spillover, reduction of silica surface by 179-183
 Hydrolysis and surface area 165-183
 tetramethoxysilane, and gel time 120
 Hydrolyzation polymerization, silicon alkoxides 297-301
 Hydronium ions in hydrated silicate 28
 Hydrosilicate composition, hydration/dehydration 280-281
 Hydrosilicate porosity as function of alkali content and dealcalization temperature 286f, 287f
 Hydrous silicate 10
 Hydroxo and oxo ligand coordination 63
 Hydroxyl, surface 73, 183

I

- Illite, alkaline consumption minerals and sand, static equilibrium studies 231f
 Impact depth and Flow Index 252-253
 Impurities, paramagnetic, in silicon-29 NMR 75
 Impurity analysis 21-25, 45f
 detection limit 21-22
 high vapor pressure compounds 23
 instrumental techniques 21-25
 mercury vapor cold trap 23
 Index, Primary Irritation 58-59
 Industry oil, recovery of crude oil using chemical flooding processes 187-211
 sodium silicate 3-13
 Infrared spectroscopy—*See* IR spectroscopy 50-58
 Ingestion 50-58
 Ingestion studies in rats, serum alkaline phosphatase activity 56
 Inhibitor, corrosion in drinking water 39-41
 Inorganic Chemicals Manufacturing Industry and National Resources Defense Council v. Costle 42
 Inorganic precipitation 165-167

- Instrumental techniques 17-29
 relative precision 19-20
 silicate impurity analysis 21-25
 silicate structural analysis 25-28
 Interdiffusion coefficient 283-285
 Interfacial tensions and emulsions 217
 International Joint Commission
 (U.S.-Canada) 32
 Ion(s)
 alkali, adsorption onto silica
 particles 95
 copper, in solution equilibria 141
 metal, interactions with silicates
 in solution 133-146
 precipitate hardness 217
 species in solution, silicon-29
 NMR 88-90
 Ion activity, hydrogen, measurement 137
 Ion chromatography 21-25
 Ion exchange, and nonreversible
 chemical consumption 233-235
 Ion-exchange reaction, diffusion ki-
 netics for dealkalization 281-285
 Ion selective electrodes 21-25, 136-146
 Ion-solvent and ion-surface inter-
 actions 135
 Iron
 adsorption 135
 impurities 21-25
 spectral lines 23, 24f
 Irritation Index, Primary 58-59
 IR spectra
 surface Si-H 182f, 179, 182-183
 trimethylsilyl polymer 323
 IR spectroscopy 26
 IR and surface silanols 167-169,
 179, 182f
 Isoteric heat of adsorption 173, 176
 Isotope, silicon-29 73
- K**
- Kaolinite, alkaline consumption
 minerals and sand, static
 equilibrium studies 231f
 Karl Fischer analysis of crude oil
 emulsions 217
 Kinetic, diffusion, for dealkalization .. 281
 Kinetics
 of aqueous silicate solutions 80-90
 of dealkalization 278-284
- L**
- Labeling 33-35, 38
 Laser Raman spectroscopy 26
 Lattice constant, tetrabutylammonium
 hydrogen silicate 306
 Laundry detergent(s)—*See*
 Detergent(s)
- Lead ion and adsorption 135
 Lentz-type extraction—substitution
 process 320
 Lethal oral dose of sodium silicate
 in man 54
 Light scattering 124, 126f, 127
 Linear and cyclic tetramer,
 silicon-29 NMR 81, 83-90
 Liquid detergent—*See* Detergent(s)
 Liquid phase separation—*See*
 Storage stability
 Liquid silicate, atomizing 10
 Litidionite 319-328
 Low-phosphate detergents 38
 Low-tension waterflooding 193, 197-199
- M**
- Magnesium
 and adsorption 135-138, 141, 144-146
 impurities 21-25
 spectral lines 23, 24f
 and water hardness in detergents 272
 Magnetic moment, proton NMR
 and gels 169
 Man, lethal oral dose of sodium
 silicate 54
 Manufacture in the US, history 3-13
 Material safety data sheet, high
 ratio powders 33, 36-37
 Mean pore diameter of solid
 silica 156-163
 Median tolerance limit 65
 Mercury vapor cold trap and
 impurity analysis 23
 Metal atoms in litidionite,
 coordination 320-321
 Metal ion
 activity 138-146
 flame photometry 19-21
 interactions with silicates in
 solution 133-146
 multivalent 202
 solution precipitate 141, 144-146
 Metasilicate
 monosilicic acid 108
 sodium
 food additive regulation status 40
 granulated 11
 and health hazards 38
 and safety regulation 31-46
 phase relationship for crystalli-
 zation 10-11
 spectrum 26
 Methanol, adsorption 173
 Methanolic solution of silicic
 acids 84, 90, 91f
 Methoxylation of an aerogel surface .. 171
 Methyl silicate and silicon-29
 NMR spectra 75, 76f

- Micellar/polymer flooding 193-195
- Microballoons for inertial confinement fusion 301
- Microwave power and dehydration of sand 255
- Microwave scan, crude oils 217-224
- Mineral
alkaline consumption, static equilibrium studies 231*t*
rock, in reservoir sand, interaction of alkali 233
- Minusil 206
- Moisture absorption rate, dehydration core sand 262-267
- Moisture loss and coated sand worklife 252-253, 262-263
- Molar ion activity 137-138
- Mold density and sand grain shape 257
- Molecular weight and connectivity 124
- Molybdc acid reaction with sodium silicate 97
- Monolithic dried gel of amorphous silica 302*f*
- Monolithic shapes, casting and drying 301
- Monomer, silicon-29 NMR 81, 83-90
- Monomeric silica determination using silicomolybdate method 19-21
- Monosilicic acid 63, 104
from metasilicate 108
pH concentration, and reaction rate 120-124
second-order rate constant for dimerization 90, 92*f*
- Montmorillonite 202, 204*f*, 206
- Montmorillonite, alkaline consumption minerals and sand, static equilibrium studies 231*t*
- Mulling 252
- Multipermeable zones 206, 210-211
- Multivalent metal cations 202
- N**
- National Resources Defense Council v. Costle and Inorganic Chemicals Manufacturing Industry 42-44
- Nernst response curve 137-138
- Neso unit 73-78
- Neutralization 115-116
- Neutron activation analysis (NAA) 21-25
- Nitrogen BTE specific surface areas 166-167
- Nitrogen retention, animal studies 54*f*
- NMR gel, proton 169-183
- NMR spectra
high-field silicon-29 85*f*
silicon-29 73-92
ethyl esters of polysilicic acids 77*f*
methyl siliconates 76*f*
- NMR spectra—*Continued*
silicon-29—*Continued*
potassium silicate 79-82, 84-85
silicate esters 73-78
sodium silicate 74*f*, 76*f*, 81, 83*f*
solid silicate 84*t*
- Nomenclature, silicon alkoxides 295-296
- Nonporous gel, preparation and behavior 165-183
- Nonreversible chemical consumption, ion exchange/reversible adsorption 233-235
- Nutritional animal studies 54-58
- Nutritional aspects 65-67
- O**
- Occupational Safety and Health Administration (OSHA) 31-33, 41-42
- Octamer, cubic 110
- Octamer, cubic, silicon-29 NMR 81, 83-90
- Oil
Aminoil LMZ 235
chemical flooding processes 187-211
emulsification phenomena in alkaline waterflooding 215-224
- Oil bank 223
- Oil gravity, reservoir rock 189*t*, 216
- Oil recovery, enhanced 187-211
- Oil recovery, enhanced, sodium hydroxide and sodium orthosilicate consumption 227-250
- Oil viscosity at reservoir temperature 189*t*, 216
- Oligomeric ethyl silicate 75
- Oligomeric species, equilibrium, silicon-29 NMR 79-92
- Optical density, gels 180*f*
- Oral dose, lethal, of sodium silicate in man 54
- Oral LD₅₀ studies 50-58
- Organic acid and alkaline flooding 215-224
- Organic cation, action size influence silicates 306
- Organic and inorganic compound, precipitation 165-167
- Organometallic reagent and surface silanols 167
- Organosilicon, fibrous, polymer 319-328
- Orthosilicate
alkaline flooding 188-192
enhanced oil recovery 215
- OSHA—*See* Occupational Safety and Health Administration
- Oxidation of volatile silicic compounds 179-183
- Oxidizing agent for prevention of discoloration by carbon 6

- Oxygen
 in litiidonite 321f
 non-bridging and bridging in alkali
 silicate glasses 26-27
- P**
- Packing distribution of silanols 170
 Packing regulations 42
 Paramagnetic impurities in silicon-29
 NMR 75
 Particle diameter 112-113
 relation to rate constant of reac-
 tion with molybdic acid 99
 in solutions 95-112
 Patents for sodium silicates 5-7
 Permeability (brine), reservoir
 rock 189t, 216
 Permeability zones 206, 210-211
 Permissible exposure limit (PEL) 33
 Pesticide formulations 41-42
 Petroleum reservoir sand, long term
 consumption of solutions 227-250
- pH
 and gelation 120, 124-126
 and NMR studies 75
 of oil emulsions 218, 221-224
 and polymerization degree 166
 and reaction rate of monosilicic
 acid 104
 and solubility 99
- Phase relationships for
 crystallization of hydrated
 sodium metasilicates 10-11
- Phase separation, liquid—*See* Storage
 stability
- Phase, solid, hydration effect 160
- Phosphatase activity, ingestion
 studies in rats 56
- Phosphate-free and low-phosphate
 detergents 38
- Phosphorus retention, animal studies 54f
- Photoelectron spectrum, x-ray tri-
 methylsilyl polymer 324f
- Photometry flame, for alkali metals 19-21
- Photon spectroscopy, sputter induced 28
- PII—*See* Primary Irritation Index
- Plants and sources of silica 62
- Plasma emission spectroscopy (PES) 19-21
- PMR—*See* Proton NMR
- Pollution control 42-44
- Polymer
 colloidal, tetrahydrofuran
 extraction 99-101, 108-110
 trimethylsilyl
 composite transmission electron
 micrograph 325f, 326f
 X-ray photoelectron spectrum .. 324f
- Polymeric silicic acid salts 75
- Polymeric siloxane, building units 73-74
- Polymerization-depolymerization
 reaction, solution chemistry 85-147
- Polymerization
 in acid solution 120
 degree 124
 interactions with cations in
 solution 133-147
 pH and aging time effect 166
 hydrolyzation and condensation,
 silicon alkoxides 297-301
 rate, silicic acid 116
- Polymer/micellar flooding 193-195
- Polysilicate connectivity 125f
- Polysilicate materials, alkaline 38-41
- Polysilicic acid, silicon-29 NMR
 spectra 77f
- Pore, aerogel 173
- Pore diameter
 alkali/surfactant 206
 consumption of reservoir sands 244-250
 interactions 206
 mean of solid silica 156-163
 ultrafiltration 110-112
- Pore volume 235
 consumption of reservoir sands 244-250
 relative reactivity of reservoir and
 berea sandstone using 232t
- Porosity
 alkaline slug 219t
 as function of alkali content and
 dealkalization tempera-
 ture 286f-287f
 reservoir rock 189t, 216
- Porous gel, preparation and
 behavior 165-183
- Porous structure, reconstitution of
 hydratable sodium silicate
 glasses 280, 285
- Potassium, spectral lines 23, 24t
- Potassium silicate
 NMR spectra 79-82, 84-85
 safety regulations 31-46
- Powders, high ratio, material safety
 data sheet 33, 36-37
- Precipitate formation—*See also*
 Storage stability
 hardness ions 217
 metal ion solutions 141, 144-146
 organic and inorganic
 compounds 165-167
 processing silicon alkoxides 295
 sepiolite 160-162
 and ultrafiltration 129
- Precision of wet chemical and instru-
 mental assay methods 19-21
- Pressure, ramming, sand 257
- Pressure dependency of solubility in
 salt water 155-163

- Preparation and behavior of porous
and nonporous gels 165-183
- Primary Irritation Index (PII) 58-59
- Prismatic hexamer, silicon-29
NMR 81, 83-90
- Processes, flooding—*See* Chemical
flooding processes 187
- Properties
high temperature, and collapsibility
of stand from aluminum
casting 267-268
- litidionite 320-322
- silica surface, and silanol
groups 165-183
- silicate, in enhanced oil
recovery 197, 200-211
- tetrabutylammonium hydrogen
silicate 306-318
- trimethylsilyl polymer 323-328
- Protonation, silicon-29 NMR 80
- Proton exchange, between silanols
and adsorbate molecules 178-179
- Proton mobility 170
- Proton NMR gels 169-183
- Public health agencies 31-46, 58-61
- Pulse nuclear magnetic resonance 172
- Pulse study, long term, consumption
of reservoir sands 244-250
- Q**
- Quadrupole coupling constant 176
- Quadrupole-inner electrical field
gradient interaction 176
- Quality control and silicate to
soda ratios 18
- Quartz 206
- Quartz cell 179
- R**
- Rabbit, esophageal test 54-55
- Radial flood using low tension
water flood system 208f, 209f
- Raman spectroscopy 21-26
- Raman spectrum of sodium silicates .. 27f
- Ramming pressure, sand 257
- Rare gases, adsorption 170
- Rare ladder silicate litidionite 319-322
- Rat studies
lethal sodium silicate dose 50-51
- reproductive ability when fed
sodium silicate 56, 57t
- serum alkaline phosphatase
activity, ingestion studies 56
- urinary excretion of sodium
silicate 56-58
- Rate, dissolution in salt water 158t
- Rate, polymerization, silicic acid 116
- Rate constant
first-order, sodium silicate, reac-
tion with molybdc acid 97
- second-order, for dimerization of
monosilicic acid 90, 92f
- solvation 95-112
- Ratio
hydrated orthosilicates 11
- silicate to soda 18
- RCRA—*See* Resource Conservation
and Recovery Act of 1976
- Reaction rate, and pH concentration
of monosilicic acid 120-124
- Reactivity of berea sandstone and
reservoir sands, using pore vol-
ume alkaline chemicals 232t
- Reagent, organometallic, and surface
silanols 167
- Reconstitution of hydratable sodium
silicate glass 277-288
- Recovery, oil 216-219
- Recovery, oil, sodium hydroxide and
sodium orthosilicate consump-
tion 227-250
- Reduction of silica surface by
hydrogen spillover 179-183
- Regulatory status of soluble
silicates 31-46
- Relaxation rate, spin-lattice .172, 176, 178
- Reproductive ability of rats fed
sodium silicate 56, 57t
- Reservoir parameters 189t
- Reservoir rock 189t, 216
- Reservoir sand
consumption
long term pulse study 244-250
- pore volume 244-250
- static equilibrium study 224-232
- petroleum, long term consumption
of caustic and silicate
solutions 227-250
- reactivity, using pore volume
alkaline chemicals 232t
- Resonance, silicon-29 NMR 80-90
- Resonance frequency 172
- Resource Conservation and Recovery
Act of 1976 (RCRA) 43
- Reversible adsorption and non-
reversible chemical consump-
tion 233-235
- Reversible adsorption of sodium
hydroxide and orthosilicate
alkalinity, THUMS Ranger
sand 234f, 236f
- Rock minerals in reservoir sand,
interaction of alkali 233
- Rosin, historical perspective and
replacement by sodium silicates 3-5

- S**
- Safety aspects 49-62
- Safety and corrosivity regulation 43-44
- Safety reviews 31-37
- Salt water solution, solubility and aging of amorphous silica 149-163
- Salts, polymeric silicic acid 75
- Sand
- alkaline consumption, static equilibrium studies 231*t*
 - aluminum casting, high temperature properties and collapsibility 267-268
 - Aminoil LMZ 232*t*, 235-244
 - Berea sandstone 228-232
 - bound, storage stability 260-267
 - dehydration 255
 - THUMS Ranger 228-250
- Sand bodies, high bulk density 257
- Sand coating 252-255
- Sand core, for aluminum casting, dehydrated sodium silicate bound 251-270
- Sand grain, raw material for silicate glasses 294
- Sand grain shape and mold density 257
- Sandstone/surfactant chemical reaction 202
- Scale expansions, silicon-29 NMR spectra 84, 86-88
- Second-order rate constant for dimerization of monosilicic acid 90, 92*f*
- Sensitivity, silicon-29 NMR 79, 90
- Sepiolite, precipitation 160-162
- Serum alkaline phosphatase activity, ingestion studies in rats 56
- Sesquisilicates 11
- Sewage and water, silica sols 12
- Shifts, enriched silicon-29 NMR 81*t*
- Shipping regulations 42
- Silanol group
- esterification 171, 172
 - properties of silica surfaces 165-183
- Silica
- amorphous, in salt water solution, solubility an aging 149-163
 - content determination 18
 - cycle 64*f*
 - gel surface, dynamics of adsorption processes 172-177
 - monomeric, determination using silicomolybdate method 19-21
 - surface properties, and silanol groups 165-183
 - thermal titration detection 19
 - titration determination 18
- Silicate esters, NMR studies 73-78
- Silicate glasses, alkali, silicon-oxygen bond 26-27
- Silicate litidionite, rare ladder 319-322
- Silicate litidionite, tube 319-322
- Silicate ratio and tensile strength 257-263
- Silicate to soda ratio 18
- Silicic acid
- aqueous methanolic solution 84, 90, 91*f*
 - conversion of sodium silicate 97
 - dissociation 155
 - polymerization 120
 - polymerization rate 116
 - solution 102-106
 - solution, aging 99
- Silicomolybdate acid complex, spectroscopic detection in visible spectrum 19-21
- Silicomolybdate method, monomeric silica determination 19-21
- Silicomolybdate reaction data 98-113
- Silicon, spectral lines 23, 24*t*
- Silicon alkoxide
- gel, application 301-303
 - in glass technology 293-303
- Siliconate, methyl, silicon-29 NMR spectra 76*f*
- Silicon-29 NMR
- high-resolution, solid silicates 84*t*
 - spectra
 - ethyl esters of polysilicic acids .. 77*f*
 - methyl siliconates 76*f*
 - sodium silicate 74*f*, 76*f*
- Silicon-oxygen bond in alkali silicate glasses 26-27
- Siloxane
- fibrous 319-328
 - polymeric, building units 73-74
- Singlet silicon-29 NMR resonance 81*t*
- SIPS—See Sputter induced photon spectroscopy
- Skin contact 58-59
- Skin and eye irritation 33
- Slug, alkaline, porosity 219*t*
- Soap and alkaline silicates 10-12
- Soap and soluble silicate, history of manufacture 3-13
- Soda ash 5
- Soda content and dealcalization of hydrosilicate 285
- Soda to silicate ratio 18
- Sodium
- adsorption onto silica particles 95
 - electrode 280
 - in glass, profile 28-29
 - hydrated metasilicates, phase relationships for crystallization 10-11
 - spectral lines 23, 24*t*
- Sodium carbonate, and low tension waterflooding 193
- Sodium fluoride reaction in fluosilicate method 18

- Sodium hydroxide, and orthosilicate alkalinity, THUMS Ranger sand, reversible adsorption and consumption 234f, 236f
- Sodium hydroxide and sodium orthosilicate consumption by alkaline flooding and enhanced oil recovery 227-250
- Sodium metasilicate, food additive regulation status 40
- Sodium metasilicate, granulated 11
- Sodium metasilicate pentahydrate in guinea pig studies 58
- Sodium metasilicate and safety regulation 31-46
- Sodium metasilicate spectrum 26
- Sodium nitrate solution and dealkalinization 281
- Sodium orthosilicate alkaline flooding 188-192
- consumption and sodium hydroxide by alkaline flooding and by enhanced oil recovery 227-250
- enhanced oil recovery 215
- Sodium polysilicate materials 38-41
- Sodium silicate glass, hydratable, glass by reconstitution 277-288
- Sodium tripoly-phosphate, and low tension waterflooding 193
- Sol-gel process for forming glass, silicon alkoxides 293-303
- Solid phase hydration effect 160
- Solid silica mean pore diameter 156-163
- high-resolution silicon-29 NMR 84f
- gel 116
- Sols silica, for clarification of water and sewage 12
- silicic acid, rate constant 99
- Solubility 95-112
- amorphous silica 116, 117f
- amorphous silica in salt water solutions 149-163
- silica 62-65
- Solution aqueous 63
- aqueous methanolic, of silicic acids 84, 90, 91f
- copper ion, equilibria 141
- degree of polymerization, effect of interactions with cations 133-147
- dilute 95-96, 101-107
- kinetics of aqueous silicate 80-90
- salt water, solubility and aging of amorphous silica 149-163
- silicic acid 102-106
- Solution—*Continued*
- silicon-29 NMR, silicate in species 88-90
- sodium silicate, colloidal components 95-112
- Solution chemistry, polymerization-depolymerization reaction 85-147
- Solvated silicate, NMR studies 73-78
- Solvent interaction 135-146
- Sources of silica 62
- Speciation 64f
- Spectra high-field silicon-29 NMR 85f
- IR 182f
- IR, trimethylsilyl polymer 323
- NMR, potassium silicate 79-82, 84-85
- NMR, sodium silicate 81, 83f
- silicon-29 NMR ethyl esters of polysilicic acids 77f
- methyl siliconates 76f
- sodium silicate 74f, 76f
- Raman 27f
- x-ray photoelectron 324f
- Spectrometer, ESCA 179
- Spectroscopic detection alkali ion 19-21
- automated, silicate in detergents 19-21
- silicomolybdate acid complex in the visible spectrum 19-21
- Spectroscopic properties 171
- Spectroscopy plasma emission 19-21
- Raman 21-25
- sputter-induced photon 28
- vibrational 26
- Spin-lattice relaxation rate 172, 176, 178
- Sputter-induced photon spectroscopy (SIPS) 28
- Stability bound sand storage 260-267
- boundary and pH 127, 128f
- in the micellar phase 193
- storage, and liquid detergent 273
- Static equilibrium studies caustic consumption of reservoir sand 230f
- consumption of reservoir sands 224-232
- Storage stability bound sand 260-267
- and liquid detergent 273
- Strain, structural 88
- Strength bound sand 255-260
- tensile, and silicate ratio 257-263
- Structural analysis, silicate, advanced instrumentation 25-28
- Structural arrangement, coordination shell 166

Structural strain 88
 Structural studies, NMR 73-92
 Sulfate impurities 21-25
 Surface,
 BET, area determinations 156
 silica, by hydrogen spillover,
 reduction 179-183
 silica, properties, and silanol
 groups 165-183
 silica gel, dynamics of adsorption
 processes 172-177
 Surface area, and hydrolysis 165-183
 Surface density in silanol groups 170
 Surface diffusion coefficient 175*f*
 Surface hydroxyls 73-183
 Surface interaction 135-146
 Surface silanol, and IR 167-169, 179, 182*f*
 Surface wettability, change rock 217
 Surfactant activity, hardness ion 202
 Surfactant/alkali systems, calcium
 concentration and electrode
 potential 203*f*
 Surfactant sensitive electrode 202
 Symmetry 173
 and coordination 81-90
 tetrabutylammonium hydrogen
 silicate 305, 306
 Synthesis
 litudionite 320-322
 tetrabutylammonium hydrogen
 silicate 306
 trimethylsilyl polymer 323-328

T

Temperature
 dealkalization, and alkali
 content 286*f*, 287*f*
 and solubility in salt water 150-155
 Temperature effects—*See* Storage
 stability
 Tensile sample, blown, and core
 production 254-255
 Tensile strength, and silicate ratio 257-263
 Tension
 interfacial, and emulsions 217
 low, waterflooding 193, 197-199
 TEOS—*See* Tetraethyl orthosilicate
 Tertiary oil recovery 223
 Testing, biological 49-62
 Tetraalkylammonium silicate,
 silicon-29 NMR 90
 Tetraalkylorthosilicate and tetrabutyl-
 ammonium hydroxide 306
 Tetrabutylammonium hydrogen
 silicate, synthesis, chemical,
 thermal and crystallographic
 properties 305-317

Tetrabutylammonium hydroxide, and
 tetraalkylorthosilicates 306
 Tetraethyl orthosilicate (TEOS) 294-303
 Tetrahedron
 bond length 166
 chains 124
 connectivity 119, 124
 Tetrahydrofuran, extraction of
 colloidal polymer 99-101, 108-110
 Tetramer, cyclic, of monosilicic acid,
 concentration and reaction rate 120
 Tetramethoxysilane hydrolysis,
 and gel time 120
 Thermal decomposition, tetrabutyl-
 ammonium hydrogen
 silicate 313*f*, 315*f*, 316*f*
 Thermal gravimetric analysis (TGA),
 tetrabutylammonium hydrogen
 silicate 312, 316*f*
 Thermal properties, tetrabutyl-
 ammonium hydrogen silicate 312
 Thermal titrator detection of alkali
 and silica 19
 Thermodynamics, pressure 155
 Thermogram, differential thermal
 analysis, trimethylsilyl polymer .. 327*f*
 THF—*See* Tetrahydrofuran
 THUMS Ranger sand 228-250
 Titanium, spectral lines 23, 24*t*
 Titration curve, tetrabutylammonium
 hydrogen silicate and its
 hydrate 310-311, 314, 317*f*
 Titration determination of alkali
 and silica 18
 Titrator, thermal, detection of
 alkali and silica 19
 Toxicity 49-62
 aquatic 65, 66*t*
 lethal dose for rat 50-57
 Toxic pollutants 42-44
 Toxic Substances Control Act
 (TOSCA) 33, 41-42, 44-45
 Transmission electron micrograph
 composite, trimethylsilyl
 polymer 325*f*, 326*f*
 litudionite crystallite 320, 322*f*
 Transportation regulations 42
 Trimethylsilylation 118-119
 Trimethylsilyl polymer, x-ray photo-
 electron spectrum 324*f*
 Tube silicate litudionite 319-322

U

Ultrafiltration 101, 110-112
 Ultrafiltration, of colloidal solutions .. 129*t*
 Unit cell, tetrabutylammonium
 hydrogen silicate 314

Urinary excretion of sodium silicate	
in rats	56-58
U.S. Department of Agriculture	40-42
U.S. Department of Transportation	
and skin contact	58-59
U.S. production of soluble silicates	3-13

V

Vail, James	12-13
Valence of metal ion, and	
adsorption	135-146
Valency	84, 87f
Vapor pressure, high, and	
impurity analysis	23
Vibrational spectroscopy	26
Viscosity	
silicate solid content	257-260
silicon alkoxides	300f
Volatile silicic compound,	
oxidation	179-183
Volume, pore, consumption of	
reservoir sands	244-250

W

Waste control	42-44
Water	
addition effect on gel time, silicon	
alkoxides	299f
content range, and humidity	278
corrosion inhibitor	39-41
drinking, reproductive ability of rats	
fed sodium silicate	56, 57f
hardness and zeolites	272

Water— <i>Continued</i>	
and sewage, silica sols	12
softening, base exchange gel	12
solution, salt, solubility and aging	
of amorphous silica	149-163
as solvent, NMR studies	73-78
Waterflooding, alkaline, of heavy	
crude oils, emulsification	
phenomena	215-224
Water vapor pressure, dehydration	
core sand	262-267
Weight gain, rat studies	56
Weight percent water, hydration of	
sodium silicate glass	281f
Wet chemical method	
assay of silicates	18, 19-21
relative precision	19-20
Wettability, change rock surface	217
Wilmington Field Crude	190f, 216, 219f
Wood preservation	4-5
Worklife, coated sand	252-254

X

X-Ray fluorescence (XRF)	19
X-Ray photoelectron spectrum, tri-	
methylsilyl polymer	324f
X-Ray powder diffraction data, tetra-	
butylammonium hydrogen	
silicate	306-310

Z

Zeolite, commercial application	272
Zeolite A	32, 58, 62